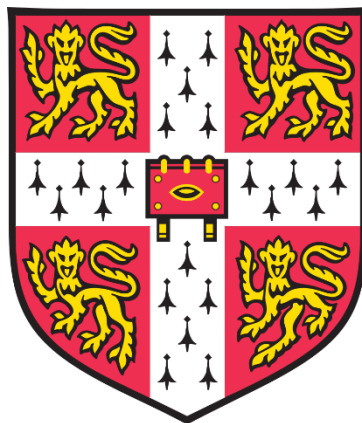

Understanding and Exploiting Viral Protein US28 During Human Cytomegalovirus Latency

Elizabeth Grace Elder

Corpus Christi College



DECEMBER 2019

This thesis is submitted for the degree of Doctor of Philosophy

Declaration

This thesis is the result of my own work and includes nothing which is the outcome of work done in collaboration except as declared in the Preface and specified in the text. It is not substantially the same as any that I have submitted, or, is being concurrently submitted for a degree or diploma or other qualification at the University of Cambridge or any other University or similar institution except as declared in the Preface and specified in the text. I further state that no substantial part of my thesis has already been submitted, or, is being concurrently submitted for any such degree, diploma or other qualification at the University of Cambridge or any other University or similar institution except as declared in the Preface and specified in the text. It does not exceed the prescribed word limit for the relevant Degree Committee.

Abstract

Understanding and Exploiting Viral Protein US28 During Human Cytomegalovirus Latency **Elizabeth Grace Elder**

Human cytomegalovirus (HCMV) is a ubiquitous herpesvirus which infects 50-100% of humans worldwide. HCMV causes a lifelong subclinical infection in immunocompetent individuals, but is a serious cause of mortality and morbidity in the immunocompromised and in neonates. Like other herpesviruses, HCMV establishes latency in specific cell types following primary infection, and reactivates periodically during the lifetime of the host. One important site of HCMV latency is early myeloid lineage cells, including hematopoietic progenitor cells and monocytes, in which the critical viral lytic promoter, the major immediate early promoter (MIEP), is repressed. This is mediated by a combination of host and viral factors, including the viral G-protein coupled receptor US28.

Here, I explore mechanisms by which US28 optimises host cells for latent carriage. Using an unbiased proteomic screen, I have assessed changes in total host proteins induced by US28 and find that interferon-inducible genes are downregulated by US28. I validate that MHC Class II and two PYHIN proteins, MNDA and IFI16, are downregulated during experimental latency in primary human CD14⁺ monocytes. By overexpressing IFI16, I show that IFI16 can activate the viral major immediate early promoter and immediate early gene expression during latency via NF- κ B, a function which explains why downregulation of IFI16 during latency is advantageous for the virus. I also show that MNDA is a potential restriction factor for HCMV latency. Since PYHIN proteins are sensors of double stranded DNA, I also investigate whether US28 interferes with the sensing of dsDNA.

I also examine the antiviral potential of two US28-targeting reagents during HCMV latency. Lowering latent viral loads in solid organ or hematopoietic stem cell transplant donors and recipients is likely to lead to lower incidence of HCMV-disease in transplant patients. The first reagent, a US28-specific nanobody, inhibits US28 function and partially reverses latency. This leads to lytic gene expression, and subsequent recognition and killing of latently infected cells by naturally existing T cells from seropositive individuals. The second, a US28-specific immunotoxin, has previously been shown to directly kill latently infected cells. I show that new derivatives of this immunotoxin are more efficacious and can kill latently infected cells after a short incubation, paving the way for their use in *ex vivo* normothermic perfusion of solid organs from seropositive individuals prior to transplantation.

Acknowledgements

My supervisor John Sinclair has been an immense source of scientific and personal support during my PhD. He has provided wonderful mentorship and training, and has, at times, been a parent to me. To begin to honour his contribution, and a vital skill he taught me during my PhD, on the next page I have set a cryptic crossword.

I'd like to thank my fellow PhD students for their invaluable contribution to my time in Cambridge. I was welcomed to the lab by (the now Dr) Ben Krishna who was responsible for both the foundations of this project, teaching me a great many lab techniques, and for an increase in my usage of profanity.

Marianne Perera has been a brilliant companion for conference travel, consolation over failed experiments, and toilet humour. I'd like to thank (now Dr) George Sedikides, the fastest lymphoprep layerer on the planet, for his help and his playfulness during the first two and a half years here. Dr Eleanor Lim helped with T cell work and both she and Martin Potts have shared my enjoyment for a good practical joke over the last three years.

I gratefully acknowledge those in working in the shared Sinclair and Wills group lab spaces. Special thanks go to Dr Mark Wills, Linda Teague, Roy Whiston, Paula Rayner, Dr Emma Poole, and Dr Ian Groves for advice and assistance, and opportunities to contribute to other projects. Esme Fowkes was an undergraduate Part II student who I was given the opportunity to supervise during my PhD, and I'm grateful for her conscientiousness and her contribution to some of the work presented here.

I'd like to gratefully acknowledge collaborators outside the Sinclair/Wills labs for various parts of this project, including Paul Lehner, James Williamson, and staff at the NIHR cell phenotyping hub, members of the Lever lab (all Cambridge University), Timo de Groof and Martine Smit (Vrije Universitet), Thomas Kledal (Synkline ApS), Mette Rosenkilde (University of Copenhagen), and Christine O'Connor (Cleveland Clinic).

Thank you to Christopher Fox for putting up with me at my most stressed, and providing some tip top pipetting advice. I'm also extremely grateful to him, and to my mum, Rachel, who proof-read parts of this thesis. Finally, thank you to all those who donated blood for experiments, and the organisations that have provided financial support, including the Wellcome Trust who funded me.

Liz Elder

December 2019

PhD Cryptic, set by Blondie

ACROSS

1. See 27

4, 25, 2. John has scrambled coral protein, I'll produce more herpesvirus DNA. (6, 4, 11)

7. El diablo oddly contains a 12 (5)

9. See 10

12. Party with country is a gift (8)

14, 15. Pet's a type of viral life cycle, secret; eats point queen and is sold for scrap metal (9, 9)

16. See 22

17. See 27

18. See 11

19. See 28

20. See 5

22. Taverners magnetise a dodgy expenses claim (9, 10)

26, 8. Rating for film is messily tearing up LA tango (8, 8)

27, 1, 17. Chromatin expert? Oh no, chlorine is spilled on dirty floor making 28, 19 (6, 10, 10)

29. Provided good person with a home for 28, 19 (1,1,5)

DOWN

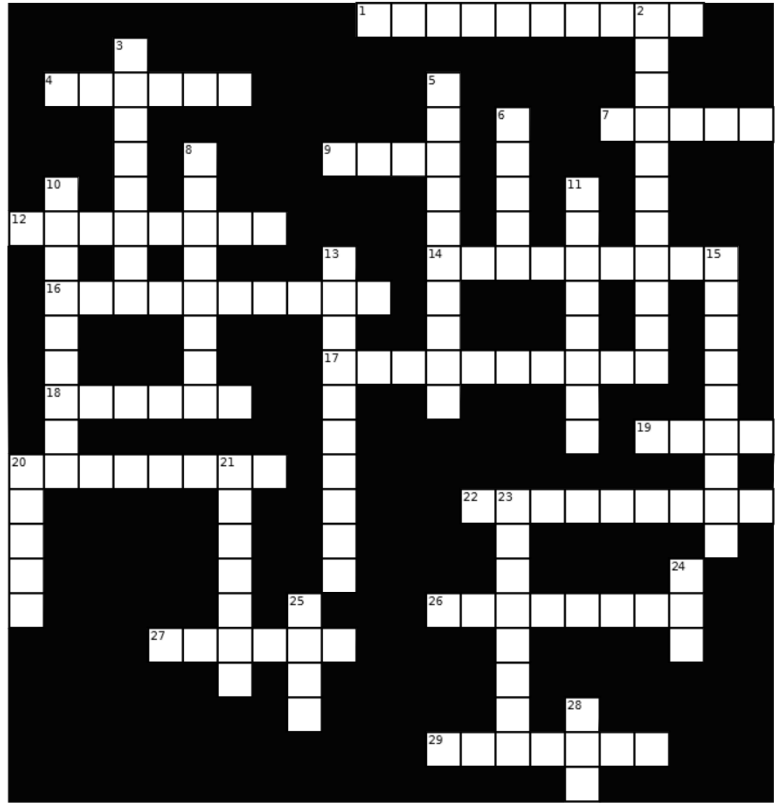
2. See 4

3. See 24

5, 20 across, 13. Eulogy is dreadful, take handkerchieves out, stay half wailing. (3, 7, 4, 4, 4, 1, 5)

6. This 12 is not odd if Frau riots? (5)

8. See 26



10, 9, 23. Christmas 12 is firm round eastern state that is sad, listener calls (9, 4, 8)

11, 18. Rue noisiest turmoil after top returns for 28, 19. (8, 6)

13. See 5

15. See 14.

20. Physician unwell for military training regime (5)

21. Eliot holds son or daughter and dries tears (7)

23. See 10

24. Travel motto for lean years: stay inside, no chocolate logs, and instigate rationing at first (3, 8)

25. See 4

28, 19. Western blotting is an example of dog labour? (3, 4)

Table of Contents

Declaration	1
Abstract	2
Acknowledgements.....	3
List of Abbreviations.....	9
List of Figures	12
List of Tables.....	13
1. Introduction	14
1.1. Natural history of human cytomegalovirus	14
1.1.1. Herpesviruses	14
1.1.2. HCMV infection in healthy individuals	15
1.1.3. Congenital HCMV infection	16
1.1.4. HCMV in the transplant setting.....	16
1.1.5. Other HCMV pathologies	17
1.1.6. HCMV treatment and prevention	17
1.1.7. Species specificity of cytomegaloviruses	18
1.2. Lytic infection of human cytomegalovirus.....	19
1.2.1. HCMV virions and genome structure.....	19
1.2.2. Tropism, entry, and tegument proteins.....	19
1.2.3. Lytic gene expression: a regulated cascade	20
1.3. HCMV latency and reactivation.....	22
1.3.1. Natural sites of HCMV latency and reactivation	22
1.3.2. HCMV latency and reactivation experimental models	22
1.3.3. Viral gene expression during latency and reactivation.....	23
1.3.4. Control of viral gene expression during latency and reactivation	25
1.4. Viral protein US28 is essential for HCMV latency	29
1.4.1. US28 structure, expression, and function during lytic infection.....	29
1.4.2. US28 is essential for HCMV latency	31
1.4.3. US28 manipulation of cell signalling during latency	33
1.5. Pattern recognition and nucleic acid sensing during HCMV infection.....	36
1.5.1. Lytic infection	36
1.5.2. Latent infection	37
1.6. The PYHIN proteins are DNA sensors and transcriptional regulators.....	39

1.6.1.	The PYHIN family of proteins: a brief overview	39
1.6.2.	AIM2	40
1.6.3.	IFIX	40
1.6.4.	IFI16	41
1.6.5.	MNDA	42
1.7.	Nanobodies as immunotherapeutic agents	44
1.7.1.	Camelid antibody domains as therapeutic agents	44
1.7.2.	Anti-US28 nanobodies modulate US28 activity	45
1.7.3.	Shock and kill for reducing latent viral loads	46
1.8.	US28-targeting immunotoxins for killing of HCMV-infected cells	48
1.8.1.	Immunotoxins as anti-cancer and anti-microbial agents	48
1.8.2.	F49A-FTP, a US28-targeting immunotoxin	48
2.	Materials and Methods	51
2.1.	Cells	51
2.2.	Inhibitors	52
2.3.	Generation of lentiviruses and retroviruses	52
2.4.	Lentiviral and retroviral transduction	53
2.5.	Preparation and transfection of DNA into THP-1 cells	53
2.6.	Human cytomegaloviruses	53
2.7.	Immunofluorescence staining and image analysis	54
2.8.	Western blotting	55
2.9.	Flow cytometry	56
2.10.	Cytokine detection by ELISA	57
2.11.	RNA and DNA extraction, reverse transcription, and quantitative PCR	57
2.12.	Proteomic analysis	59
2.13.	Gene ontology analysis	59
2.14.	Interferome analysis	59
2.15.	Nanobody production	59
2.16.	Nanobody binding ELISA	59
2.17.	Nuclear Factor of Activated T-cells reporter gene assay	60
2.18.	Detection of IE gene expression in nanobody-treated monocytes	60
2.19.	PBMC and T cell co-culture and virus reactivation	60
2.20.	Immunotoxin treatments	61

2.21.	Statistical analysis.....	61
3.	US28 downregulates interferon-responsive genes in myeloid cells	62
3.1.	Analysis of the US28-associated proteome	62
3.1.1.	Introduction.....	62
3.1.2.	GO-term enrichment analysis	66
3.1.3.	Interferome analysis.....	67
3.1.4.	US28 expression reduces STAT1 phosphorylation	70
3.2.	Validation of selected proteins from the US28-associated proteome.....	72
3.2.1.	MNDA and IFI16 are downregulated by US28-WT.....	72
3.2.2.	Downregulation of steady-state levels of HLA-DR by US28.....	75
3.3.	Mechanism of US28-mediated downregulation	77
3.4.	Downregulation of IFI16, MNDA, and HLA-DR during latency.....	80
3.4.1.	Introduction.....	80
3.4.2.	Initial observations with TB40/E IE2-2A-eGFP SV40mCherry virus.....	80
3.4.3.	Time course of downregulation with TB40/E SV40eGFP	81
3.4.4.	IFI16 is downregulated in a US28-dependent manner, but only in undifferentiated myeloid cells	84
3.4.5.	Long-term downregulation of IFI16 and MNDA.....	91
3.4.6.	Latently infected THP-1 cells show loss of IFI16 and MNDA mRNA.....	94
3.4.7.	The role of incoming pUS28 in IFI16 downregulation.....	96
3.5.	Discussion.....	99
4.	IFI16 can activate IE gene expression during latency and needs to be targeted for latency-associated IE suppression	101
4.1.	Introduction	101
4.2.	Overexpression of IFI16.....	101
4.3.	IFI16 overexpression drives IE gene expression.....	102
4.4.	IFI16 activates the MIEP independently of other viral factors.....	103
4.5.	IFI16 drives IE gene expression via NF- κ B at the MIEP	104
4.6.	Discussion.....	107
5.	MNDA is a potential restriction factor for HCMV latency.....	109
5.1.	Introduction	109
5.2.	Overexpression of MNDA.....	109
5.3.	MNDA-overexpressing cells fail to drive fluorescent reporter expression following latent infection	111

5.4.	MNDA-overexpressing cells do take up viral genome following latent infection.....	112
5.5.	Discussion.....	114
6.	US28-mediated interference with DNA sensing	115
6.1.	Introduction	115
6.2.	Undifferentiated THP-1 cells make far smaller responses to DNA stimuli compared with PMA-differentiated THP-1 cells.....	115
6.3.	US28-WT expression in myeloid cells may interfere with DNA sensing	117
6.4.	IFI16 and MNDA super-expression drive Type I interferon responses to DNA in undifferentiated THP-1 cells	121
6.5.	Discussion.....	122
7.	Selective shock and kill using anti-US28 nanobodies.....	124
7.1.	Introduction	124
7.2.	US28 nanobodies induce immediate early gene expression	124
7.2.1.	Bivalent nanobody VUN100b binds US28 and inhibits US28-mediated signalling	124
7.2.2.	VUN100b induces IE gene expression in latently infected monocytes	127
7.2.3.	VUN100b does not drive full virus reactivation	130
7.3.	US28-specific nanobody treatment of latent monocytes directs their T cell killing.....	133
7.4.	Discussion.....	136
8.	Improved US28-specific immunotoxins kill latently infected monocytes.....	138
8.1.	Introduction	138
8.2.	US28-specific immunotoxins kill US28-expressing THP-1 cells	138
8.3.	US28-specific immunotoxins kill latently infected monocytes	141
8.4.	Discussion.....	147
9.	General Discussion	150
10.	References.....	154
	Appendix A: Publications authored during this project	195

List of Abbreviations

AIDS	Acquired immunodeficiency syndrome
AIM2	Absent in melanoma 2
ANOVA	Analysis of variance
AP1	Activator protein 1
APC	Allophycocyanin
ATF	Activatory transcription factor
aTTP	Acquired thrombotic thrombocytopenic purpura
BAC	Bacterial artificial chromosomes
BSA	Bovine serum albumin
C/EBP	CCAAT-enhancer-binding protein
CC ₅₀	50% cellular cytotoxicity
cCMV	Congenital cytomegalovirus
ChIP	Chromatin immunoprecipitation
CI	Confidence intervals
CREB	cAMP response element binding protein
crs	cis-repression sequence
CTL	Cytotoxic T lymphocyte
Cy7	Cyanine 7
d.p.i.	Days post infection
DAMP	Danger associated molecular pattern
DC	Dendritic cells
DMSO	Dimethyl sulfoxide
DRY	Aspartate-arginine-tyrosine
dsDNA	Double stranded DNA
EBV	Epstein-Barr virus
EdU	5-Ethynyl-2'-deoxyuridin
ELISA	Enzyme-linked immunosorbent assay
ERF	Ets-repressor factor
EV	Empty vector
EVNP	Ex vivo normothermic perfusion
FACS	Fluorescence associated cell sorting
FBS	Fetal bovine serum
FITC	Fluorescein-isothiocyanate
FTP	Fusion-toxin protein
GAPDH	Glyceraldehyde phosphate dehydrogenase
GCV	Ganciclovir
Gfi-1	Growth factor independent 1 transcriptional repressor
GM-CSF	Granulocyte-macrophage colony-stimulating factor
GO	Gene ontology
GPCR	G protein coupled receptor
h.p.i.	Hours post infection

H3K27me3	Histone-H3-lysine-27-trimethylation
H3K9me3	Histone-H3-lysine-9-trimethylation
H3S10P	Histone H3-serine-10
HBV	Hepatitis B virus
HCMV	Human cytomegalovirus
HDAC	Histone deacetylase
HDACi	Histone deacetylase inhibitors
HHV-6A	Human herpesvirus-6A
HHV-6B	Human herpesvirus-6B
HHV-7	Human herpesvirus-7
HIV	Human immunodeficiency virus
HPCs	Hematopoietic progenitor cells
HPV	Human papilloma virus
HRP	Horseradish peroxidase
HSCT	Hematopoietic stem cell transplant
HSV-1	Herpes simplex virus type 1
HSV-2	Herpes simplex virus type 2
HTLV-1	Human T-lymphotropic virus type 1
huNSG	Humanised NOD-scid IL2R γ c null
IFI16	Gamma interferon-inducible protein 16
IFIX	interferon-inducible protein X
IFN α	Interferon alpha
IFN β	Interferon beta
IFN γ	Interferon gamma
IL-1 β	Interleukin-1 beta
IL-4	Interleukin-4
IL-6	Interleukin-6
IP	Immunoprecipitation
iPSC	Inducible pluripotent stem cell
ISG	Interferon stimulated gene
KSHV	Kaposi sarcoma associated herpesvirus
LANA	Latency-associated nuclear antigen
LPS	Lipopolysaccharide
MACS	Magnetic-activated cell sorting
MCMV	Murine cytomegalovirus
MDBP	Methylated DNA binding protein
MIEP	Major Immediate Early Promoter/Enhancer region
MNDA	Myeloid cell nuclear differentiation antigen
MOI	Multiplicity of infection
MRF	Modulator recognition factor 1
MTS	3-(4,5-dimethylthiazol-2-yl)-5-(3-carboxymethoxyphenyl)-2-(4-sulfophenyl)-2H-tetrazolium, inner salt)
Nbs	Nanobodies

NF1	Nuclear factor 1
NFAT	Nuclear Factor of Activated T cells
NF- κ B	Nuclear factor kappa B
ORF	Open reading frame
p.f.u.	Plaque forming unit
PBMC	Peripheral blood mononuclear cells
PBS	Phosphate buffered saline
PE	Phycoerythrin
PerCP/Cy5.5	Peridinin-Chlorophyll protein/Cyanine 5.5
PMA	Phorbol 12-myristate 13-acetate
PML	Promyelocytic leukemia
POP3	Pyrin domain-only protein 3
PPAR γ	peroxisome proliferator activated receptor gamma
pUS28	US28 protein
PVDF	Polyvinylidene difluoride
RSV	Respiratory syncytial virus
RT	Reverse transcriptase
SDS-PAGE	Sodium dodecyl sulfate-polyacrylamide gel electrophoresis
SFFV	Spleen focus forming virus
SOT	Solid organ transplant
SP1	Sp1 transcription factor
SRF	Serum response factor
SYNx	Synklino ApS US28-targeting immunotoxin
TBP	TATA-box binding protein
TLR	Toll-like receptor
TSS	Transcription start site
US28-WT	Wild-type US28
VHH	Variable heavy chain domain
VWF	von Willebrand factor
VZV	Varicella Zoster virus
YY1	Yin yang 1

List of Figures

Figure 1-1 Organisation of the Major Immediate Early locus.	21
Figure 1-2 Regulation of HCMV latency and reactivation during myeloid differentiation	28
Figure 1-3 Serpentine diagram of US28, highlighting functional domains, motifs, and amino acids.....	30
Figure 1-4 US28 controls several signaling pathways to suppress the MIEP in early myeloid lineage cells	35
Figure 1-5 HCMV evasion of pattern recognition receptors and interferon induction.....	37
Figure 1-6 Domain architecture of the PYHIN proteins.....	39
Figure 1-7 A comparison of the domain architectures of human IgG (A), camelid heavy-chain only immunoglobulin (B), VHH domains/nanobodies (C), and a bivalent nanobody (D).	44
Figure 3-1 US28 proteomic analysis reveals US28 signalling-dependent and independent changes in myeloid cell environment.	63
Figure 3-2 GO-term enrichment analysis of genes downregulated by US28-WT.....	67
Figure 3-3 US28 downregulates Type I and Type II interferon-inducible proteins..	69
Figure 3-4 US28-WT decreases STAT1 and phosphorylated STAT1.	71
Figure 3-5 Generation of independently-transduced US28-expressing cell lines..	73
Figure 3-6 Steady state levels of MNDA and IFI16 mRNA in US28-expressing cells.....	74
Figure 3-7 US28-WT downregulates MNDA and IFI16.....	75
Figure 3-8 US28-WT downregulates cell surface HLA-DR.....	77
Figure 3-9 Effect of Janus kinase and c-fos inhibition on IFI16 and HLA-DR expression.	79
Figure 3-10 HCMV latent infection is associated with downregulation of IFI16, MNDA, and HLA-DR..	81
Figure 3-11 Time course of US28-target gene downregulation.	84
Figure 3-12 IFI16 is rapidly downregulated in a US28-dependent manner during latent infection.....	87
Figure 3-13 US28 immunostaining in transduced THP-1 cells.....	87
Figure 3-14 Fibroblasts which overexpress US28 do not downregulate IFI16..	88
Figure 3-15 Lytic infection of fibroblasts and epithelial cells leads to downregulation of IFI16 independently of US28.....	90
Figure 3-16 Lytic infection of fibroblasts with the Titan strain of HCMV leads to downregulation of IFI16 independently of US28.....	91
Figure 3-17 IFI16 and MNDA downregulation during long term latency.....	93
Figure 3-18 Latently infected THP-1 cells have lower levels of PYHIN mRNAs but not HLA-DRA.	95
Figure 3-19 Incorporation of V5-tagged US28 into virions.	97
Figure 3-20 Incoming US28 may help to drive IFI16 downregulation.....	98
Figure 4-1 Overexpression of IFI16 in THP-1 cells.....	102
Figure 4-2 IFI16 overexpression drives IE gene expression.....	103
Figure 4-3 IFI16 drives MIEP activity.....	104
Figure 4-4 IFI16 activates IE gene expression via NF- κ B.....	106
Figure 4-5 IFI16 overexpression increases nuclear NF- κ B.	107
Figure 5-1 Overexpression of MNDA.	110
Figure 5-2 MNDA-mediated restriction of virus-associated fluorescent reporter expression.	112
Figure 5-3 Relative HCMV DNA levels in infected control and MNDA-overexpressing cells.	113
Figure 6-1 PMA pre-treatment of THP-1 cells leads to greater responses to transfected DNA.	116
Figure 6-2 US28-WT expressing THP-1 cells make attenuated cytokine responses to transfected DNA.	118

Figure 6-3 Infected monocyte interferon and IL-1beta responses.	120
Figure 6-4 IFI16 and MDA overexpression drives interferon but not IL-1beta responses to transfected DNA.	122
Figure 7-1 Characterisation of VUN100b and comparison with VUN100.	126
Figure 7-2 VUN100 and VUN100b increase IE gene expression in latently infected monocytes.	128
Figure 7-3 VUN100b consistently upregulates IE gene expression in latently infected monocytes.	129
Figure 7-4 VUN100b is only capable of activating IE gene expression in monocytes in the presence of US28.	130
Figure 7-5 VUN100 and VUN100b treatment does not lead to full lytic replication in monocytes.	132
Figure 7-6 T cell separations from PBMC.	134
Figure 7-7 VUN100b directs T cell killing of latently infected monocytes.	135
Figure 8-1 US28-specific immunotoxins kill US28-expressing THP-1 cells but not control THP-1 cells.	139
Figure 8-2 US28-specific immunotoxins kill US28-expressing cells after short incubation times.	140
Figure 8-3 US28-specific immunotoxins do not kill uninfected primary monocytes at relevant concentrations	142
Figure 8-4 SYN002 and SYN005 kill latently infected monocytes.	143
Figure 8-5 SYN002 and SYN005 have similar antiviral activities against lytic and latent infections	145
Figure 8-6 SYN002 and SYN005 kill latently infected monocytes and reduce reactivation.	147
Figure 8-7 Ex vivo normothermic perfusion configuration	149

List of Tables

Table 1-1 Human herpesviruses	15
Table 1-2 Selected functions of US28	31
Table 1-3 Immunotoxins: examples and modes of action	48
Table 2-1 List of primers used in this project.	58
Table 3-1 Proteins upregulated by US28-WT compared with US28-R129A.	64
Table 3-2 Proteins downregulated by US28-WT compared with US28-R129A.	65
Table 8-1 CC₅₀ and respective 95% confidence intervals (CI) for immunotoxins at given incubation times.	141

1. Introduction

1.1. Natural history of human cytomegalovirus

1.1.1. Herpesviruses

The *herpesvirales* are an order of large, double-stranded DNA viruses which infect vertebrate and invertebrate species (<https://talk.ictvonline.org/taxonomy/>) [1]. The *herpesviridae* family, which infect reptiles, birds, and mammals, are subdivided into three subfamilies: alpha-, beta-, and gamma-herpesviruses. There are nine herpesviruses known to infect humans (Table 1-1). The most recent of these to be discovered was the gamma herpesvirus HHV-8, Kaposi sarcoma associated herpesvirus (KSHV), in 1994 [2], while the betaherpesvirus human cytomegalovirus (HCMV, HHV-5) was isolated in the 1950s [3].

During primary infection, herpesviruses typically replicate (lytic infection) in a wide array of tissues and cell types [4]. Herpesviruses also establish a latent infection in specific cell types within the host (Table 1-1). During latent infection, the viral genome is maintained in the absence of the production of new infectious virions. However, under certain conditions, the virus can reactivate from latency to produce new infectious viral particles. In the next section I will explain how latency and reactivation underpins lifelong carriage of herpesviruses, including human cytomegalovirus.

Table 1-1 Human herpesviruses

Subfamily	Virus	Formal name	Cellular site(s) of latency
<i>Alphaherpesvirinae</i>	Herpes simplex virus type 1 (HSV-1)	HHV-1	Sensory neurons (trigeminal ganglia) [5]
	Herpes simplex virus type 2 (HSV-2)	HHV-2	Sensory neurons (trigeminal ganglia) [5]
	Varicella-Zoster virus (VZV)	HHV-3	Neurons (predominantly dorsal root ganglia) [6]
<i>Betaherpesvirinae</i>	Human cytomegalovirus (HCMV)	HHV-5	Hematopoietic progenitors and early myeloid lineage cells [7]
	Human herpesvirus-6A (HHV-6A); <i>Roseolovirus</i>	HHV-6A	Likely hematopoietic lineage [8,9]
	Human herpesvirus-6B (HHV-6B); <i>Roseolovirus</i>	HHV-6B	Likely myeloid lineage [8,9]
	Human herpesvirus-7 (HHV-7); <i>Roseolovirus</i>	HHV-7	Unknown, likely hematopoietic lineage [8]
<i>Gammaherpesvirinae</i>	Epstein-Barr virus (EBV)	HHV-4	B lymphocytes [10]
	Kaposi sarcoma associated herpesvirus (KSHV)	HHV-8	B lymphocytes [11]

1.1.2. HCMV infection in healthy individuals

HCMV is a ubiquitous pathogen which infects 45-99% of individuals worldwide [12]. HCMV seroprevalence is correlated with socioeconomic status and, in the UK, approximately 50% of adults contain anti-CMV IgG in their serum [12,13]. Primary infection of healthy children and adults with HCMV is often asymptomatic but can result in mild flu-like symptoms [14] and HCMV shedding is routinely detectable in bodily fluids including saliva, urine, breast milk, semen, and vaginal fluid [15–17]. Broad and robust immune responses are generated during primary infection with HCMV, incorporating both cellular and humoral immunity [18]. In particular, strong T cell responses against a variety of viral epitopes are made which enable control of virus replication and, after resolution of infection, extremely high frequencies of CMV-specific T cells are routinely detected in HCMV-seropositive individuals [18].

Despite this effective control of lytic replication, healthy individuals never clear HCMV, and individuals can also be re-infected with additional strains of HCMV during their lifetime [19]. In healthy virus carriers, circulating HCMV-specific effector T cells predominantly recognise viral epitopes that are expressed during lytic infection, but not during latent infection [20]. This general inability of effector T

cells in HCMV seropositive carriers to recognise latently infected cells helps the virus to remain undetected by the immune system during latency, which is routinely established in CD34⁺ hematopoietic progenitor cells and early myeloid lineage cells such as CD14⁺ monocytes [20].

Reactivation of HCMV from latency, discussed in much greater detail later, occurs sporadically throughout the lifetime of healthy individuals as myeloid progenitor cells which carry latent genomes differentiate into mature dendritic cells and macrophages [21,22]. Reactivation events in healthy carriers are also well controlled by existing immune responses and, therefore, asymptomatic but likely result in reseeded of the latent viral reservoir [20]. This model of latency and continual reactivation supports the view that HCMV can cause a lifelong subclinical infection in healthy individuals and helps explain the maintenance of high levels of HCMV-specific T cells in normal healthy carriers.

1.1.3. Congenital HCMV infection

Transfer of HCMV from mother to foetus during pregnancy is a leading cause of HCMV-associated disease. Congenital HCMV (cCMV) infection occurs in an estimated 0.8% of live births in the UK [23]. While many cCMV infections are asymptomatic at birth, approximately 15% will go on to develop long term developmental problems, including sensorineural hearing loss, vestibular dysfunction, and mental retardation [23]. Indeed, cCMV is the leading non-genetic cause of hearing loss.

Transfer of HCMV from mother to foetus can occur in three ways: (1) primary infection of a seronegative mother; (2) secondary infection of a seropositive mother; and (3) reactivation of an existing HCMV infection in a seropositive mother [23,24]. In an individual mother, the risk of transmission to the foetus and clinical disease is highest if she undergoes primary HCMV infection [24,25]. However, since the majority of world populations have high HCMV seropositivity, the majority of cCMV cases are attributed to non-primary infection [26].

1.1.4. HCMV in the transplant setting

Both allogeneic hematopoietic stem cell transplant (HSCT) and solid organ transplant (SOT) patients are at serious risk of HCMV-associated disease. Both types of transplant procedures require immunosuppression to avoid organ rejection or graft-versus-host disease. Coupled with inflammation associated with surgery, and allogeneic reactions, transplant patients often develop viremia and disseminated HCMV infection, which can, in some cases, be fatal [14,27–30]. The risk of symptomatic CMV disease depends on the type of transplant, and the serostatus of the donor (D) and recipient (R) [27]. Seropositive HSCT patients are at highest risk of disease if the donor is seronegative (D⁻R⁺) and

intermediate risk if both recipient and donor are seropositive (D⁺R⁺); seronegative recipients are at low risk from a seropositive donor (D⁺R⁻), and, clearly, the lowest risk if both recipient and donor are seronegative. In SOT patients, seropositive recipients are at low risk if the donor is seronegative (D⁻R⁺), and intermediate if the donor is seropositive (D⁺R⁺). Seronegative recipients are at high risk from a seropositive donor (D⁺R⁻).

Managing HCMV in the transplant setting varies from centre to centre; antiviral drugs (See §1.1.6) are used in prophylactic regimens in some cases and only after detecting HCMV DNA in the blood in others [28,30]. Unfortunately, these antivirals are not well-tolerated in all patients, often causing marrow suppression and renal impairment, and the development of resistance mutations is commonplace [28,30]. Ensuring successful engraftment via immunosuppression, whilst preventing HCMV disease by allowing immune function, is a delicate balancing act for transplant physicians.

1.1.5. Other HCMV pathologies

HCMV is linked with other pathologies in both healthy and immunocompromised hosts. Human immunodeficiency virus (HIV)-acquired immunodeficiency syndrome (AIDS) patients are at risk of HCMV disease, most commonly CMV retinitis [31], while intensive care patients, such as those with sepsis, frequently experience disease linked to HCMV reactivation [32]. Meanwhile, older HCMV seropositive individuals have higher all-cause mortality, atherosclerosis and arterial hypertension in the absence of symptomatic infection [33–35]. Finally, HCMV has been linked with various cancers, most notably breast cancer and glioblastoma [36–40]. This link remains controversial, since HCMV does not readily transform cells, and whole genomes are not detected in cancers, but results showing improvement in patient survival upon treatment with HCMV antivirals mean that the link merits further investigation [39,41].

1.1.6. HCMV treatment and prevention

There is no licensed HCMV vaccine, though several candidates are under development [14,24,42–44]; an incomplete understanding of the correlates of protection against HCMV in a given clinical setting (e.g. pregnancy, SOT) likely limits progress towards an effective vaccine. Efforts towards preventing cCMV by educating pregnant women about risks and hygiene measures are under investigation [45,46].

Ganciclovir (GCV), and its orally-available derivative valganciclovir, are the first-line treatments for HCMV disease, and are also used as prophylaxis in SOT patients [44]. GCV, a guanosine analogue, is phosphorylated by the viral kinase UL97 to become a monophosphorylated species, and then subsequently phosphorylated by cellular kinases to become a nucleotide analogue and competitive

inhibitor for viral DNA polymerase catalytic subunit UL54 [47]. While largely efficacious in the transplant setting, resistance to GCV does occur via mutations in UL97 and UL54 [44], and it can cause neutropenia and thrombocytopenia leading to susceptibility to bacterial and fungal infections [30,44]. GCV can also inhibit myeloid reconstitution following HSCT [44]. GCV can reduce some cCMV-associated pathologies, but it is by no means fully efficacious, and works best for infants diagnosed within the first 30 days after birth [20]. Second-line therapies include cidofovir, acyclovir, and foscarnet also all target the viral DNA polymerase subunit UL54. These are also susceptible to resistance mutations and also associated with toxicity [44]. Letermovir has recently been approved for prophylactic treatment of HSCT patients, and targets the viral terminase complex, inhibiting capsid assembly [44,48,49]; unfortunately, antiviral resistance can also develop for this compound during the course of treatment [49]. No licensed therapy targets latently infected cells, and thus current antiviral regimens will always leave latent reservoirs intact [44].

1.1.7. Species specificity of cytomegaloviruses

There are many mammalian cytomegaloviruses described, including, but not limited to, murine, rat, guinea pig, bovine, equine, canine, swine, rhesus macaque, and chimpanzee [50]. Each cytomegalovirus is specific to its host; that is, murine cytomegalovirus (MCMV) does not productively infect human cells or, indeed, human beings, and HCMV does not productively infect mouse cells or mice [51]. This important feature means that when using a model organism, the cytomegalovirus used is that which naturally infects that organism.

Many animal cytomegaloviruses are used to dissect aspects of CMV biology; particularly *in vivo* phenomena, which cannot be studied in humans for ethical reasons. These models, which include murine, rat, guinea pig, and rhesus macaque, are described extensively elsewhere [50,52–57]. Like all animal models for human diseases, there are advantages and disadvantages to each. In general, many HCMV genes have clear homologues in animal CMVs, but there has been extensive gene duplication and diversion, as well as gains and losses of function for individual genes during the course of evolution.

MCMV is perhaps the most commonly used animal model for cytomegalovirus infection, and has been incredibly useful to CMV researchers. Two differences, highly pertinent to this project, exist: the major immediate early promoter (see §1.2.3 and 1.3.4) has a different arrangement of transcription factor binding sites, and hence may be regulated differently, and the cellular site of MCMV latency remains controversial [58–61]. For these reasons, studies of MCMV latency and reactivation must be interpreted with some caution by those interested in HCMV latency and reactivation.

1.2. Lytic infection of human cytomegalovirus

1.2.1. HCMV virions and genome structure

Lytic viral infections follow a basic pattern: virus particles enter cells, viral genes are expressed, the viral genome is replicated, new viral particles are assembled, and these particles egress from cells. HCMV is an enveloped virus of approximately 200 nm in diameter [62,63]. The tegument layer, containing many soluble proteins, lies in the space between the envelope and the capsid. The capsid, which has icosahedral symmetry, contains one copy of the HCMV genome in a linear form [63].

The HCMV genome is a non-segmented double stranded DNA (dsDNA) molecule of approximately 230 kb, making it the largest genome of any human viral pathogen [63]. While it is linear within virions, it circularises within cells and is rapidly chromatinised in host nuclei [64,65]. The genome is organised into a short and a long arm, each flanked by inverted repeat sequences [63]. The portion of the genome on which a given HCMV gene resides determines the name of the gene, and so, for example, genes in the unique long arm are denoted UL(XX), or US(XX) for those resident in the unique short region where XX designates the number of the open reading frame (ORF) within that region. There are over 200 ORFs encoded by HCMV, located on both the positive and negative DNA strands, with many genes overlapping [63]. As well as viral proteins, the genome encodes for multiple microRNAs and long non-coding RNAs; the functions of many HCMV genes have yet to be fully elucidated [66–68].

1.2.2. Tropism, entry, and tegument proteins

HCMV productively infects a wide range of cell types, including fibroblasts, epithelial cells, endothelial cells, smooth muscle cells, astrocytes, dendritic cells, and macrophages [69]. HCMV can enter cells via several different mechanisms, including direct fusion with the outer membrane, endocytosis, and pinocytosis [69–74], depending on the specific cell type involved. HCMV particles interact with heparan sulfate proteoglycans, but the co-receptors for HCMV entry are subjects of ongoing study, and likely vary by cell type and entry mechanism; co-receptors identified include integrins, PDGFR α , and neuropilin2 [70,73].

One very important determinant of cell tropism is the glycoprotein composition of the virion envelope. The glycoproteins can form a trimeric complex (gH/gL/gO) or a pentameric complex (gH/gL/UL128/UL130/UL131). Virions with pentameric complexes can enter endothelial cells and fibroblasts, whereas virions containing only trimeric complexes can only enter fibroblasts [73]. This is important since serial passage of laboratory viruses in fibroblasts leads to deletion of a genomic region

called ULb', which contains the UL128/UL130/UL131 components of the pentamer, leading to a loss of tropism for endothelial cells [75,76].

At least some of the incoming proteins and RNAs associated with HCMV particles are known to be functional before their *de novo* transcription during infection [77]. Lots of these are the tegument proteins, which have roles including immune evasion, capsid trafficking to the nucleus, and activation of viral gene expression [77–79]. In particular, incoming tegument protein pp71 (encoded by UL82) induces the degradation of components of promyelocytic leukemia (PML) bodies which repress viral gene transcription in the nuclei of permissive cells [77] – this is discussed in greater depth in §1.3.4.

1.2.3. Lytic gene expression: a regulated cascade

Herpesvirus gene transcription is temporally regulated. Classically, there are three major kinetic classes of viral genes: immediate early, early, and late,[80], but additional, intermediate classes of genes have been described, such as 'leaky-late' [81,82]. Nevertheless, temporal regulation is critical to the biology of HCMV replication.

Immediate early (IE) genes are the first to be transcribed. They transactivate early gene transcription, modulate cell cycle, and counteract a variety of host defence responses [83,84]. The Major Immediate Early (MIE) gene products IE1 and IE2 (also known as IE72 and IE86) are expressed from the Major Immediate Early Promoter/Enhancer region (henceforth referred to as the MIEP). This region, shown in Figure 1-1, consists of core, enhancer, unique, and modulator sequences upstream of the transcription start site [83,85,86], as well as regulatory sequences in the first intron that can also act as a promoter for alternative IE transcripts [87–89]. Since HCMV DNA is rapidly chromatinised upon entry into the nucleus, the MIEP is subject to regulation by chromatin structure [85,86,90–92].

Once the MIEP is activated, and IE gene products are expressed, early gene expression is transactivated. As a generalisation, early gene products encode the viral DNA replication machinery, a step necessary for late gene expression. Late genes encode for structural components of the virion, such as the envelope glycoproteins and tegument proteins.

HCMV genes of all kinetic classes, as well as tegument proteins, have immune evasion functions. This spans the disruption of sensing mechanisms, the antagonism of interferon responses and innate immunity, cell death pathways, antigen presentation, cytokine and chemokine responses, and T-, B-, and NK-cell immunity [93–97]. Despite this, healthy individuals control HCMV replication and carry HCMV

asymptotically for the duration of their lifetimes; it is viral latency that underpins persistence. In this next section, I will explain where and how latent viral infections are established and maintained in hosts.

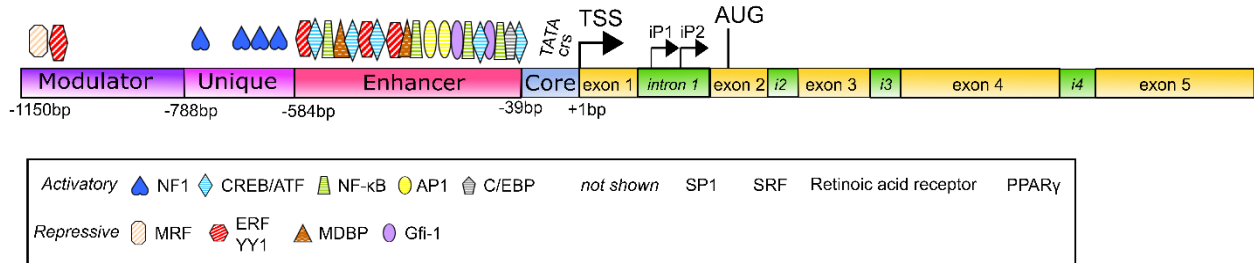


Figure 1-1 **Organisation of the Major Immediate Early locus, based on [83,86].** The MIEP consists of modulator, unique, enhancer, and core regions which are bound by the indicated activatory or repressive transcription factors. NF1, nuclear factor 1; CREB/ATF, cAMP response element binding protein/activatory transcription factor; NF-κB, nuclear factor-kappa B; AP1, activator protein 1; C/EBP, CCAAT-enhancer-binding protein; SP1, Sp1 Transcription Factor; SRF, serum response factor; PPAR γ , peroxisome proliferator activated receptor gamma; MRF, modulator recognition factor 1, HUGO name ARID5A; ERF, Ets-repressor factor; YY1, ying yang 1; MDBP, methylated DNA binding proteins; Gfi-1, growth factor independent 1 transcriptional repressor. The approximate positions of the TATA-box and cis-repression sequence (crs) is indicated; the crs is bound by IE2 protein at late times of infection to repress transcription of MIE gene products. The canonical transcription start site (TSS) is indicated at +1bp. Exons (yellow) and introns (green) are numbered. The intronic promoters iP1 and iP2 also contribute to full-length IE1 and IE2 proteins; the position of the initiator AUG codon is indicated. IE1 is comprised of coding regions from exons 2, 3, and 4; IE2 is comprised of coding regions from exons 2, 3, and 5; these, and other MIE proteins, are generated by alternative splicing from this locus.

1.3. HCMV latency and reactivation

1.3.1. Natural sites of HCMV latency and reactivation

By definition, latent carriage of HCMV requires the maintenance of the viral genome in the absence of the production of infectious virus particles; however, under certain conditions, virus is able to reactivate and produce new virus particles [98]. This ability to reactivate sets latency apart from so-called 'abortive infection', and cellular differentiation is intimately linked with both latency and reactivation [98].

One important natural site of HCMV latency is in cells of the early myeloid lineage. CD34⁺ hematopoietic progenitors (HPCs) and their derivatives, including granulocyte-macrophage progenitors and CD14⁺ monocytes, are latently infected in seropositive individuals [99–102]. Reactivation of HCMV has been observed directly *ex vivo* in differentiated myeloid cells [21,22] and *in vitro* upon differentiation of CD34⁺ progenitor cells and CD14⁺ monocytes into mature dendritic cells or macrophages [103,104]. While differentiation-independent virus reactivation has been recently reported in an immortal myeloid cell line [105], the mechanism of reactivation from latency has only been extensively described during myeloid cell differentiation (described in the next three sections).

Some groups have suggested that endothelial cells might also be sites of HCMV latency [27,106]. However, to date, no group has been able to take these cell types from a seropositive donor, show that they are latently infected, and then show that they can reactivate virus; however, this does not preclude that these cell types may contribute to long-term persistence of HCMV.

1.3.2. HCMV latency and reactivation experimental models

The most relevant experimental models of HCMV latency and reactivation are infections of primary early myeloid lineage cells from healthy donors. CD34⁺ HPCs are typically resident in the bone marrow and, because they are stem cells, these are thought to represent the long term site of latency in humans [107]. For *ex vivo* work, HPCs can be derived directly from bone marrow, after cytokine-mediated mobilisation from bone marrow into blood, as well as from umbilical cord blood. These can be cultured in a simple, serum- and cytokine- free medium, or can be expanded using cytokines/serum, and can also be co-cultured with supporting stromal cells. Reactivation is induced using further cytokines that induce differentiation [108–110]. Thus, while CD34⁺ HPCs are a highly relevant model for HCMV latency and reactivation, there are several challenges associated with their use: they are difficult to obtain in large numbers, they are a heterogeneous population within any single experiment, and additional experimental sources of heterogeneity mean that repeating observations is not always straightforward.

Similarly, granulocyte-macrophage progenitor cells are also an experimental model of latency and reactivation [101], with the source material being fetal liver from aborted fetuses. The source material is therefore limited and subject to heterogeneity. CD14⁺ monocytes can be obtained via venepuncture and thus are a much more readily available cell type compared with CD34⁺ HPCs [111,112]. Some groups work with monocytes in a serum- and cytokine-free media, and the work presented here uses this system, which aims to avoid differentiation. Others culture monocytes in serum and/or cytokines to more closely mimic circulating monocytes *in vivo* [113,114]

In addition to practical and ethical considerations, a major disadvantage of primary cell models is that they cannot readily be genetically modified. Therefore, several cell lines have been used for the study of HCMV latency and reactivation. A great deal of early work was performed in human embryonal NTera2 carcinoma cells [115,116], while Kasumi-3 cells are a CD34⁺ myeloblastic cell line [117], and THP-1 cells are a myelomonocytic leukemia cell line [118,119]. Each supports a form of latency and reactivation, but none recapitulates all aspects of latency and reactivation known to occur in primary cells [120], with a major difficulty being the dilution of viral genome as cells divide during the course of latent infection.

Recently, an inducible pluripotent stem cell (iPSC) line has been identified which supports latency and reactivation [121], and can combine the ability to track latency through all stages of myeloid differentiation with an ability to genetically modify cells. Finally, a humanised NOD-scid IL2R γ null (huNSG) mouse model of HCMV latency and reactivation might allow interrogation of viral processes that are only observable *in vivo* [122], but results from this mouse model need to be interpreted carefully since the mouse cells of non-hematopoietic origin do not get productively infected.

1.3.3. Viral gene expression during latency and reactivation

Viral latency was once believed to be equivalent to viral quiescence, involving little or no viral transcription or modulation of host cell gene expression and function. However, HCMV latency is now well established to mediate multiple changes in host processes such as antigen presentation, cytokine production, apoptosis, differentiation, and motility [112,113,123–128], and these can be related to the expression of viral gene products during latency.

Viral gene expression during experimental and natural latency is a subject of ongoing study. Prior to recent advances in transcriptomics, only a handful of viral transcripts were known to be expressed during latency, including the protein coding genes UL138, UL144, US28, UL111a, and LUNA, as well as some long non-coding RNAs and micro RNAs [20,129,130]. These analyses were based on microarrays or

targeted RT-PCR studies [124,131–133], but unbiased methods, including single-cell RNAseq, has identified that latency-associated gene expression is more broad and complex than previously conceived, though the absolute levels of transcripts are much lower during HCMV latency than during lytic infection [134–136]. However, besides the lack of production of infectious virions, a key hallmark of latency is still accepted to be the suppression of immediate early (IE) gene expression in latently infected cells, both *ex vivo* and in *in vitro* models [101–103,131,137,138].

Conversely, the initiating step in reactivation is transcription of IE1/IE72 and IE2/IE86 transcripts to begin the lytic transcription programme [7,103,104]. As described in §1.2.3, these transcripts can originate from the canonical transcription start site (Figure 1-1), and the intronic promoters iP1 and iP2. One group has recently suggested that iP1 and iP2 are the major sources of IE1 and IE2 during reactivation, and proposed a ‘promoter-switching’ paradigm [89]. They drew these conclusions after measuring levels of the three promoter-derived transcripts during the phorbol ester-induced differentiation of THP-1 cells as well as knocking out iP1 and iP2 and seeing reduced reactivation in CD34⁺ HPCs. However, unpublished work from our own laboratory, and that of collaborators (C. O’Connor, personal communication) has failed to recapitulate the strong bias towards iP1 and iP2 driven transcripts during reactivation in both primary monocytes and THP-1 or Kasumi-3 cells. However, in these unpublished studies, while the canonical transcripts predominate, iP2 was more prevalent when using reactivation stimuli that promote macrophage differentiation, rather than dendritic cell differentiation. Mutagenesis in the intronic region as carried out in the studies defining iP1 and iP2, must, I believe, be interpreted with caution, since regulatory elements in that region may act upstream as well as downstream; for example, a CTCF site (a well-established chromatin insulator) is present in the first intron of the major IE region [88].

Following recent insights into the apparent broad range of viral transcription during HCMV latency, it is now incumbent upon groups to identify latency-associated functions for transcripts detected in latently infected cells, for example by knocking out these genes in the context of a latent infection. Such approaches have identified important roles for latency-associated expression of UL111a, which is involved in immune evasion [123,139], LUNA, which disperses promyelocytic leukemia (PML) bodies and is essential for reactivation [109,140], and the microRNA miR-UL112-1, which represses IE1 translation [141]. Many viral genes, as I will outline below, play important roles in controlling viral gene expression during latency.

1.3.4. Control of viral gene expression during latency and reactivation

HCMV latency and reactivation is intimately linked with myeloid differentiation (§1.3.1) and, consistent with this, some latency-associated viral gene promoters contain elements that are differentially regulated during myeloid differentiation. For example, the promoters of LUNA and UL144 (in some viral isolates) contain GATA2 responsive elements, and GATA2 is expressed in myeloid cells allowing expression of these genes during latency [129,130,142].

Perhaps the most important determinant of latency and reactivation is control of IE gene expression. As described in §1.2.3, IE gene expression is regulated by chromatin structure at the MIEP. Analyses of chromatin structure at the major immediate early promoter reveals that latency correlates with a repressive chromatin structure around the MIEP, including the presence of the heterochromatin marker HP1 [103,104,143], as well as the histone modifications histone-H3-lysine-27-trimethylation (H3K27me3) and histone-H3-lysine-9-trimethylation (H3K9me3) [136,144] (see also Figure 1-2). Histone deacetylase (HDAC) activity is also important for maintaining a repressed chromatin state as treatment of latently infected monocytes with HDAC inhibitors leads to transient activation of IE gene expression [145].

The differentiation of CD34⁺ progenitor cells, which can carry latent HCMV *in vivo*, into mature dendritic cells results in the removal of repressive H3K27me3 and H3K9me3 marks and associated HP1 from the MIEP [103,104,136,144]. Additionally, phosphorylation of histone H3-serine-10 (H3S10P) at the MIEP has been shown to precede the removal of repressive marks during the differentiation of experimentally infected monocytes into immature dendritic cells [146]. Acetylation of histone H4 has also been demonstrated during reactivation from latency in maturing dendritic cells [103,104]. As such, an open chromatin structure around the MIEP permits the initiation of IE transcription which is necessary for reactivation.

Clearly, a repressive chromatin structure around the MIEP must be established during latency in myeloid progenitors and then modified during reactivation to permit efficient IE gene expression in differentiated dendritic cells and macrophages (Figure 1-2). We know that this process relies upon both cellular and viral factors; these can function by direct binding to the MIEP or by indirect mechanisms and have either activatory or repressive functions. A long-standing hypothesis states that it is the balance of these activatory or repressive factors that then controls whether or not the MIEP drives IE gene transcription, and that cellular differentiation must alter this balance [147–149].

Some host cell transcription factors bind directly to the overlapping 18, 19, and 21 bp repeats within the MIEP as well as other motifs in more upstream sequences (direct acting factors)[86]. This includes the repressive factors YY1 and ERF, and the activatory factors NF- κ B and CREB. In undifferentiated, non-permissive cells, the repressive factors YY1 [116] and ERF [150,151] bind to the 21 bp repeats. ERF is thought to recruit HDAC1 to the MIEP, thus providing a link between transcription factors binding to specific DNA sequence motifs and epigenetic modification. Interestingly, absolute levels of YY1 decreased during differentiation of the non-permissive NT2 cell line [116].

KAP1 was more recently identified as a chromatin organiser that can mediate repression during latency in CD34⁺ HPCs [144]. While not strictly a DNA-binding protein, KAP1 was found to constitutively associate with HCMV DNA in CD34⁺ progenitor cells, and KAP1 deposition across the viral genome correlated with the presence of the KAP1 effector SETDB1, as well as HP1 and H3K9me3 marks at the MIEP. When KAP1 was depleted, these marks were lost and the virus entered lytic replication in the absence of cellular differentiation. Furthermore, KAP1 activity was shown to be repressed during lytic infection by mTOR-mediated phosphorylation, thus providing a potential mechanism for exiting latency.

Other host factors which do not, themselves, bind to viral DNA are thought to control the presence or activation of other direct-acting factors. As discussed, mTOR-mediated phosphorylation of KAP1 abrogates the repressive activity of KAP1, implying that mTOR is important for regulating latency. Other host kinases are also important. Linking reactivation with cellular differentiation, interleukin-6 (IL-6)/lipopolysaccharide (LPS)-stimulated activation of ERK-MAPK pathways was shown to be crucial for inducing MIEP activity in maturing dendritic cells [146,152]. In this study, CREB was phosphorylated by the downstream kinase MSK, which is required for its activation at the MIEP. The absence of this MSK signalling cascade during latency in myeloid progenitors may therefore prevent CREB activity and help MIEP suppression.

The role of viral factors during latency is becoming more appreciated [129]. These include viral factors that may enter myeloid cells as components of the virion. For example, the viral long non-coding RNA 4.9, has been reported to bind the MIEP and recruit the repressor complex PRC2 to the MIEP [136]. The viral transactivator pp71, which activates the MIEP, is excluded from the nucleus of undifferentiated myeloid cells and, since pp71 has been shown to be important for antagonising the suppressive functions of PML bodies on the MIEP during lytic infection, exclusion of pp71 may help an initial PML-mediated repression of the MIEP upon infection [153]. However, other reports in different systems note that knockdown of PML components had no effect on the establishment of latency [154,155] and,

furthermore, a recent study found that the viral factor LUNA actually disperses PML bodies during latent infection in CD34⁺ cells [109].

Transcribed viral genes also contribute to latency and reactivation. For example, the latency-associated gene product UL138 manipulates cellular signalling pathways from the ER, probably in concert and in opposition with other members of the ULb' region [156]. UL138 has been reported to repress MIEP activity, in part by blocking histone lysine-demethylase activity during latency [157] and also likely via manipulation of EGFR signalling [157,158]. Meanwhile, other viral factors promote reactivation from latency, including LUNA and UL7 [109,128,140].

The virally-encoded G-protein coupled receptor US28 is expressed during lytic and latent infections, as well as coming in with the virion [159] and has recently gained prominence as an essential protein for latency. In §1.4, I will describe how US28 is able to alter cell signalling in a differentiation dependent manner, and thus promote latency in myeloid progenitor cells.

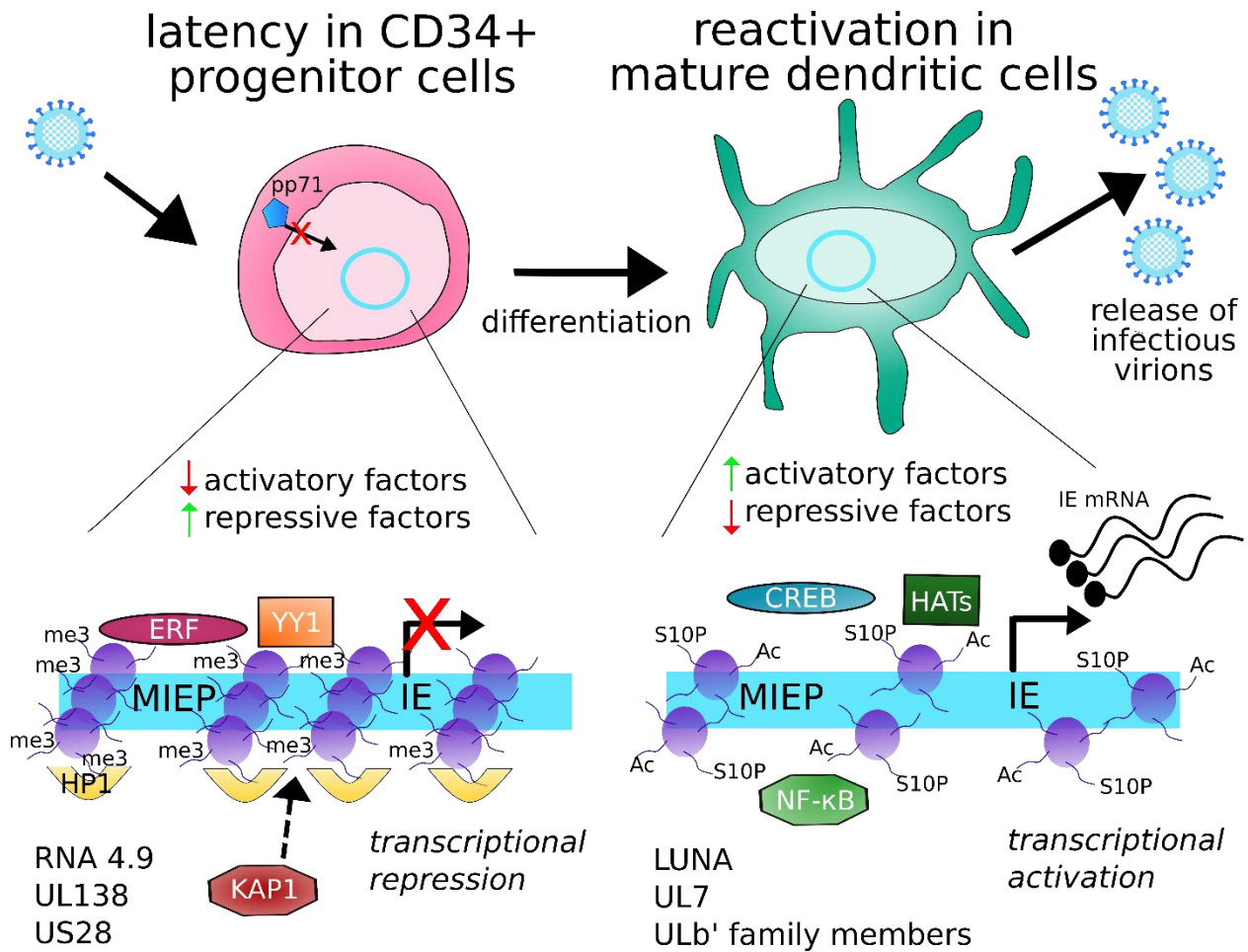


Figure 1-2 **Regulation of HCMV latency and reactivation during myeloid differentiation, taken from [160].** HCMV infects CD34⁺ progenitor cells and establishes latency (top left). The HCMV genome is maintained in the nucleus as an episome (blue circle) and is chromatinised. The MIEP (represented bottom left) is prevented from driving IE gene expression by a repressive chromatin state. Histones (purple) are trimethylated at H3K9 and H3K27. The repressive factor HP1 associates with the MIEP, as do ERF and YY1, and KAP1 acts to suppress the MIEP from distal binding sites. Latency-associated viral factors (listed) contribute to MIEP suppression, and the activatory factor pp71 is excluded from the nucleus. During differentiation-induced reactivation in mature dendritic cells or macrophages (top right), transcription of IE genes is activated leading to full lytic replication and release of infectious virions. As a result of differentiation, the chromatin structure around the MIEP is more open (bottom right), and activatory histone marks including histone acetylation (Ac) and H3-serine-10-phosphorylation (S10P) are present. Activated CREB and NF-κB become associated with the MIEP, as do histone acetyl transferases (HATs). Several viral factors are reported to be important for reactivation in myeloid cells, including LUNA, UL7, and certain members of the ULb' family.

1.4. Viral protein US28 is essential for HCMV latency

1.4.1. US28 structure, expression, and function during lytic infection

HCMV encodes four G protein coupled receptors (GPCRs), namely US27, US28, UL33, and UL78 [161,162]. One of these, US28, is a seven transmembrane domain protein coupled to host trimeric G proteins via an aspartate-arginine-tyrosine (DRY) amino acid motif [163] (Figure 1-3). US28 is a chemokine receptor homologue, binding CC and CX3C chemokines via a variety of binding mechanisms involving the N terminus; residue Y16 in particular is known to be important for binding CCL5 and CX3CL1 [164]. However, ligand binding is not required for all signalling activity of US28 and US28 can signal constitutively [163,165–168]. The C terminal region also has multiple serine residues that can be phosphorylated and is an important regulatory region that binds beta-arrestins [166,169].

Expressed in both lytic and latent HCMV infections [67,159,163,170–173], US28 protein (pUS28) is incorporated into infectious virions [159] and, during lytic infection, pUS28 is localised to endocytic vesicles and is constitutively recycled to/from the cell surface [174]. Pharmacological studies indicate that at least some proportion of US28 is localised to the cell surface during latent infection [172].

During lytic infection, the functions of US28 depend on the specific cell type infected [163,166] (Table 1-2). Part of this 'functional selectivity' of US28 owes to the ability of US28 to interact with host G proteins which vary in a context and cell type-dependent manner [163,166], and which also interact with a swathe of different CC and CX3C chemokines [165], but, as described above, not all US28-functions are dependent on ligands. US28 can, in a cell-type dependent manner, induce calcium influx, cell adhesion, angiogenic signalling, and cell migration and, during lytic infection, activate pathways including MAPK, NF- κ B, and STAT3 (references in Table 1-2). US28 is also likely to function as a chemokine sink during lytic infection, to aid in immune evasion [175]. Furthermore, US28 is a positive regulator of transcription from the MIEP in cells permissive for lytic infection, a process dependent on p38 MAP kinase activation and NF- κ B activation [176]. Despite these functions, US28 is not essential for lytic infection *in vitro* [159,177], but does enhance cell-to-cell spread in epithelial cells [178]. Possible *in vivo* functions of US28 are not informed by e.g. MCMV, in part because MCMV encodes only one GPCR, M33, which could therefore be homologous to any of the four HCMV GPCRs. However, US28 may be important for dendritic cell trafficking *in vivo* [179], and contribute to glioblastoma growth [36,40,180–182].

Table 1-2 **Selected functions of US28, adapted from** [163]. US28 activates the pathways, unless otherwise stated.

Signalling pathway/ cellular function	Cell type	Ligand/domain dependency	References
Intracellular calcium release	Fibroblasts Arterial smooth muscle cells	CCL5, CXCL3	[169,184]
	Endothelial cells	CCL7, CCL5	[185]
Adhesion to endothelial cells	THP-1 cells	DRY motif	[126,186]
Cellular migration	Smooth muscle cells Macrophages	CC chemokines (positive regulator) CX3CL1 (negative regulator)	[187,188]
	MAPK	Embryonic kidney Differentiated myeloid cells	DRY motif (positive regulator)
	Endothelial cells Neural progenitor cells	CCL5 (positive regulator)	[190]
	Undifferentiated myeloid cells	DRY motif (negative regulator)	[189]
NF-κB	Fibroblasts Glioblastoma cell line Epithelial cells	Ligand independent (positive regulator)	[176,181,191]
	Undifferentiated myeloid cells	DRY motif (negative regulator)	[189]
STAT3	Endothelial cells	CCL5	[190]
	Glioblastoma cell line	Ligand independent	[191]
	Undifferentiated myeloid cells	unknown	[173]
VEGF secretion	Glioblastoma cell line Fibroblasts	Ligand independent	[40,181,192]

1.4.2. US28 is essential for HCMV latency

Three research groups, including my own laboratory, have independently found that US28 gene deletion viruses (Δ US28) fail to establish latency in early myeloid lineage cells [159,173,189]. Cord blood-derived and bone marrow-derived CD34⁺ progenitor cells [159,173,193], Kasumi-3 cells [159,193], CD14⁺ monocytes [189], and THP-1 cells [189,193] all show this phenotype and, in each setting, the lack of US28 leads to the failure to repress the MIEP, thus driving IE expression and the full lytic replication cycle with the eventual release of infectious viral particles. Removing US28 from the virus uncouples

permissiveness for lytic infection from cellular differentiation, since monocytes infected with Δ US28 HCMV abnormally undergo lytic infection, though they do not show differentiation-specific cell surface markers [189]. US28 is expressed and translated *de novo* as well as entering the cell with the virion [159] and both incoming US28 and *de novo* expressed US28 are important for the establishment and ongoing maintenance of latency in myeloid progenitor cells [193].

Use of characterised mutants of US28 has elucidated some US28-mediated functions that are important for latency. As described in §1.4.1, the Y16F mutant removes some ligand binding activity [164] and the R129A mutant abrogates coupling of G-proteins to the DRY box motif of US28 [181,184,194]. Expression of wild-type US28 (US28-WT) *in trans* rescues latency-establishment in THP-1 cells with the Δ US28 virus [189]. Similarly, expression of US28-Y16F *in trans* could also complement the US28 deletion virus suggesting that certain modes of ligand binding may not be necessary for the latency-associated function of US28 [189]. However, deletion of the entire ligand binding domain of US28 in the virus causes lytic infection in myeloid cells [193], which is perhaps explained by work demonstrating the multiple modes by which US28 can bind a wide array of ligands [165]. It is clear, however, that infection with virus carrying US28-R129A or infection of THP-1 cells expressing US28-R129A with Δ US28 virus fails to lead to latency establishment, providing clear evidence that US28-signalling via G proteins is essential for latency [189,193]. The way that US28 signalling manipulates the host environment to support latency is therefore of great interest and under intense study, and will be described in the next section.

However, one group has produced findings that seemingly contradict these studies [195]. They constructed a virus with two stop codons close to the 5' end of the US28 ORF, as well viruses with the US28-R129A and US28-Y16F mutations, and a destabilising domain attached to US28 (ddFKBP) which causes protein degradation unless in the presence of a molecule called Shield-1. However, neither the growth characteristics of these viruses nor US28 protein expression were validated by the authors. They infected fetal liver-derived CD34⁺ progenitor cells to examine the maintenance of HCMV latency and subsequent reactivation by transfer to fibroblasts or genome copy number. The authors concluded that the US28-stop virus can establish latency but fail to reactivate in long-term culture (over 14 d.p.i.), but did not show earlier time points; previous analyses have demonstrated that infection of myeloid cells with Δ US28 viruses leads to lytic gene expression and infectious virus production within 7 days [159,189], providing one potential explanation for the discrepancy. Quite strangely, in that same study, the US28-stop virus reactivated following stimulus, however, the lack of error bars throughout the study does not allow one to be certain about the precision of their analysis. Furthermore, the authors found that the

US28-Y16F virus failed to establish latency, with high levels of immediate virus production. It is unclear how this observation could fit with any model of US28 function during latency and reactivation, and the lack of controls for protein production, virus growth kinetics, or time course of how latent infection progresses does not lead one to feel confident in their results. As an explanation for the discrepancy between their study and previously published studies [159,173,189], the authors suggest that (i) there are differences between the cells used and (ii) that while their study uses stop mutants, the previous work used whole ORF deletions, and “US28 is encoded on a polycistronic transcript that also includes US27 and US29 which could affect the expression of US27 and US29”. While US28 is certainly encoded on a polycistronic transcript encoding US27, as well as a monocistronic transcript [66,67], I could find no evidence that US29 is encoded by such a transcript, and the authors do not provide a citation. Furthermore, unpublished data from the O’Connor laboratory suggests that US28 ORF deletions do not affect US27/US29 expression and that, in their system, a US28-stop virus also fails to establish latency (C. O’Connor, personal communication, manuscript in preparation). On the basis of the strength of the evidence provided by the four different laboratories, it seems most likely that US28 is essential for the both establishment and maintenance of latency.

1.4.3. US28 manipulation of cell signalling during latency

One argument in favour of an essential role of US28 in latency establishment and maintenance is the body of mechanistic data linking US28 signalling in myeloid cells with the suppression of lytic gene expression.

Analyses of the activation states of cellular kinases during latent infection, or in myeloid cells overexpressing US28 in isolation have revealed several signalling pathways that are important for latency (summarised in Figure 1-4). Infection of CD34⁺ progenitor cells with WT virus, but not Δ US28 HCMV, drives activation of the STAT3-iNOS pathway, and the resultant nitric oxide production was shown to suppress the MIEP [173]. Furthermore, these authors showed that presence of US28 in the context of latent infection may reprogramme infected cells to become immunosuppressive monocytes akin to myeloid-derived suppressor cells, rather than conventional monocytes or, indeed, parts of other myeloid or lymphoid lineages.

Additionally, US28 has been found to attenuate several cellular signalling pathways, such as ERK, MSK, NF-KB, and STAT5 [189] when expressed in isolation in undifferentiated myeloid cells. It is interesting to note that ERK signalling is crucial for CREB phosphorylation at the MIEP and subsequent deposition of the activatory mark H3S10P on the MIEP upon differentiation-induced reactivation [146]. Consistent

with this, and the ability of US28 to attenuate ERK signalling, infection of monocytes with Δ US28 HCMV (which no longer suppresses the MIEP) is also associated with activated CREB and phosphorylated H3S10 on the MIEP. Furthermore, pharmacological inhibition of ERK in combination with NF- κ B could prevent lytic replication of Δ US28 HCMV in monocytes and, conversely, treatment of monocytes with small molecule inhibitors of US28 also results in a lytic infection rather than latency [189].

Attenuation of these cellular signalling pathways by US28 is reversed when US28-expressing cells are differentiated into macrophage-like cells using phorbol esters such as phorbol 12-myristate 13-acetate (PMA) [189]. The implication, then, is that US28 helps to maintain latency via the attenuation of MIEP-activatory cascades but does not block signalling from these pathways during reactivation, and may even support their function during cellular differentiation. Indeed, in reporter systems, US28 represses the MIEP in undifferentiated THP-1 monocytes, but activates the MIEP in PMA-differentiated THP-1 derived macrophages [189].

Recent work has also shown that US28 decreases c-fos levels during latency. Binding to the AP-1 site within the MIEP by fos/jun dimers activates the MIEP and so, in decreasing c-fos, US28 enacts MIEP suppression via an additional mechanism. As such, treatment of myeloid cells with a c-fos inhibitor reduced lytic gene expression when infecting with Δ US28 HCMV [193].

The functions of US28 during latency extend beyond MIEP suppression. US28 has been linked to hematopoietic reprogramming during latency, to ensure latently infected CD34⁺ HPCs differentiate into myeloid lineage cells [173,195]. Given the wide array of signalling pathways modulated by US28, there are likely further functions of US28 that are important for the establishment and maintenance of HCMV latency. In Chapter 3, I will present the results of a proteomic screen that aims to address the additional functions of US28 in myeloid cells.

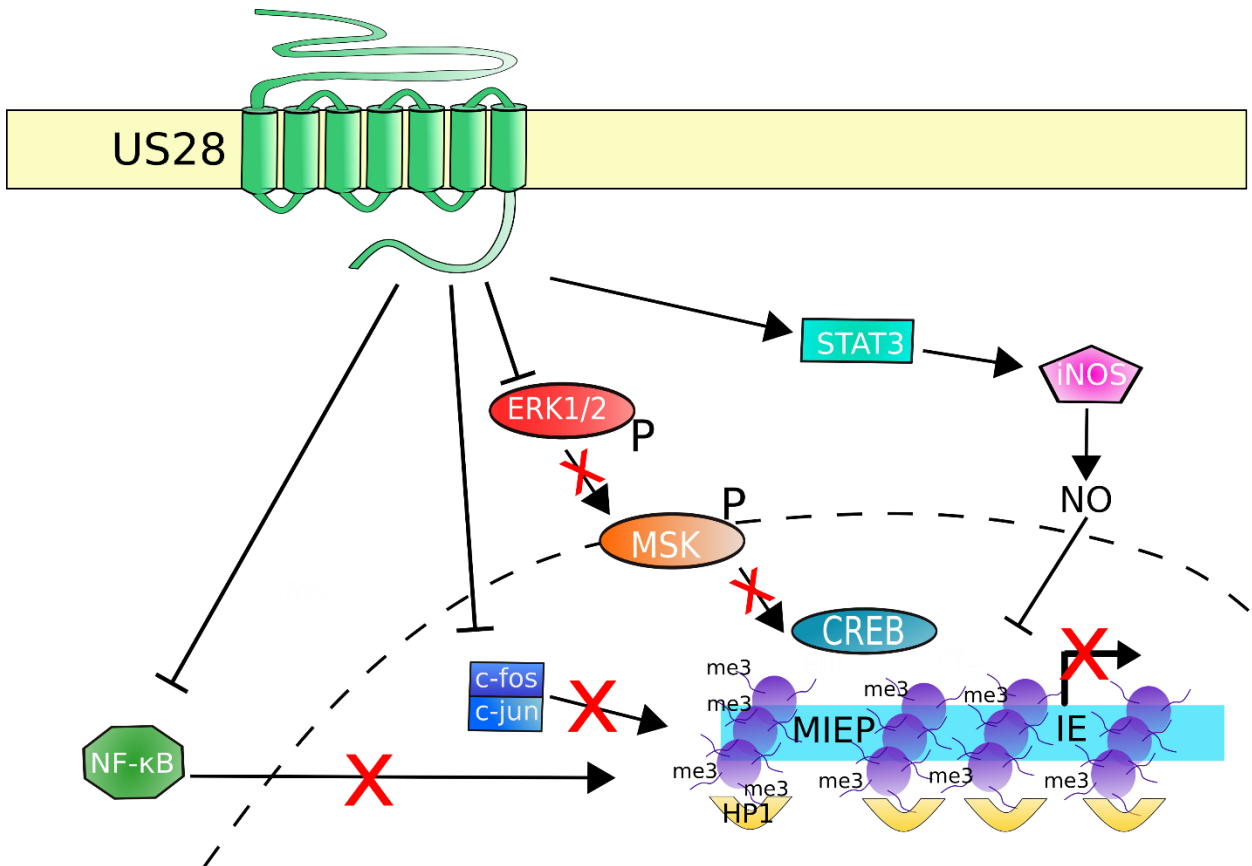


Figure 1-4 **US28 controls several signalling pathways to suppress the MIEP in early myeloid lineage cells, taken from [160].** US28 is present at the cell surface, and probably other membranes, of latently infected cells. Here, it attenuates several signalling pathways and transcription factors, including NF- κ B, c-fos, and ERK1/2. NF- κ B can no longer enter the nucleus (dashed line), nor bind and activate the MIEP. c-fos typically forms a dimer with c-jun to form the AP1 complex; US28 causes loss of c-fos, the AP1 complex does not form and thus cannot activate the MIEP. Attenuation of ERK1/2 causes loss of ERK1/2 phosphorylation (P) and subsequent activation of MSK and, therefore, MSK does not phosphorylate and activate CREB. Inactive CREB cannot activate the MIEP. US28 is also reported to activate the STAT3-iNOS signalling axis, leading to nitric oxide (NO) production. NO suppresses the MIEP in myeloid cells by unknown mechanisms. By these, and probably other pathways, US28 helps establish and maintain a repressive chromatin structure at the MIEP, and a lack of IE gene expression.

1.5. Pattern recognition and nucleic acid sensing during HCMV infection

1.5.1. Lytic infection

HCMV is a large double stranded DNA virus that replicates its genome in the nucleus. However, viral nucleic acids are substrates for pattern recognition receptors (PRR) in the cytosol as well as in the nucleus [196]. PRR induction leads to activation of both IRF3 and NF- κ B transcription factors, leading to Type I interferon induction and production of pro-inflammatory cytokines. Early activation of PRRs, via HCMV envelope glycoproteins and HCMV DNA, is likely pro-viral and depends on Toll-like receptors (TLR) 2 and TLR9, cGAS, STING, and IFI16 [196–198]. Cytosolic HCMV DNA likely results from early uncoating of viral capsids [199], while intact viral capsids deliver HCMV DNA to the nucleus. In certain contexts, cGAS and IFI16 can be either nuclear or cytosolic proteins [199–205], explaining how both are reported to contribute to innate sensing of HCMV DNA [78,94,209,196–199,203,206–208].

During lytic infection, HCMV interferes with pattern recognition receptor signalling, and the downstream effects of interferon, suggesting that some portions of this innate immune signalling must be evaded, modulated, or co-opted to ensure efficient viral replication. There are numerous viral factors known to play a role in this evasion [78,79,94,198,203,208,210,211]; a summary of these is presented in Figure 1-5.

As well as innate sensing, HCMV must overcome intrinsic immunity that suppresses HCMV gene transcription. This centres around the heterochromatinization of incoming HCMV DNA and association with PML nuclear bodies, and is evaded by tegument proteins and immediate early genes during lytic infection [65,86,90,153,155,212–215]. Interestingly, PML nuclear bodies have more recently been proposed as signalling platforms that contribute to induction of innate immunity, making evasion of these structures beneficial to the virus on multiple levels [216,217]. After the onset of viral transcription, viral dsRNA is a substrate for innate sensing and effectors such as RIG-I and PKR; this is also evaded by HCMV gene products [196,218–221]. Overall, HCMV lytic infection is associated with the generation of large quantities of pathogen-associated molecular patterns (PAMPs) that are, or can be, sensed by components of host intrinsic and innate immunity. These are actively evaded or manipulated by HCMV to enable efficient viral replication.

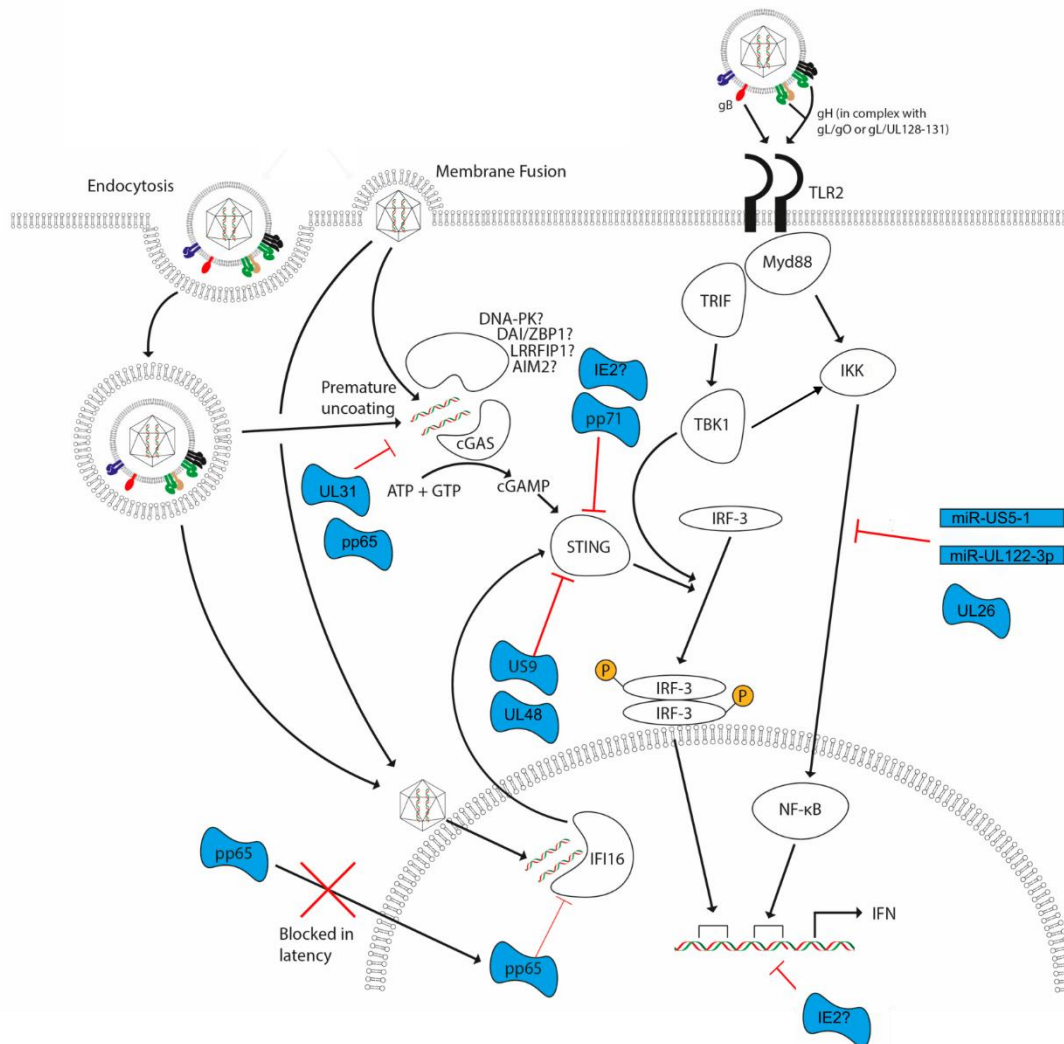


Figure 1-5 HCMV evasion of pattern recognition receptors and interferon induction, adapted from [198]. HCMV glycoproteins can be detected by TLR2, leading to activation of IRF3 and NF-κB pathways and Type I interferon induction. Premature uncoating of viral capsids leads to HCMV DNA availability in the cytosol; this may be sensed by cGAS leading to STING activation, which also activates IRF3 and NF-κB pathways, leading to Type I interferon induction. HCMV DNA in the nucleus is a substrate for IFI16-mediated sensing, leading to interferon induction via cGAS and/or STING. Viral antagonists of these processes are shown in blue. Other DNA sensors, such as DNA-PK/DAI/LRRFIP1/AIM2 have been proposed, but no viral antagonist identified.

1.5.2. Latent infection

In contrast to lytic infection, latency is associated with far less viral gene transcription, and little-to-no genome replication. It is therefore questionable whether viral PAMPs are detectable during HCMV latent infection [198]. No study, to date, has analysed whether viral DNA/RNA is sensed during entry of virus into cellular sites of HCMV latency, or whether it is sensed during the ongoing maintenance of latency.

PML bodies are dispersed during HCMV latency by the latency-associate gene product LUNA [109], which one could argue is one example of suppression of intrinsic immunity during latency. However, many of the evasins described in Figure 1-5 are not expressed during latency, and, importantly, the tegument protein pp65, which disrupts IFI16 functions [203,208,215,222], does not reach the nucleus of CD34⁺ HPCs [223]. Furthermore, while many studies have analysed DNA sensing in differentiated THP-1 cells, which are permissive for HCMV lytic infection [197,199,206,209,224], none have looked at undifferentiated THP-1 cells (a model for HCMV latency). Therefore, what intrinsic anti-viral functions are active in undifferentiated myeloid cells, and what, if any, viral nucleic acid sensing occurs during HCMV latency and how this is abated by the latent virus is yet to be investigated.

1.6. The PYHIN proteins are DNA sensors and transcriptional regulators

1.6.1. The PYHIN family of proteins: a brief overview

Located in the 1q23 locus of the human genome, the PYHIN family of proteins have relatively recently come to light as innate immune sensors or mediators of host defences. PYHIN proteins, unique to eutherian and marsupial mammals [225], contain a Pyrin domain (a member of the death domain superfamily) which can oligomerise, and at least one of three HIN-200 domain subtypes, which can bind DNA. The five members of the human PYHIN family are annotated in Figure 1-6. These are myeloid cell nuclear differentiation antigen (MNDA), interferon-inducible protein X (IFIX; formally denoted as PYHIN1), pyrin domain-only protein 3 (POP3), gamma interferon-inducible protein 16 (IFI16), and absent in melanoma 2 (AIM2). There is large diversity of the PYHIN family between species both in sequence and number of families, which makes the use of animal models to study the function of these proteins challenging [225]. For example, mice have at least 13 PYHIN proteins, and only gene *Aim2* has true orthology with its human counterpart, AIM2 [225]. POP3 lacks a HIN-200 domain and likely regulates inflammasome structures of the other PYHIN proteins [226]; this function, and other PYHIN protein functions will be described in more detail in the next sections.

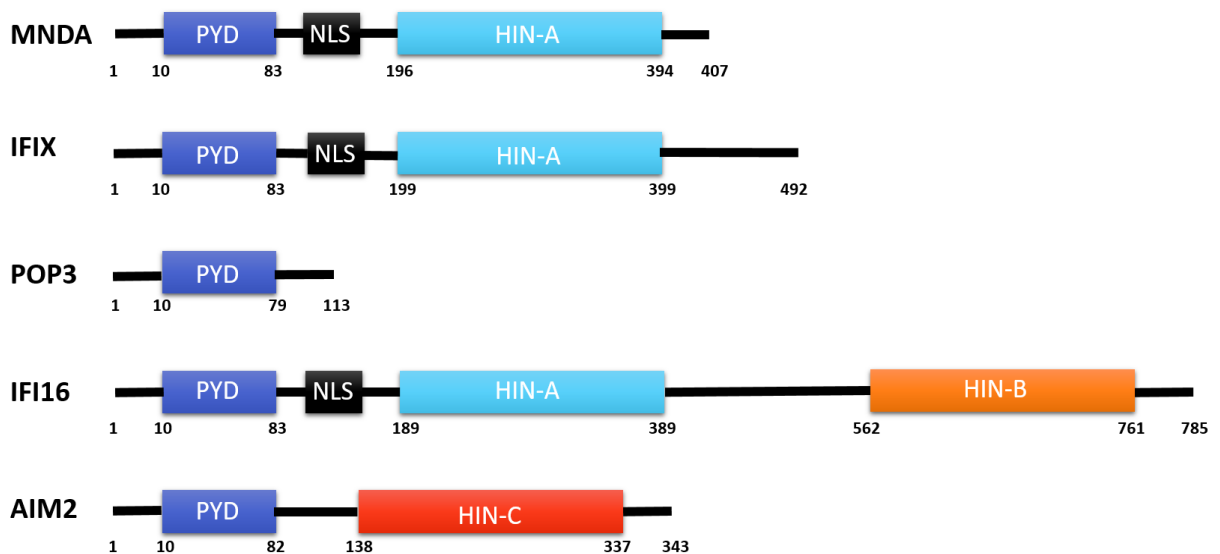


Figure 1-6 **Domain architecture of the PYHIN proteins.** Pyrin domains (PYD) are annotated based on a review by Connolly and Bowie [227], and nuclear localisation sequences (NLS) and HIN domains are labelled based on UniProt annotations. The PYHIN proteins are shown in order corresponding to the arrangement of the genes along chromosome 1. Where multiple isoforms exist (IFI16 has 4, IFIX has 6), the longest is shown.

1.6.2. AIM2

AIM2 was first reported as an interferon-inducible gene with a role in cancer biology [228,229]. Later, it was found to respond to cytosolic DNA in mice and human cells [230–233]. AIM2 can respond to microbial DNA as well as cytosolic host DNA, and these responses are comprehensively reviewed elsewhere [234]

AIM2 was found to play such a role in 2009 [7–10] in the cytosol of mice and human cells. AIM2, and its responses to bacterial, viral, and other pathogenic DNA is comprehensively reviewed elsewhere [234,235]. The key function of AIM2 is the activation of inflammasome responses in response to cytosolic DNA. AIM2 is believed to exist in an auto-inhibitory state whereby the HIN domain blocks sites in the Pyrin domain required for signalling. Upon binding DNA in the cytosol in a sequence independent manner via the HIN domain, the Pyrin domain can now mediate an interaction with ASC (apoptosis-associated speck-like protein containing a CARD). ASC now binds caspase-1, which cleaves the pro-inflammatory cytokines IL-1 β and IL-18, and Gasdermin D, which initiates pyroptosis. AIM2 (Aim2 in mice) has been shown to be activated by murine cytomegalovirus (MCMV), and Aim2 deficient mice had higher viral titres at 36 hours post infection [236]. Furthermore, AIM2 is activated by HCMV infection, which may be antagonised by pp65; the subsequent production of IL-1 β is antagonised by IE2 protein [237–239]. AIM2 also has antiviral effects against human papillomavirus (HPV) [240] and hepatitis B virus (HBV) [241], and HSV-1 encodes an antagonist of AIM2 [242].

1.6.3. IFIX

IFIX, or PYHIN1, has recently been identified by one group as a nuclear antiviral factor and sensor for HSV-1 [243]. In their study, Diner et al. defined an interactome for all four of the HIN domain-containing PYHIN proteins in HEK293 cells. They noted that IFIX was able to interact with PML body components. As described in §1.5.1, PML bodies are critical components of intrinsic immunity, inducing chromatinization and repression of viral gene expression. Knockdown of IFIX increased HSV-1 titres in infected fibroblasts, suggesting that IFIX is a restriction factor for HSV-1. IFIX could bind DNA in a sequence independent manner, responded to transfected DNA by inducing the expression of interferon-beta (IFN β), and chromatin immunoprecipitation (ChIP) analyses found HSV-1 DNA is associated with IFIX. A follow-up study found that IFIX is antagonised by an early HSV-1 gene product, a hallmark of an antiviral factor, and that IFIX could repress HSV-1 gene transcription [244]. However, no additional antiviral roles have been reported.

1.6.4. IFI16

IFI16 was first identified as a transcript constitutively expressed in T- and B- lymphocytes but interferon- γ -inducible in myeloid U937 and HL60 cells [245]. Quite a number of roles have been described for IFI16, for example in cellular senescence [246,247], the DNA damage response [224,248,249], pro-inflammatory pathways [250–253], and in innate defence against viruses (reviewed in [227,254,255]). IFI16 has both transcriptional and signalling functions that contribute to the restrictive role of IFI16 for numerous viral pathogens; I will describe the most pertinent of these below.

IFI16 was first identified as a sensor of transfected DNA in the cytosol where, via an interaction with STING, it induces IFN β [256]. Since then, IFI16 has been shown to respond to transfected DNA insults to induce Type I interferon responses or silence transcription from transfected plasmids [206,257,258]. IFI16 has also been identified as a restriction factor for the DNA viruses HSV-1 [201,204,215,259–262], HSV-2 [263], HCMV [208,215,264], KSHV [204,265–268], EBV [265], and HPV [269]. IFI16 can also respond to or restrict transcription of DNA intermediates during HIV [270–272], Human T-lymphotropic virus type 1 (HTLV-1) [273], HBV infections [274] and, perhaps counter intuitively, IFI16 is also a reported restriction factor for the RNA viruses Zika virus, Chikungunya virus, and Sendai virus [258,275].

As alluded to earlier, IFI16 is reported to contribute to innate sensing of herpesviral DNA in both the cytosol [199,206,270] and the nucleus [215,261,265,269,276]. This likely involves cooperative aggregation of IFI16, via Pyrin domains [215,277], to generate either an AIM2-like inflammasome [265,267,276] or a structure capable of activating cGAS or STING [201,209,261] and subsequent induction of IL-1 β or Type I interferon, respectively. How IFI16 can discriminate between self- and non-self DNA in the nucleus has been of great interest; in one model, IFI16 binds DNA via its HIN domains in a sequence-independent but length-dependent manner, and the minimum length is longer than the distance between nucleosomes and transcription bubbles [256,277–279]. The clustering of IFI16 occurs as IFI16 tracks along DNA duplexes in a 1D manner and contacts other scanning IFI16 molecules [279]; nuclear IFI16 puncta are observable during the first 15 minutes of HSV-1 infection [259,280]. However, other structures are proposed to be substrates for IFI16 recognition [281,282] and, at low multiplicity of infection (MOI), IFI16 can only lead to innate signalling once HSV-1 viral transcription and replication is initiated, suggesting that more complex DNA structures are sensed by IFI16 [262].

IFI16 also restricts viral infections by modulating viral transcription. In the vast majority of cases, IFI16 represses lytic gene transcription, and this can be via interaction with PML body components [259,283,284], the sequestration of Sp1 transcription factor [264,271], and promoting repressive histone

marks [268,274,283]. In fact, transcriptional repression by IFI16 makes the presence of IFI16 essential for the maintenance of EBV latency [285], and IFI16 must be degraded for efficient KSHV reactivation from latency [267]. It is worth noting that there is only weak evidence that IFI16 directly binds to DNA to exert transcription repression.

The transcriptional role of IFI16 during HCMV infection is slightly more complex. During HCMV infection of fibroblasts, IFI16 is co-opted by the viral tegument protein UL83 (pp65) [79,208]. This binding serves multiple roles: firstly, the IFI16/UL83 complex may bind and does activate the MIEP during the first 6 hours of infection [79,264]. The binding of UL83 blocks oligomerisation of IFI16 Pyrin domains, thus preventing innate immune signalling and cytokine induction [215] but, likely, also prevents the repression of HCMV early gene expression (UL54, UL44) [208,264,286]. Thus, at low multiplicities of infection, IFI16 is both required for efficient HCMV lytic infection (for IE gene expression) but is then restrictive to HCMV replication. Since the MIEP must be transcriptionally repressed for efficient latency establishment, it might be predicted that the regulation of IFI16 expression by HCMV is important for latency.

1.6.5. MNDA

MNDA was the first human PYHIN protein to be identified; it is interferon- α -inducible, and its expression is specific to cells of the myeloid lineage [287–290]. No antiviral functions associated with MNDA are published, though in at least two settings viral gene products have been found able to interact with MNDA. Firstly, the KSHV Latency-associated nuclear antigen (LANA) was identified as an MNDA interactor by a yeast-2-hybrid screen and by immunoprecipitation when both genes are transfected into 293T cells [291]. Secondly, again in an overexpression analysis in 293T cells, UL83 can bind and disrupt aggregation of the Pyrin domain of MNDA [215]. Of note, unpublished data presented at a conference from the Bowie lab has suggested that MNDA can contribute to Type I interferon induction (Andrew Bowie, personal communication), which is consistent with the ability of MNDA to bind DNA [292].

MNDA is relatively uncharacterised compared to AIM2 or IFI16. MNDA bears hallmarks of an important transcriptional regulator for myeloid differentiation [293–297]; for example, ectopic expression of MNDA in conjunction with three other transcription factors induced reprogramming of fibroblasts that drove changes in morphology, and increases in phagocytosis, chemotaxis, and cytokine production consistent with monocyte-like behaviour [294]. In support of transcriptional activity, MNDA can stimulate the binding of the transcription factor YY1 to its target DNA sequences [298], which is intriguing since YY1 is a known repressor of the MIEP [116].

Reduced levels of MNDA transcripts have been associated with myelodysplastic syndrome [299–301], a syndrome thought to involve aberrant myeloid cell apoptosis [302]. As such, two reports have sought to define the behaviour of MNDA during apoptosis. In the myeloid cell line HL-60, MNDA is exported to the cytoplasm upon stimulation with hydrogen peroxide, a crude stimulus designed to induce apoptosis, [303] thus showing that MNDA has dynamic behaviour in response to cell stresses. In the same study, the authors found that exogenous MNDA expression in K652 cells increased protection for TRAIL-induced apoptosis [303]. The second study monitored the behaviour of MNDA in *ex vivo* neutrophils from healthy patients and septic patients, a condition that involves the failure of neutrophils to undergo apoptosis [304]. *Ex vivo* neutrophils from healthy patients underwent apoptosis within 24 hours, and this was characterised by cytoplasmic redistribution of MNDA and cleavage of MNDA to distinct ~27 and ~35 kDa products. Levels of MNDA cleavage correlated with Annexin-V positivity, a well-established early marker of apoptosis. In neutrophils from septic patients, these events did not occur. Knockdown of MNDA in HL-60 cells protected these cell lines from UV light-induced apoptosis, as characterised by Annexin-V positivity, mitochondrial membrane potential, and caspase-3 activity. Interestingly, MNDA interacted with Mcl-1 (a critical myeloid pro-survival protein) in the cytoplasm and promoted the degradation of Mcl-1 in response to apoptotic stimuli. This interaction is extremely pertinent to HCMV latency, since Mcl-1 is known to be upregulated as a result of the binding/internalisation of virus into monocytes and to promote the survival of latently infected CD34⁺ cells and monocytes [112,114,305]. The upregulation/stabilisation of Mcl-1 has thus far been shown to be dependent on ERK and PI3K signalling, and critical to allow long-term survival of what are typically short-lived circulating monocytes. It is, therefore, an interesting question as to how MNDA might be regulated by, and regulate responses to, HCMV latent infection.

1.7. Nanobodies as immunotherapeutic agents

1.7.1. Camelid antibody domains as therapeutic agents

Typical IgG molecules from mammals, including humans and mice, are dimers of dimers containing a heavy and a light chain. In turn, the heavy chain contains 3 constant domains and one variable domain, while the light chain contains one constant domain and one variable domain (Figure 1-7). Together, the variable domains of the heavy and light chains compose the complementarity determining region, i.e. the antigen binding portion of the antibody [306].

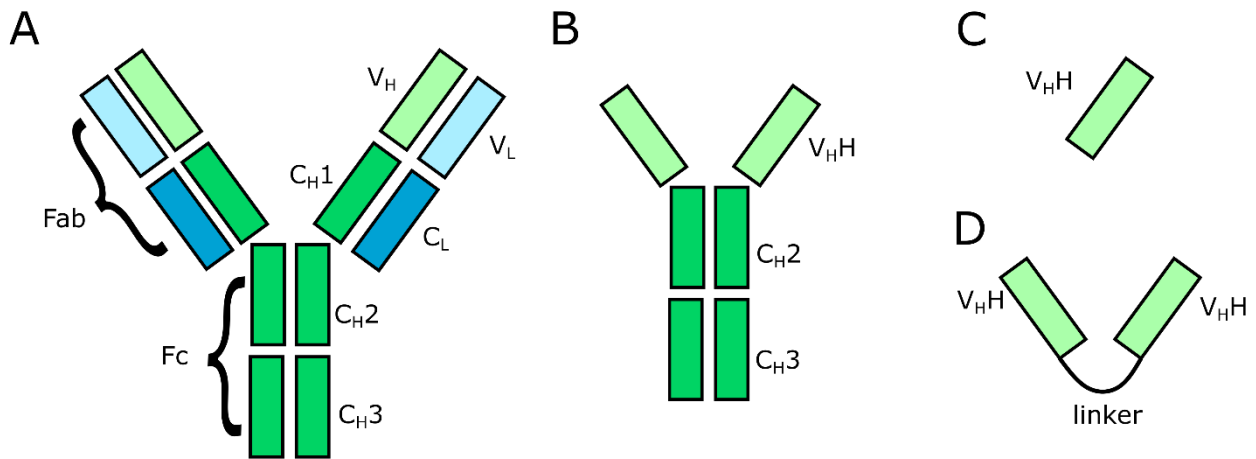


Figure 1-7 **A comparison of the domain architectures of human IgG (A), camelid heavy-chain only immunoglobulin (B), VHH domains/nanobodies (C), and a bivalent nanobody (D).** (A) Human IgG contains heavy (green) and light (blue) chains that contain constant domains (C_H and C_L) and variable domains (V_H and V_L). Together, C_{H2} and C_{H3} form the Fc portion of the molecule, and 2x (C_{H1}, C_L, V_H, and V_L) form the Fab fragment. (B) Camelid heavy-chain only immunoglobulin molecules are dimers of constant (C_{H2} and C_{H3}) and variable (V_HH) polypeptides. (C) VHH domain antibodies are known as nanobodies, can contain only a V_HH domain. (D) Nanobodies may be multimerised by chemical or genetic mechanisms. This bivalent nanobody represents the bivalent US28 nanobody VUN100b, discussed later; the C terminus of one nanobody is connected to the N terminus of the next by an encoded polypeptide linker.

In contrast, camelid species (camels, llamas, alpacas) naturally produce heavy chain-only antibodies as part of their array of immunoglobulin molecules [307]. The variable domain of these heavy chains (V_HH) therefore confers the antigen specificity of the molecule (Figure 1-7). Camelids can be immunised in manners similar to the immunisation of mice and rabbits in order to generate antibodies to an antigen of interest, and the resulting V_HH domain coding sequences can be cloned from immunised animals and used to generate libraries from which high-affinity V_HH genes can be isolated [307,308]. These single-domain antibodies, henceforth termed nanobodies (Nbs), are much smaller than monoclonal antibodies

(15 kDa when unmodified), have higher solubility in water, are expressed from only one coding sequence, and can more easily access active sites or ligand binding regions of target proteins [307].

Nanobodies have potential applications as experimental, imaging, diagnostic, and therapeutic tools [309–311]. There is one currently licensed nanobody for therapeutic use, Caplacizumab, for the treatment of acquired thrombotic thrombocytopenic purpura (aTTP). Patients with aTTP suffer from inappropriate and life-threatening blood clotting due to an abundance of unprocessed von Willebrand factor (VWF) strings [312,313]. This is typically due to an autoimmune antibody response to the enzyme which cleaves VWF. Caplacizumab is a bivalent humanized anti-VWF nanobody that prevents VWF binding to platelets and reduces the length of acute TTP episodes [314].

Other nanobodies have been investigated for the treatment of acute viral infections, including respiratory syncytial virus (RSV) and rotavirus [307,315], though a Phase IIb clinical trial of the RSV nanobody therapeutic was stopped in 2018 due to a lack of efficacy (<https://clinicaltrials.gov/ct2/show/NCT03418571>). In addition, nanobodies targeting human G protein coupled receptors have been investigated for therapeutic potential [316–318], as well as nanobodies targeting HCMV US28 [182,308], which I will discuss in the next section.

1.7.2. Anti-US28 nanobodies modulate US28 activity

HCMV nucleic acids and US28 protein can be detected in tumour samples from glioblastoma patients [36,190]. US28 is thought to be oncomodulatory in glioblastoma, and constitutive signalling from US28 was recently shown to accelerate glioblastoma growth in an experimental setting [40,181,182]. On this basis, Martine Smit's group (Vrije Universiteit, Amsterdam) developed an anti-US28 nanobody (US28-Nb) [182]. The monovalent nanobody could displace the ligands CCL5 and CX3CL1 from binding US28 in competition assays, with a K_d (US28 binding) of approximately 340 nM. Binding was enhanced approximately 100-fold by the linking of two US28-Nb molecules together to form a bivalent nanobody. Interestingly, this bivalent format was then also able to block US28 constitutive signalling as measured by US28's known ability to activate NF- κ B in reporter assays in some cell models, while the monovalent format was not able to do this. The bivalent US28-Nb could then block the acceleration of glioblastoma spheroid growth in an experimental setting [182].

The group then developed a higher-affinity monovalent US28-targeting nanobody termed VUN100 [308]. VUN100 was developed with the aim of conjugating a photosensitiser to the nanobody such that it could be used in photodynamic therapy for the treatment of glioblastoma. Briefly, the nanobody-

photosensitiser conjugate binds US28 on the surface of glioblastoma cells, and when illuminated by the correct wavelength of light, the photosensitiser is activated and produces reactive oxygen species leading the death of the bound cell [308].

Subsequently, the group developed a bivalent form of VUN100, termed VUN100b, which I will describe in more detail in Results. In a collaboration between our two laboratories, and in particular Timo de Groof and myself, we investigated the effect of these nanobodies on HCMV latency, since US28 is expressed on the cell surface of latently infected cells [172]. In Chapter 7, I will describe how anti-US28 nanobodies induce IE gene expression during latency and how this leads to recognition and killing by cytotoxic T cells. Therefore, I will provide some background to this potentially therapeutic concept, often termed 'shock and kill', in the next section.

1.7.3. Shock and kill for reducing latent viral loads

Latent reservoirs of viral pathogens are significant barriers to eradication of these viruses from their hosts [20,319,320]. During latency, human herpesviruses and retroviruses maintain their viral genomes in the absence of infectious virus particle production, often with little-to-no viral gene expression [321]. As such, latent infections are refractory to treatment with typical antivirals that target replication of the virus [320]. Furthermore, the relatively low levels of viral gene expression during latency reduces the levels of viral antigens that would otherwise be readily detectable by host immune cells e.g. cytotoxic T lymphocytes (CTLs) [20].

The shock and kill strategy aims to reverse latency and drive lytic viral gene expression (shock) leading to recognition and elimination by naturally present immune responses (kill), and has been extensively explored by HIV-1 biologists and clinicians [319,320]. HIV-1 latency, like herpesvirus latency, is dependent on repressive chromatin structures around its key viral promoter [86,321–323]. Approaches to target the epigenetic machinery, such as with inhibitors of histone deacetylases (HDACi) and histone methyl transferases have been trialled [319,320]. Some have shown promising results in cell line models, and have induced detectable HIV-1 replication in patients, but none has led to a reduction in the latent viral reservoir [319,320]. This is presumed to be a result of an inability to target deep tissue latent virus reservoirs, failure to induce killing, because of drug interference with CTL function, and subversion of apoptotic pathways by the reactivated virus [319,324,325].

More recently, herpesvirologists have begun to explore latency reversal and shock and kill [20,320,326,327]. Work from my own laboratory has shown that HDACi induce transient activation of

lytic IE gene expression in latently infected monocytes, resulting in CTL-mediated killing of infected cells [145]. Ongoing work by colleagues aims to use additional epigenetic machinery-targeting small molecules to improve shock and kill, and preliminary data suggests that seropositive individuals who are already taking these drugs for other conditions have lower latent viral loads. As described in §1.1.2, up to 5% of a seropositive individual's CD8⁺ T cells are capable of recognising lytic IE antigen [74], which might aid in the efficiency of the 'kill' part of shock and kill.

However, host-targeting antivirals have off-target effects, and it may be preferable to use a specific virus-targeting molecule to induce shock and kill. In §1.4.2, I presented the evidence for US28 being essential for HCMV latency due to the ability of US28 to suppress the MIEP. In Chapter 7, I will show how US28-targeting nanobodies inhibit US28 function in myeloid cells and induce IE gene expression, leading to T cell recognition and killing.

1.8. US28-targeting immunotoxins for killing of HCMV-infected cells

1.8.1. Immunotoxins as anti-cancer and anti-microbial agents

Ligand-toxin fusion proteins, or immunotoxins, have shown promise for targeting cancer and infectious diseases [328,329]. The principle of an immunotoxin is that a toxin is conjugated to a molecule that binds and is internalised by a receptor on target cells. The toxin is then cleaved within cells and, if enough immunotoxin has been internalised, the target cell is killed. The ligand can be based upon the native ligand for a given receptor, or be a receptor-targeting antibody. Cancerous cells and pathogen-infected cells frequently have upregulation of cell-surface receptors, or the presence of unique receptors, making these diseases targets for immunotoxin-based treatments. Some have been licensed as therapies, such as trastuzumab emtansine (T-DM1), a conjugate which targets HER2-positive breast cancers [330,331]. Some examples of immunotoxins in development or clinical use are given in Table 1-3.

Table 1-3 Immunotoxins: examples and modes of action

Disease	Ligand	Toxin
HER2-positive breast cancer [331]	Anti-HER2 monoclonal antibody (trastuzumab)	DM1/Mertansine, inhibitor of microtubule formation
Hairy cell leukemia [332]	Anti-CD22 monoclonal antibody	<i>Pseudomonas aeruginosa</i> Exotoxin A, translation inhibitor
Latent HIV-1 [333]	Anti-CD30 monoclonal antibody	Monomethyl auristatin E, inhibitor of microtubule formation
Acute myeloid leukemia [332]	Granulocyte-macrophage colony stimulating factor (GM-CSF)	Diphtheria toxin
HCMV [334]	CX3CL1 (fractalkine), bound by HCMV US28	<i>Pseudomonas aeruginosa</i> Exotoxin A, translation inhibitor

1.8.2. F49A-FTP, a US28-targeting immunotoxin

US28 binds the chemokine CX3CL1/fractalkine with higher affinity than the host native receptor, CX3CR1 [334,335]. US28 is also expressed during both lytic and latent infection (§1.4) and, therefore, represents a target in patients with active CMV disease and those who harbour latent virus. Spiess and colleagues

[334] designed an immunotoxin to take advantage of these properties. The immunotoxin ligand consisted of the soluble domain of CX3CL1 (after removal of its mucin stalk domain) containing an F49A mutation, decided upon following rational mutagenesis. The toxin was the cytotoxic domain of *Pseudomonas aeruginosa* Exotoxin A, which is cleaved from CX3CL1 by the host protease furin following internalisation. The immunotoxin, termed F49A-FTP, had a 182-fold greater affinity for US28 than for CX3CR1. It also killed lytically infected cells and showed antiviral activity in an infected humanised mouse, with greater potency than the established CMV antiviral ganciclovir.

In a collaboration with members of my own laboratory, F49A-FTP was then shown able to specifically kill latently infected cells and block reactivation at a concentration of 5×10^{-8} M following a 72 hour incubation [172]. This was true for experimentally latent monocytes, CD34⁺ cells, and naturally latent monocytes from seropositive donors. The results suggested that F49A-FTP could be used to target the latent viral reservoir. Perhaps not unexpectedly, resistance mutants did arise during serial passage of virus in lytic infection [334,336] and, in all but one case, this involved a premature stop codon resulting in a truncated pUS28. This truncated pUS28, though expressed, was present at lower levels at the cell surface and was less able to bind and initiate responses to chemokines; it was therefore postulated that this viral mutant might lack *in vivo* fitness.

Other than antiviral resistance, there are additional potential problems with an F49A-FTP strategy for treatment of HCMV. Immunotoxins tend to be immunogenic because they contain 'foreign' antigens [337]. Anti-drug antibodies are induced and neutralise any efficacy during long term treatment of a patient. However, the possibility of treating an HCMV positive graft *ex vivo* prior to transplantation could negate such problems. One such system which would lend itself to such an approach is the *ex vivo* normothermic perfusion system for solid organs [338,339]. *Ex vivo* normothermic perfusion (EVNP) is a novel technique that can recondition an organ and restore function in sub-optimal organs prior to transplantation. During this procedure, a solid organ can be perfused with buffers that could contain a drug, such as the F49A-FTP. Indeed, in collaboration with our laboratory, transplant physicians at the University Health Network (Toronto, Canada) are attempting to reduce the latent load in cadaveric lung prior to transplant. To optimise such an intervention, the immunotoxin needs to be able to kill infected cells following less than 6 hours of incubation (a typical maximum length of normothermic perfusion). Furthermore, since their original study, the designers of the immunotoxin had been experimenting with variations in the FTP construct [340], and a company (Synkline ApS) had been established to perform preclinical testing of newer FTP constructs. In Chapter 8, I will address whether these new FTP

constructs can kill latently infected cells with greater efficacy and in a shorter window, to permit more efficient killing of latent reservoirs during their normothermic perfusion.

2. Materials and Methods

2.1. Cells

All cells were maintained at 37 °C in a 5% CO₂ atmosphere. THP-1 cells (ECACC 88081201) were cultured in RPMI-1640 media (Sigma) supplemented with 10% heat-inactivated fetal bovine serum (FBS; PAN Biotech), 100 U/mL penicillin and 100 µg/mL streptomycin (Sigma), and 0.05 mM 2-mercaptoethanol (Gibco). Kasumi-3 cells (ATCC® CRL-2725) were cultured in RPMI-1640 media (Sigma) supplemented with 20% heat-inactivated fetal bovine serum (PAN Biotech), 100 U/mL penicillin and 100 µg/mL streptomycin (Sigma). During infections, THP-1 and Kasumi-3 cells were cultured in a low-serum (1%) version of this media for a minimum of 24 hours prior to inoculation, and maintained in this low-serum media throughout the infection. MIEP-eGFP reporter THP-1 cells [118] were a gift from M Van Loock, Johnson & Johnson. RPE-1 cells (ATCC® CRL-4000™) and Human foreskin fibroblasts (Hff1; ATCC® SCRC-1041™) were maintained in DMEM (Sigma) supplemented with 10% heat-inactivated FBS and 100 U/mL penicillin and 100 µg/mL streptomycin. 293T cells (ECACC 12022001) were maintained in DMEM (Sigma) supplemented with 10% heat-inactivated FBS but without penicillin or streptomycin. Hff-TERT and Hff-TERT US28-V5 cells were a gift from L. Nobre, University of Cambridge. These were also maintained in DMEM 10% FBS plus penicillin/streptomycin. Phorbol 12-myristate 13-acetate (PMA, Sigma) was used to induce myeloid cell differentiation at a concentration of 20 ng/mL in primary monocytes, and 100 ng/mL in THP-1 cells.

Primary CD14⁺ monocytes were isolated from apheresis cones (NHS Blood & Transplant Service) or from peripheral blood taken from healthy volunteers as previously described [111]. Briefly, CD14⁺ monocytes were isolated from total peripheral blood mononuclear cells (PBMC) by magnetic-activated cell sorting (MACS) using CD14⁺ microbeads (Miltenyi Biotec). The monocytes were plated on tissue culture dishes (Corning) or slides (Ibidi), or kept in suspension in X-Vivo 15 media (Lonza) supplemented with 2 mM L-glutamine. Mature dendritic cells were generated by treating CD14⁺ monocytes with granulocyte-macrophage colony-stimulating factor (GM-CSF, Miltenyi, 1000U/mL) and interleukin-4 (IL-4, Miltenyi, 1000U/mL) for 5 or 6 days before addition of lipopolysaccharide (LPS, Invivogen, 50 ng/mL) for 2 further days. CD4⁺ and CD8⁺ T cells were isolated by MACS from monocyte-depleted PBMC using CD4 and CD8 microbeads (Miltenyi Biotec). These primary cells were cultured in X-vivo 15 (Lonza) supplemented with 2 mM L-glutamine (Gibco) at 37°C in 5% CO₂. Phorbol myristate acetate (PMA, Sigma-Aldrich) was used as described in figure legends at 20 ng/mL.

Primary human CD34⁺ hematopoietic progenitor cells, isolated from adult bone marrow, were purchased from STEMCELL Technologies and cultured in X-Vivo 15 media (Lonza).

2.2. Inhibitors

The c-fos inhibitor T5524 was purchased from Cayman Chemical, solubilised in dimethyl sulfoxide (DMSO) and used at 10 μ M. The Janus kinase inhibitor Ruxolitinib was purchased from Cell Guidance Systems, solubilised in DMSO and used at 5 μ M. The IKK α inhibitor/NF- κ B pathway inhibitor BAY11-7082 was purchased from Santa Cruz, solubilised in DMSO, and used at a concentration of 5 μ M.

2.3. Generation of lentiviruses and retroviruses

The lentiviral vectors encoding US28 from the VHL/E strain of HCMV have been described previously [189]; US28 is expressed in these vectors from the Spleen Focus-Forming Virus (SFFV) promoter. The lentiviral vectors pHRsIN UbEm and pHRsin SV40blast were a kind gift from D. van den Boomen, University of Cambridge, and were based upon a previously published lentiviral system [341,342]. Briefly, expression of the gene of interest is also driven by the SFFV promoter, and the selectable markers Emerald and blasticidin resistance are driven by the Ubiquitin promoter (UbEm) and the SV40 promoter (SV40blast), respectively. The sequence encoding US28 from the VHL/E strain of HCMV was cloned into pHRsIN UbEm using the EcoR1 and Spe1 sites. The sequence encoding IFI16 was cloned into pHRsin SV40blast using the BamHI and NotI sites. The coding sequence of MNDA was cloned from a TrueClone[®] cDNA clone (Origene) into pHRsin SV40blast using XhoI and NotI sites. Correct plasmid sequences were verified by Sanger Sequencing (Department of Biochemistry, University of Cambridge). Primer sequences are given in Table 2-1.

The retroviral vector pBABE eGFP US28-3XFLAG was a gift from C. O'Connor (Cleveland Clinic, USA). The Q5 site directed mutagenesis kit (New England Biotech) was used to generate the US28-R129A mutant of this vector, which was verified by Sanger Sequencing (Department of Biochemistry, University of Cambridge). Expression of US28 in these vectors is driven by the HIV-1 long terminal repeat and partial gag.

Generation of VSV-G pseudotyped lentiviral particles was conducted generally in line with the Broad Institute Protocols. Five hundred thousand 293T cells were transfected with 1250 ng of lentiviral expression vector, 625 ng of lentiviral packaging vector psPAX and 625 ng of envelope vector pMD.2G (both gifts from S. Karniely, Weizmann Institute, Israel) using transfection reagent FuGene6 (Promega) according to the manufacturer's instructions. For generation of VSV-G pseudotyped retrovirus particles,

1250 ng of the murine leukemia virus retroviral packaging vector KB4 [343] (a gift from H. Groom, University of Cambridge) was transfected along with 625 ng pMD.2G and 1250 ng retroviral expression vector.

2.4. Lentiviral and retroviral transduction

Supernatants from transfected 293T cells were harvested at 36 and 60 hours post transfection, filtered through a 0.45 µm syringe filter, and used to transduce THP-1 cells in the presence of 2 µg/mL polybrene. When necessary, lentiviral titres were determined by in-house p24 enzyme-linked immunosorbent assay (ELISA) by Isobel Jarvis (Department of Medicine, University of Cambridge). For transduction with puromycin-resistance vectors, puromycin (2 µg/mL, Sigma) was added to media and refreshed every 2-5 days until all control non-transduced THP-1 cells were dead. Similarly, where blasticidin-resistance vectors were used, blasticidin (10 µg/mL, Invivogen) was added to media. Emerald positive cells were isolated by fluorescence associated cell sorting (FACS) using a BD FACSAriaIII instrument.

2.5. Preparation and transfection of DNA into THP-1 cells

All DNA transfections used a mock-transfected control, which contained equivalent levels of the transfection reagent, Fugene6 (Promega). Poly dA:dT was purchased from Invivogen and transfected at a final concentration of 1 µg/mL. pUC19 (Addgene #50005) [344] was digested with BglI and purified by phenol/chloroform/isoamyl alcohol extraction [345]. THP-1 cells (2×10^5) were transfected with 1 or 2 µg of the digested plasmid using transfection reagent FuGene6 (Promega) for 24 hours prior to RNA extraction. The plasmid pmaxGFP was a component of the Amaxa Nucleofection Kit R (Lonza) and drives GFP expression from a modified 780bp HCMV MIEP. EF1alpha GFP was a gift from P. Upton (Department of Medicine, University of Cambridge). These, and pHRsin UbEm (described above), were transfected into THP-1 cells (750 ng / 2×10^5 cells) using transfection reagent FuGene6 (Promega) and GFP expression was analysed by flow cytometry using a BD Accuri Instrument 24 hours after transfection.

2.6. Human cytomegaloviruses

Infection of monocytes and THP-1 cells were carried out at a multiplicity of infection (MOI) of 3 as determined by titration on RPE-1 cells. When required, latently infected, mCherry positive THP-1 cells were sorted using a BD FACSAriaIII instrument. Hff1 and RPE-1 cells were infected at indicated MOIs as determined by titration on Hff1 and RPE-1 cells, respectively.

TB40/E BAC4 strains, recombinant viruses derived from bacterial artificial chromosomes (BAC), were propagated in RPE-1 cells by seeding 50% confluent T175 flasks with virus at an MOI of 0.1. Spread of virus was monitored for 2-6 weeks following inoculation by fluorescence microscopy, and infected monolayers were subcultured twice during this period. When cells were 95-100% infected (on the basis of fluorescent tag detection), supernatants were harvested on three occasions spaced over 7 days and stored at -80°C. In the final harvest, the monolayer was scraped and also stored at -80°C. After thawing the virus-containing media, cell debris was pelleted by centrifugation at 1500 x *g* for 20 minutes at RT. Then, the clarified supernatant was concentrated by high speed centrifugation at 14500 x *g* for 2 hours at 18°C. Virus-containing pellets were then resuspended in X-vivo-15 media in aliquots at -80°C.

TB40/*EmCherry*-US28-3XFLAG and TB40/*EmCherry*-US28Δ have been described previously [159]. TB40/*Egfp* [346] and TB40/E BAC4 SV40 mCherry IE2-2A-GFP[121] were kind gifts from E.A. Murphy, SUNY Upstate Medical University. TB40/E BAC4 IE2-eYFP has been described previously [347,348]. TB40/E BAC4 GATA2mCherry has been described previously[349]. TB40/E with deleted NF-κB sites in the MIEP at positions -94, -157, -262 and -413, and the revertant virus, were a kind gift from Jeffery Meier and Ming Li (University of Iowa, United States), and have been described previously[146].

UV-inactivation of virus was performed by placing a 100 μL aliquot of virus in one well of a 24-well plate and placing this within 10cm of a UV germicidal (254 nm) lamp for 15 minutes, which routinely results in no detectable IE gene expression upon infection of Hff1 cells.

2.7. Immunofluorescence staining and image analysis

Cells were fixed with 2% paraformaldehyde for 15 minutes and permeabilised with 0.1% Triton-X100 for 10 minutes at RT. Blocking and antibody incubations were performed in phosphate buffered saline (PBS) with 1% bovine serum albumin and 5% normal goat serum. Primary antibodies used: anti-IFI16 (Santa Cruz sc-8023, 1:100), anti-FLAG (Sigma F1804, 1:1000), anti-MNDA (Cell Signaling Technology 3329, 1:100), anti-IE (Argene 11-003, 1:1000 or directly conjugated to FITC, 1:100), anti-GFP (directly conjugated to FITC, Abcam ab6662, 1:200), anti-mCherry (Abcam ab167453, 1:500), anti-HLA DR (conjugated to Brilliant Violet 421, Biolegend Clone L423 or Abcam ab92511 1:100), anti-NF-κB (Abcam ab16502, 1:500). Secondary antibodies used: goat anti-mouse Alexa 488 (Thermo Fisher A11001, goat anti-mouse Alexa 594 (Thermo Fisher, A11005), chicken anti-rabbit Alexa 488 (Thermo Fisher A21441) goat anti-rat Alexa 488 (Abcam ab150157), donkey anti-rat Alexa 594 (Thermo Fisher, A21209). Cells were imaged with a widefield Nikon TE200 microscope and images were processed using ImageJ. For contingency analyses of IFI16 expression during experimental latency, cells were assigned as 'IFI16

positive/negative', and 'infected/uninfected' and then counted. These results were then analysed using Fisher's Exact statistical test for significance. For analysis of signal intensity, nuclear stained images were used to create a mask from which intensity values of the corresponding IFI16/MNDA stained image were derived using the Analyze Particles feature of ImageJ. Cells were assigned as infected or uninfected based on signal from the GFP/mCherry stain. The average signal intensity of uninfected cells was used to normalise the signal intensity in order to compare different fields of view.

For nanobody binding experiments, THP-1 cells were pelleted and resuspended in 4% paraformaldehyde (Sigma-Aldrich) and seeded in a 96 well U-bottom plate. Cells were fixed for 10 minutes at room temperature. After fixation, cells were permeabilized with 0.5% NP-40 (Sigma-Aldrich) for 30 minutes at room temperature. Nanobodies were incubated for 1 h at RT and detected using Mouse-anti-Myc antibody (1:1000, 9B11 clone, Cell Signaling Technology). US28 was visualized with the rabbit-anti-US28 antibody (1:1000, Covance). Subsequently, cells were washed and incubated with Goat-anti-Rabbit Alexa Fluor 546 (1:1000 in 1% (v/v) FBS /PBS, Thermo Fisher Scientific) and Goat-anti-Mouse Alexa Fluor 488 (1:1000 in 1% (v/v) FBS/PBS, Thermo Fisher Scientific).

2.8. Western blotting

Except for US28, virion, and ERK blots, cells were lysed directly in Laemmli Buffer and separated by sodium dodecyl sulfate-polyacrylamide gel electrophoresis (SDS-PAGE). Following transfer to nitrocellulose, the membrane was blocked in 5% milk in tris buffered saline (TBS) with 0.1% Tween-20. Primary antibodies used: anti-IFI16 (Santa Cruz sc-8023, 1:500), anti-MNDA (Cell Signaling Technology 3329, 1:250), anti-STAT1 (Cell Signaling Technology 14994, 1:1000), anti-phosphoSTAT1 Tyr701 (Cell Signaling Technology 9167, 1:1000), anti-beta actin (Abcam ab6276, 1:5000), (GAPDH, Abcam ab8245, 1:5000). Secondary antibodies used: anti-mouse-horse radish peroxidase (HRP) conjugate, (Santa Cruz sc-2005 or Thermo Fisher 31430), anti-rabbit HRP (Santa Cruz sc-2004), anti-rat HRP (Cell Signaling Technology 7077). These membranes were developed using electrochemiluminescence (standard or prime) reagents from GE Healthcare.

For US28 blots of THP-1 cells, cells were pelleted, washed once in ice cold PBS, then lysed in lysis buffer (25 mM Tris HCl pH 7.4, 150 mM NaCl, 1 mM EDTA, 1% NP40, 5% glycerol, plus protease inhibitors) for 30 minutes, vortexing every 10 minutes. After the addition of non-reducing Laemmli buffer, samples were heated at 42°C for 10 minutes and then separated by SDS-PAGE. Polyvinylidene difluoride (PVDF) membranes were used for transfer, and blocked membranes were incubated with the rabbit anti-US28 antibody [191] (a gift from M. Smit, Vrije University) at 1:1000 dilution. To quantify western blots, the

Analyze Gels feature of Image J was used to plot the band intensities. These membranes were developed using electrochemiluminescence (standard or prime) reagents from GE Healthcare.

For US28-V5 blots of Hff-TERT cells and virions, Hff-TERT cells were pelleted, washed once in ice cold PBS, then lysed in radioimmunoprecipitation assay buffer (25 mM Tris pH 7.5, 150 mM NaCl, 0.5% sodium deoxycholate, 1% Triton X-100, and 1% NP-40 with protease inhibitor cocktail) on ice for 30 minutes. Cell debris was removed by centrifugation at 13,000 x *g*. HCMV virions were pelleted by high speed centrifugation at 14500 x *g* for 2 hours at 18°C. Virus-containing pellets were then resuspended in solubilisation buffer (10 mM Tris-Cl, pH 8.0, 400 mM NaCl, and 10 mM EDTA) on ice for 1 hour, vortexing every 15 minutes. After the addition of non-reducing Laemmli buffer, cell and virion samples were heated at 42°C for 10 minutes and then separated by SDS-PAGE. PVDF membranes were used for transfer, and blocked membranes were incubated with anti-V5 (Thermo Fisher R960-25, 1:1000), anti pp65 (Santa Cruz sc56976 1:1000), and anti-beta actin (Abcam ab6276, 1:5000). These membranes were developed using electrochemiluminescence (standard or prime) reagents from GE Healthcare.

For analysis of ERK phosphorylation following nanobody treatment, mock transduced or US28-expressing THP-1 cells were seeded in a 6 wells plate and incubated with 100 nM nanobodies. After 48 h, cells were lysed in native lysis buffer (25 mM Tris HCL pH7.4, 150 mM NaCl, 1 mM EDTA, 1% NP-40, 5% Glycerol, 1 mM NaF, 1 mM NaVO₃, cOmplete™ protease inhibitor cocktail) for 10 minutes on ice. Cell debris was removed by centrifugation at 13,000 x *g*. Lysates were then separated on a 10% SDS-PAGE gel under reducing conditions and transferred to 0.45 µm PVDF blotting membrane (GE healthcare). Total ERK1/2 and phospho-ERK1/2 were detected using p44/42 MAPK antibody (1:1000 in 5% bovine serum albumin (BSA)/TBS-T, #9102, Cell Signaling Technology) and phospho-p44/42 MAPK (Thr202/Tyr204) (1:1000 in 5% BSA/TBS-T, #9101, Cell Signaling Technology). Actin was detected using anti-actin antibody (1:2000 in 5% BSA/TBS-T, Clone AC-74, Sigma-Aldrich). Antibodies were detected using Goat anti-Rabbit IgG-HRP conjugate (1:10000, #1706515, Bio-Rad) or Goat anti-Mouse IgG-HRP conjugate (1:10000, #1706516, Bio-Rad). Blots were developed using Western Lightning Plus-ECL (Perkin-Elmer, Waltham, MA, USA) and visualized with Chemidoc™ (Bio-Rad).

2.9. Flow cytometry

Transduced THP-1 cells and MIEP-reporter THP-1 cells were analysed on a BD Accuri C6 Instrument. Live cells were gated using forward and side scatter. Paraformaldehyde-fixed cells were stained using anti-HLA-DR Allophycocyanin (APC) conjugate (Biolegend, Clone L243, 1:50).

T cell/PBMC preparations were analysed for purity using anti-human CD3 antibody conjugated to fluorescein-isothiocyanate (FITC) (BD Biosciences), anti-human CD4 antibody conjugated to phycoerythrin (PE) and anti-human CD8 antibody conjugated to Peridinin-Chlorophyll protein/Cyanine 5.5 (PerCP/Cy5.5) (both from BioLegend). Antibodies were incubated with samples for 30 minutes and fixed with 2% paraformaldehyde before analysis by flow cytometry on the BD Accuri C6 Instrument.

Latently infected CD14⁺ monocytes were fixed with 1% paraformaldehyde and stained using anti-HLA-DR Pacific blue conjugate (Biolegend, Clone L243, 1:50) and anti-HLA-A,B,C, PE-Cyanine 7 (Cy7) conjugate (Biolegend, Clone W6/32, 1:50), before analysis on the Nxt Attune Instrument (Thermo Fisher).

2.10. Cytokine detection by ELISA

Commercial ELISA kits were used to detect interleukin 1-beta (IL-1 β) (Thermo Fischer), interferon beta (IFN β) (Elabscience), and interferon alpha (IFN α) (PBL Assay Sciences). These were used according to the manufacturer's instructions and absorbance at 490 nm was read using an iMarkTM Microplate Absorbance Reader (BioRad).

2.11. RNA and DNA extraction, reverse transcription, and quantitative PCR

RNA was extracted and purified using Direct-Zol RNA MiniPrep kit (Zymo Research) according to the manufacturer's instructions. A total of 5 ng of purified RNA was used in one-step RT-qPCR reactions, performed using QuantiTect SYBR[®] Green RT-PCR Kit reagents (Qiagen) on a StepOne Real-Time PCR instrument (Applied Biosystems). For two-step RT-qPCR analysis, reverse transcription was performed using the Qiagen QuantiTect Reverse Transcription kit, and then cDNA was used in qPCR analysis using New England Biotech LUNA SYBR Green qPCR reagents. TATA-box binding protein (TBP) or Glyceraldehyde phosphate dehydrogenase (GAPDH) were used as reference genes and relative gene expression was analysed using ΔC_t or $\Delta\Delta C_t$ values. Primer sequences are given in Table 2-1.

To extract DNA from HCMV infected cells, cells were pelleted and washed in citrate wash buffer (40mM sodium citrate, 10mM KCl, 135mM NaCl pH 3.0) for one minute before washing in PBS. Cells were then resuspended at 5×10^6 /mL in Buffer A (100 mM KCl, 10 mM Tris-HCl pH 8.3, 2.5 mM MgCl₂) followed by the addition of an equal volume of Buffer B (10 mM Tris-HCl pH 8.3, .5 mM MgCl₂, 1 % Tween-20, 1% NP-40, 0.4 mg/mL Proteinase K) and then incubated at 60°C for 1 hour followed by 95°C for 10 minutes. HCMV DNA abundance was then analysed using New England Biotech LUNA SYBR Green qPCR reagents using the GAPDH promoter region as a reference sequence, and the UL44 promoter region as the HCMV

genomic target. Relative HCMV DNA levels were then analysed using ΔC_t or $\Delta\Delta C_t$ values. Primer sequences are given in Table 2-1.

Table 2-1 **List of primers used in this project.** Application (Appⁿ) is denoted by 'Q' for (RT)-qPCR, 'C' for cloning, 'M' for site directed mutagenesis. Targets in the promoter region are denoted by 'prom'. All primer sequences are 5'-3'.

Target	App ⁿ	Forward	Reverse
IE72/IE1	Q	GTCCTGACAGAACTCGTCAAA	TAAAGGCGCCAGTGAATTTTTCTTC
UL44	Q	TACAACAGCGTGTCTGTCTCCG	GCGTAAAAAACATGCGTATCAAC
UL138	Q	ACGACGAAGACGATGAACCC	CCCAGTATGAGATCTTGGTCCG
UL32	Q	GGTTTCTGGCTCGTGGATGTCTG	CACACAACACCGTCTGTCGATTAC
US11	Q	TACTCCGAAACATCGGGCAG	CGCGGGTAGTATGCCTGAAT
GAPDH	Q	TGCACCACCAACTGCTTAGC	GGCATGGACTGTGGTCATGAG
US28	Q	AATCGTTGCGGTGTCTCAGT	TGGTACGGCAGCCAAAAGAT
TBP	Q	CGGCTGTTAACTTCGCTTC	CACACGCCAAGAAACAGTGA
IFNB	Q	AAACTCATGAGCAGTCTGCA	AGGAGATCTTCAGTTTCGGAGG
CXCL10	Q	TTCAAGGAGTACCTCTCTCTAG	CTGGATTCAGACATCTCTTCTC
MNDA	Q	GGAAGAAGCATCCATTAAGG	GTTTGTCTAGACAGGCAAC
IFI16	Q	CTGCACCCTCCACAAG	GTTTGTCTAGACAGGCAAC
HLA-DRA	Q	TGTAAGGCACATGGAGGTGA	TAGGGCTGGAAAATGCTGA
BETA2.7	Q	ATCACGATGGATCGTTGCGA	CACTCTCCTGTCACGACACC
AIM2	Q	CAGGAGGAGAAGGAGAAAGTTG	GTGCAGCACGTTGCTTTG
IFIX	Q	GAGACTGGAACCAAAAAGGC	CGCGATTATTGGGTCTTC
NFKBIA	Q	ACATCAGCACCCAAGGACACC	CCGCACCTCCACTCCATCC
UL44 prom	Q	AACCTGAGCGTGTGTTGTG	CGTGCAAGTCTCGACTAAG
GAPDH prom	Q	CGGCTACTAGCGGTTTTACG	AAGAAGATGCGGCTGACTGT
US28	C	GCACGAATTCCATATGACGCCGACGACGAC C	CTGCACTAGTTTACGGTATAATTTGTGAG AC
IFI16	C	GATTGCGGCCGCATGGGAAAAAATACA AGAACATTGTTC	GATCGGATCCTTAGAAGAAAAAGTCTGGT GAAGTTTC
MNDA	C	GATCCTCGAGATGGTGAATGAATACAAG	GATCCAATTGTCAATTAACATTCAATTTGG
US28-R129A	M	TGCACTCGATGCCTACTACGCTATTG	ATCTCCGTGATAAAACACAAAC

2.12. Proteomic analysis

These procedures were performed prior to the beginning of this project but an abridged version of these methods is included to aid interpretation of the analyses presented later.

Cells were harvested lysed in 2% SDS/50 mM Triethylammonium bicarbonate and 50 µg of each sample was digested with trypsin using a modified Filtered Aided Sample Preparation protocol. Samples were further purified by acid precipitation and two-phase partitioning, and dried under vacuum. Samples were then labelled with tandem mass tag reagents and pooled prior to high pH reverse-phase fractionation. High pH fractions were pooled orthogonally into 24 samples for analysis by Liquid chromatography–mass spectrometry on an Orbitrap Fusion, using synchronous precursor selection mode to isolate reporter ions. Data were analysed using the MASCOT search node within Proteome Discoverer.

2.13. Gene ontology analysis

The gene ontology (GO)-term enrichment database search feature of geneontology.org was used to compare a given subset of genes identified in the proteomic analysis with either all human genes or all proteins identified in the proteomic analysis. Biological process GO-terms were analysed for enrichment using the FDR correction within the enrichment analysis tool.

2.14. Interferome analysis

The gene IDs of the top 40-downregulated proteins identified in the proteomic analysis (§3.1), or those of the 40 proteins which showed zero fold change, or the whole list of identified proteins, were entered in the Interferome database search function and noted if they were positively inducible by either Type I or Type II interferon using a cut-off of 2-fold induction.

2.15. Nanobody production

Nanobody gene fragments were recloned in frame with a myc-His6 tag in the pET28a production vector. The bivalent format VUN100b was constructed by addition of a 30GS-linker in frame with the two VUN100 nanobody fragments. Nanobodies were produced as described previously [350]. Purity of the nanobodies was verified by SDS-PAGE.

2.16. Nanobody binding ELISA

Nanobody binding was performed as described previously [308]. Briefly, US28-expressing membrane extracts were coated in a 96 well MicroWell™ MaxiSorp™ flat bottom plate (Sigma-Aldrich) overnight at

4 °C. Wells were then washed and blocked with 2% (w/v) skimmed milk (Sigma-Aldrich) in PBS. Different concentrations of nanobodies were incubated. Nanobodies were detected with mouse-anti-Myc antibody (1:1000, clone 9B11, Cell Signaling Technology) and Goat anti-Mouse IgG-HRP conjugate (1:1000, #1706516, Bio-Rad). Optical density was measured at 490 nm with a PowerWave plate reader (BioTek).

2.17. Nuclear Factor of Activated T-cells reporter gene assay

HEK293T cells were transfected with 50 ng pcDEF3-HA-US28 VHL/E, 2.5 µg Nuclear Factor of Activated T-cells (NFAT)-reporter gene vector (Stratagene) and 2.5 µg empty pcDEF3 DNA as described previously [308]. Six hours post-transfection, cells were lifted using Trypsin-EDTA 0.05% (Gibco) and 50000 cells were seeded per well in a Poly-L-lysine (Sigma-Aldrich)-treated white bottom 96-well assay plate. Nanobodies were added at a final concentration of 100 nM. After 24 h, medium was removed and 25 µL Luciferase reagent (0.83 mM D-Luciferine, 0.83 mM ATP, 0.78 µM Na₂HPO₄, 18.7 mM MgCl₂, 38.9 mM Tris-HCl (pH 7.8), 2.6 µM DTT, 0.03% Triton X-100 and 0.39% Glycerol) was incubated for 30 min at 37°C. Luminescence (1 s per well) was measured using a Clariostar plate reader (BMG Labtech, Ortenberg, Germany).

2.18. Detection of IE gene expression in nanobody-treated monocytes

CD14⁺ monocytes were isolated as described above and seeded into a 96 well or 12-well plates. The next day, medium was removed and cells were infected with TB40/E IE2-eYFP. Two hours post infection, medium was aspirated and replaced with medium containing nanobodies at a final concentration of 100 nM. Nanobody-containing medium was refreshed every 2-3 days. IE-expression was detected by means of IE2-YFP tag or immunostaining of IE as described above. This was either counted manually or imaged by the ArrayScan XTI instrument (Thermo Fischer) and data processed using the Target Activation experimental tool.

2.19. PBMC and T cell co-culture and virus reactivation

Following PBMC isolation from healthy donor peripheral blood, CD14⁺ monocytes were isolated, plated on 96 well plates, and treated with nanobodies as described above. The remaining PBMC were frozen in liquid nitrogen until one day prior to co-culture. At this time, the PBMC were thawed and rested overnight. CD4⁺ and CD8⁺ T cell fractions were isolated as described in §2.1 above and pooled, and these, or the remaining PBMC were added to the monocyte cultures at an effector:target cell ratio of 5:1. After

two days, the T cells/depleted PBMC were washed away using PBS + 2 mM EDTA, and the medium on the monocytes was replenished with X-vivo 15 + L-glutamine containing IL-4 and GM-CSF at 1,000 U/ml in order to stimulate differentiation to immature dendritic cells. After 5 days, this medium was aspirated and replaced with X-vivo 15 + L-glutamine supplemented with 50 ng/mL LPS for 2 days to induce maturation of dendritic cells.

2.20. Immunotoxin treatments

Immunotoxins were sent by Synklino ApS on dry ice, thawed on wet ice, and aliquoted and flash frozen in liquid nitrogen until use. Immunotoxin dilutions were made in immunotoxin assay buffer (1 mM acetic acid, 0.5% w/v BSA) and if not used immediately, these were stored at -20°C for up to 14 days and could be thawed once more before discarding. For analysis of cell viability, the CellTiter 96® AQueous One Solution Cell Proliferation Assay (Promega), commonly known as the MTS assay (MTS = 3-(4,5-dimethylthiazol-2-yl)-5-(3-carboxymethoxyphenyl)-2-(4-sulfophenyl)-2H-tetrazolium, inner salt), was used according to the manufacturer's instructions. Specifically, cells were treated with immunotoxins, or blasticidin (100 µg/mL, Invivogen) in 96 well plates for variable time periods in 100 µL culture volume. To assess viability, 20 µL of assay reagent was added to culture and the plate incubated for between 1 and 4 hours. The reaction was stopped by the addition of 25 µL of 10% SDS, and the absorbance at 490 nm was measured using an iMark™ Microplate Absorbance Reader (BioRad).

2.21. Statistical analysis

Statistical analysis, including hypothesis testing (t test, analysis of variance (ANOVA), corrections for multiple comparisons, non-parametric tests), regression analysis, and 'curve-fitting' was performed using GraphPad Prism 8.0 software. Specific statistical tests are described in figure legends.

3. US28 downregulates interferon-responsive genes in myeloid cells

3.1. Analysis of the US28-associated proteome

3.1.1. Introduction

The virally encoded G protein coupled receptor US28 is likely essential for the establishment and maintenance of HCMV latency in myeloid cells [159,173,189,193]. Furthermore, US28 coupling to G proteins is required for HCMV latency; loss of G protein coupling via the signalling mutation R129A results in lytic infection of myeloid cells [193]. Similarly, while expression of US28-WT *in trans* complements for US28-deletion viruses, expression of US28-R129A or an empty vector control leads to lytic infection with US28-deletion viruses [189].

While previous work has looked at the global effects of US28 expression in myeloid cells on the phosphorylation status of important signalling pathways by phosphoarray [189], or examined transcription by microarray [173,193], these methods are inherently biased as the cellular targets are pre-selected. Therefore, an unbiased proteomic screen was undertaken in our laboratory by Benjamin Krishna in collaboration with James Williamson and Paul Lehner (all University of Cambridge). This screen compared the host proteomes THP-1 cells which express an empty vector, US28-WT, or US28-R129A. Employing a tandem-mass-tag labelling approach, the screen identified 7458 host proteins present in all cell lines. The full results are presented in the appendix and summarised in Figure 3-1, Table 3-1, and Table 3-2.

The power of this screen was that it allowed identification of changes in host proteins enacted by US28 in a signalling-dependent and -independent manner. Changes in host protein abundance common between US28-WT and US28-R129A when compared to empty vector represent signalling independent changes, and these included CD44 and CD82 proteins, which were each downregulated by both sets of US28-expressing cells.

While I do not rule out that signalling independent changes in myeloid cells driven by US28 may be important for HCMV latency, G-protein dependent signalling is absolutely required for latency, and therefore we were particularly interested in the direct comparison of host protein abundances in THP-1 cells expressing US28-WT and US28-R129A. This comparison revealed 42 host proteins whose expression was two-fold or more increased or decreased by US28-WT, and my subsequent analyses focussed on these signalling-dependent changes.

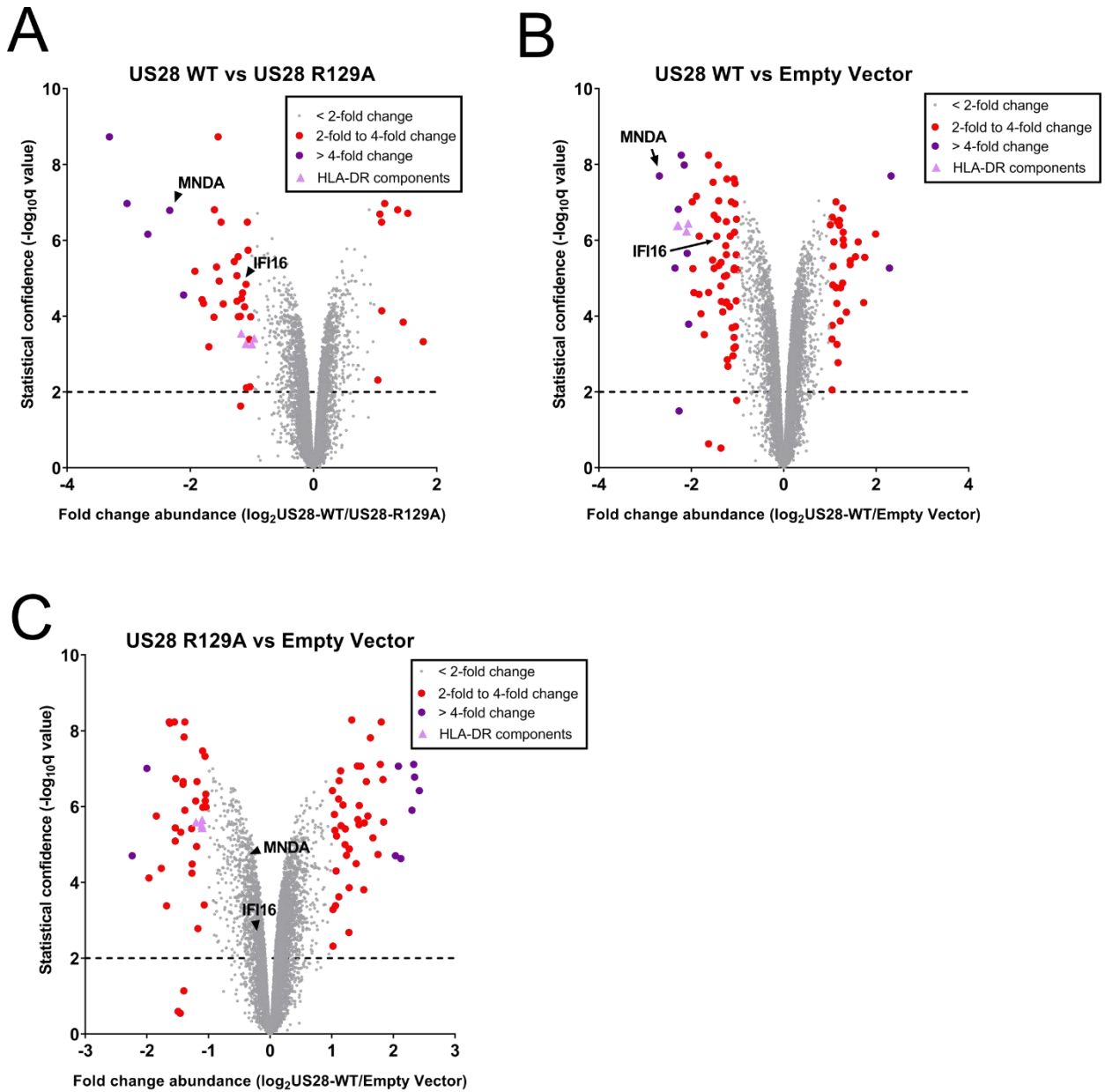


Figure 3-1 US28 proteomic analysis reveals US28 signalling-dependent and independent changes in myeloid cell environment. A, B, C) Empty vector, US28-WT, and US28-R129A THP-1 cells were subject to total cell proteomic analysis using a tandem-mass-tag labelling approach as described in Materials and Methods. Each dot represents one human protein and is shown in grey if its abundance changes by a factor of less than 2, in red if between 2- and 4-fold, and in purple if greater than 4-fold. The exception is components of the HLA-DR complex which are represented by pink triangles. A) Shows a comparison of US28-WT and US28-R129A, B) compares US28-WT and empty vector, and C) compares US28-R129A and empty vector. In each case, the relative abundance of human proteins MND and IFI16 is marked with an arrow.

Table 3-1 **Proteins upregulated by US28-WT compared with US28-R129A**. The Uniprot accession numbers, HUGO Gene IDs, number of Unique Peptides quantified, and log₂(fold change abundance) between cell lines is presented for the top 40-most upregulated proteins (US28-WT vs US28-R129A) after filtering for q value of <0.01. The proteins are presented from most upregulated to least upregulated (US28-WT vs US28-R129A)

Accession	# Unique Peptides	Gene ID	US28-WT/EV	US28-R129A/EV	US28-R129A/US28-WT
P13928	6	ANXA8	1.286881148	-0.739372092	-2.023269779
O94851	1	MICAL2	0.101650076	-1.680382066	-1.780908942
Q12965	11	MYO1E	0.325386415	-1.20756107	-1.531156057
Q8WWN9	1	IPCEF1	1.051720116	-0.401634795	-1.454031631
P15144	27	ANPEP	0.742437445	-0.623709617	-1.365871442
P20701	17	ITGAL	0.645240513	-0.510457064	-1.15521265
Q11206	2	ST3GAL4	1.232660757	0.123003954	-1.10780329
O00151	15	PDLIM1	0.980390956	-0.125006361	-1.104697379
Q6YHK3	20	CD109	0.645240513	-0.432454552	-1.077041036
P04083	20	ANXA1	1.752748591	0.768925336	-0.98279071
Q9NP71	1	MLXIPL	0.388465097	-0.577766999	-0.965784285
Q96PC3	3	AP1S3	0.092207438	-0.833927324	-0.924125133
Q9HBU1	2	BARX1	0.207892852	-0.717856771	-0.924125133
Q9NUU6	13	FAM105A	0.297484916	-0.60823228	-0.905088353
O00421	1	CCRL2	0.070389328	-0.805912948	-0.875671865
Q8TF42	14	UBASH3B	1.204140717	0.368489001	-0.836501268
Q13642	5	FHL1	1.286289758	0.468843943	-0.81857936
Q9BRF8	11	CPPED1	-0.023269779	-0.805912948	-0.783389931
P08133	47	ANXA6	-0.087733372	-0.803392956	-0.717856771
Q8IU85	3	CAMK1D	0.232660757	-0.483984853	-0.715485867
P11169	5	SLC2A3	0.396159489	-0.320125852	-0.715485867
Q658P3	6	STEAP3	-0.045431429	-0.734563104	-0.689659879
P30405	9	PPIF	0.618238656	-0.067938829	-0.687334826
Q8IX19	4	C19orf59; MCEMP1	0.286881148	-0.386468347	-0.673462652
Q9BX10	13	GTPBP2	0.353887836	-0.312939312	-0.666576266
Q7L266	2	ASRGL1	-0.744197163	-1.384583703	-0.639354798
P09525	23	ANXA4	-0.407363571	-1.043943348	-0.637109357
P20020	15	ATP2B1	0.34596403	-0.286304185	-0.632628934
O00458	7	IFRD1	0.318461465	-0.305788392	-0.623709617
Q04726	5	TLE3	0.138814469	-0.477944251	-0.61705613
Q96PY5	3	FMNL2	0.195347598	-0.413115187	-0.610433188
Q13683	4	ITGA7	0.100304906	-0.490050854	-0.590744853
P50281	7	MMP14	0.291603558	-0.295128036	-0.586405918

Q9BPW9	5	DHRS9	0.093560176	-0.490050854	-0.584241333
Q13480	2	GAB1	0.606915942	0.024319679	-0.582079992
Q96TA1	9	FAM129B	-0.416962376	-0.988504361	-0.57132159
Q9NQ86	4	TRIM36	0.137503524	-0.434402824	-0.57132159
Q8IWB7	14	WDFY1	0.03562391	-0.526992432	-0.560642822
Q9P2M4	1	TBC1D14	0.658097205	0.097610797	-0.560642822
Q6PI78	1	TMEM65	0.187767747	-0.371459681	-0.55851652

Table 3-2 **Proteins downregulated by US28-WT compared with US28-R129A**. The Uniprot accession numbers, HUGO Gene IDs, number of Unique Peptides quantified, and log₂(fold change abundance) between cell lines is presented for the top 40-most downregulated proteins (US28-WT vs US28-R129A) after filtering for q value of <0.01. The proteins are presented from most downregulated to least downregulated (US28-WT vs US28-R129A)

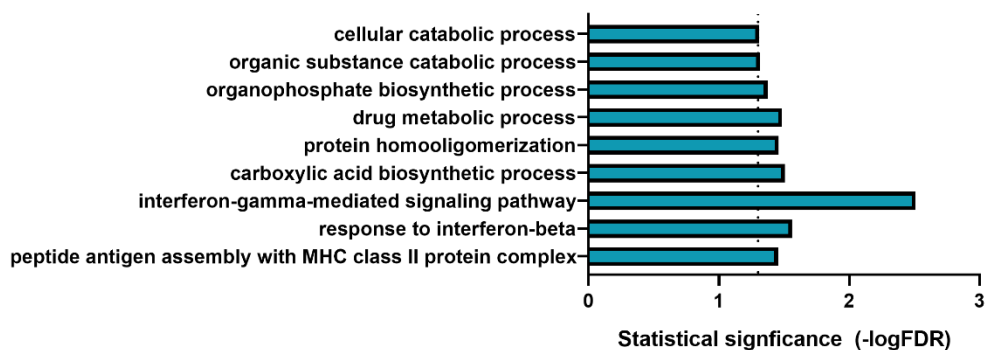
Accession	# Unique Peptides	Gene ID	US28-WT/EV	US28-R129A/EV	US28-R129A/US28-WT
Q03135	2	CAV1	-1.50635	1.803227	3.311212
P22090	5	RPS4Y1	-0.69432	2.329985	3.025206
P13591	4	NCAM1	-0.26708	2.421156	2.688852
P41218	9	MNDA	-2.68966	-0.35476	2.331992
Q9Y2J8	7	PADI2	-0.71076	1.395611	2.107688
Q16719	4	KYNU	-0.08314	1.840765	1.92372
P20292	2	ALOX5AP	-1.96578	-0.15521	1.807355
Q92506	1	HSD17B8	-0.03357	1.750178	1.784504
Q9Y243	1	AKT3	-1.01742	0.679874	1.697774
P25815	2	S100P	0.506907	2.121347	1.614945
O15523	2	DDX3Y	-0.13765	1.470407	1.608336
P32929	6	CTH	-0.35476	1.218471	1.573375
O75155	8	CAND2	-0.22263	1.325386	1.54745
O15394	8	NCAM2	-1.82623	-0.2969	1.53057
Q6ZMU5	11	TRIM72	0.58111	2.082362	1.500802
Q9NRW1	1	RAB6B	-0.71786	0.747602	1.465713
P50225	5	SULT1A1	0.16092	1.446786	1.286881
Q16666	4	IFI16	-1.45008	-0.20923	1.24245
Q96T66	4	NMNAT3	-0.92687	0.312665	1.239398
P29728	17	OAS2	-2.152	-0.93236	1.223423
Q9Y4D7	2	PLXND1	-1.16488	0.051024	1.217851
P05091	19	ALDH2	-2.27928	-1.09234	1.187134
P01911	4	HLA-DRB1	-2.27928	-1.1078	1.172488
Q9BRX8	4	FAM213A	-0.6416	0.526069	1.168642
P31327	9	CPS1	1.151209	2.30188	1.15056

Q96BZ4	7	PLD4	-1.02621	0.092207	1.119688
Q6P5R6	2	RPL22L1	0.326537	1.422771	1.096262
P01903	6	HLA-DRA	-2.30045	-1.20423	1.094912
P12277	8	CKB	0.342555	1.415759	1.073135
Q9UMS6	20	SYNPO2	0.049631	1.111031	1.060739
Q01628	1	IFITM3	-1.25498	-0.21591	1.039138
B011T2	28	MYO1G	-0.57132	0.448901	1.020058
P04229	3	HLA-DRB1	-2.1016	-1.1016	1
P52895	3	AKR1C2	0.561693	1.560715	0.999278
Q30154	3	HLA-DRB5	-2.06492	-1.1047	0.961994
P10153	1	RNASE2	-0.66658	0.290424	0.9568
P37268	15	FDFT1	-0.32193	0.598365	0.921436
P29966	6	MARCKS	0.096262	1.010064	0.913033
P15104	10	GLUL	-0.32013	0.587845	0.908429
P48163	16	ME1	-1.52699	-0.63039	0.896078

3.1.2. GO-term enrichment analysis

Gene ontology (GO) terms are key phrases annotated to genes and proteins in public databases that describe associated biological processes, molecular functions, and cellular components. GO-term enrichment analysis is a way to analyse larger datasets such as transcriptomes and proteomes and ask whether any particular biological pathways or functions are common features in genes that are differentially regulated in one's dataset. To do this, I used the GO-term enrichment tool available at geneontology.org [351–353], analysing biological process terms, and input the top 40 upregulated proteins (fold changes), or the top 40 downregulated proteins (fold changes) after applying a filtering criterion of q value <0.01. As a comparator, I used both the automatically generated list of human genes, and a list of all 7458 proteins identified in the screen. Statistical significance was associated with a False Discovery Rate (FDR)-corrected p value of <0.05. There were no significantly enriched terms for the upregulated proteins (not graphed). I found between five and nine GO-terms enriched for the downregulated proteins, including several terms relating to antiviral defence such as interferon-gamma signalling pathway and MHC Class II assembly (Figure 3-2). This was intriguing as US28 has not previously been associated with modulation of interferon responses nor MHC Class II (which is itself interferon-gamma inducible [354]), though it can bind human chemokines and act as a 'chemokine sink' during productive infection [166].

GO-term enrichment: Downregulated by US28-WT vs All Human Genes



GO-term enrichment: Downregulated by US28-WT vs Proteome

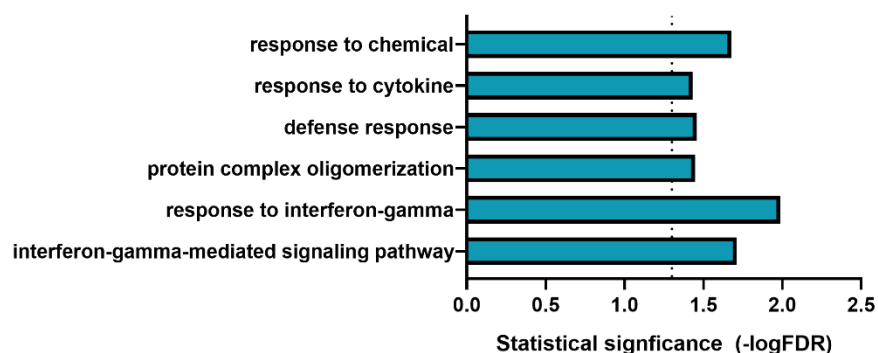


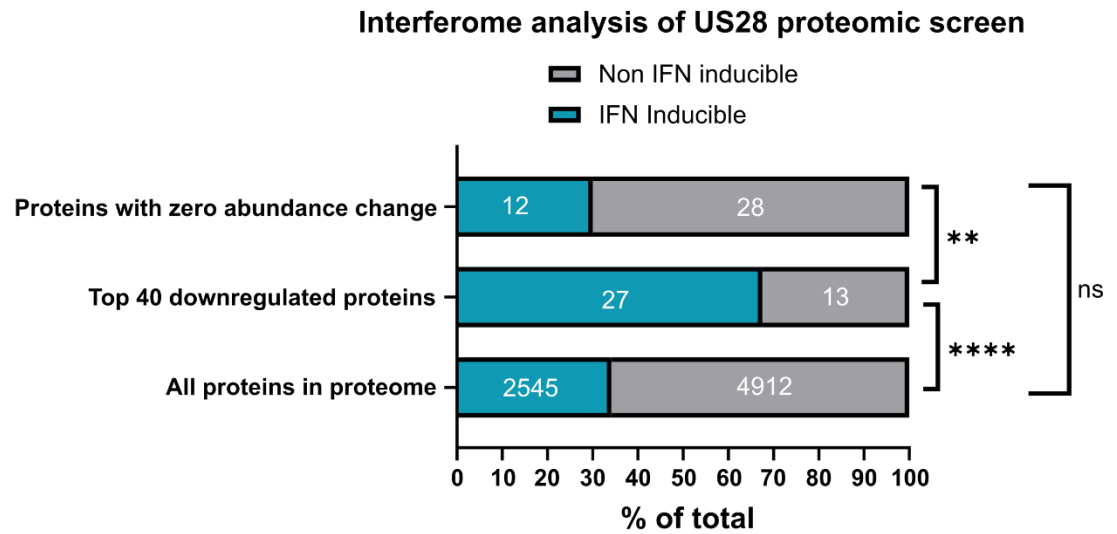
Figure 3-2 **GO-term enrichment analysis of genes downregulated by US28-WT.** Gene IDs from were input into the GO-term enrichment database search feature of geneontology.org and compared with either all human genes (upper panel) or all proteins identified in the proteomic screen (lower panel). Biological process GO-terms enriched in each comparison with a FDR-corrected value of <0.05 are graphed.

3.1.3. Interferome analysis

Following GO-term analysis, I wanted to use a specialist tool, Interferome, (v2.01, www.interferome.org) [355] to analyse the downregulated proteins in my dataset. Interferome uses existing microarray and transcriptomic datasets for genes induced or downregulated by treating cells with Type I, Type II, or Type III interferon. I input the 40-most significantly downregulated genes, or the 40 genes which showed zero change in abundance, or the entire dataset into the tool, filtering for human genes and those which are induced at least 2.0-fold. Two-thirds (27/40) of the most downregulated proteins we identified are Type I or Type II interferon-inducible (Figure 3-3). In contrast, of the 40 proteins which showed no changes (fold change = 0) in abundance between US28-WT and US28-R129A, 12/40 (30%) were included in the Interferome database, and 34% of all proteins in the proteome were included in the Interferome

database. Fisher's Exact contingency analysis supports that downregulated proteins are significantly more likely to be interferon-inducible (Figure 3-3). One of the downregulated proteins was annotated as Type III interferon-inducible, but it is worth noting that there are far fewer datasets for Type III interferon included in the Interferome database. Overall, global analyses of the US28-proteomic dataset reveal that US28 likely reduces the basal levels of Type I and Type II interferon-inducible genes in a signalling-dependent manner.

A



B

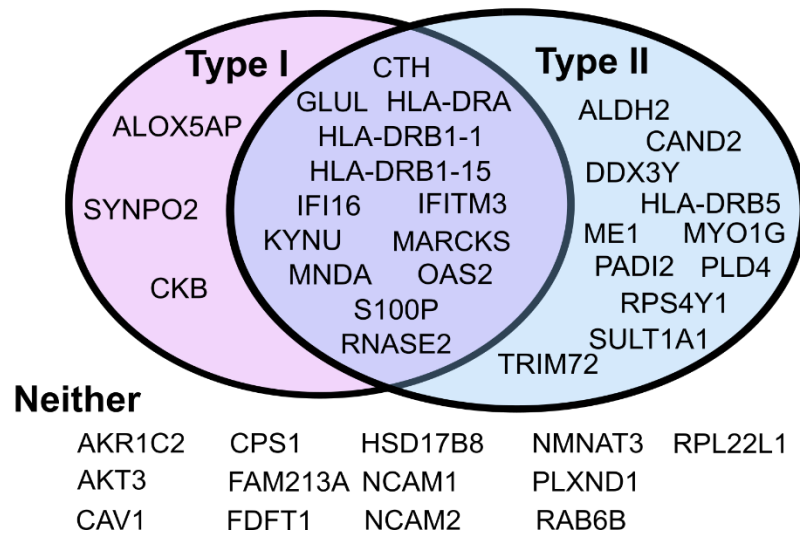


Figure 3-3 **US28 downregulates Type I and Type II interferon-inducible proteins.** The gene IDs of the top 40-downregulated proteins identified in the screen (Table 3-2), or those of the 40 proteins which showed zero fold change, or the whole list of identified proteins, were entered in the Interferome database search function and noted if they were positively inducible by either Type I or Type II interferon. A) The proportions of each of these datasets which were positively interferon inducible was calculated and graphed (raw numbers of proteins in white). Contingency analysis of these groups (Fisher's Exact) was performed comparing each group in turn. **: $p < 0.01$; ****: $p < 0.0001$; ns: not significant. B) Interferome-based annotation of Type I and Type II interferon-inducible proteins downregulated by US28, as well as those in the group of 40 which were not recorded as interferon-inducible ('Neither').

3.1.4. US28 expression reduces STAT1 phosphorylation

To follow up the global effect on Type I and Type II interferon-inducible proteins, I decided to assess STAT1 abundance and phosphorylation status, since STAT1 mediates both Type I and Type II signalling pathways. I predicted that relative phosphorylated STAT1 levels (Tyr701 phosphorylation) would be lower in the US28-WT cells compared with US28-R129A and empty vector cells. By Western blot, I found that US28-WT decreases the absolute levels of total STAT1 and phosphorylated STAT1 compared with both empty vector cells, and US28-R129A cells. Furthermore, and as expected, after correcting for total levels of STAT1, I found that the relative levels of phosphorylated STAT1 were decreased in US28-WT compared with empty vector and US28-R129A cells (Figure 3-4). Unexpectedly, US28-R129A cells had higher levels of STAT1 and phosphorylated STAT1 compared with empty vector cells. This apparent induction of STAT1 and STAT1 activation by US28-R129A is unexplained and not predicted by the proteomic data. Nevertheless, US28-WT overexpression decreases STAT1 levels and phosphorylation, providing an obvious mechanism for the downregulation of Type I and Type II interferon-inducible genes during the steady state.

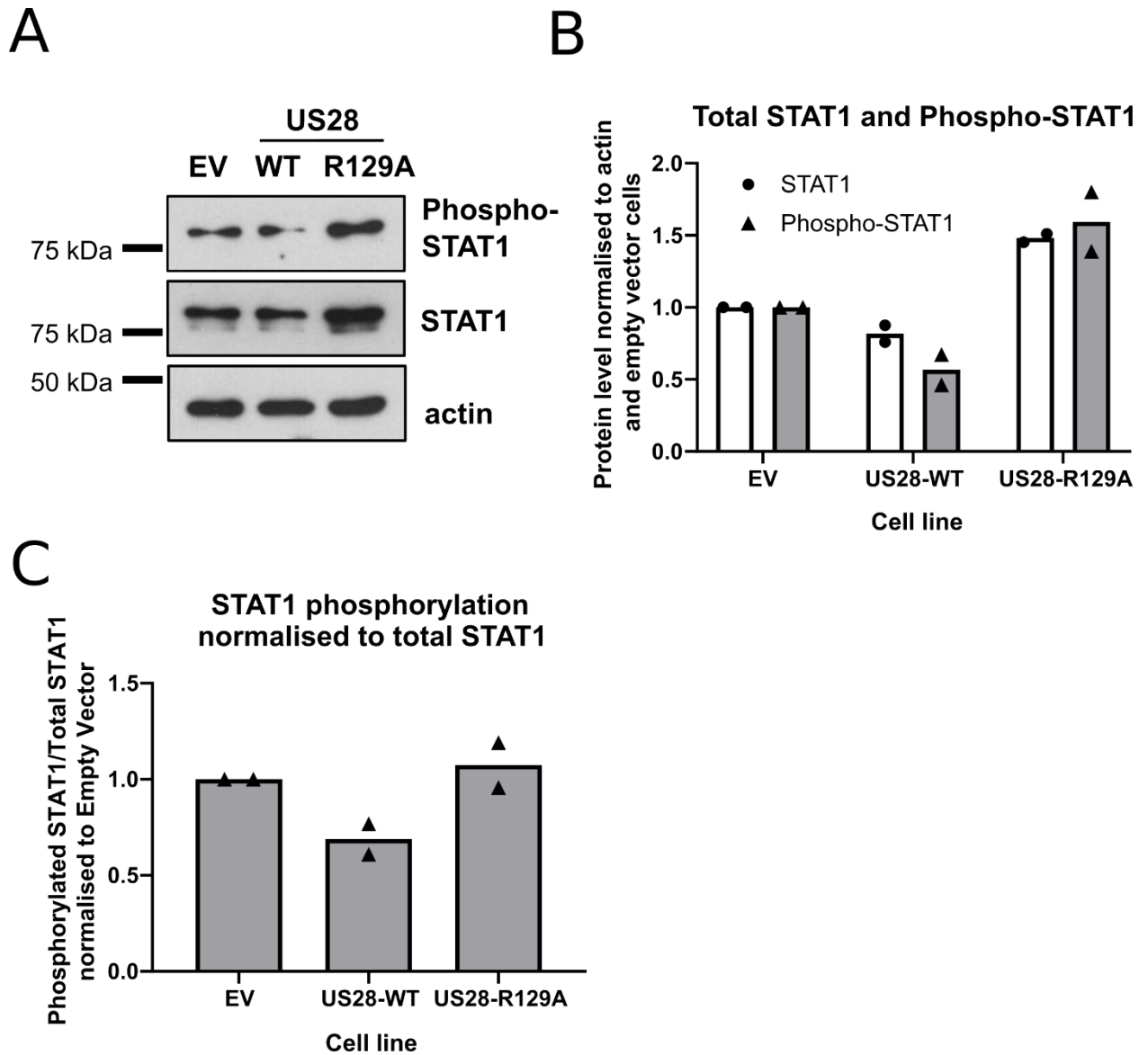


Figure 3-4 **US28-WT decreases STAT1 and phosphorylated STAT1**. A) Western blot of lysates from EV, US28-WT, and US28-R129A THP-1 cells for phospho-STAT1 (Tyr701), total STAT1, and beta-actin. B and C) Quantification of STAT1 and phospho-STAT1 band intensity from two Western blots from two independent samples of transduced THP-1 cells. B) shows bands normalised to actin, and C) shows phospho-STAT1 levels relative to total STAT1.

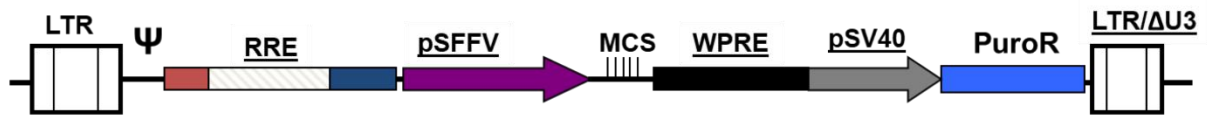
3.2. Validation of selected proteins from the US28-associated proteome

3.2.1. MNDA and IFI16 are downregulated by US28-WT

Several interferon-inducible proteins showing decreased expression were of interest as potentially important targets for US28 during HCMV latency. These included PYHIN-family proteins MNDA (9 unique peptides; 5.0-fold downregulated compared to US28-R129A) and IFI16 (4 unique peptides; 2.4-fold downregulated compared to US28-R129A). These two related proteins piqued my interest because, as detailed in the introduction, IFI16 is a restriction factor for viral replication, and MNDA is a myeloid-specific PYHIN protein with a putative role in myeloid cell apoptosis. I began by confirming US28-WT-mediated downregulation of these proteins in independently-transduced US28-expressing THP-1 cells. I used the same lentiviral constructs as were used in the proteomic screen and in Krishna et al [189] to transduce THP-1 cells. A map of the construct, which drives US28 expression from the SFFV promoter, is given in Figure 3-5. After generating these fresh US28-expressing cell lines, I checked expression levels of US28-WT or US28-R129A by RT-qPCR and Western Blot (Figure 3-5) to confirm near-equivalent protein expression. The multiple species of US28 detected by Western blot is consistent with previously published western blot detection of US28 [186,193], and likely in part reflects differential levels of glycosylation on the predicted N-glycosylation site in the US28 N-terminal domain (Predicted in UniProt entry P69332). While the overall average levels of US28 protein expression was near-equivalent in the different US28-expressing cell lines, it is possible that there were differences in the relative levels of the individual US28 species. This could have potential consequences for localisation and subsequent function of US28, particularly if any differences are due to glycosylation differences. It would be beneficial to check this by deglycosylation of proteins within cell lysates, and confocal microscopy of immunostained US28-expressing cells with relevant organelle markers.

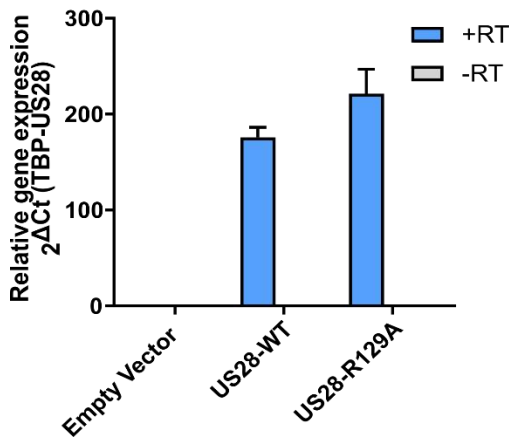
A

#1253 pHRsin pSFFV MCS(-) pSV40 Puro

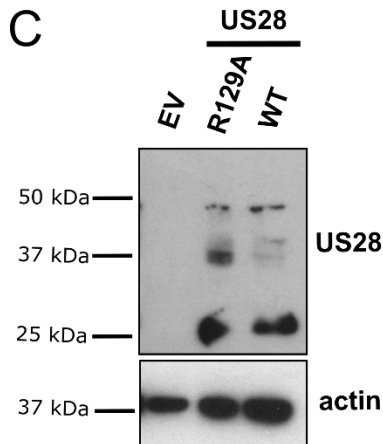


B

US28 steady state mRNA



C



D

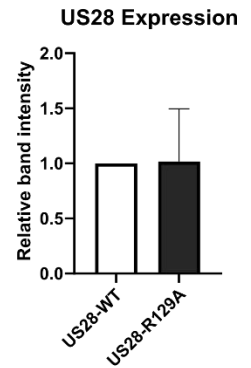


Figure 3-5 **Generation of independently-transduced US28-expressing cell lines.** A) The lentiviral vector into which the sequence encoding US28-WT or US28-R129A had previously been cloned. LTR: long terminal repeat; Ψ : the psi lentiviral packaging element; RRE: rev response element; pSFFV: the spleen focus-forming virus promoter; MCS: multiple cloning site; WPRE: Woodchuck Hepatitis Virus Posttranscriptional Regulatory Element; pSV40: the SV40 promoter; PuroR: the puromycin resistance gene; LTR/ Δ U3: long terminal repeat deleted for the 3' unique region. B) RT-qPCR analysis of US28 expression in transduced cell lines. +RT reactions included reverse transcriptase. -RT reactions did not include reverse transcriptase and control for genomic DNA contamination. C) Cells from B were lysed and subject to western blot for US28, and actin as a loading control. D) Quantification of three western blots for US28 expression. Intensities of all US28-specific bands shown in (C) were summed to generate these data.

I then used RT-qPCR confirmed that IFI16 and MNDA are both downregulated in US28-WT-expressing cells compared to those expressing the signalling mutant R129A (Figure 3-6). Subsequently, I confirmed this US28-WT mediated downregulation of IFI16 and MNDA at the protein level by western blot (representative blots and quantification of four independent experiments are shown in Figure 3-7). Unexpectedly, and similarly to the observations with STAT1, US28-R129A seemed to induce IFI16 and MNDA above empty vector cell lines. This was not predicted by the US28 proteomic data, where the relative abundance of US28-R129A:empty vector was 0.865 for IFI16 and 0.765 for MNDA, a slight drop compared with empty vector control.

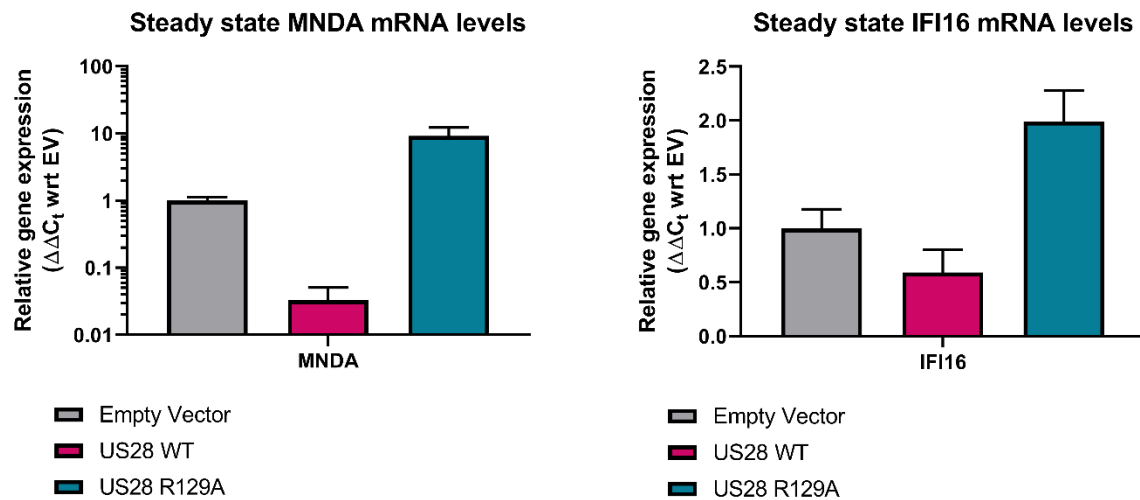


Figure 3-6 **Steady state levels of MND A and IFI16 mRNA in US28-expressing cells.** Relative levels of IFI16 and MND A mRNA were assessed by RT-qPCR in US28-expressing THP-1 cells. Levels of IFI16, and MND A, were normalised to TBP and then to Empty Vector using the $\Delta\Delta C_t$ method.

Despite the unexpected result for US28-R129A cells, it still stands that US28-WT expressing THP-1 cells downregulate IFI16 and MND A compared with cells expressing a mutant US28 at similar levels but which is deficient for latency establishment. This US28-mediated downregulation of IFI16 and MND A appears to be occurring at the level of steady state RNA, leading to a lack of protein expression of these two PYHINS.

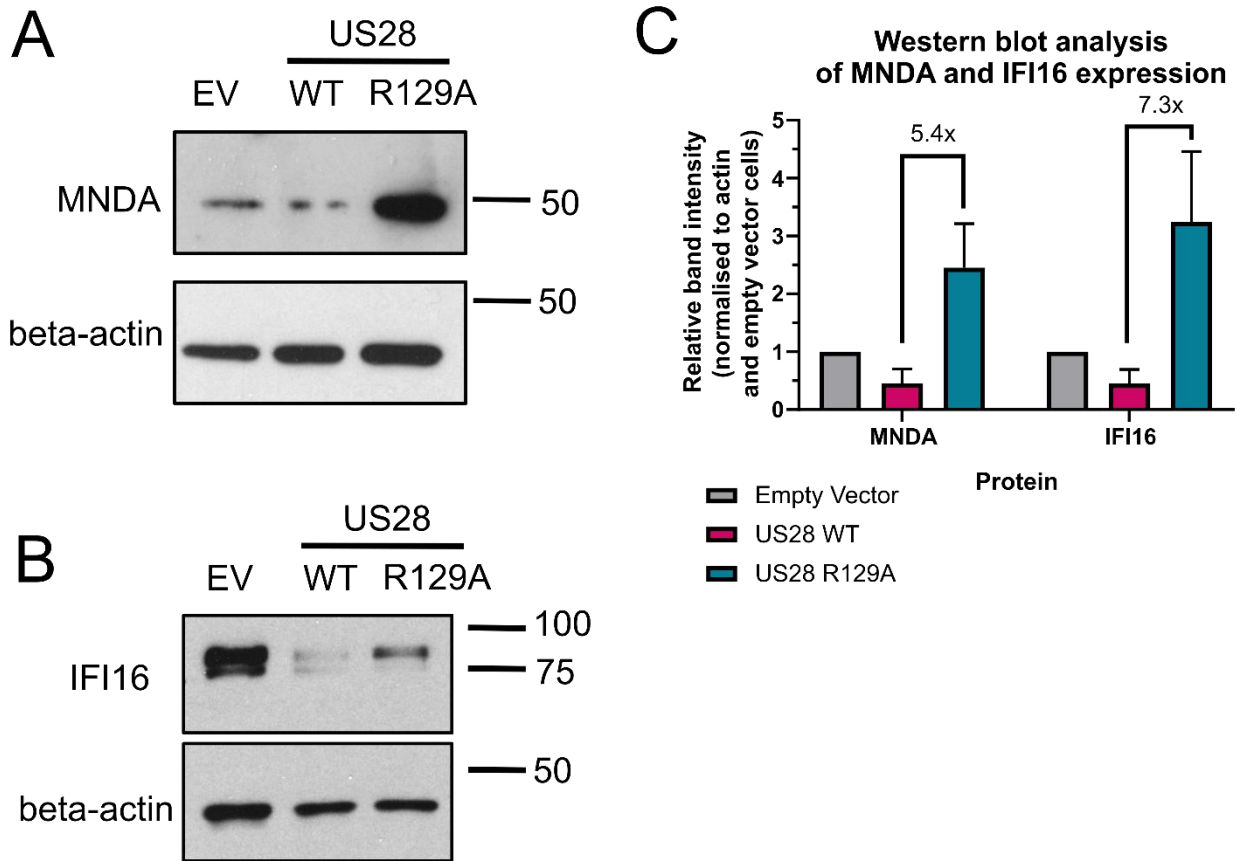


Figure 3-7 **US28-WT downregulates MNDA and IFI16.** Lysates from US28-expressing THP-1 cells and controls were separated by SDS-PAGE and analysed for MNDA (A) and IFI16 (B) levels by Western blotting. C) Four independent Western blot analyses were subject to band intensity analysis using the 'Analyse Gels' feature of ImageJ and the relative levels of MNDA and IFI16 calculated compared to empty vector cells. US28-R129A had 5.4X and 7.3X higher levels of MNDA and IFI16, respectively, compared to US28-WT cells.

3.2.2. Downregulation of steady-state levels of HLA-DR by US28

The apparent downregulation of MHC Class II components HLA-DRA, HLA-DRB1-15, HLA-DRB1-1, and HLA-DRB5, was also an interesting observation as this has clear and documented implications for CD4⁺ T cell recognition [139]. Interestingly, the proteomic data predicts that both US28-WT and US28-R129A expressing THP-1 cells downregulate these MHC Class II components compared with empty vector control cells, but that US28-WT more extensively downregulates these proteins. To validate these observations, I first examined HLA-DRA RNA expression by RT-qPCR; HLA-DRA was chosen as it aids primer selection because it is not as polymorphic as the HLA-DRB genes. These data suggest that, for at least HLA-DRA, US28-WT expressing cells have similar levels of transcript to empty vector cells, but US28-R129A cells have more HLA-DRA transcript (Figure 3-8). Again, this is not predicted by the proteomic data, but is in accordance with my observations of STAT1, MNDA, and IFI16.

I next decided to look at cell-surface expression of HLA-DR protein by flow cytometry, since that is ultimately the place where HLA-DR will likely be functional. Here, the results were in good accordance with the proteomic dataset (Figure 3-8) and showed that US28-WT cells have approximately half as much cell-surface HLA-DR compared with US28-R129A cells, and these in turn have 85% less HLA-DR than empty vector cells.

I then decided to examine whether the inhibition of cell surface expression of HLA-DR by US28 could be overcome by addition of interferon-gamma (IFN γ), which is a known potent inducer of HLA-DR expression at the level of transcription. In a single experiment, I found that a 24 hour treatment with 1 ng/mL of IFN γ increased cell-surface expression of HLA-DR on US28-WT and R129A cells to similar levels, potentially suggesting that US28-WT does not prevent the cell from responding to IFN γ despite lower levels of STAT1. However, a titration of IFN γ with a number of repeats is required to draw strong conclusions.

Taking these results together, I propose that there are at least two mechanisms by which US28-WT is able to target cell-surface HLA-DR. One of these mechanisms is signalling dependent, as evidenced by the lower levels of HLA-DRA transcript and cell-surface HLA-DR on US28-WT cells compared with US28-R129A cells. The second mechanism is G protein signalling-independent, as evidenced by the lower levels of cell-surface HLA-DR of US28-R129A cells compared with empty vector cells. This could be mediated via ligand-inducible signalling and/or a beta-arrestin dependent pathway which can act on G protein downstream targets independently of G protein signalling [356,357].

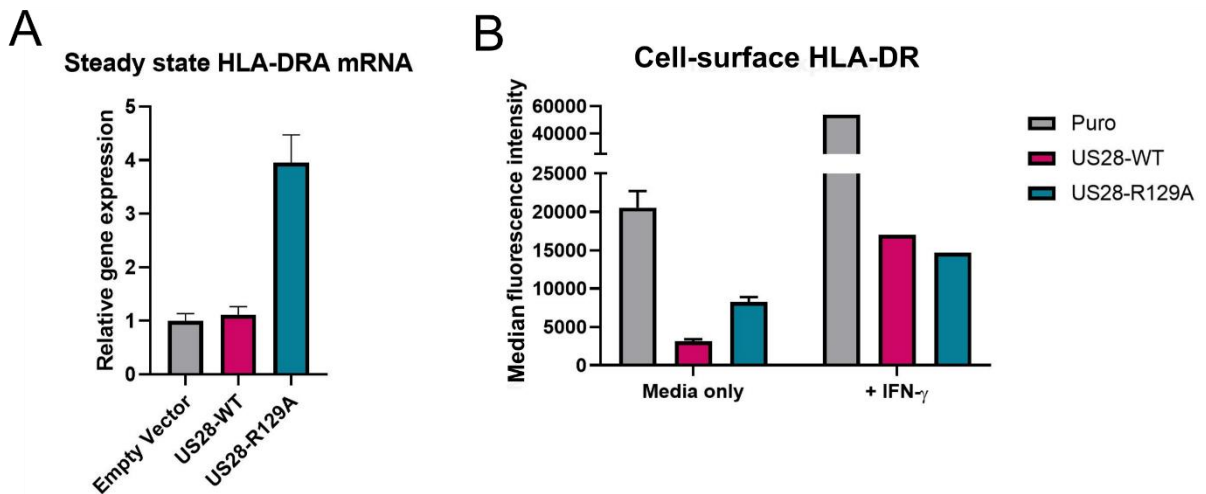


Figure 3-8 **US28-WT downregulates cell surface HLA-DR.** A) RT-qPCR of HLA-DRA in US28-expressing THP-1 cells. Levels of HLA-DRA were normalised to TBP and then to Empty Vector using the $\Delta\Delta C_t$ method. B) Flow cytometry analysis of cell-surface HLA-DR expression in the steady state (media only) or in the presence of IFN γ .

3.3. Mechanism of US28-mediated downregulation

An obvious next question is how US28 downregulates IFI16, MNDA, and HLA-DR. Global analysis of the proteome and subsequent analysis of STAT1 phosphorylation suggests that attenuation of the interferon response pathway, including STAT1, is involved (§3.1). However, c-fos, a component of the activator protein-1 complex, is also capable of activating IFI16 and HLA-DR transcription [358–360], and is attenuated by US28-WT in myeloid cells [193]. The best way to determine which signalling pathways US28 uses/attenuates to downregulate these genes would be to use pharmacological activators of the pathways to try to restore host gene expression; however, no such activator exists as far as I am aware. As an alternative, I used inhibitors of these pathways: Ruxolitinib is a pan-Janus kinase inhibitor, upstream of STAT signalling, and T-5224 blocks c-fos binding to DNA. Both inhibitors had to be solubilised in DMSO, which becomes a confounding factor because DMSO itself likely activates the AP-1 pathways [361,362] and activates transcription of p204 (often thought of as the IFI16 homologue) in mice [363]. Due to the respective solubilities of the inhibitors, the final concentration of DMSO in T-5224- treated samples was 0.5%, and the final concentration of DMSO in Ruxolitinib-treated samples was 0.03%. Despite this potential confounding factor, I proceeded with these treatments. I validated that Ruxolitinib blocked STAT1 phosphorylation (Figure 3-9 A). I then looked at expression of IFI16 and HLA-DR (Figure 3-9 B, D, E) and found that Ruxolitinib partially reduced IFI16 expression in all three cell lines, but

downregulated HLA-DR only in the US28-R129A cell line. IFI16/HLA-DR expression in empty vector or US28-R129A expressing cells could not be 'normalised' to levels found in US28-WT by Ruxolitinib. Therefore, phosphorylated STAT1 likely plays a role, but cannot be the entire mechanism by which IFI16 and HLA-DR are attenuated in US28-WT cells. In the case of T-5224, inhibition of c-fos partially reduced IFI16 and HLA-DR expression in US28-R129A cells, and almost reduced expression of these genes to US28-WT levels in the empty vector cells (Figure 3-9 C,D,E). While the interpretation of these observations is not straightforward, I believe these data indicate that c-fos is also playing a role in the US28-mediated downregulation of IFI16 and HLA-DR. Quite unexpectedly, T-5224 induced HLA-DR and IFI16 expression in US28-WT cells. I think this could be due to a basal level of c-fos being required for the expression of a host gene that is needed by US28-WT to attenuate the numerous cellular signalling pathways; one candidate gene for this is the AP-1 inducible phosphatase DUSP1 [364] which will require further investigation.

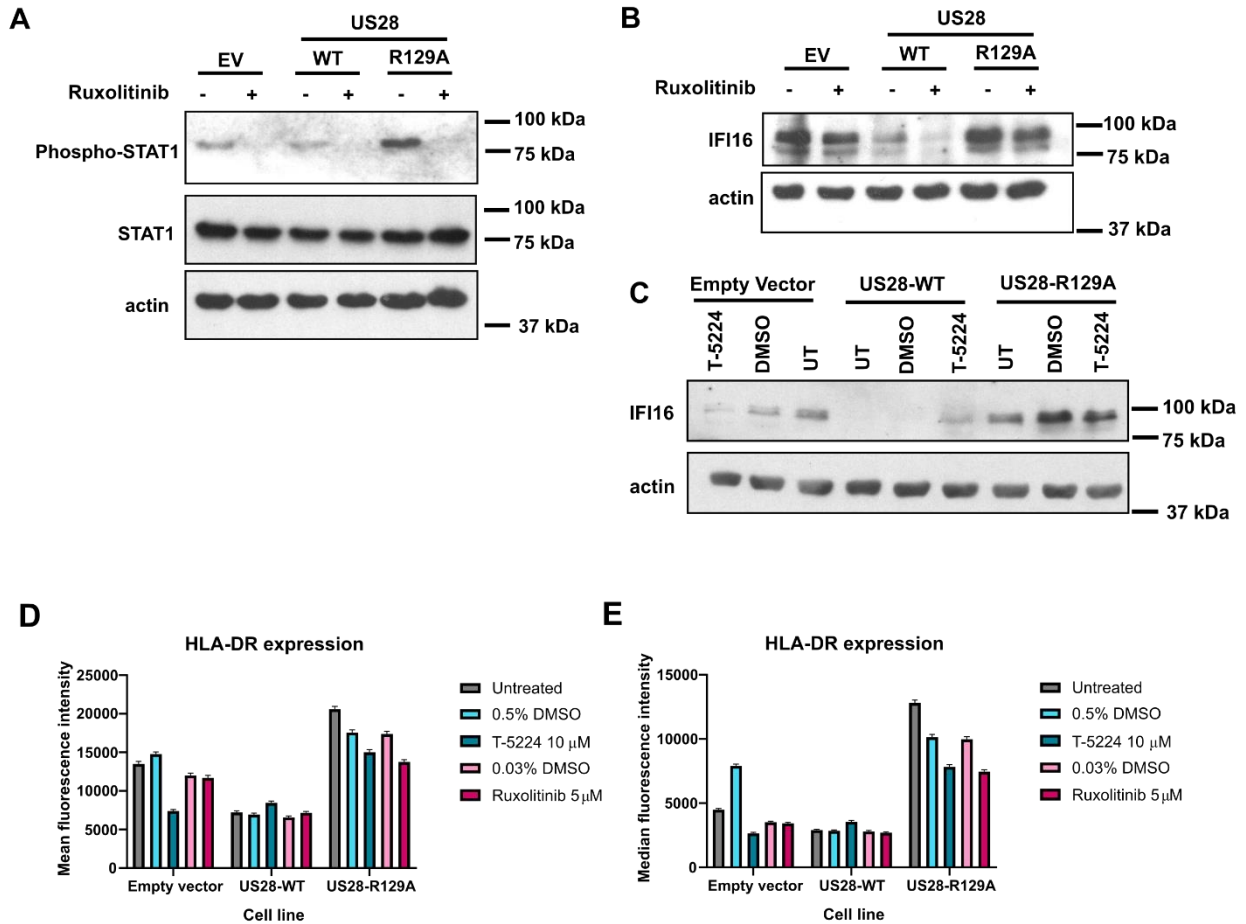


Figure 3-9 Effect of Janus kinase and c-fos inhibition on IFI16 and HLA-DR expression. A) Empty vector, US28-WT, and US28-R129A THP-1 cells were treated with 10 μ M ruxolitinib or DMSO as a control for 48 hours. Lysates from these cells were then subject to western blot for phospho-STAT1 (Tyr701), STAT1, and actin as a control. B) As (A) but instead membrane was probed for IFI16 and actin. C) Empty vector, US28-WT, and US28-R129A THP-1 cells were treated with 5 μ M T-5224 or DMSO as a control for 48 hours. Lysates from these cells were then subject to western blot for IFI16 and actin. D and E) Cells were treated as A) and C) and then subject to cell surface HLA-DR analysis by flow cytometry. Similar-coloured DMSO controls indicate corresponding concentrations of DMSO to inhibitors. D) Shows the mean fluorescence intensity and E) the median fluorescence intensity. I treated the cells with the inhibitors, and a colleague, Eleanor Lim, performed the cell-surface staining for HLA-DR and flow cytometry. I analysed the data generated.

3.4. Downregulation of IFI16, MNDA, and HLA-DR during latency

3.4.1. Introduction

IFI16, MNDA, and HLA-DR were all downregulated in THP-1 cells expressing US28-WT compared with US28-R129A, the signalling mutant that is deficient for latency establishment. The next logical step was to determine whether these three selected proteins were also downregulated during HCMV latency, itself.

To analyse whether HCMV latent infection downregulates IFI16, MNDA, and HLA-DR, I needed to use fluorescently labelled viruses because (i) our model never results in more than 20% infected cells, with an average closer to 5%, and (ii) expression of viral proteins during latency is not readily detectable by immunofluorescence (though I will show later that US28 expression is detectable when a C-terminal tag is incorporated into the ORF). I use immunofluorescence or flow cytometry to detect infection throughout this section, and analyse genes of interest in comparison with fluorescent marker negative bystander cells, which have previously been shown to be uninfected on the basis of viral gene expression and differentiation-induced reactivation [349].

3.4.2. Initial observations with TB40/E IE2-2A-eGFP SV40mCherry virus

I analysed CD14⁺ monocytes infected with TB40/E SV40 mCherry/IE2-2A-GFP. This virus drives constitutive mCherry expression in both latently and lytically infected cells via the SV40 promoter, but GFP expression is restricted to lytically infected cells as a result of IE2 expression, which is linked to GFP by the self-cleaving peptide 2A. Therefore, I was able to distinguish IE2-positive (lytic) from IE2-negative cells (one hallmark of latency) amongst infected, mCherry positive cells. At four days post infection (d.p.i.), I fixed and immunostained the monocytes for our cellular proteins of interest in mCherry positive, IE2-2A-GFP negative cells (Figure 3-10). As a control, I also differentiated monocytes with phorbol 12-myristate 12-acetate (PMA), which drives IE2-2A-GFP expression through differentiation-dependent reactivation [365]. I found that IFI16, MNDA, and HLA-DR were all downregulated in latently infected, mCherry positive but IE2-negative, CD14⁺ monocytes.

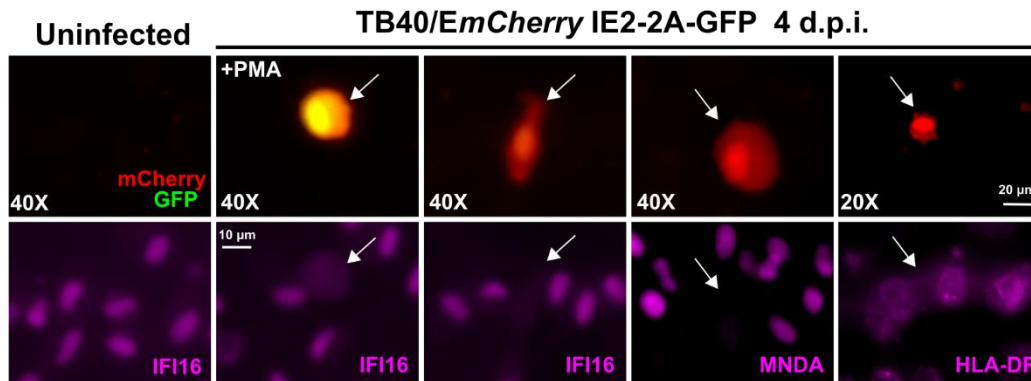


Figure 3-10 **HCMV latent infection is associated with downregulation of IFI16, MNDA, and HLA-DR.** Primary CD14⁺ monocytes were isolated from peripheral blood or apheresis cones as described in Materials and Methods. The monocytes were latently infected with TB40/E SV40-mCherry IE2-2A-GFP and stained by immunofluorescence for IFI16, MNDA, or HLA-DR as indicated at four d.p.i and imaged by widefield fluorescence microscopy. Top left image: Uninfected monocytes. Second from the left: Monocytes were treated +PMA (to permit lytic infection). mCherry (red) serves as a marker for infection and GFP (green) denotes expression from the IE2-2A-GFP cassette. Remaining panels: Monocytes were cultured in the absence of PMA. The absence of green fluorescence results from suppressed expression of the IE2-2A-GFP cassette and scored as IE negative. The magnification is indicated (40X or 20X). White arrows indicate corresponding cells in the upper and lower panels.

3.4.3. Time course of downregulation with TB40/E SV40eGFP

I then sought to look at expression of these proteins at earlier time points. US28 is a virion-associated protein [159], and incoming US28 is reported to have rapid effects on host cells [193]. I speculated that the downregulation of IFI16, MNDA, and HLA-DR might occur early during the establishment of latency, perhaps mediated by incoming functional US28. For these experiments, I used TB40/*Egfp* which marks infected cells with GFP expression via the SV40 promoter and confirmed the establishment of latency in this system by coculture of monocytes with fibroblasts either with or without PMA-induced reactivation (Figure 3-11 A, B). In this latency system, I found a stark and specific loss of IFI16 in infected monocytes from 24 hours post infection (h.p.i.) (Figure 3-11 C), a phenotype maintained at 48 and 72 h.p.i as measured by immunofluorescence. I quantified these observations in several fields of view for each of these three time points, and performed contingency analyses (Fisher's Exact), which confirmed specific loss of IFI16 in latently infected cells (Figure 3-11 D). Loss of IFI16 was observed in *ex vivo* infected monocytes at these time points in a total of four separate donors with TB40/*Egfp* virus.

I found a partial downregulation of MNDA by 72 h.p.i (Figure 3-11 E, F), with a very small downregulation at 48 h.p.i and no effect at 24 h.p.i, suggesting that modulation of MNDA is delayed compared with fellow PYHIN family member, IFI16.

For analysis of HLA-DR, I worked with monocytes infected in suspension and analysed cell surface expression by flow cytometry, working together with two PhD students in Mark Wills's laboratory, namely George Sedikides and Eleanor Lim. Together, we observed that HLA-DR, but not corresponding MHC Class I HLA-A,B,C, were downregulated at 72 h.p.i specifically in GFP positive, latently infected monocytes (Figure 3-11 G, H). Therefore, IFI16, MND4, and HLA-DR are indeed downregulated at early times during the establishment of latency in monocytes, with IFI16 showing downregulation within 24 hours of infection.

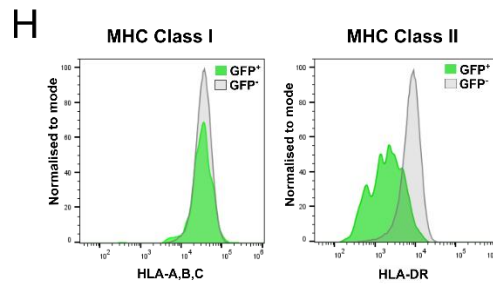
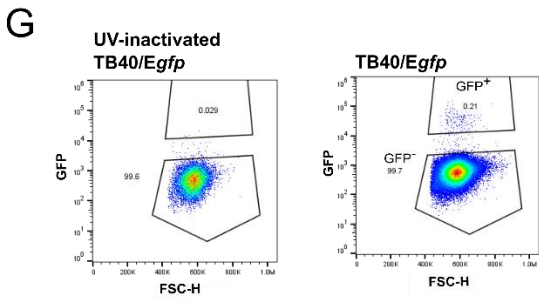
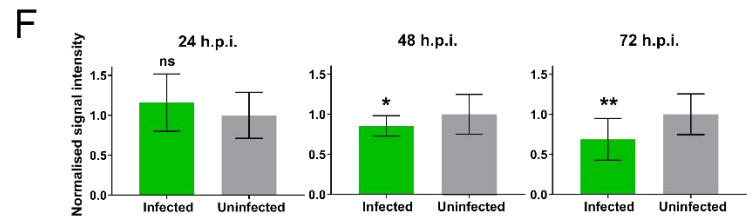
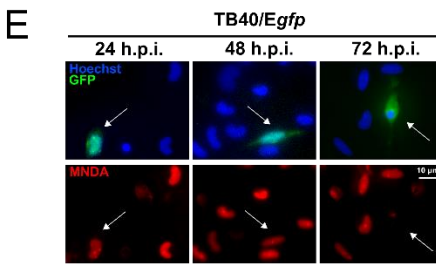
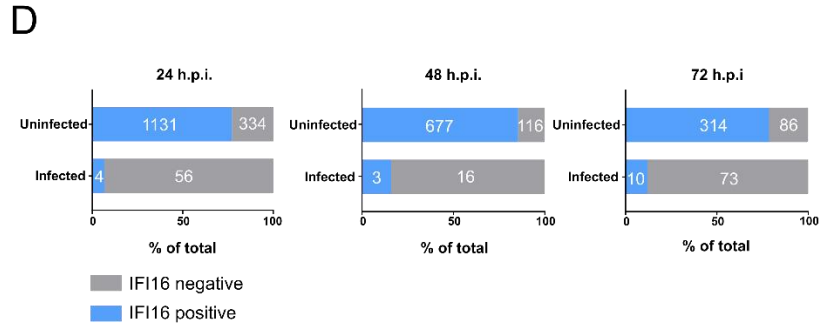
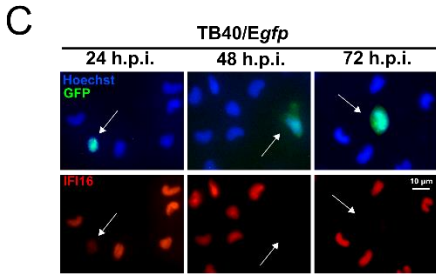
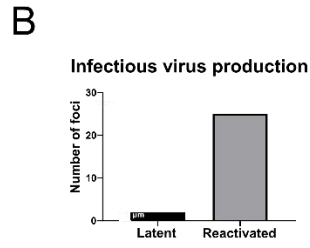
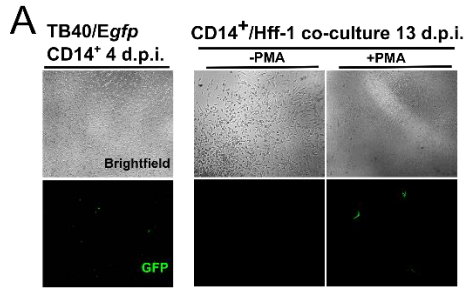


Figure 3-11 Time course of US28-target gene downregulation. A) Validation of experimental latency using TB40/*Egfp* virus. CD14⁺ Monocytes were infected and allowed to establish latency for 4 days (left panel, 10X magnification). Citrate wash buffer was used to remove externally bound virions. These latently infected cells were cultured +/-PMA for 3 days, and at 7 d.p.i, Hff-1 cells were added to the culture to demonstrate production of infectious virions. Transfer of virus to Hff-1 was monitored by fluorescence microscopy up to 13 d.p.i., B) Infected Hff-1 foci form (A) were counted and summed across the experiment (three wells of CD14⁺ monocytes per condition, graphed). C) CD14⁺ monocytes infected with TB40/*Egfp* stained by immunofluorescence for IFI16 at 24, 48, and 72 h.p.i. and imaged as before using 60X magnification. D) Quantification of IFI16 positive and negative monocytes in the uninfected and infected populations from two donors per time point. Raw numbers of cells are indicated in white text. Fisher's exact test indicates a statistically significant difference between uninfected and infected populations for each time point ($P < 0.0001$). E) CD14⁺ monocytes infected with TB40/*Egfp* were stained by immunofluorescence for MNDA at the indicated times and imaged as before using 60X magnification. F) Quantification of the signal intensity from infected monocytes at the indicated time points (n=9,7,10, respectively). MNDA signal intensity in each nucleus was normalised to the average of uninfected monocytes from each field of view. A *t*-test with Welch's correction was used to determine statistical significance. ns, not significant, * $P < 0.05$, ** $P < 0.01$. G) CD14⁺ monocytes infected with TB40/*Egfp* (+/- UV inactivation) were analysed for HLA-ABC and HLA-DR expression at three d.p.i. by flow cytometry. The gating strategy for identifying infected cells (GFP⁺) is shown. H) Histogram showing HLA-ABC and HLA-DR staining in HCMV-uninfected GFP-negative (grey) monocytes, and latently infected GFP positive (green) monocytes.

3.4.4. IFI16 is downregulated in a US28-dependent manner, but only in undifferentiated myeloid cells

Having confirmed that IFI16 is downregulated very early during latent infection of monocytes, I then sought to establish whether this effect is dependent on US28. I predicted this would be the case because of the results of our US28 proteomic screen and the established functionality of incoming virion-associated US28 [193]. I infected monocytes with either the US28-WT TB40/*EmCherry*-US28-3XFLAG HCMV (US38-3XF), or the corresponding US28 deletion virus TB40/*EmCherry*-US28 Δ (Δ US28). These viruses establish latent and lytic infections, respectively, in CD34⁺ progenitor cells, Kasumi-3 cells, and THP-1 cells [159,193], and I confirmed these phenotypes are also maintained in primary CD14⁺ monocytes by supernatant transfer to permissive fibroblasts (Figure 3-12 A). I was also able to detect US28 protein during the establishment of latency in monocytes by immunostaining for the FLAG epitope tag on the C terminus of US28 (Figure 3-12 B). This staining is the first time in our laboratory that we have been able to clearly observe intracellular expression of US28 using immunofluorescence during latency. The pattern of staining is could be an indication of ER or Golgi localisation, in addition to cell surface expression, and is in accordance with expression patterns of US28-3XFLAG via retroviral transduction in THP-1 cells (Figure 3-13) and US28 expression during lytic infection [366]. However, without using confocal microscopy and organelle markers, it is not possible to be certain of the subcellular localisation of US28.

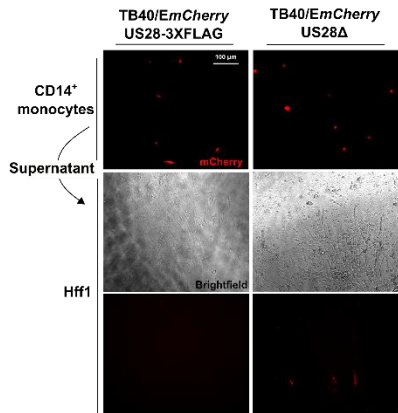
To determine if US28 specifically downregulates IFI16 in the context of infection, I compared the expression of this cellular protein in monocytes infected with US28-3XF or Δ US28. Consistent with Figure 3-11, I found that monocytes infected with the US28-3XF virus showed downregulation of IFI16 at 24 and 48 h.p.i., while monocytes infected with Δ US28 displayed robust IFI16 expression at 24 h.p.i. (Figure 3-12 C, D) and only partial downregulation at 48 h.p.i (Figure 3-12 C, E). These data demonstrate that the early downregulation of IFI16 in CD14⁺ monocytes is dependent on US28.

It would have been interesting to see whether the downregulation of MND4 and HLA-DR is also dependent on US28, but the delayed kinetics/partial phenotype associated with MND4 downregulation, and the requirement for large number of cells to perform quantitative assessment of HLA-DR expression on latently infected monocytes, precluded these studies.

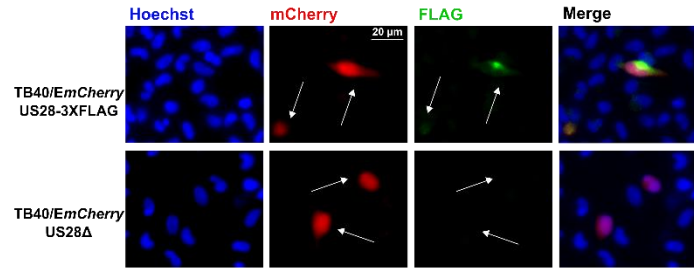
Work from the laboratory has previously showed that US28 modulates cellular signalling pathways in undifferentiated, but not differentiated THP-1 cells [189]. I was therefore curious as to whether the effects on IFI16 expression were dependent on cellular differentiation status. This is significant because differentiated THP-1 cells and mature dendritic cells are permissive for HCMV lytic infection. To analyse whether these effects are differentiation-dependent, I transduced THP-1 cells with a lentiviral vector that co-expresses US28 and the fluorescent protein Emerald (US28-UbEm), or co-expresses eGFP and Emerald (empty UbEm), as a control. For each population, the Emerald-positive THP-1 cells were isolated by FACS (Figure 3-12 F) and I validated US28 expression by RT-qPCR (Figure 3-12 G). I treated half of these cells with PMA in order to induce cellular differentiation. I found that undifferentiated US28-expressing THP-1 cells downregulated IFI16, but PMA-differentiated cells did not downregulate IFI16 (Figure 3-12 H), suggesting latency-associated expression of US28 attenuates IFI16 expression.

I also analysed the effect of cellular differentiation on IFI16 expression following infection in mature dendritic cells derived by treating *ex vivo* CD14⁺ monocytes with GM-CSF/IL-4/LPS. Again, I found that undifferentiated infected CD14⁺ monocytes downregulate IFI16 in a US28-dependent manner at 48 h.p.i, while infected mature dendritic cells do not downregulate IFI16 with WT or Δ US28 HCMV (Figure 3-12 I). Taken together, these results indicate that US28 rapidly downregulates IFI16 during latent infection of monocytes, but not during lytic infection of mature dendritic cells.

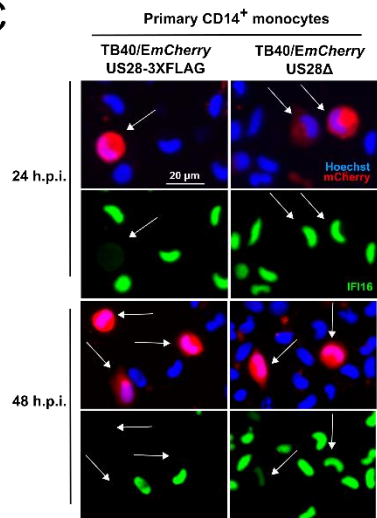
A



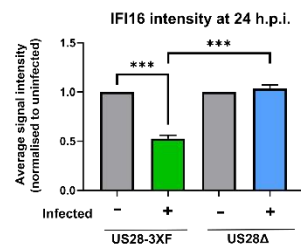
B



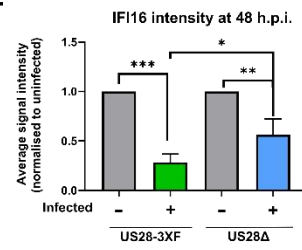
C



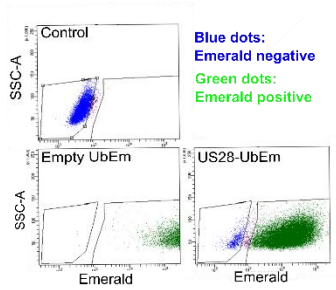
D



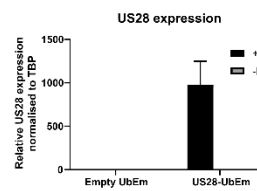
E



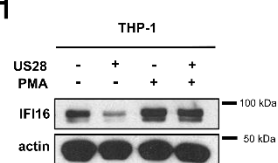
F



G



H



I

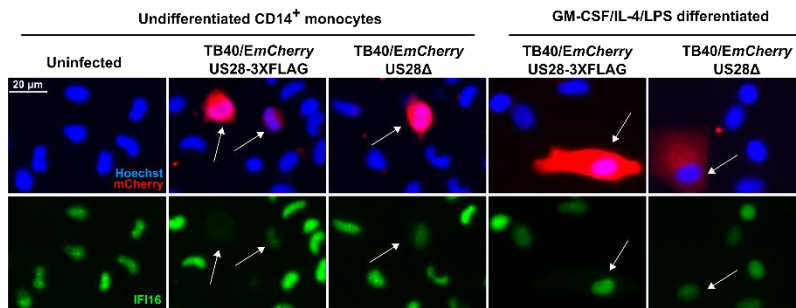


Figure 3-12 IFI16 is rapidly downregulated in a US28-dependent manner during latent infection. CD14⁺ monocytes were infected with either US28 WT TB40/EmCherry-US28-3XFLAG HCMV or the Δ US28 equivalent. A) Validation of the latent and lytic phenotypes associated with US28-3xF and Δ US28 monocyte infections, respectively. At 7 d.p.i., supernatant from infected CD14⁺ cells (upper panel) were transferred to Hff1 cells (middle brightfield and lower mCherry panels) and formation of plaques was monitored and imaged at 20X magnification. B) Detection of US28-3XFLAG during the establishment of latency in CD14⁺ monocytes. At 2 d.p.i. US28-3xF or Δ US28-infected CD14⁺ monocytes were fixed and stained by immunofluorescence for US28-3XFLAG using an anti-FLAG antibody and imaged at 40X magnification. C) US28-3xF and Δ US28-infected monocytes were stained by immunofluorescence for IFI16 at the indicated times and imaged using 40X magnification. White arrows indicate corresponding cells. D and E) IFI16 signal intensity in each nucleus was normalised to the average of the uninfected cells in a field of view. The results of three fields of view were then averaged to derive the resulting average signal intensities for each subpopulation of monocytes at the indicated time points infected with US28-3xF or Δ US28 HCMV. Statistical significance was determined using one-way ANOVA. *** indicates $P < 0.001$, ** indicates $P < 0.01$, and * indicates $P < 0.05$. F) The sequence encoding US28 was cloned into the lentiviral plasmid pUbEm (US28-UbEm), and this or empty UbEm plasmid was used to transduce THP-1 cells, which were subsequently cell-sorted for Emerald expression. G) US28 expression was validated in the cells from (F) by RT-qPCR. US28 RNA was normalised to cellular TBP and presented as 2- Δ Ct. H) US28 expressing and empty vector THP-1 cells were either left untreated or treated with PMA for 48 hours before cell lysates were harvested. These lysates were then subject to western blotting for IFI16 and beta-actin as a loading control, with molecular weight markers annotated. I) At 48 h.p.i, either undifferentiated CD14⁺ monocytes, or monocytes pre-differentiated for 7 days with GM-CSF/IL-4/LPS, were fixed and stained for IFI16 and imaged as before at 40X magnification. White arrows indicate corresponding infected cells.

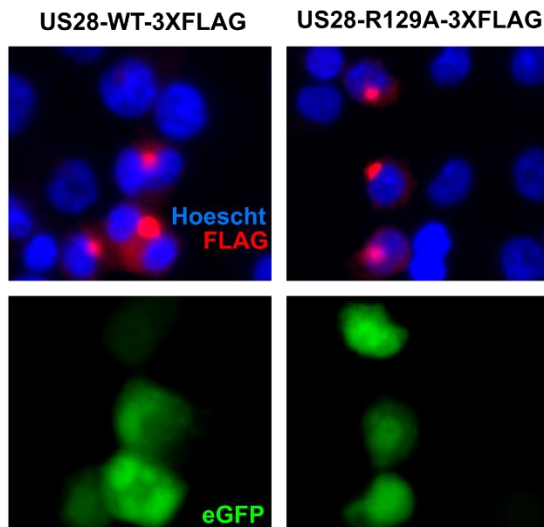


Figure 3-13 US28 immunostaining in transduced THP-1 cells. Retroviral plasmids encoding US28-WT (from TB40/E) or R129A, each with a C-terminal 3XFLAG tag, and an eGFP marker, were used to transduce THP-1 cells. They were then subject to immunofluorescence staining for the 3XFLAG tag.

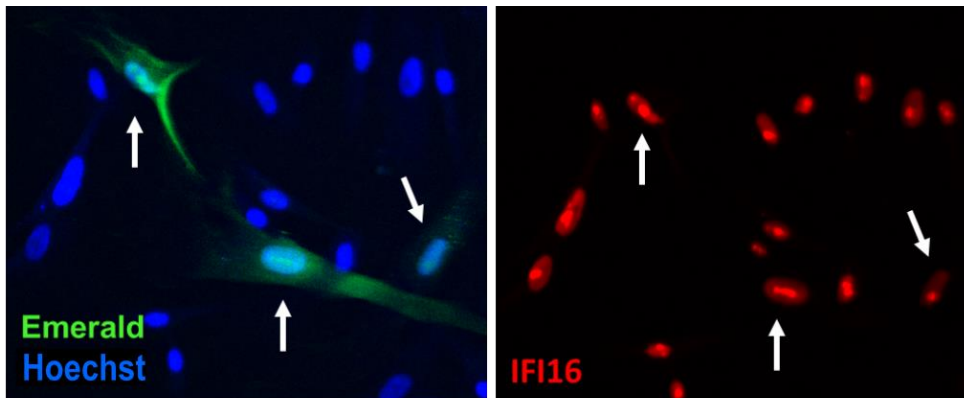


Figure 3-14 **Fibroblasts which overexpress US28 do not downregulate IFI16.** Hff1 cells were transduced with the US28-UbEm lentiviral vector as in Figure 3-12 and then fixed and stained for IFI16 expression. White arrows indicate transduced cells.

Additionally, I used the US28-UbEm to transduce fibroblasts (Hff1) cells, and left these as a mixed population. Indirect immunofluorescence of transduced Hff1 cells shows no difference in IFI16 expression with or without US28 expression (Figure 3-14).

I also analysed IFI16 expression in fibroblasts (Hff1) and epithelial cells (RPE-1), which both undergo lytic infection. Previous work suggests that IFI16 expression is not modulated by lytic infection of fibroblasts [79,208,367]. In contrast, when I infected both fibroblasts and epithelial cells with the TB40/E SV40mCherry strain of HCMV at a MOI of 0.5, I found that IFI16 was downregulated in the majority of infected cells at both 24 and 48 hours post infection (Figure 3-15). This was also true for the corresponding Δ US28 virus, indicating that downregulation of IFI16 is not dependent on US28 in these cell lines. Supporting this, I found the same downregulation using the Titan strains of HCMV, both WT and Δ US28 (Figure 3-16), when infecting fibroblasts with an MOI <1.

Clearly, there is some discrepancy between my data and those previously published. Biollati et al [208] found increased expression of IFI16 over a time course of infection of fibroblasts (MOI of 1) by western blotting; however, in such analyses using whole cell lysates, increases in IFI16 expression in bystander cells would have masked any downregulation in infected cells, which is pertinent because I saw clear upregulation of IFI16 in uninfected bystander fibroblasts compared with uninfected wells (Figure 3-15 A). Additionally, although Cristea et al [79] did not conclude that infection of fibroblasts resulted in a decrease in IFI16 expression, close examination of the immunofluorescence data in that paper does appear to show a decrease in IFI16 expression. More recently, Nightingale et al [367] have presented a comprehensive proteome of fibroblasts at 24, 48, and 72 h.p.i. using an MOI of 5 to 10 in which they did not detect any changes in IFI16 expression. The reason for the discrepancy between that study and my

data are unclear but it is possible that it results from differences in MOIs, or that there are strain dependent differences (in particular a difference between effects of TB40/E and Titan, used in my analysis, and Merlin, used in their study) in IFI16 regulation during lytic infection.

The downregulation of IFI16 I observe during lytic infection of fibroblasts and epithelial cells, as well as during Δ US28 infection of monocytes, perhaps merits further investigation: which viral gene product is responsible, and what functional outcome does this have for viral infection? Since IFI16 can repress transcription of the early genes UL44 and UL54 [264], downregulation of IFI16 during lytic infection could be pro-viral. However, since my research question was focussed on latent infections, I did not pursue these lines of investigation further.

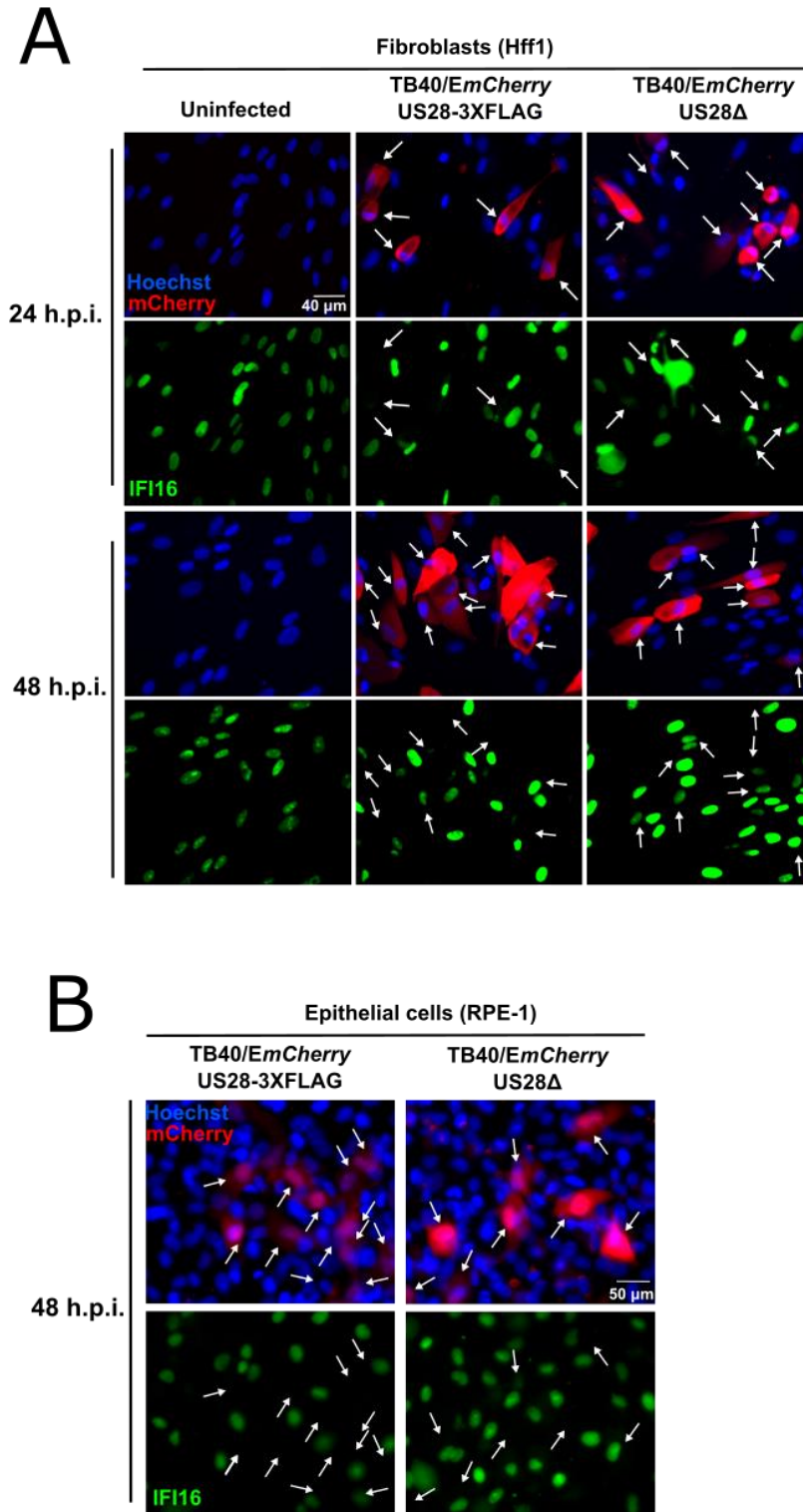


Figure 3-15 Lytic infection of fibroblasts and epithelial cells leads to downregulation of IFI16 independently of US28. Hff1 (A) and RPE-1 (B) cells were infected with TB40/*e mCherry* with US28-3XFLAG or ΔUS28 at MOIs of 0.5. At the indicated times, cells were fixed and stained for IFI16 expression. White arrows indicate the position of infected cells.

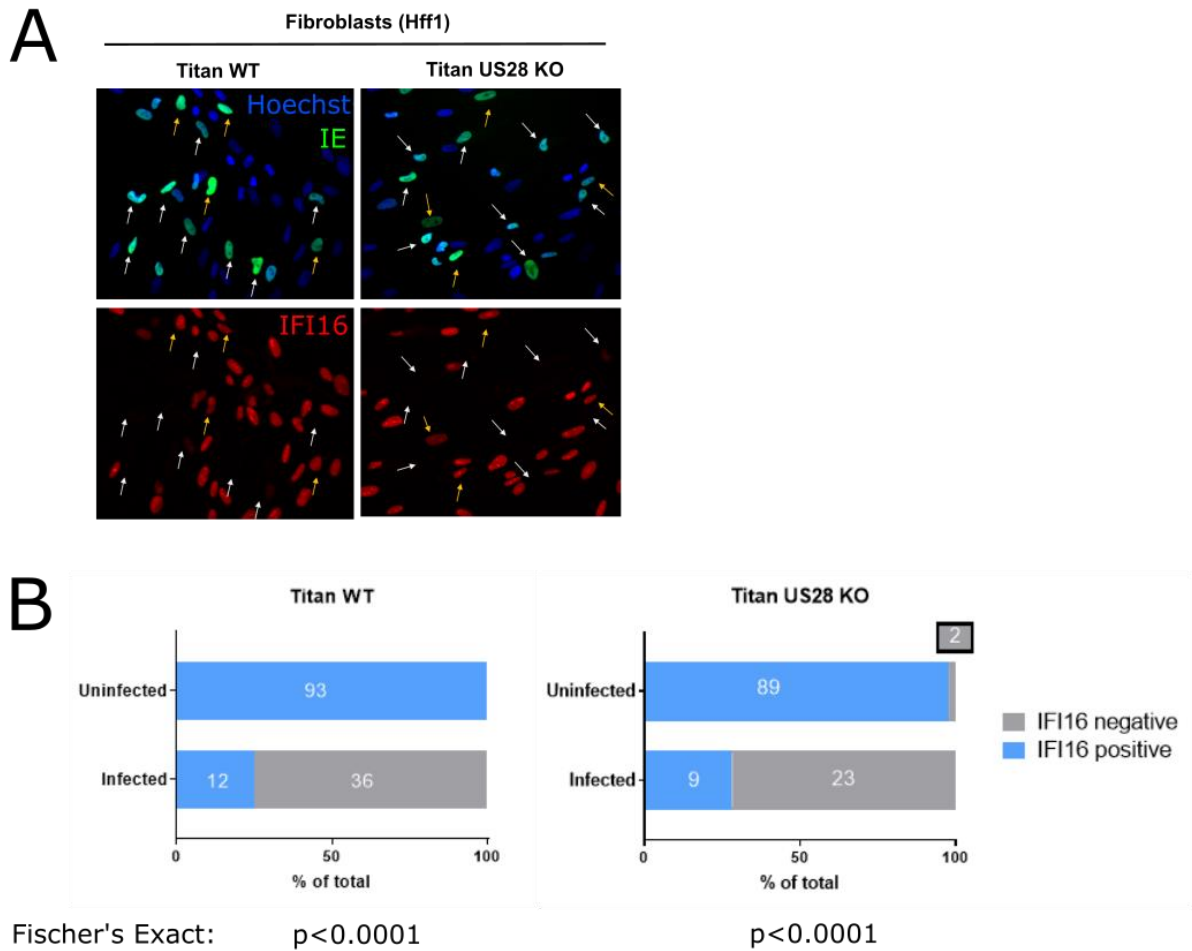


Figure 3-16 **Lytic infection of fibroblasts with the Titan strain of HCMV leads to downregulation of IFI16 independently of US28.** (A) Hff1 cells were infected with the Titan strain of HCMV at MOI 0.5. Cells were fixed and stained for IE and IFI16 at 24 h.p.i. White arrows indicate the position of infected cells which do downregulate IFI16; yellow arrows indicate the position of infected cells which do not downregulate IFI16. (B) Quantification and subsequent Fisher's Exact test of IFI16 positive and negative cells in the infected and uninfected populations in (A). Raw numbers of cells are given in white.

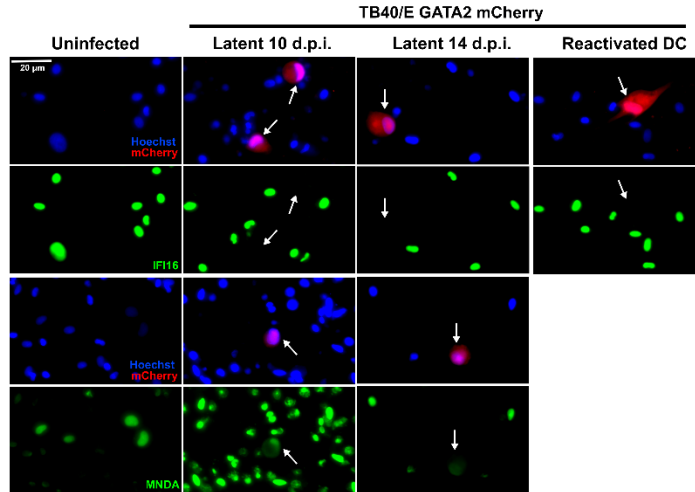
3.4.5. Long-term downregulation of IFI16 and MNDA

I next assessed whether downregulation of IFI16 and MNDA occurs during long term maintenance of latency; long term downregulation of HLA-DR is already known to be important for latent carriage of HCMV [139]. I infected monocytes with HCMV that drives mCherry from GATA2 promoter, and maintains this marker for far longer during latency than SV40 promoter-driven tags[349]; this virus is denoted as virus TB40/E GATA2mCherry. At 10 and 14 d.p.i., IFI16 remained absent and MNDA remained partially downregulated in infected cells (Figure 3-17 A). I also differentiated latently infected monocytes to

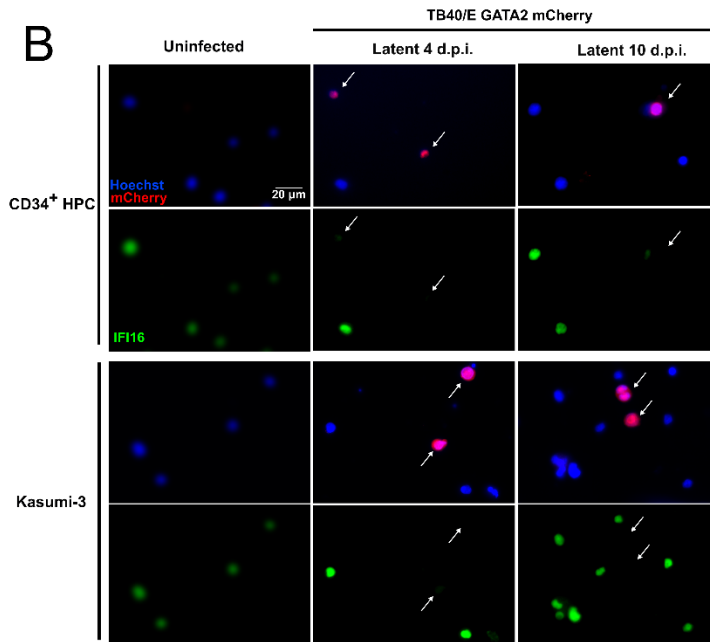
mature dendritic cells to induce reactivation of latent virus, and stained for IFI16 expression, and found that IFI16 was also downregulated in this instance. This is not what happened when I infected mature dendritic cells (essentially a lytic infection of a now permissive cell type, Figure 3-12). This might reflect differences between reactivation and primary infection, but since both observations are snapshots of long and complex processes, it would be wrong to conclude too much without further investigation.

I also analysed latently infected primary CD34⁺ hematopoietic progenitor cells (HPCs), a site of long-term *in vivo* latent carriage, as well as the Kasumi-3 cell line, an experimental model for HCMV latency [117]. Consistent with my observations in monocytes, and RNAseq experiments in cord blood derived CD34⁺ cells [108], IFI16 levels were low or absent in almost all infected cells imaged at 4 and 10 d.p.i (Figure 3-17 B, C). Thus, it seems likely that downregulation of IFI16 is a conserved process in cellular sites of HCMV latency.

A



B



C

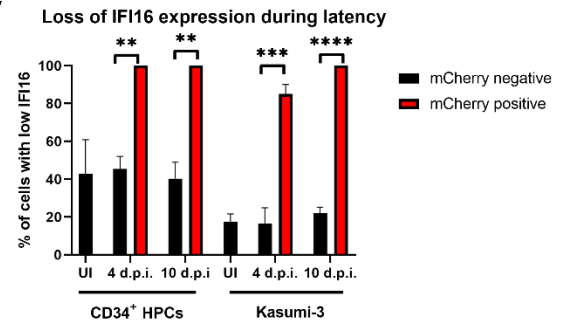


Figure 3-17 **IFI16 and MNDA downregulation during long term latency.** (A) Monocytes were latently infected with TB40/E GATA2 mCherry HCMV. Cells were fixed and stained for MNDA and IFI16 at the indicated times. For reactivated dendritic cells (DC), latently infected monocytes were differentiated with GM-CSF/IL-4 at 2 d.p.i. and then matured with LPS 5 days later. Cells were fixed and stained for IFI16 3 days after maturation. (B) Primary CD34⁺ HPCs and Kasumi-3 cells were latently infected with HCMV and fixed and stained for IFI16 at the indicated time points. (C) The number of infected and uninfected cells with low and high levels of IFI16 were tallied across a minimum of three fields of view per time point. The mean proportion of cells with low IFI16 is then graphed along with the results of a Fisher's Exact test of the sum of cells counted. ** $p < 0.01$; *** $p < 0.001$; **** $p < 0.0001$.

3.4.6. Latently infected THP-1 cells show loss of IFI16 and MNDA mRNA

I was also interested in whether the latency-associated downregulation of IFI16, MNDA, and HLA-DR was occurring at the level of mRNA. The analysis of US28-expressing cells suggests that IFI16 and MNDA mRNA levels are downregulated by US28, but that HLA-DR downregulation is more complex. I initially tried to perform these analyses on FACS-sorted primary monocytes, but too few cells were infected. Consequently, I performed the experiment using THP-1 cells infected with the TB40/E GATA2mCherry virus. At 24 h.p.i, I extracted RNA from the mCherry negative and the mCherry positive population, that had been cell-sorted by staff at the NIHR cell phenotyping hub (Figure 3-18 A), and analysed US28, IFI16, MNDA, and HLA-DRA RNA levels by RT-qPCR. I also included the additional PYHIN genes IFIX and AIM2, which were not detected by the US28-proteomic screen (Figure 3-18 B). All four PYHIN transcripts were clearly downregulated in the infected mCherry positive population compared with the bystander mCherry negative population and this is consistent with immunofluorescence data from latently infected monocytes and RNA data from US28-expressing THP-1 cells. HLA-DRA mRNA levels were slightly increased in the infected cell population, which is in line with Figure 3-8 A, where US28-WT expressing cells have a very similar level of HLA-DRA transcript compared with empty vector control cells. While I did not verify that cell-surface HLA-DR is downregulated in the THP-1 model of latency, these data suggest that latency-associated targeting of HLA-DR might rely on either transcriptional regulation of the other HLA-DR components, or post-transcriptional regulation of HLA-DR expression.

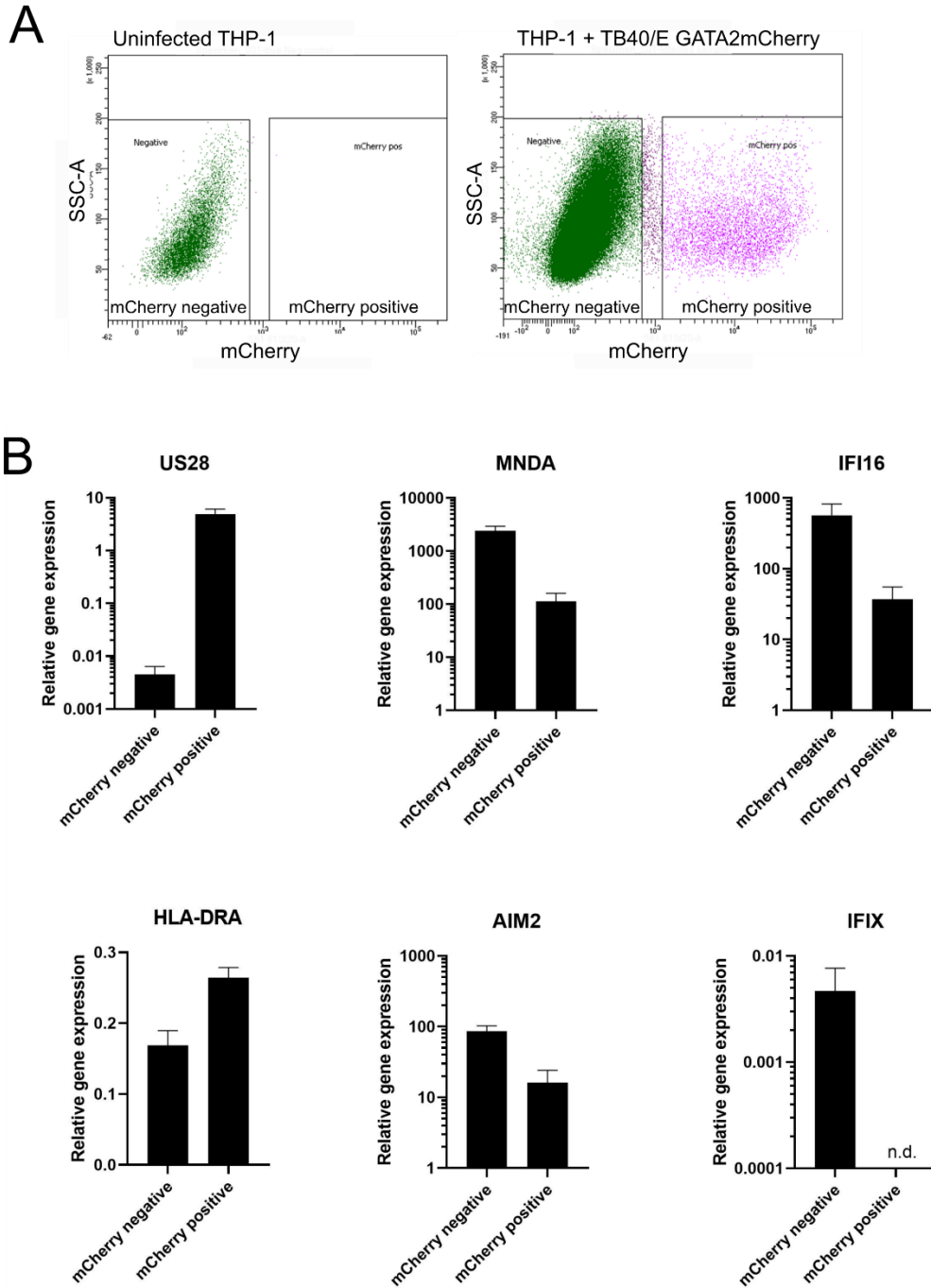


Figure 3-18 **Latently infected THP-1 cells have lower levels of PYHIN mRNAs but not HLA-DRA.** (A) THP-1 cells were latently infected with TB40/E GATA2mCherry for 24 hours before fluorescence associated cell sorting. Uninfected THP-1 cells were used to define the mCherry negative and mCherry positive populations. (B) RNA was isolated from the populations sorted in (A) and analysed by RT-qPCR for the indicated genes. All are displayed as relative gene expression with respect to TBP housekeeping control ($2^{\Delta Ct}$); HLA-DRA is plotted on a linear scale, the others on a log scale; n.d., not detected.

3.4.7. The role of incoming pUS28 in IFI16 downregulation

So far, I have shown that HCMV downregulates IFI16 during latency in a US28 dependent manner. IFI16 levels remain low during the long term maintenance of latency in CD34⁺ HPCs and CD14⁺ monocytes. Downregulation of IFI16 is initiated within 24 hours of latent infection of monocytes, and this likely results from downregulation of IFI16 mRNA levels.

Interestingly, incoming, virion associated, US28 protein (pUS28) has recently been shown to be functional [193] and able to help support suppression of IE gene expression. Therefore, I hypothesised that incoming pUS28 may play a role in the very quickly observed downregulation of IFI16 I had noted.

To address this, I grew a US28 gene deletion virus in a cell line that expresses US28, with the aim of generating infectious virions that contained pUS28 but not the US28 gene. I based my approach on the publication that showed incoming pUS28 was functional [193]. I grew the TB40/E *mCherry* US28 Δ virus in TERT-immortalised Hff1 cells that had been transduced with a US28-V5 lentiviral vector. These cells were a gift from Luis Nobre (University of Cambridge). Once I had purified virions, I solubilised these in a high-salt buffer (see Materials and Methods) and subjected them to SDS-PAGE followed by Western blotting. I used pp65 as a marker of virions, and actin as a marker of cells, and blotted for these first, before stripping and reprobing the membrane for US28-V5 (Figure 3-19). The stripping process was unsuccessful however, and US28-V5 (mouse detection antibody) signal is partially masked by pp65 and actin (also mouse detection antibodies). However, if these images are overlaid, it becomes clear that virions contained pUS28 when grown in the US28-V5 cell line. This virion preparation will be referred to as *US28comp*.

I then infected CD14⁺ monocytes with TB40/E *mCherry* US28-3XF (which encodes for US28), TB40/E *mCherry* US28 Δ , and the *US28comp* virus. At 24 h.p.i., I fixed and stained for IFI16 (Figure 3-20), since I knew from previous experiments that IFI16 is downregulated by WT but not US28 Δ viruses. Furthermore, US28 protein is likely degraded within 48 hours [193], so I needed to pick a window which maximised any observable effects on IFI16. IFI16 expression was clearly downregulated by TB40/E *mCherry* US28-3XF, but remained present in TB40/E *mCherry* US28 Δ infected cells, as expected. Cells infected with *US28comp* showed an intermediate phenotype. This suggests that incoming pUS28 may, indeed, contribute to IFI16 downregulation, but is likely insufficient for full IFI16 downregulation. This investigation merits repeating, and further validation of the virion composition, and changes in viral gene expression would aid the interpretation of this type of analysis.

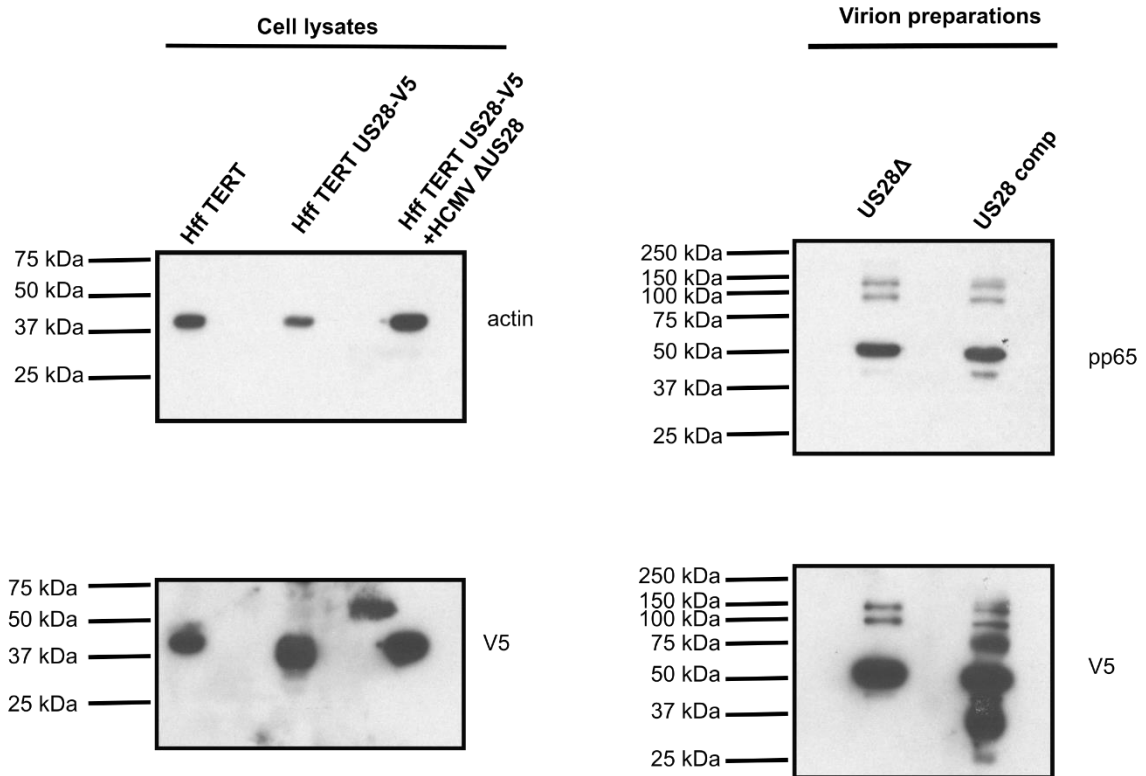


Figure 3-19 **Incorporation of V5-tagged US28 into virions.** Left hand panels: lysates from TERT immortalised Hff1 cells (Hff TERT), or Hff-TERT cells transduced with US28-V5 expression vector, or the latter cell line infected with TB40/*EmCherry* US28Δ, were subjected to western blot firstly for actin (upper panel), then stripped unsuccessfully and reprobed for V5 tag (lower panel). Hff V5 cell lines appear to have signal with the V5 antibody that is lower than the actin band, and not present in non-transduced Hff TERT cells. Right hand panels: concentrated virions were subjected to western blot firstly for pp65 (upper panel), then stripped unsuccessfully and reprobed for V5 tag (lower panel). US28 comp refers to TB40/*EmCherry* US28Δ grown in Hff V5 cell lines, and this track appears to have additional signal with the V5 antibody both above and below the pp65 bands, and which is not present in TB40/*EmCherry* US28Δ virions grown in non-transduced cells.

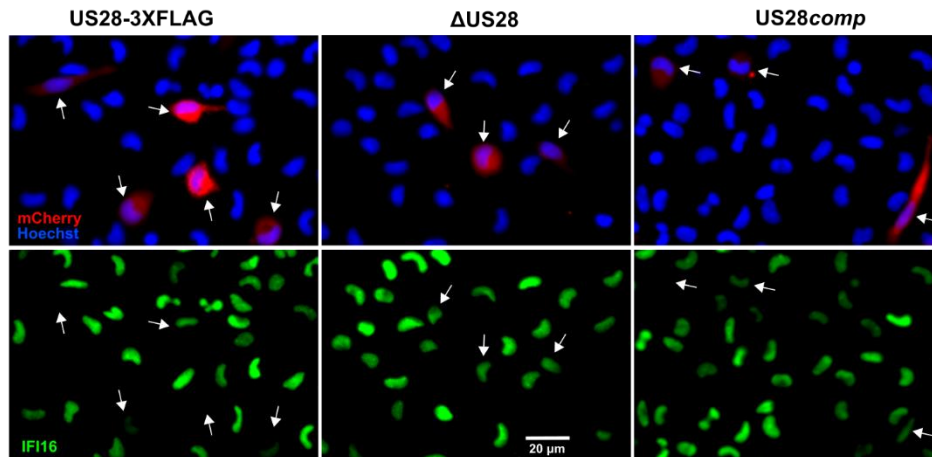
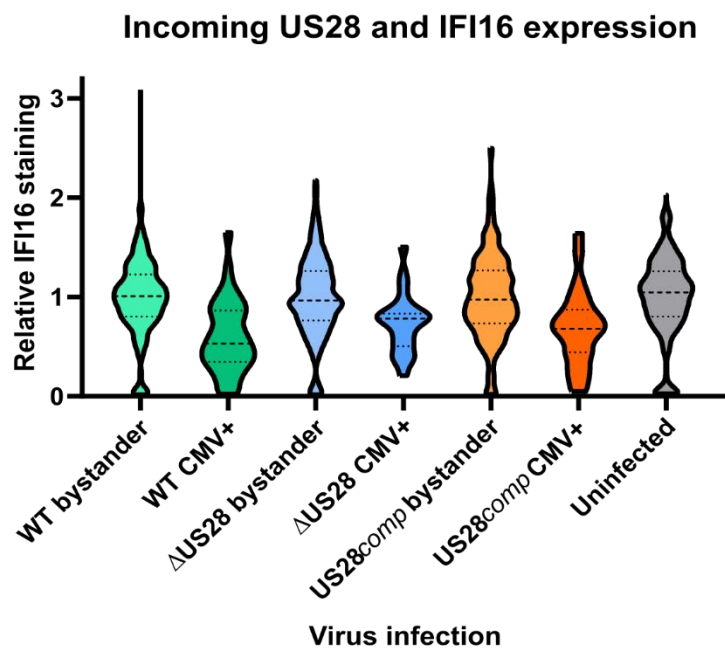
A**B**

Figure 3-20 **Incoming US28 may help to drive IFI16 downregulation.** A) CD14⁺ monocytes were infected with either TB40/EmCherry-US28-3XFLAG HCMV (WT), the ΔUS28 equivalent, or US28_{comp}. At 24 h.p.i., cells were fixed and stained by immunofluorescence for IFI16 and imaged at 40X magnification. B) Distribution of IFI16 intensities derived from a minimum of four fields of view (as per (A)). IFI16 intensities were measured using the Measure Particles feature of ImageJ. Each cell was assigned as bystander or CMV+ by mCherry intensity. Then, IFI16 intensities for each cell was normalised to the mean intensity of bystander cells for each field of view. The distribution of relative IFI16 levels are represented by the violin plot, with heavy dotted line representing the median value.

3.5. Discussion

The viral GPCR US28 is expressed during both lytic and latent infection of HCMV. While US28 is dispensable for lytic replication *in vitro* [177,178], it is essential for the establishment and maintenance of HCMV latency in early myeloid lineage cells [159,173,189,193]. This is attributable, in part, to the ability of US28 to suppress the major immediate early promoter; a US28 function specific for undifferentiated myeloid cells [160,173,189,193].

Prior to the beginning of my project, others in my laboratory had hypothesised that this ability of US28 to so profoundly regulate viral IE gene expression in undifferentiated myeloid cells was likely via US28-mediated modulation of host protein abundance and, therefore, they wanted to determine whether such US28-driven changes could be important for the establishment or maintenance of HCMV latency. Previous work has used targeted arrays to assess US28-mediated effects on myeloid cells [173,189,193] but, here, my colleagues performed an unbiased proteomic screen to understand how US28 reprograms host cells in order to support latent infection. This screen compared host protein abundance in control THP-1 cells or THP-1 cells which express either US28-WT or the US28 signalling mutant, US28-R129A. As such, I was then able to assess the signalling-dependent and signalling-independent effects of US28. I then chose to focus on signalling-dependent changes because G protein coupling via the residue R129A is essential for experimental latency [189,193]. However, I predict that some of the signalling-independent changes driven by US28 could also be important for HCMV latency, since these changes included alterations in several cell-surface molecules such as co-stimulatory molecule CD82, adhesion molecule CD44, and in receptor tyrosine kinase FLT3. The latter two cellular factors are implicated in myeloid cell differentiation, which is intimately linked with HCMV latency and reactivation [107,160,368–370]. As such, modulating these cell-surface molecules could help to control interactions with immune effectors and cellular differentiation-linked reactivation.

By analysing changes in host protein abundance between US28-WT and US28-R129A expressing THP-1 cells, I found a number of significant changes in the host proteome which likely result specifically from US28 signalling. Interestingly, I found US28-WT downregulated a large number of interferon-inducible proteins, including canonical interferon-stimulated genes (ISGs) like OAS2 and IFITM3, as well as MNDA, IFI16, and several HLA-DR components. I found that levels of both total STAT1 and phosphorylated STAT1 were reduced in US28-WT expressing cells, providing a potential mechanism for this effect, but analysis conducted using a c-fos inhibitor indicated that c-fos likely also plays a role. Modulation of interferon signalling has not previously been reported for US28, but in the context of the latently infected

monocyte, a general block in downstream interferon signalling may be important for maintaining the polarisation of the monocyte [371,372], or perhaps to avoid the anti-viral activities of ISGs. I believe these questions merit further interrogation.

I chose to focus on the two PYHIN proteins and the set of HLA-DR components which are downregulated by US28. I confirmed downregulation of IFI16, MND4, and HLA-DR in THP-1 cells which overexpress US28 and recapitulated these effects in experimental latency in primary CD14⁺ monocytes. HLA-DR was previously reported to be downregulated during experimental latency in granulocyte-macrophage progenitor cells, which prevents CD4⁺ T cell recognition and activation [125,139,373]. Whilst this downregulation of MHC Class II involved the expression of the latency-associated gene UL111A [139], my data argue that viral US28 could also contribute to this phenotype. I will discuss the functional effects of MND4 and IFI16 downregulation in later chapters.

My results clearly characterised a rapid downregulation of IFI16 during the establishment of latency in monocytes, which occurred within the first 24 h of infection and was also maintained during long term latency in monocytes and CD34⁺ HPCs. This effect was clearly US28-dependent as Δ US28 virus failed to display immediate IFI16 down-regulation. However, we did observe a partial downregulation of IFI16 in Δ US28-infected monocytes at later time points of infection. I think it likely that this involves an unidentified lytic-phase viral gene product, which may be required for overcoming the known IFI16-mediated restriction of HCMV lytic infection [208,215,264,286] and occurs as a result of Δ US28 virus initiating a lytic infection in undifferentiated monocytes.

My observation that the US28-dependent downregulation of IFI16 occurred rapidly (within 24h of infection) may, in part, be attributable to incoming US28, which has been shown by others to be functional [193]. IFI16 protein has a short half-life of approximately 150 minutes in fibroblasts [374] and therefore, incoming US28 protein may rapidly target IFI16 transcription in latently infected monocytes, as it does in both US28-expressing THP-1 cells and latently infected THP-1 cells, resulting in loss of IFI16 within 24 hours of infection; this is then maintained by subsequent latency-associated *de novo* US28 expression. By generating virions that contained pUS28 but not US28 coding sequence, I generated evidence that pUS28 contributes, but is not sufficient, for IFI16 downregulation at 24 h.p.i.; since US28 mRNA is detectable within 24 hours of latent infection (Figure 3-18), it is feasible that *de novo* synthesis of pUS28 'finishes the job' of downregulating IFI16.

4. IFI16 can activate IE gene expression during latency and needs to be targeted for latency-associated IE suppression

4.1. Introduction

In Chapter 3, I demonstrated that HCMV latency induces IFI16 downregulation in a US28 dependent manner. An obvious question is how this might be beneficial to the virus during latency. In §1.6.4, I outlined the evidence for IFI16 being a sensor of double stranded DNA, other mechanisms of viral restriction, and modulation of human and viral gene expression. While I will discuss DNA sensing in Chapter 6, here I focus on applying known IFI16-mediated modulation of HCMV gene expression during lytic infection to what might be happening during HCMV latency.

In fibroblasts, IFI16 can activate MIEP activity while restricting the transcription of UL54, and perhaps UL44; this is possibly dependent on the tegument protein pp65/UL83 [79,208,264]. Since IE gene expression must be suppressed in order to establish latency, I hypothesised that downregulation of IFI16 would be important for repressing the MIEP.

Here, I demonstrate the merit in that hypothesis by overexpressing IFI16, and showing that this drives IE gene expression in myeloid cells via NF- κ B activation.

4.2. Overexpression of IFI16

I cloned the sequence encoding IFI16 (isoform IFI16-B, NM_001206567.1, nucleotides 291–2482) into the lentiviral expression vector pHRsin SV40 Blast, which drives transgene expression from the SV40 promoter. I generated control empty vector and IFI16 overexpressing THP-1 cell lines via lentiviral transduction twice to generate two independent sets of cell lines, and verified overexpression of IFI16 by western blot and by immunofluorescence (Figure 4-1). The IF staining also demonstrated that I had a heterogeneous population of IFI16-transduced cells.

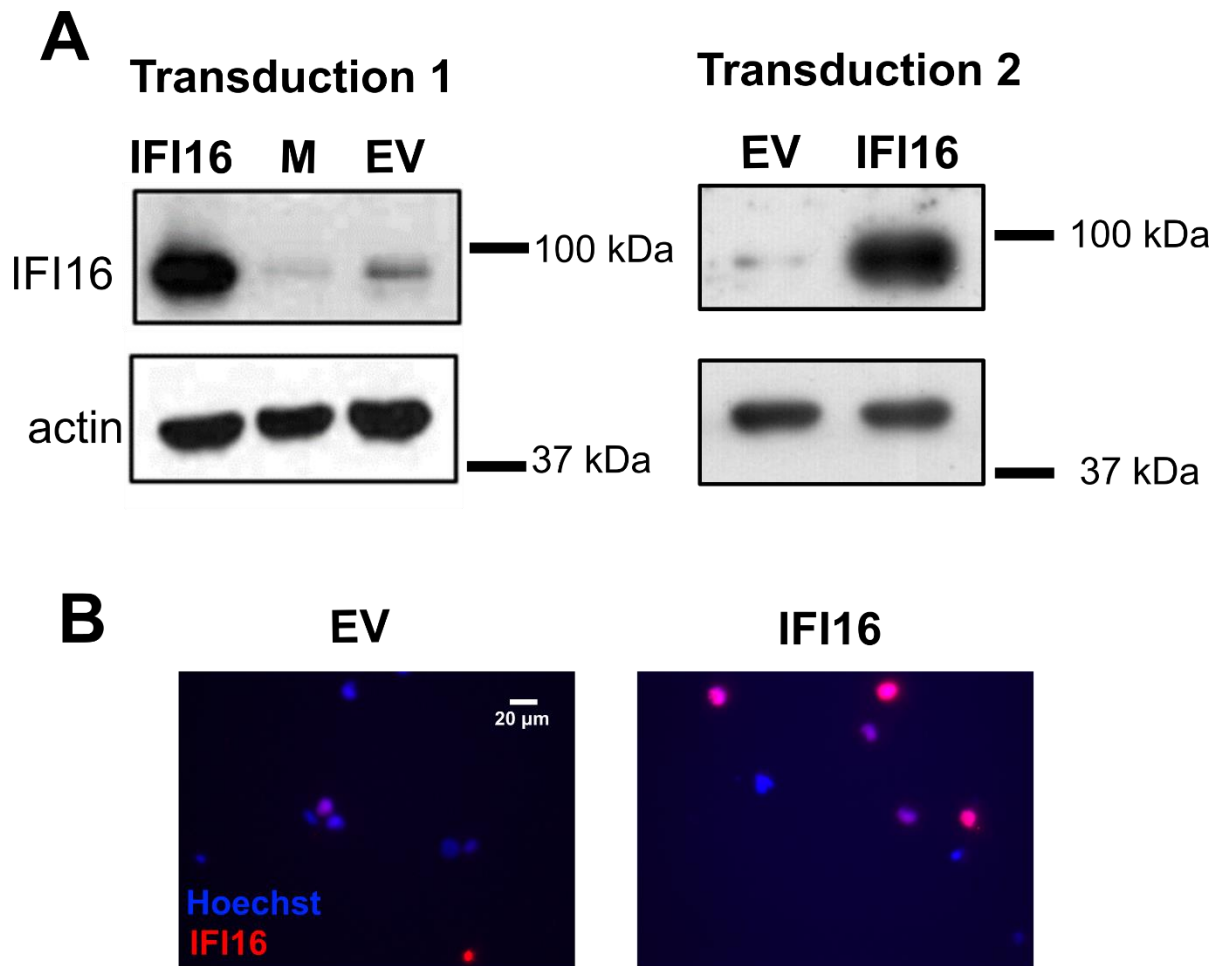


Figure 4-1 **Overexpression of IFI16 in THP-1 cells.** (A) Western blots of IFI16 expression from two independent transductions of THP-1 cells with IFI16 overexpression vectors, empty vectors (EV), or MNDA overexpression vector (M, described in Chapter 5). Actin is used as a loading control. (B) Immunofluorescence staining of IFI16 expression of cell lines generated in A, left hand panel, M not included.

4.3. IFI16 overexpression drives IE gene expression

I then infected control empty vector and IFI16 overexpressing THP-1 cells with HCMV strain TB40/E IE2-eYFP [348]. This results in expression of IE2 (also known as IE86, UL122) as an IE2 yellow fluorescent protein fusion. Typically, undifferentiated THP-1 cells infected with HCMV express only low amounts of IE [119,141]. I found that IFI16 overexpression significantly increased IE2 expression in THP-1 cells over a number of paired experiments (Figure 4-2). These experiments were analysed as pairs, to account for a number of factors. Firstly, passage of THP-1 cells over time decreases overall infectability of the cell lines: experiments were all performed on passage-matched cells, but over several months and different batches of cells which had been stored in liquid nitrogen. I also made two independently transduced sets

of cell lines. The matching also controls for differences between batches of IE2-eYFP virus such as particle-to-plaque forming unit (p.f.u.) ratio.

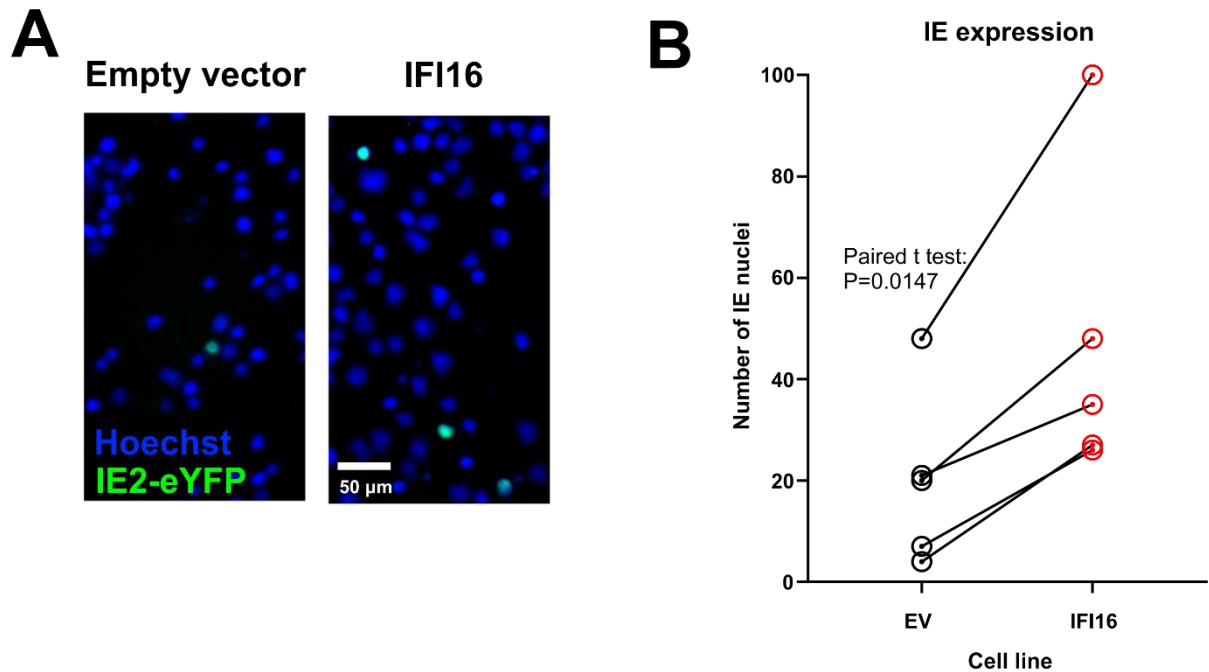


Figure 4-2 **IFI16 overexpression drives IE gene expression**. Empty vector or IFI16-overexpressing cells were infected with TB40/E IE2-eYFP virus, and IE2-eYFP positive nuclei were imaged (A) and counted by fluorescence microscopy (B). Results from five paired experiments are shown, which were analysed by paired two-tailed Student's t-test.

4.4. IFI16 activates the MIEP independently of other viral factors

To understand whether IFI16 mediated induction of IE gene expression was an effect on the MIEP, and whether other virion components were required for this activity, I used an MIEP-eGFP reporter cell line [118]. These are THP-1 cells in which an integrated 1151 bp region of the MIEP drives the expression of eGFP [118]. In these undifferentiated THP-1 cells, the MIEP is epigenetically repressed unless stimulated (for example by differentiation) [118]. I treated these MIEP-eGFP THP-1 cells with control lentiviruses or lentiviruses which drive the overexpression of IFI16, ensuring equivalent lentivirus infection of reporter cells by correcting for p24 concentration. The p24 ELISA was performed by Isobel Jarvis, University of Cambridge, and gave the following values: empty vector lentivirus, 411 ng/mL; IFI16 lentivirus, 67.0 ng/mL. Transduced cultures were maintained for two weeks, after which I validated IFI16 expression by

immunofluorescence and then analysed eGFP expression by flow cytometry (Figure 4-3 A, B). I found that the IFI16-overexpressing cells had increased eGFP expression compared with controls, suggesting that IFI16 overexpressed in isolation and in the absence of additional HCMV components, drives MIEP activity. Furthermore, culturing THP-1 MIEP-eGFP reporter cells with supernatants from the empty vector or IFI16-overexpressing cell lines in Figure 4-1 resulted in no significant MIEP activity, suggesting that the effect is mediated intracellularly, and not by a secreted factor (Figure 4-3 B).

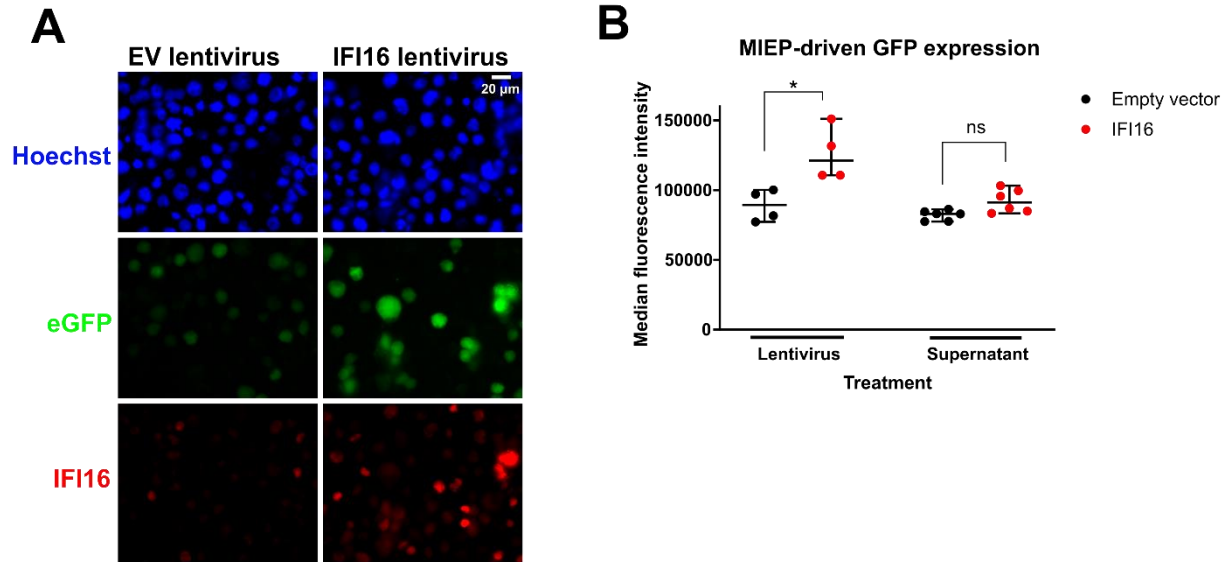


Figure 4-3 **IFI16 drives MIEP activity.** (A) EV and IFI16 lentivirus concentration was determined by p24 ELISA and 15 ng p24 equivalents of each lentivirus was used to transduce MIEP-eGFP THP-1 cells. Cells were maintained for two weeks in culture, and IFI16 overexpression was validated by immunofluorescence. (B) Left hand comparison: cells described in (A) were assessed for eGFP fluorescence by flow cytometry. Right hand comparison: non-transduced MIEP-eGFP expressing cells were incubated with supernatants from cells described in Figure 4-1 for two days. eGFP expression was quantified by flow cytometry. A statistical comparison of the median fluorescence intensity was performed using two-tailed Mann-Whitney test; ns, not significant and * P<0.05.

4.5. IFI16 drives IE gene expression via NF- κ B at the MIEP

IFI16 activates NF- κ B signalling in a number of contexts [224,250], and our previous work indicates that US28-mediated attenuation of NF- κ B signalling is important for the establishment of latency [189]. Therefore, I hypothesised that IFI16 activates the MIEP via NF- κ B. By using the NF- κ B pathway inhibitor, BAY11-7082, we were able to ameliorate the effect of IFI16 overexpression on IE, suggesting that NF- κ B plays an important role in this pathway (Figure 4-4 A, C). I also infected IFI16-overexpressing cells with a recombinant HCMV that lacks NF- κ B sites within the MIEP [146] to check whether activation of the MIEP

by IFI16 requires the well-established NF- κ B binding sites present within the MIEP. In this analysis, IFI16 overexpression failed to induce IE gene expression in the NF- κ B site deletion virus, unlike IFI16 cells infected with the revertant strain (Figure 4-4 B,C). Taken together, these data are consistent with the view that IFI16 activates IE gene expression in early myeloid lineage cells through NF- κ B binding to the MIEP.

To begin to unpick how NF- κ B is activated by IFI16, I analysed nuclear NF- κ B localisation in IFI16 overexpressing cells (Figure 4-5), since localisation of NF- κ B is a principle way by which its activity is regulated [375]. Undifferentiated THP-1 cells have only a small cytoplasmic volume, making quantification challenging, but I appeared to see greater nuclear NF- κ B in cells which overexpress IFI16. This is consistent with previously published observations in epithelial cells [250]. In that study, Caposio et al [250] demonstrated that IFI16 activates NF- κ B via the attenuation of I κ B α expression. I κ B α , known formally as NFKBIA, inhibits NF- κ B by binding and preventing NF- κ B translocation to the nucleus [375]. Caposio et al [250] suggest that IFI16 overexpression sequesters Sp1 transcription factors, thus preventing binding of Sp1 to the I κ B α promoter. To see if this was occurring in my system, I analysed NFKBIA/ I κ B α gene expression by RT-qPCR in empty vector and IFI16 overexpressing cell lines, as well as in US28 expressing THP-1 cells described in Chapter 3. I found that, contrary to what one might have predicted from the Caposio et al [250] study, IFI16 overexpression increased I κ B α RNA expression. Furthermore, US28-WT expressing cell lines, which have reduced nuclear NF- κ B, also have reduced I κ B α RNA levels. This suggests that the Sp1 mechanism is not at play in my system. Indeed, I κ B α is induced by NF- κ B as part of a negative feedback loop [376], and so my results are consistent with IFI16 increasing NF- κ B activity, and US28-WT decreasing NF- κ B activity. IFI16 can also contribute to NF- κ B activity by etoposide-induced DNA damage sensing pathway, via ATM and STING [224]; whether a DNA/DNA damage sensing pathway explains IFI16-mediated activation of NF- κ B merits further investigation.

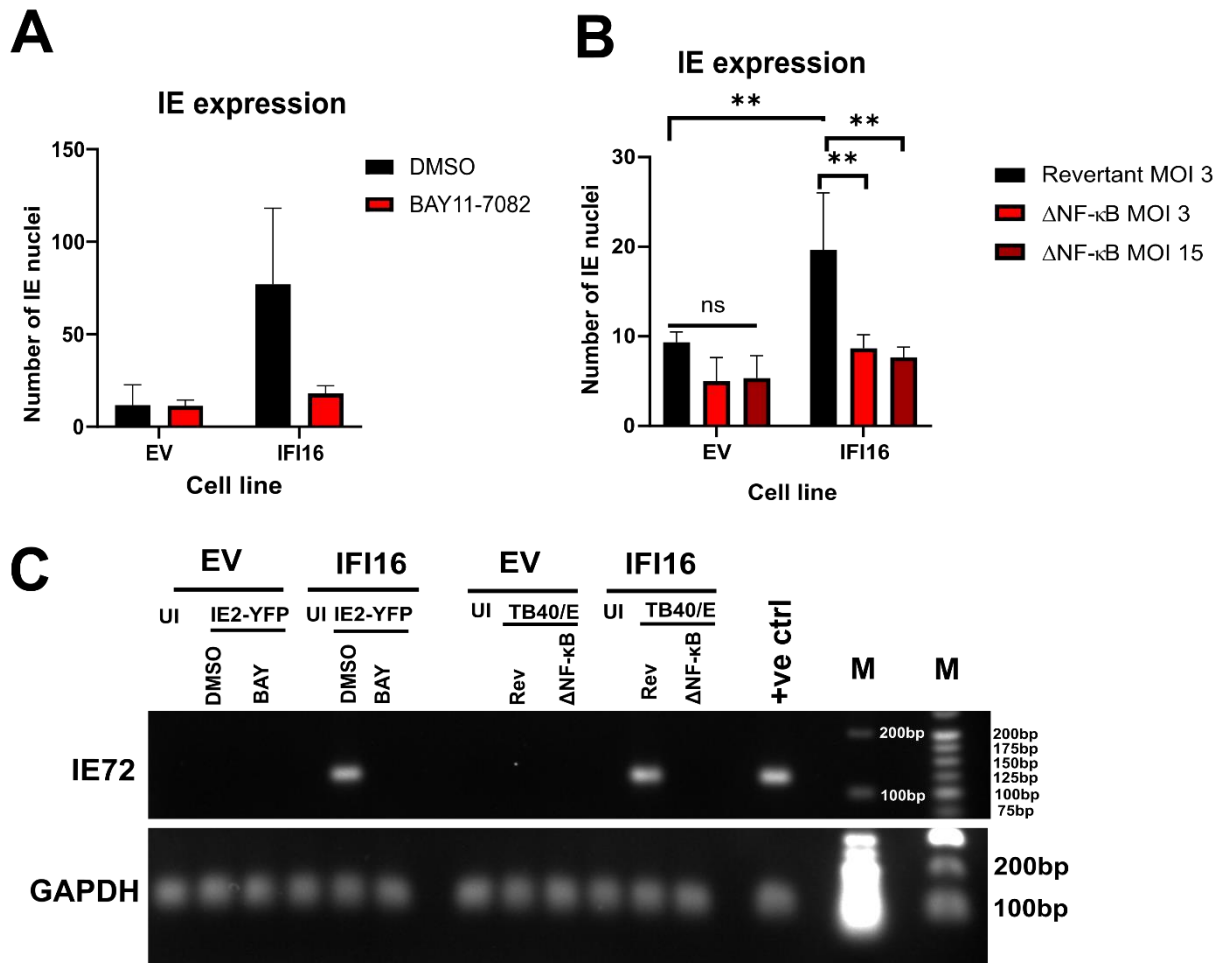


Figure 4-4 **IFI16 activates IE gene expression via NF-κB.** (A) Empty vector or IFI16-overexpressing cells were infected with TB40/E IE2-eYFP virus in the presence of the IKKα inhibitor BAY11-7082 which inhibits the NF-κB pathway, or DMSO as a control. IE2-eYFP positive nuclei were imaged and counted by fluorescence microscopy at 48 hours post infection. (B) Empty vector or IFI16-overexpressing cells were infected with a revertant WT-like TB40/E at MOI 3, TB40/E with NF-κB binding sites deleted from the MIEP (ΔNF-κB) at MOI 3 or MOI 15. At 48 h.p.i., cells were fixed and stained for IE and the number of IE positive nuclei were counted. Graph shows the results of three experiments and statistical analysis by 2-way ANOVA using Sidak's multiple comparison test. ** P<0.01, ns, P > 0.05. C) Empty vector or IFI16-overexpressing cells were infected as per A) and B) at MOI 3, but cells were instead analysed for IE72 expression by RT-qPCR. PCR products were then run on a 2% (upper panel, IE72) or 1.2% (lower panel, GAPDH) agarose gel. UI refers to uninfected cells, DMSO is the solvent control, BAY refers to BAY11-7082, Rev refers to the revertant TB40/E and ΔNF-κB to the NF-κB binding site mutant virus. The positive control (+ve ctrl) was HCMV-infected PMA-differentiated monocytes. Molecular weight markers (M) are annotated.

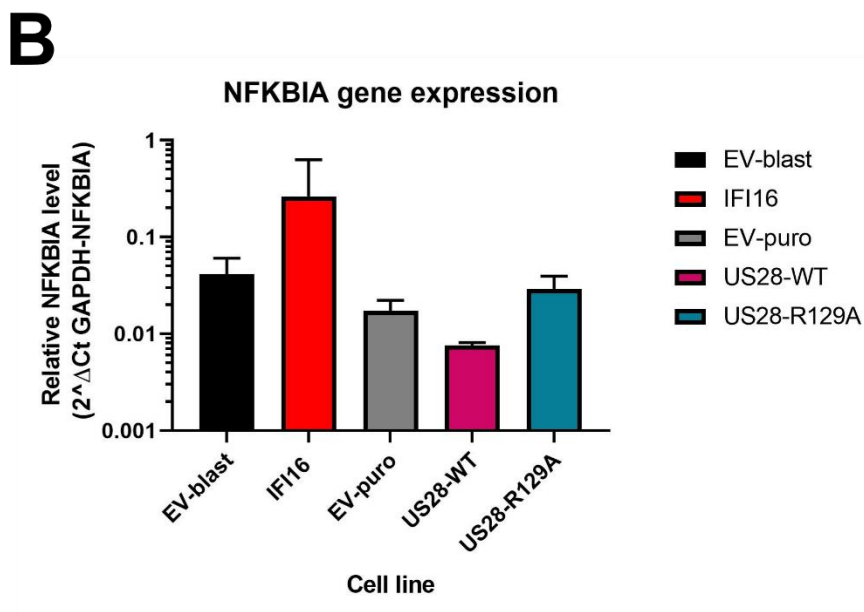
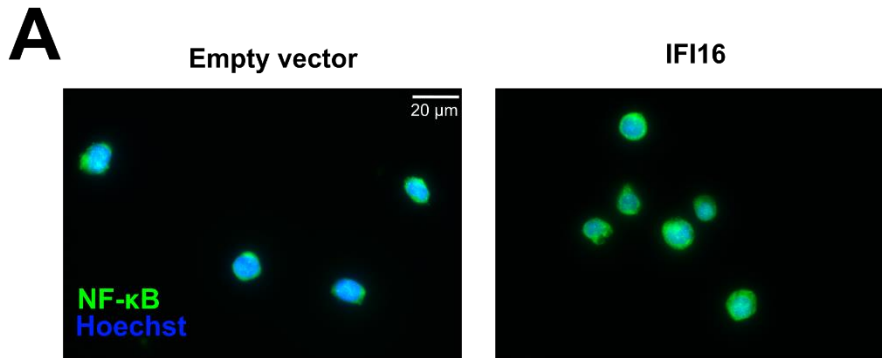


Figure 4-5 **IFI16 overexpression increases nuclear NF-κB**. (A) Empty vector or IFI16-overexpressing cells were fixed and stained for NF-κB, with Hoechst as a nuclear stain, at 40X magnification to assess levels of nuclear NF-κB. (B) IκBα, gene name NFKBIA, RNA level was assessed by RT-qPCR in the indicated cell lines, and normalised to GAPDH levels. EV-blast is the control for IFI16 transduced cell lines, and EV-puro is the control for US28-WT and -R129A cell lines.

4.6. Discussion

Here I found that preventing IFI16 expression has a clear benefit to the establishment of HCMV latency. This contrasts with previous analyses of latency in other viral systems, where IFI16 expression is necessary to repress lytic viral transcription [271,285]. In my model, IFI16 overexpression activated MIEP activity in the absence of additional viral proteins, and, furthermore, IFI16 overexpression increased IE

positive nuclei in latently infected THP-1 cells. IFI16 activates the MIEP during lytic infection [79,264], though in these cases an additional viral gene product, UL83, is thought to be required. My results suggest that UL83 is not required for IFI16-mediated activation of the MIEP in undifferentiated myeloid cells, and suggest that IFI16 activates NF- κ B to achieve this, as use of either an NF- κ B pathway inhibitor or deletion of NF- κ B binding sites from the MIEP prevented IFI16-mediated IE expression. I believe this provides one mechanism by which US28 blocks NF- κ B activity early during latency, a phenomenon previously shown to be important for the establishment of latency in myeloid cells [189].

5. MNDA is a potential restriction factor for HCMV latency

5.1. Introduction

In Chapter 3 I demonstrated that HCMV latency induces partial MNDA downregulation, and that, in THP-1 cells, US28 expression alone is sufficient for MNDA downregulation. Very little is known about the function of MNDA, and thus it was not obvious why MNDA might be a target for downregulation during HCMV latency. In the Introduction, I outlined what is known about MNDA: it is a PYHIN protein, it can bind DNA [292]; it may enhance YY1 binding to DNA [298]; it has a potential role in myeloid cell death [303,304]; it displays the properties of a master transcriptional regulator of the myeloid lineage [293–297]. Here, I overexpress MNDA in THP-1 cells and find that these cells show lower levels of latent infection based on a reduction in the numbers of cells expressing fluorescent reporters in recombinant HCMV strains routinely used to detect latently infected myeloid cells. Some of the follow up studies, including the use of independently generated sets of MNDA-overexpressing cell lines, were performed by an undergraduate Part II student, Esme Fowkes, under my supervision and will be attributed to her where applicable. These analyses show that this effect is unlikely to be explained by a failure of virus to enter cells. The data suggest that MNDA could be a restriction factor for HCMV latency, but further analysis is required, including the mechanism of restriction.

5.2. Overexpression of MNDA

I cloned the sequence encoding MNDA (NM_002432) into the lentiviral expression vector pHRsin SV40 Blast, which drives transgene expression from the SV40 promoter. I generated control empty vector and MNDA overexpressing THP-1 cell lines via lentiviral transduction on multiple occasions, to generate three independent sets of cell lines during the course of this project. I, or Esme Fowkes in the case of the second and third transduction, verified overexpression of MNDA by western blot and by immunofluorescence (Figure 5-1). The IF staining also demonstrated that I had a heterogenous population of MNDA-transduced cells.

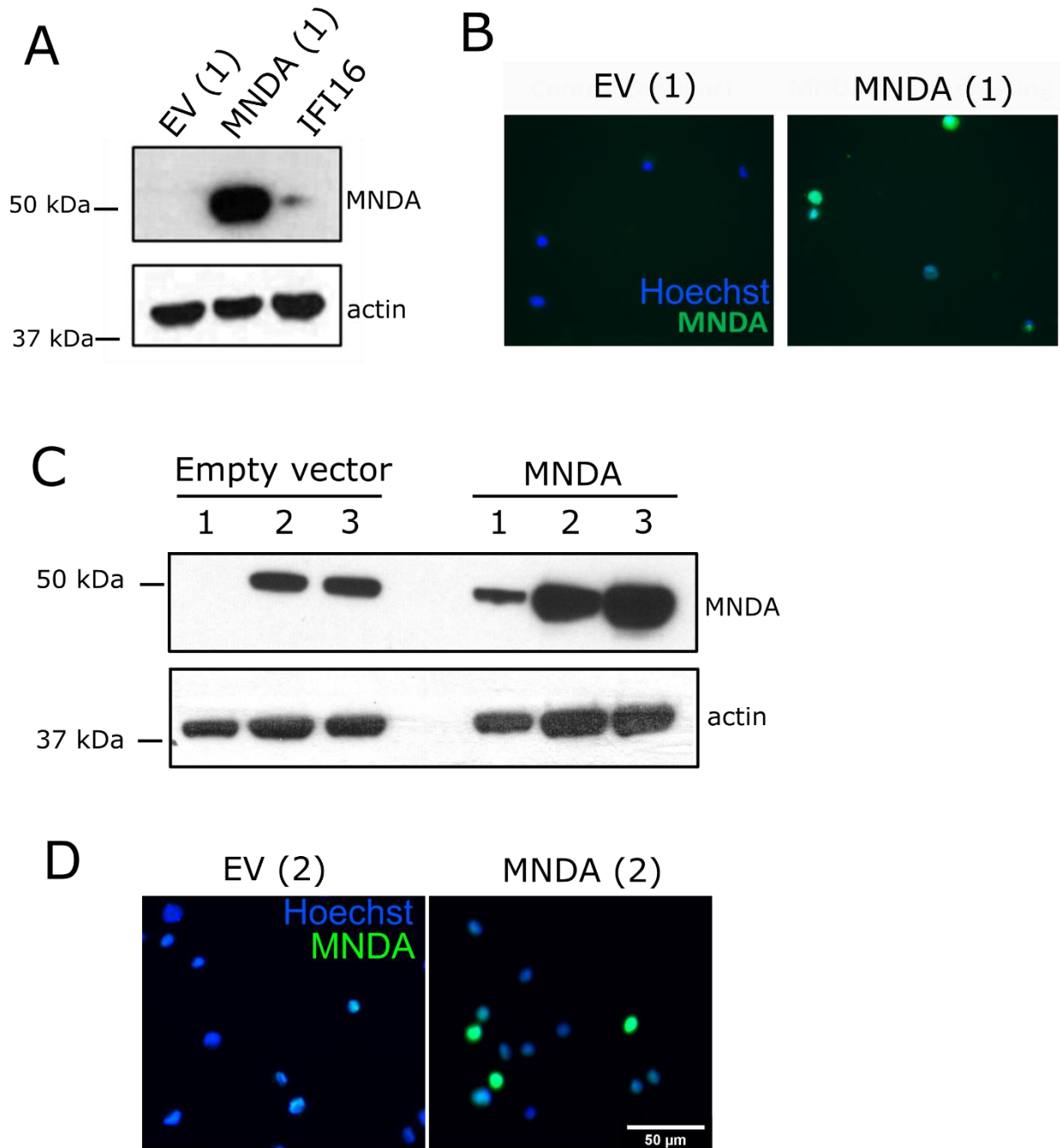


Figure 5-1 **Overexpression of MNDA.** (A) Western blot of MNDA expression from the first transduction of THP-1 cells with MNDA overexpression vectors, empty vectors (EV), or IFI16 overexpression vector (described in Chapter 4). Actin is used as a loading control. (B) Immunofluorescence staining of IFI16 expression of cell lines generated in A, IFI16 not included. (C) Western blot of MNDA expression from the three independent transductions (1, 2, 3). (D) As (B), but for the second set of transduced cell lines (2). C and D were experiments performed by Esme Fowkes under my supervision.

5.3. MNDA-overexpressing cells fail to drive fluorescent reporter expression following latent infection

To begin to understand why MNDA is targeted during HCMV latency, I infected empty vector or MNDA-overexpressing cells with TB40/E viruses that, in our models of HCMV latent infection, express fluorescent proteins. These contain SV40 GFP or GATA2 mCherry expression cassettes, and I introduced these in Chapter 3. I found, using the cell obtained in the first transduction, a clear and significant reduction in the numbers of cells which become infected, and measured by GFP or mCherry fluorescence by microscopy (Figure 5-2 A, B). I was then able, in conjunction with Esme Fowkes, to reproduce the observations with the GATA2mCherry virus in the independently-transduced cell lines (Figure 5-2 C, D). Because the reduction in apparent levels of HCMV latent infection occurred using two different reporter proteins, expressed from different promoters, I believe it unlikely that this is a simple effect of MNDA non-specifically affecting reporter gene expression outside the context of a viral genome. However, it would be prudent to rule that out by performing reporter assays on transfected plasmids, for example with a GATA2-luciferase construct.

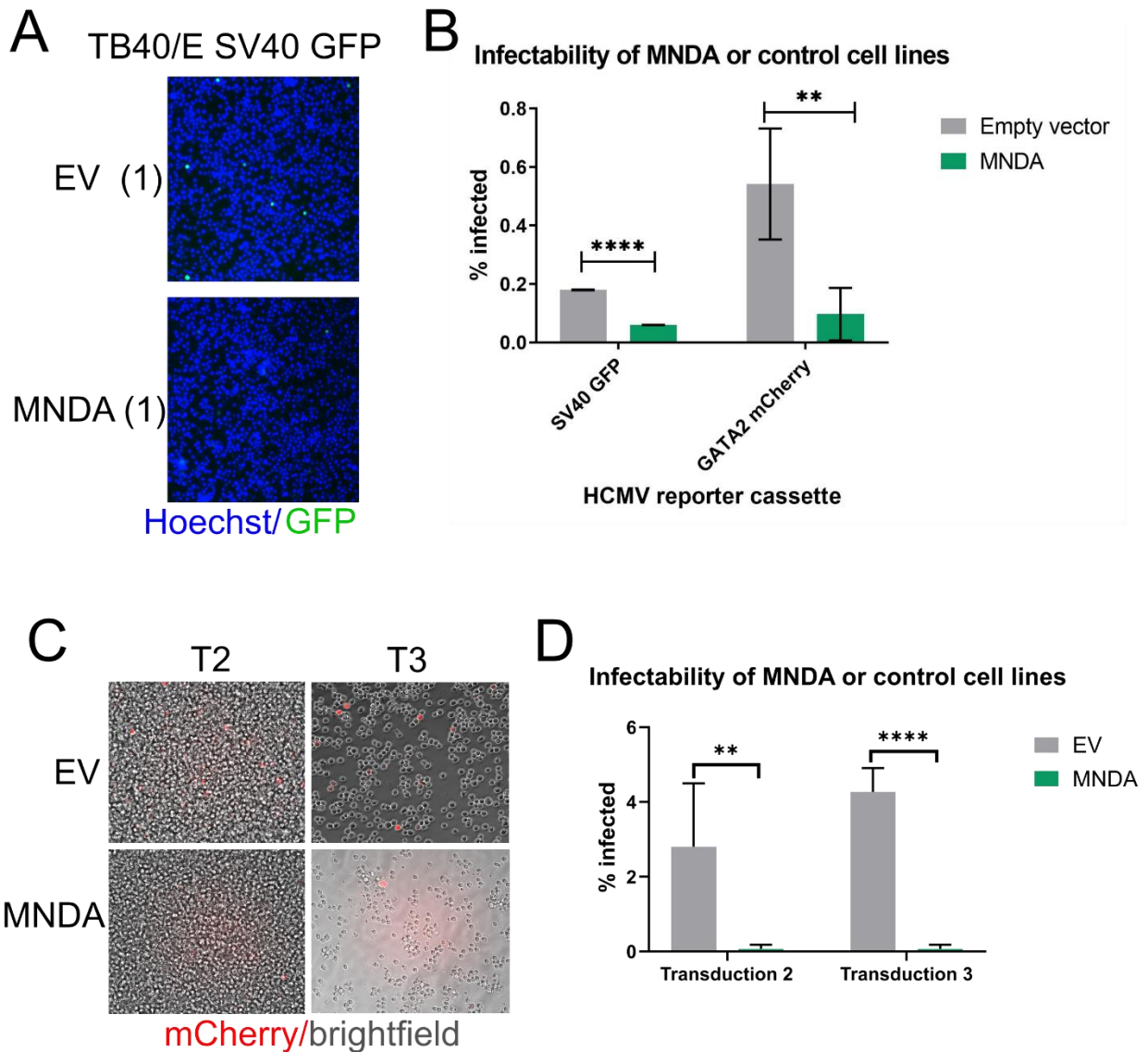


Figure 5-2 **MNDA-mediated restriction of virus-associated fluorescent reporter expression.** A) Empty vector (EV) or MNDA-overexpressing cells from transduction 1 were infected with TB40/E SV40 GFP. At 3 d.p.i., cells were counterstained for Hoechst and imaged. B) Quantification of GFP positive cells from (A) and those from a similar experiment except using TB40/E GATA2mCherry virus. C) EV and MNDA cells from transductions 2 and 3 (T2, T3) were infected with TB40/E GATA2mCherry virus. The next day, cells were imaged. D) Quantification of mCherry positive cells from (C). C and D were experiments performed by Esme Fowkes. Statistical analysis by two-way ANOVA and Sidak's multiple comparison test, **, $P < 0.01$; ****, $P < 0.0001$.

5.4. MNDA-overexpressing cells do take up viral genome following latent infection

The observations outlined in Figure 5-2 suggested that MNDA may act as a restriction factor for HCMV latency. There are many potential mechanisms by which this could be occurring, which I will discuss in §5.5. One mechanism I was able to begin to explore was whether MNDA overexpression leads to a

failure to take up and maintain viral genome. In a straightforward analysis, DNA from infected cells from the latter two independent transductions was harvested at 24 h.p.i. and analysed for relative HCMV DNA content (Figure 5-3). These data were accrued from the same experiments as shown in Figure 5-2 C/D, where, for transductions 2 and 3, there was a 10-to-20-fold difference between the proportions of mCherry positive cells. When analysing relative HCMV content, there was a decrease in HCMV DNA in both MNDA-overexpressing cell lines, compared with control empty vector cells. However, empty vector cells had only 1-to-2-fold increases in HCMV DNA, which seems unlikely to be sufficient to explain the 10-to-20-fold difference seen in fluorescence reporter. To further understand the differences in DNA levels, I would perform an extension of this analysis and analyse the relative HCMV DNA content at 3 h.p.i., 24 h.p.i., 48 h.p.i, 72 h.p.i, and 6 d.p.i., to distinguish between an entry phenomena and genome maintenance phenomena, both of which would clearly impact latent carriage and latency-associated gene expression.

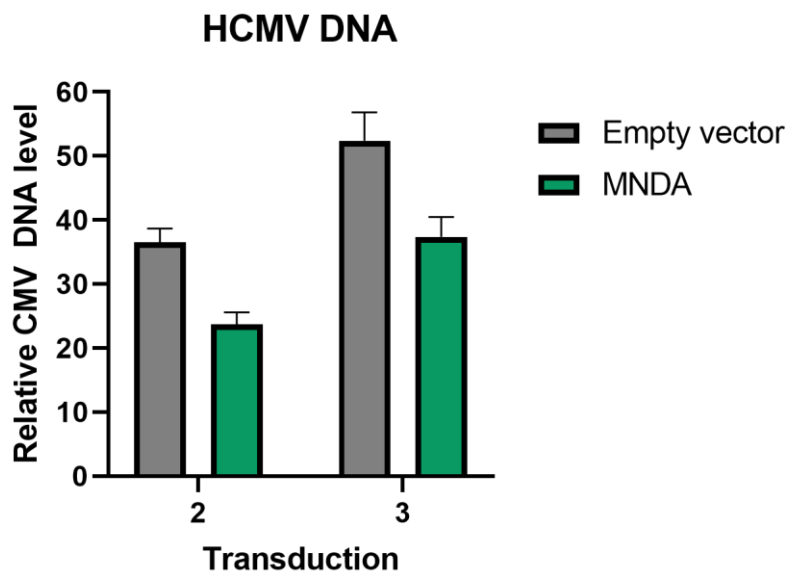


Figure 5-3 **Relative HCMV DNA levels in infected control and MNDA-overexpressing cells.** EV and MNDA cells from transductions 2 and 3 were infected with TB40/E GATA2mCherry virus. The next day, after imaging, cells were washed in a low pH citrate buffer to remove any cell-surface bound but uninternalized HCMV particles. Total DNA was then harvested and subject to qPCR for HCMV DNA using the UL44 promoter region as the HCMV target and GAPDH promoter region as host genomic DNA control. Results are expressed as $2^{-\Delta\Delta Ct}$ (GAPDH promoter-UL44 promoter). This analysis was performed by Esme Fowkes under my supervision.

5.5. Discussion

Very little is known about the function of the myeloid specific PYHIN protein MNDA, but it is partially downregulated during HCMV latency. In this Chapter, I began to address why it may be targeted during latency by overexpressing MNDA in THP-1 cells. I found that MNDA-overexpressing cells show lower levels of latent infection based on a reduction in the numbers of cells expressing fluorescent reporters in recombinant HCMV strains routinely used to detect latently infected myeloid cells, suggesting a form of antiviral restriction mediated by MNDA. Though viral genome levels were decreased in MNDA-overexpressing cells, I reasoned that this was insufficient to explain the difference in fluorescent reporter expression. While the analysis of genome uptake and carriage requires additional analysis, I am interested in analysing potential additional mechanisms of antiviral restriction.

The most important of these would be to analyse expression (both RNA, and protein if possible) of viral latency-associated transcripts such as US28, UL138, LUNA, and beta2.7. LUNA is particularly of interest because its promoter activity is driven by GATA2 sites during latency [142], which would provide a good comparison for mCherry expression in the GATA2mCherry virus. As described previously, IFI16 transcriptionally represses many different viral genes/promoters (for example HCMV UL54, HIV lytic transcription [264,271]). It is therefore feasible that the related protein MNDA could be performing a similar role.

If I were to find that MNDA enacts antiviral restriction by repression of HCMV latent transcription, there would be many potential lines of further investigation. I would wish to see if MNDA restricts transcription of all foreign DNA, for example by transfection of GFP expression plasmids. I would also look at other viruses, including herpesviruses such as HSV-1, other DNA viruses, retroviruses, and possibly RNA viruses. I would also investigate whether MNDA restricts transcription during HCMV lytic infection, by differentiating the cells prior to infection. It might be informative to transduce cells that do not typically express MNDA, for example fibroblasts, to see if MNDA is able to act as a restriction factor in these cell types.

Overall, my data appear to show a potentially very interesting and, as yet, undescribed function of MNDA as an antiviral restriction factor. However, there are multiple confounding issues which need to be addressed (such as whether this effect is a result of MNDA action specifically on SV40/GATA2 promoters) and, of course, detailed additional studies will eventually need to be carried out to identify the mechanism of any such restriction.

6. US28-mediated interference with DNA sensing

6.1. Introduction

I have already shown that US28 downregulates interferon-inducible genes when expressed in isolation, including IFI16, and that one US28-mediated effect on IFI16 appears to result in inhibition of IFI16-mediated activation of the viral MIEP. However, IFI16 is also involved in the double stranded DNA sensing pathway (see §1.6.4). An attractive hypothesis would, therefore, be that the expression of US28 also interferes with the ability of myeloid cells to sense double stranded DNA and induce a Type I interferon response. Furthermore, as US28 is expressed during latent infection, US28 could be required to evade sensing of the viral genome or viral transcription intermediates during the establishment or maintenance of HCMV latency.

Here, I explore whether US28 is capable of interfering with DNA sensing in myeloid cells, and the potential contributions of IFI16 and MND4 to such a phenomenon. Some experiments described were performed by Esme Fowkes, an undergraduate Part II student under my supervision, and these will be clearly detailed.

6.2. Undifferentiated THP-1 cells make far smaller responses to DNA stimuli compared with PMA-differentiated THP-1 cells

I wanted to take a reductionist approach and analyse the effect of US28 expression on responses to transfected DNA, a well-established insult for the induction of the interferon response, in undifferentiated THP-1 cells overexpressing US28. However, the vast majority of publications that examine interferon or pro-inflammatory responses in THP-1 cells differentiate their cells with PMA prior to analysis [206,224,256,377]. This was not an option for my studies, because, as previously reported [189], and shown again in Chapter 3, US28 alters cellular signalling and transcription in a differentiation dependent manner; in particular, US28 does not downregulate IFI16 in differentiated myeloid cells.

Consequently, I compared the response of undifferentiated and PMA-differentiated THP-1 cells to transfected DNA. I decided to use pUC19 plasmid that had been digested with the restriction enzyme BglI in order to create 'DNA ends' which are established to be good substrates for DNA sensing in some settings [378,379] (Figure 6-1 A). I first analysed IL-1 β production by ELISA, as IL-1 β is reported to be generated by IFI16-induced sensing in some settings [380,381]. As shown in Figure 6-1 B, PMA-differentiated THP-1 cells make detectable IL-1 β responses to LPS (a positive control), mock transfection, and transfection of digested pUC19. The response to mock transfection likely results from a cell-type

dependent pro-inflammatory response to the liposome-based transfection reagent [382], and the magnitude of the response to transfected DNA is increased with respect to mock. However, undifferentiated THP-1 cells did not produce quantifiable levels of IL-1 β under either mock or DNA transfection conditions.

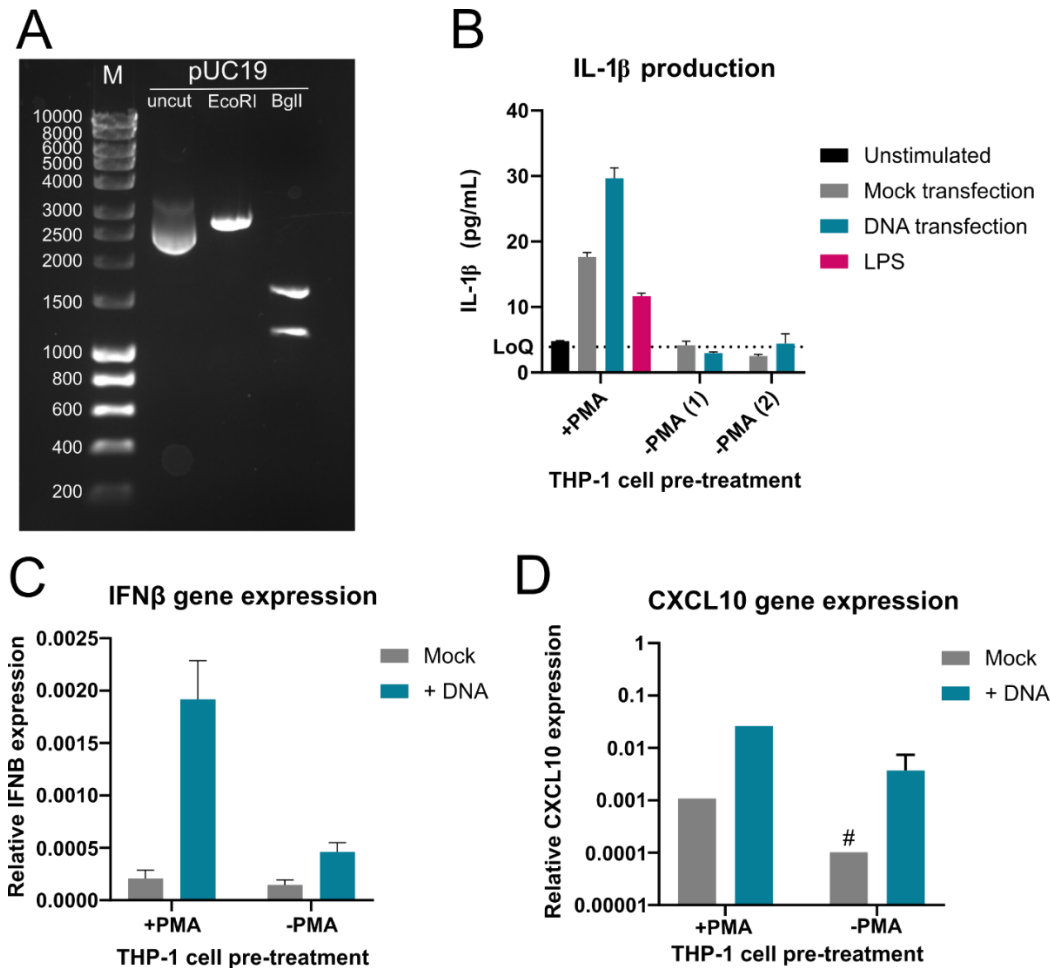


Figure 6-1 PMA pre-treatment of THP-1 cells leads to greater responses to transfected DNA. A) The 2698 bp plasmid pUC19 was digested with the restriction enzyme EcoRI to generate a single-cut, linear fragment, or with BglI to generate a 1118 bp and a 1580 bp fragment. Uncut plasmid, and molecular markers (M), were also separated on a 1 % agarose gel. Plasmid digestion and separation was performed by Esme Fowkes under my supervision. B) THP-1 cells were differentiated with PMA or left undifferentiated (-PMA) for 48 hours prior to stimulation with indicated reagents. Two independent undifferentiated samples were assessed. Mock transfection contained Fugene6, the liposome-based transfection reagent. 2 μ g/mL of BglI-digested pUC19 was used for DNA transfections and 100 ng/mL LPS was used for LPS stimulation. After 24 hours, the cell culture supernatants were assayed for IL-1 β by ELISA. LoQ indicates the lower limit of quantification for the ELISA. Single biological replicates were analysed by ELISA in duplicate. C) As B, except RNA from the stimulated cells was analysed for interferon beta (IFN β) expression. The graph shows single biological replicates analysed in triplicate by RT-qPCR. D) As B, except RNA from the stimulated cells was analysed for CXCL10 expression. The graph shows a single biological replicate analysed in triplicate by RT-qPCR for the +PMA condition, and two biological replicates for the -PMA condition. However, only one sample from the -PMA/mock condition had detectable levels of CXCL10 by RT-qPCR; this is indicated by '#'.

I also analysed IFN β and CXCL10 RNA levels in a similar experiment. IFN β is a Type I interferon and has been shown many times to be produced in response to transfected DNA and viral infections, and this involves IFI16 [256]. CXCL10 is often used as a 'surrogate' for Type I interferon because its expression can be activated by NF- κ B and IRF3, just like Type I interferons [383]. These analyses showed similar results to those for IL-1 β ; PMA-differentiated cells made measurable, substantial responses to transfected DNA (Figure 6-1 C,D), but undifferentiated THP-1 cells made much smaller responses. This meant that detecting differences in responses between undifferentiated THP-1 cells overexpressing genes of interest would be difficult.

6.3. US28-WT expression in myeloid cells may interfere with DNA sensing

Despite identifying potential difficulties assessing interferon responses in undifferentiated THP-1 cells, I pursued this line of investigation in undifferentiated THP-1 cells which express US28-WT or US28-R129A, or empty vector control THP-1 cells (described in Chapter 3). I transfected US28-WT and US28-R129A cells with uncut pUC19, or the dsDNA analogue poly dA:dT, and analysed IFN β mRNA levels the following day (Figure 6-2 A). I found a clear trend suggesting that US28-WT cells have attenuated responses to both plasmid and poly dA:dT, which is consistent with these cells expressing lower levels of the DNA sensor IFI16; however, the magnitude of the response is generally very low even in US28-R129A cells. I also found an attenuation of CXCL10 gene expression after transfecting BglI-digested pUC19 into US28-WT THP-1 cells compared with US28-R129A or empty vector cell lines (Figure 6-2 B), though it was difficult to be sure that US28-R129A cells responded to the stimulus over and above the CXCL10 levels found in mock transfected cells. I also found what appeared to be a weakened response to the same DNA stimulus when analysing IL-1 β production, but a lack of replicates and the existence of only a weak trend make these results inconclusive. Finally, I also tried to analyse both IFN α and IFN β protein production by ELISA following stimulus with digested or undigested plasmid, but the ELISA failed to detect any IFN α or IFN β protein in the cell culture supernatants (data not shown). Overall, these experiments do not lead me to draw strong conclusions about whether US28 expression interferes with DNA sensing, but I believe the trend shown in Figure 6-2 A hints at such an effect and merits further repetition and optimisation of the transfection conditions. For example, it may be that these genetically modified THP-1 cells were of too high a passage number to make responses, and early passage transduced cells are required to see an effect.

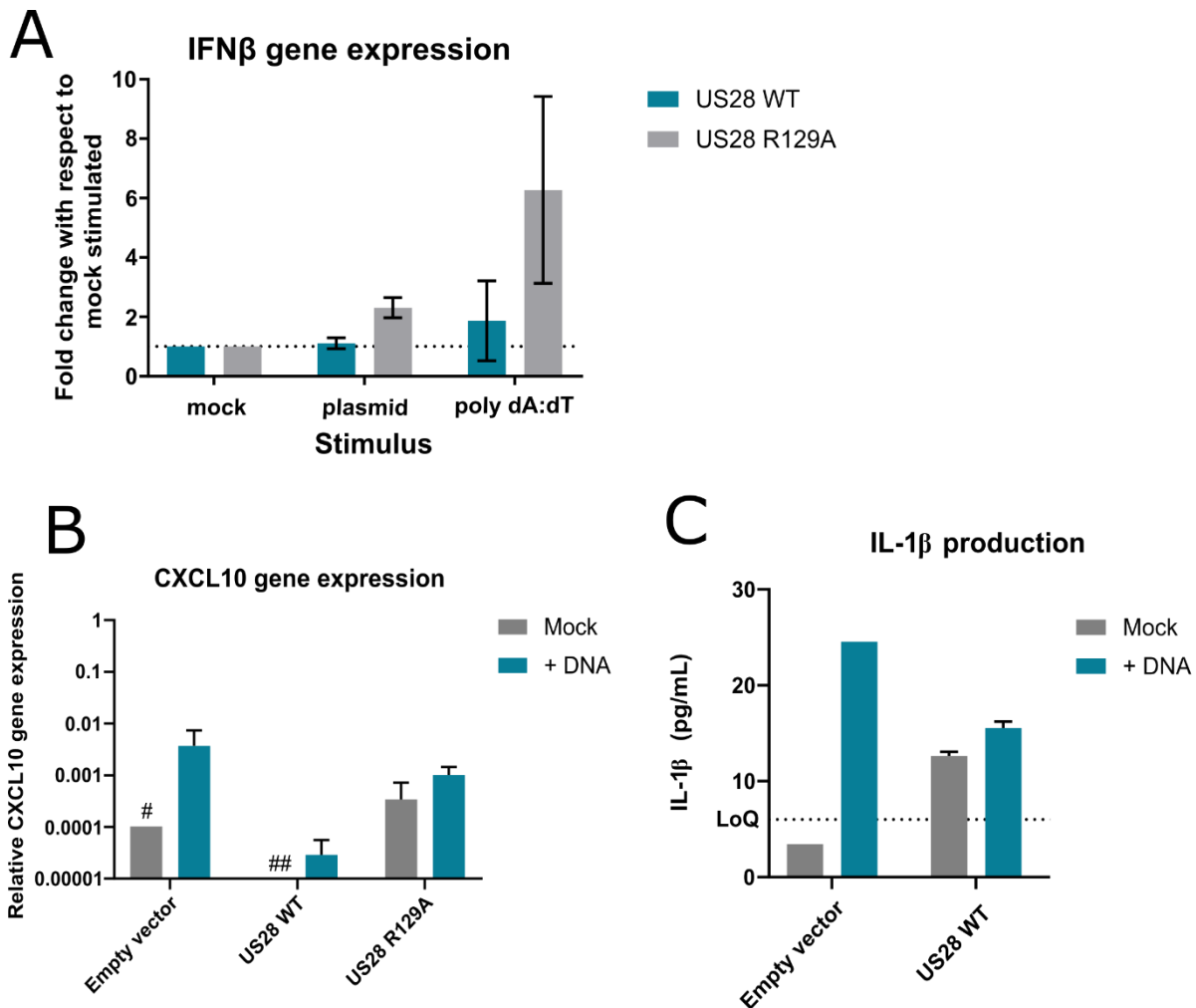


Figure 6-2 **US28-WT expressing THP-1 cells make attenuated cytokine responses to transfected DNA.** A) US28-WT or US28-R129A –expressing THP-1 cells (2×10^5) were mock transfected, or transfected with 1 μ g of uncut pUC19, or 1 μ g of the dsDNA analogue poly dA:dT. After overnight incubation, RNA was extracted and analysed for levels of IFN β mRNA, using GAPDH as a housekeeping gene. Results represent the average of two biological replicates analysed in technical triplicate and are displayed as $2^{-\Delta\Delta C_t}$ with respect to mock transfected cells. B) Empty vector, US28-WT or US28-R129A –expressing THP-1 cells (2×10^5) were mock transfected, or transfected with 2 μ g of digested pUC19. After 24 hours, RNA was extracted and analysed for levels of CXCL10 mRNA, using GAPDH as a housekeeping gene. Results represent the average of two biological replicates analysed in technical triplicate and are displayed as $2^{\Delta C_t}$ with respect to GAPDH. Where one or both of those biological replicates did not contain detectable CXCL10 mRNA, the bar is marked with a # or ##, respectively. C) As B, except cell culture supernatants were subject to ELISA for IL-1 β . Results represent the average of one (empty vector) or two (US28-WT) biological replicates analysed in technical duplicate. LoQ indicates the lower limit of quantification for the ELISA.

One prediction from these data, and data presented in Chapter 3, might be that latently infected primary CD14⁺ monocytes make lower interferon responses following infection in comparison with monocytes infected with Δ US28 HCMV. To that end, I compared the secretion of IFN α , IFN β , and IL-1 β (Figure 6-3) following infection by ELISA. In the first analysis, I found that IFN β is produced by monocytes and is measurable by ELISA (Figure 6-3 A). Addition of poly dA:dT to the media (no transfection reagents) was

sufficient to drive IFN β secretion. Infection with Titan WT also appeared to induce IFN β secretion, over and above uninfected and UV-inactivated virus-treated monocytes. A higher level of IFN β was detected in monocytes infected with Titan Δ US28, which is consistent with the hypothesis. However, analysis of the viral inoculum itself showed that all three viral conditions (UV-inactivated, Titan WT, Titan Δ US28) contained high levels of IFN β . Though the inoculum is removed after 2 hours of infection, and the cells washed with PBS, it is not possible to rule out the contribution of contaminating IFN β in the viral inocula. Furthermore, the particle:p.f.u. ratio is not known for each virus isolate, and it is feasible that a higher induction of IFN β in Titan Δ US28-infected monocytes could be due to an increase in the proportion of non-infectious particles in the inoculum.

The same potential confounders are present when interpreting the analysis of IFN α and IL-1 β in the supernatants of monocytes infected with TB40/*EmCherry* US28-3XFLAG ('WT') or TB40/*EmCherry* Δ US28 (Figure 6-3 B,C). Indeed, one donor had higher IFN α secretion after 24 hours infection with WT virus than with Δ US28 HCMV. Two further independent donors had similar IFN α secretion after 48 hours infection with both viruses. Monocytes from the third donor were differentiated to dendritic cells and the infections repeated; here no induction of IFN α was detected. This might be because dendritic cells secrete different profiles/subtypes of Type I interferons to monocytes [384,385]. Because the infection and washing protocol was identical for differentiated and undifferentiated monocytes, it does suggest that the induction of IFN α was likely due to detection of virus particles or other danger associated molecular patterns (DAMPs), and it was not due to contaminating IFN α in the viral inoculum, though I can not entirely rule this out. The particle:p.f.u. ratio was also not known for these TB40/E viruses. The results of an analysis of IL-1 β production were consistent with the hypothesis that latent infection is in some way anti-inflammatory, but given the confounders described in this section it is not possible to draw strong conclusions from this experiment.

To truly understand whether there is a difference in interferon/inflammatory responses between latent infection with WT HCMV, and infection in the absence of US28, I would need to work with highly purified infectious virions, with near-to-identical particle:p.f.u. ratio, and no contaminating cytokines or DAMP. I would also look at the relevant cytokines by RT-qPCR.

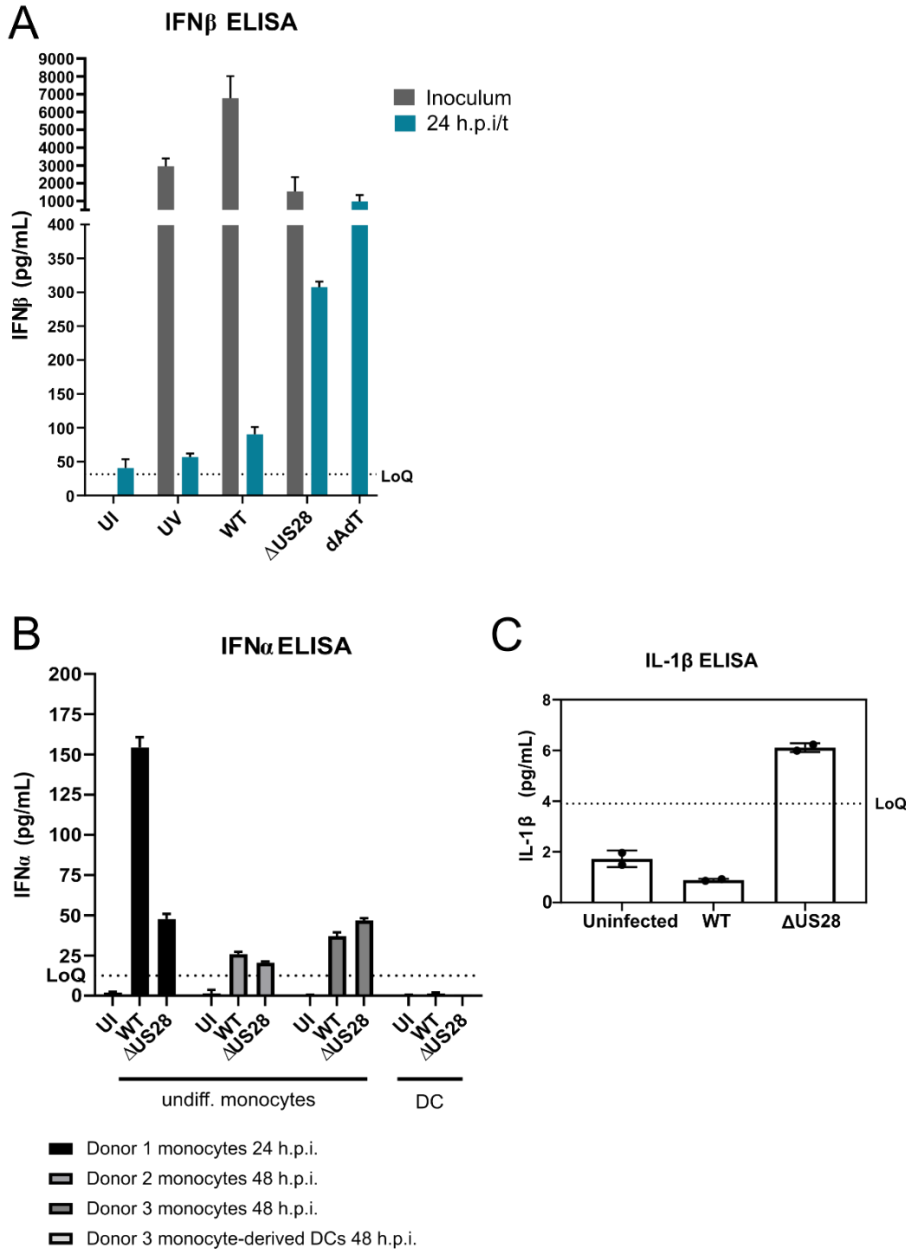


Figure 6-3 Infected monocyte interferon and IL-1beta responses. A) CD14⁺ monocytes were left uninfected (UI), treated with UV-inactivated Titan WT, infected with Titan WT or Titan Δ US28, or treated with 1 μ g/mL poly dA:dT. For UV or live virus treatments, these viruses were aspirated after two hours and the cells washed three times with PBS. After 24 hours, before the supernatants were harvested and assayed for IFN β by ELISA (teal bars, 24 hours post infection (i)/treatment (t)). To measure incoming IFN β , viral inocula were placed into empty wells and harvested after 2 hours before assay for IFN β by ELISA (grey bars, Inoculum). LoQ, lower limit of quantitation. B) Undifferentiated CD14⁺ monocytes were left uninfected (UI) or infected with TB40/E *mCherry* US28-3xFLAG (WT), or TB40/*EmCherry* Δ US28. Alternatively, CD14⁺ monocytes were differentiated to mature dendritic cells (DC) with GM-CSF/IL-4/LPS as described in Materials and Methods prior to infection. At the indicated time post infection, supernatants were harvested and assayed for IFN α by ELISA. LoQ, lower limit of quantitation. C) As B, but supernatants from undifferentiated monocytes were harvested after 48 hours of infection and assayed for IL-1 β by ELISA. LoQ, lower limit of quantitation.

6.4. IFI16 and MNDA super-expression drive Type I interferon responses to DNA in undifferentiated THP-1 cells

While I could not draw strong conclusions about whether US28 interferes with DNA sensing, I was still interested in whether IFI16 and MNDA were part of the DNA sensing machinery in undifferentiated myeloid cells. I took THP-1 cells overexpressing IFI16 and MNDA, or empty vector controls (described in Chapter 4 and Chapter 5, IFI16 transduction 2 and MNDA transduction 1) and transfected these with BglI-digested pUC19, as described in §6.2. I then analysed IFN β and CXCL10 by RT-qPCR, and IL-1 β by ELISA (Figure 6-4). As described in §6.2, empty vector control THP-1 cells made little-to-no response to the transfected DNA. However, in a single experiment, overexpression of IFI16 and MNDA substantially increased the IFN β and CXCL10 response to transfected DNA, though, interestingly, not IL-1 β responses. From this, I conclude that IFI16 contributes to interferon responses to transfected DNA in undifferentiated myeloid cells, as it does in differentiated myeloid cells, and other cell types such as keratinocytes [201,206,224,256]. Excitingly, MNDA also contributed to interferon responses to transfected DNA, which has not been previously published. MNDA overexpressing cells had higher levels of IFN β and CXCL10 in both mock and DNA transfected conditions, and I can rule out that MNDA overexpression simply increased IFI16 expression by the western blot presented in Figure 4-1 in Chapter 4. The same effect on IL-1 β did not occur, indicating that an inflammasome type response is unlikely to be a function of IFI16 and MNDA in undifferentiated myeloid cells. If these results can be repeated, it would be the first step to identifying MNDA as a myeloid-specific component of the DNA sensing machinery.

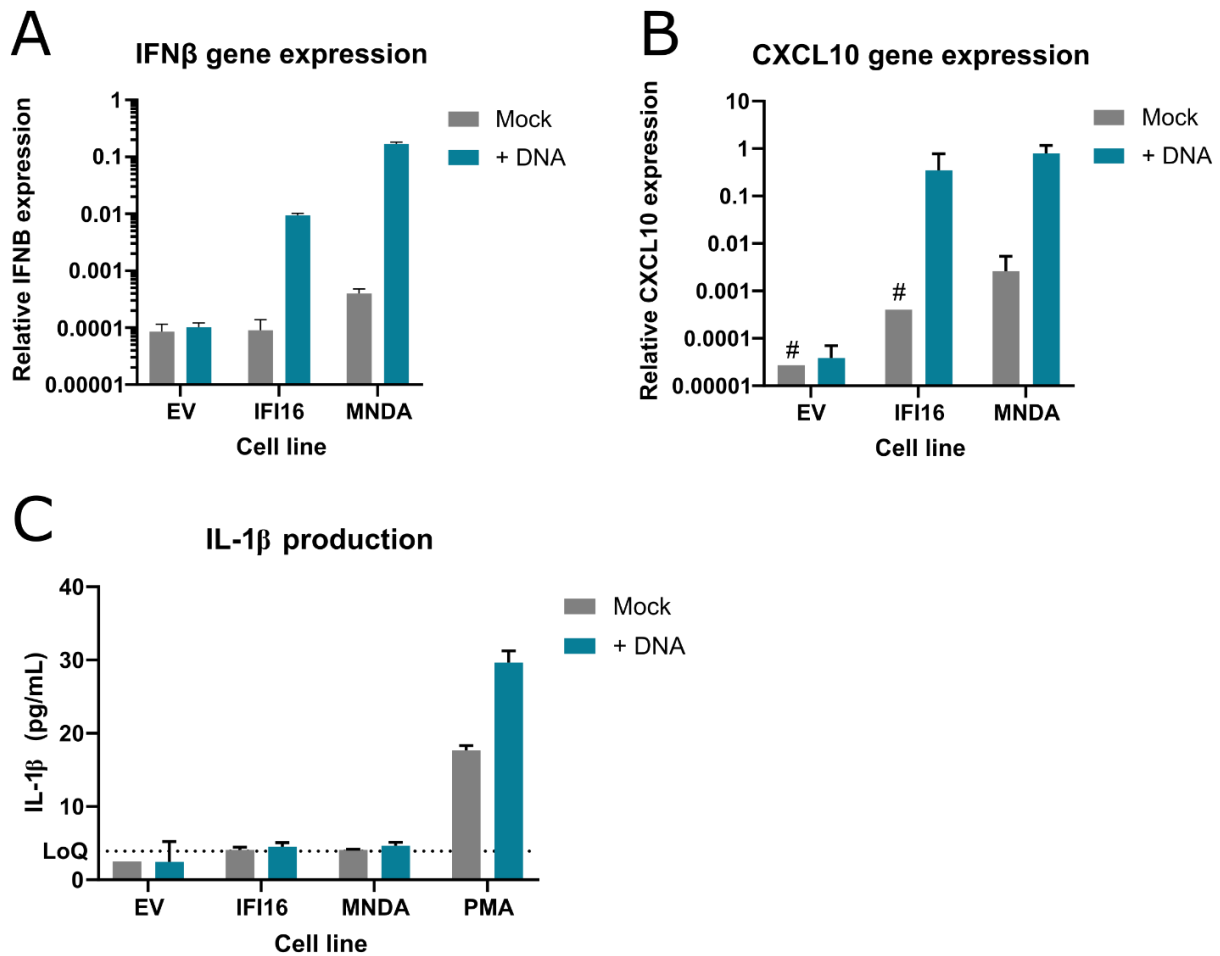


Figure 6-4 **IFI16 and MNDA overexpression drives interferon but not IL-1beta responses to transfected DNA.** A) Empty vector (EV), IF16-overexpressing, and MNDA overexpressing THP-1 cells (2×10^5) were mock transfected or transfected with 2 μ g of digested pUC19. After 24 hours, RNA was extracted and analysed for levels of IFN β mRNA, using GAPDH as a housekeeping gene. Results represent the mean of one biological replicate analysed in technical triplicate, displayed as $2^{\Delta Ct}$ with respect to GAPDH B) As A), except RNA was analysed for levels of CXCL10 mRNA, using GAPDH as a housekeeping gene. Results represent the average of two biological replicates analysed in technical triplicate and are displayed as $2^{\Delta Ct}$ with respect to GAPDH. Where one of those biological replicates did not contain detectable CXCL10 mRNA, the bar is marked with a '#'. C) As B, except cell culture supernatants were subject to ELISA for IL-1 β . Results represent the average of two biological replicates analysed in technical duplicate. LoQ indicates the lower limit of quantification for the ELISA. Results for PMA differentiated THP-1 cells (from Figure 6-1) are plotted on this graph to indicate that the ELISA was able to detect IL-1 β in cell culture supernatants.

6.5. Discussion

In this Chapter, I have investigated whether US28 may be preventing DNA/other nucleic acid sensing in the context of latent infection of undifferentiated myeloid cells, and whether this is linked to the US28-mediated downregulation of IFI16 and/or MNDA. I analysed the ability of US28 to interdict in DNA

sensing in a reductionist system (THP-1 cells transfected with DNA or DNA analogues), and in the context of latently infected monocytes.

I was greatly hindered in this investigation by a general failure of undifferentiated THP-1 cells to make robust and substantial interferon/inflammatory cytokine responses to transfected DNA, and the presence of confounding factors during virus infections. Furthermore, I did not assess whether interferon treatment has any impact on the efficiency of latency establishment and downstream reactivation. This analysis would be greatly needed to correctly interpret any US28-mediated effects seen. These important experiments could not be performed due to time limitations.

While differentiated THP-1 cells were competent for generating interferon responses to transfected DNA, I could not use differentiated THP-1 cells for my analyses because US28 expression has a very different phenotype in differentiated myeloid cells [189], and does not downregulate IFI16 in this context (Chapter 3). I found some indications and trends that suggested that US28 may interdict in DNA sensing when expressed in isolation in myeloid cells; it is possible that further extensive optimisation of the system would lead to the kind of reproducible data necessary to draw robust conclusions. My overall view of the data generated during infections of monocytes is that it is impossible to interpret without knowing the particle:p.f.u. ratio and having highly purified virion preparations.

Perhaps the most interesting pieces of data generated here were results suggesting that MNDA could be acting as a DNA sensor, like the other three PYHIN proteins. MNDA overexpression clearly resulted in increased interferon responses to transfected DNA. A more detailed, mechanistic understanding of the role of MNDA in such a response is now required. To gain such an understanding, I would generate MNDA knock-out THP-1 cells, or iPSCs, by CRISPR-Cas9, to determine whether MNDA is *necessary* for interferon responses, or just enhances these responses. I would transduce cells that do not normally express MNDA (e.g. fibroblasts, 293T, keratinocytes) with MNDA-overexpression constructs to determine if MNDA can also contribute to DNA sensing there. I would determine whether MNDA binds DNA as part of the mechanism by CHIP, and/or whether it interacts with canonical components of DNA sensing pathways (e.g. STING, cGAS). I would also determine if MNDA functions independently of STING, cGAS, etc, by repeating the analysis presented in Figure 6-4 in STING/cGAS knockout cells. Finally, I would like to determine whether MNDA interactions with DNA sensing pathways are independent of, or linked to, the restriction on HCMV latency as presented in Chapter 5.

7. Selective shock and kill using anti-US28 nanobodies

7.1. Introduction

Single-domain camelid antibodies, termed nanobodies (Nb) are promising molecules for experimental, diagnostic, and therapeutic tools [307,309,310]. Collaborators at the Vrije Universiteit, The Netherlands, have developed several US28-targeting nanobodies that can interfere with aspects of US28 ligand binding and signalling [182,308,318]. I worked closely with Timo de Groof, a PhD student from Martine Smit's group at Vrije Universiteit, to analyse the effect of two US28-targeting nanobodies on latently infected cells. The first, VUN100, has previously been characterised [308], and inhibits US28 ligand binding. The second is a bivalent form of VUN100, termed VUN100b. Our collaboration aimed to address whether either of these nanobodies could interfere with US28 functions that are important for the maintenance of latency. In particular, if either nanobody were to block MIEP suppression, we would predict IE gene expression during HCMV latency – a phenomenon we have previously shown to make latently infected monocytes vulnerable to T cell killing [145].

Here, I will present the characterisation of VUN100b, the effect of VUN100 and VUN100b on latently infected monocytes, and the subsequent impact on T cell killing and reactivation. Timo de Groof performed the binding studies, immunostaining, and analysis of the effect on US28 signalling in cell lines. I performed the majority of the studies on latently infected monocytes, with Timo de Groof performing some of these during a month-long visit to our laboratory. Eleanor Lim, a PhD student in Mark Wills's laboratory here at the Department of Medicine, performed T cell isolations and assisted with assays involving T cell killing.

7.2. US28 nanobodies induce immediate early gene expression

7.2.1. Bivalent nanobody VUN100b binds US28 and inhibits US28-mediated signalling

The existing US28-specific nanobody VUN100 is an antagonist of US28 – it inhibits ligand binding to US28 and ligand-dependent US28 activity [308]. By generating a bivalent format of VUN100, termed VUN100b, it was hoped that a higher affinity molecule displaying inverse agonist properties would be generated; in several cases, bivalent nanobodies that target chemokine receptors are already known to be inverse agonists [309,311]. In the case of a US28 inverse agonist, the molecule would block US28 signalling independently of ligand presence. VUN100b is composed of: N-VUN100-30GS-VUN100-C, where N and C

are the N and C termini, VUN100 is the monovalent Nb in the N-C orientation in both arms, and 30GS is a 30 amino acid glycine-serine linker.

Characterisation of VUN100b binding by ELISA found that it had a 5-to-10 fold higher affinity for US28 than VUN100, as defined by the concentration that gave 50% binding (Figure 7-1 A). While VUN100 can bind US28, and has previously been shown to inhibit ligand binding [308], we found that VUN100 was not able to impact constitutive US28 signalling in a reporter assay; however, VUN100b could block the ability of US28 to activate a Nuclear Factor of Activated T-cells (NFAT)-luciferase reporter by 50% (Figure 7-1 B). This indicated that VUN100b had additional activity against US28 compared with VUN100, consistent with the bivalent format being an inverse agonist. To test the specificity of VUN100 and VUN100b binding to US28, THP-1 cells expressing US28-WT (see Chapter 3) were incubated with these nanobodies, or an irrelevant nanobody, and immunostained for US28 expression and the Myc epitope tag used for nanobody production and purification. This showed that only US28 expressing cells were co-stained with nanobody (Figure 7-1 C). Finally, an analysis of the effect of these nanobodies (at saturating concentrations) on US28 signalling in myeloid cells showed that US28 expression attenuates ERK1/2 phosphorylation in THP-1 cells, a phenomenon that is important for MIEP suppression and the establishment of latency [189]. In contrast, neither irrelevant Nb nor VUN100 treatment could block ERK1/2 dephosphorylation in the presence of US28, but that VUN100b treatment increased ERK1/2 phosphorylation (Figure 7-1 D), demonstrating that VUN100b can block US28 signalling in undifferentiated myeloid cells.

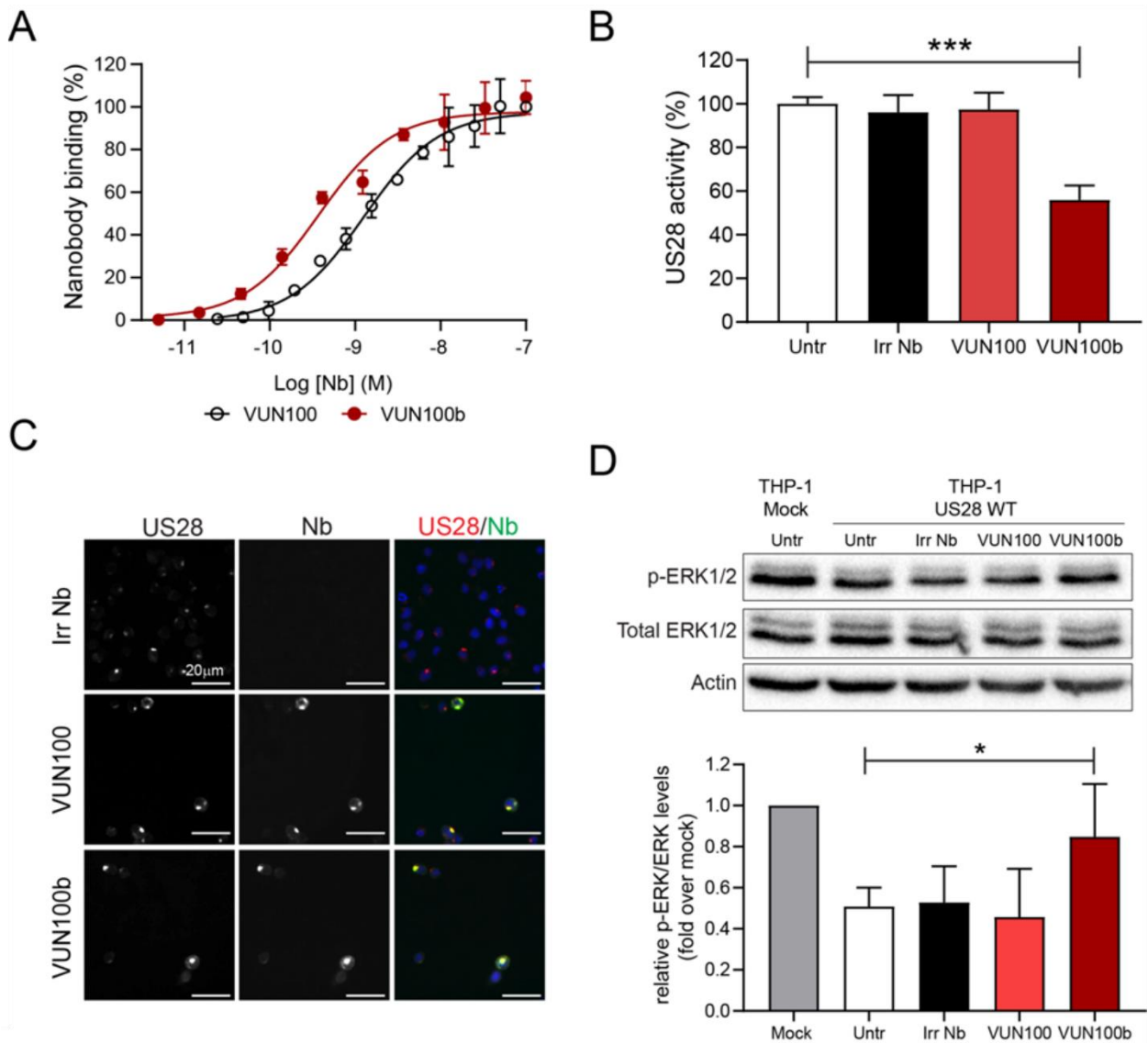


Figure 7-1 Characterisation of VUN100b and comparison with VUN100. A) VUN100 and VUN100b binding to membrane extracts from US28-expressing HEK293T cells was analysed by ELISA. B) HEK293T cells expressing US28 and containing a Nuclear Factor of Activated T-cells (NFAT)-luciferase reporter were untreated (untr) or treated with an irrelevant nanobody (Irr Nb), VUN100 or VUN100b for 24 h prior to luminescence measurement. C) Immunofluorescence microscopy of nanobody binding to US28-expressing THP-1 cells. US28 was detected using a polyclonal rabbit-anti-US28 antibody (US28, red). Bound nanobody was detected using the Myc-tag present on the nanobodies and an anti-Myc antibody (Nb, green). D) lysates of THP-1 empty vector transduced cells (Mock) or US28-expressing THP-1 cells were probed for phospho-ERK1/2 levels by western blot. Cells were untreated (untr) or treated with an irrelevant nanobody (Irr Nb), VUN100 or VUN100b at 100 nM for 48 h prior to harvest of the lysate. Levels of phosphorylated ERK1/2 relative to total ERK1/2 protein levels were determined and normalized to actin protein levels. Subsequently, relative phosphorylated protein levels were normalized to untreated THP-1 mock cell lysates. Representative figure is shown while data is plotted as mean \pm S.D. and is obtained from three or four independent experiments. Statistical analyses were performed using unpaired two-tailed t-test. *, $p < 0.05$; ***, $p < 0.001$. These analyses were performed by Timo de Groof and panels C and D use US28-expressing THP-1 cells, described in Chapter 3, which I provided.

7.2.2. VUN100b induces IE gene expression in latently infected monocytes

Given that US28 signalling is essential for latency in monocytes, and that VUN100b inhibits US28 signalling in monocytic THP-1 cells, I reasoned that VUN100b would likely inhibit some US28 activity during latency in CD14⁺ monocytes, leading to derepression of the MIEP and activation of IE gene expression. The monovalent VUN100 inhibits ligand binding activity, which, based on previously published data, we predicted would have a lesser effect on US28-mediated suppression of the MIEP [189,193].

I used the IE2-eYFP reporter virus to monitor IE2 gene expression during experimental latency. As described in Chapter 4, IE2 expression is generally repressed in latently infected monocytic cells but can be reactivated using differentiation or other stimuli (such as IFI16 overexpression). I was able to monitor IE2 gene expression in living cells, but I was also able to fix and stain for total IE at 2 or 6 d.p.i.. This latter protocol then enabled automated analysis of the number of IE positive cells and was useful when there were very large numbers of IE positive cells in each well. This type of analysis was performed for five independent donors, and showed that both VUN100 and VUN100b increased IE gene expression in latently infected monocytes (Figure 7-2, Figure 7-3). VUN100b consistently caused a 2-to-10-fold increase in IE gene expression, but VUN100 significantly increased IE gene expression in some, but not all, donors (Figure 7-3).

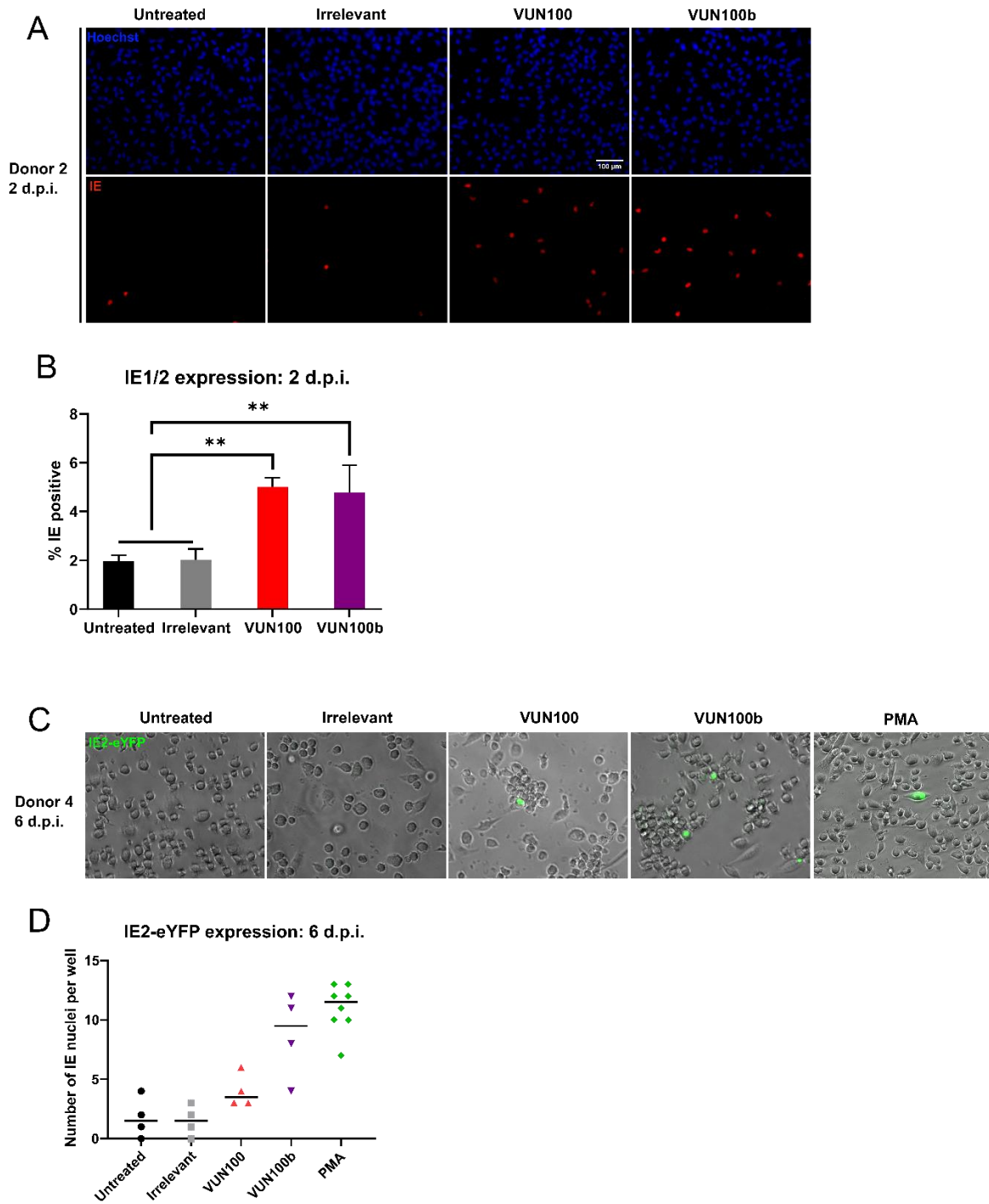


Figure 7-2 VUN100 and VUN100b increase IE gene expression in latently infected monocytes. Primary CD14⁺ monocytes were latently infected with TB40/E IE2-eYFP for 2 hours prior to incubation with the indicated nanobodies, left untreated, or treated with PMA to induce differentiation. Nanobodies were replenished every 2 or 3 days A) At 2 d.p.i., latently infected monocytes from Donor 2 were fixed and stained for total IE protein. B) Proportions of IE positive cells in A were analysed by Cellomics ArrayScan plate reader. Statistical analysis performed by one-way ANOVA followed by Tukey's multiple comparison test. **, P<0.01. C) At 6 d.p.i., latently infected monocytes from Donor 4 were imaged. Merged Brightfield and YFP channel images are shown. D) IE2-eYFP positive cells from C were counted.

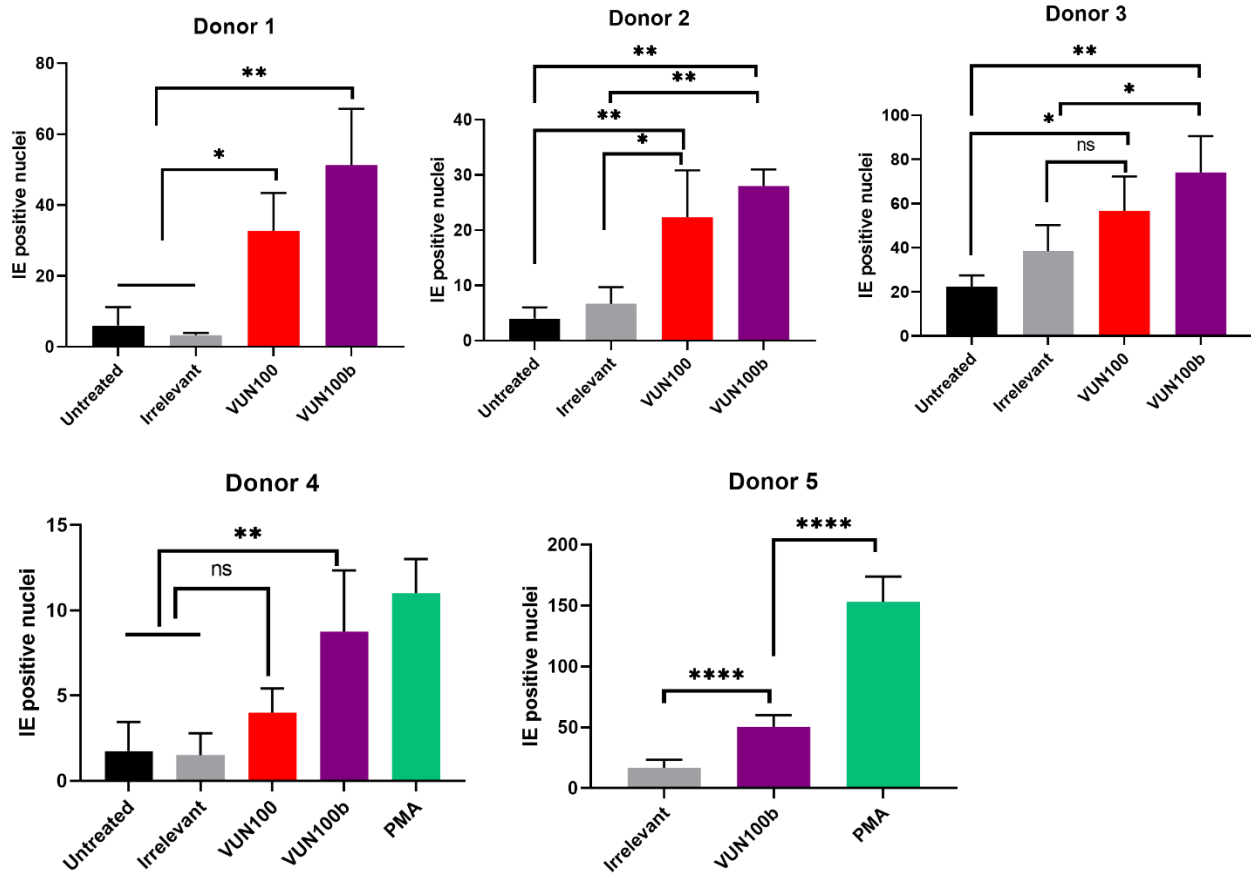


Figure 7-3 **VUN100b consistently upregulates IE gene expression in latently infected monocytes.** Primary CD14⁺ monocytes were latently infected with TB40/E IE2-eYFP for 2 hours prior to incubation with the indicated nanobodies, or left untreated, or treated with PMA to induce differentiation. Nanobodies were replenished every 2 or 3 days. At 6 d.p.i., latently infected monocytes were imaged and IE2-eYFP positive cells from were counted. The mean number of IE positive nuclei in each well is shown, statistical analysis performed by one-way ANOVA followed by Tukey's multiple comparison test. *, P<0.05; **, P<0.01; ***, P<0.001; ****, P<0.0001; ns, P>0.05.

I wished to confirm the specificity of VUN100b for US28 during latency by performing a similar analysis on cells latently infected with either WT, or Δ US28 HCMV. I was unable to perform a direct comparison of matched strains, but I did perform a small-scale comparison of monocytes from Donor 3 infected with TB40/E IE2-eYFP with those infected with Titan Δ US28. As predicted, while VUN100b increased the number of IE expressing monocytes latently infected with IE2-eYFP, VUN100b failed to have any effect on IE expression in monocytes infected with Titan Δ US28 (Figure 7-4). This is important because it indicates that VUN100b does not drive a general increase in permissiveness for lytic infection in monocytes. However, this should be repeated with matched virus strains, and quantified.

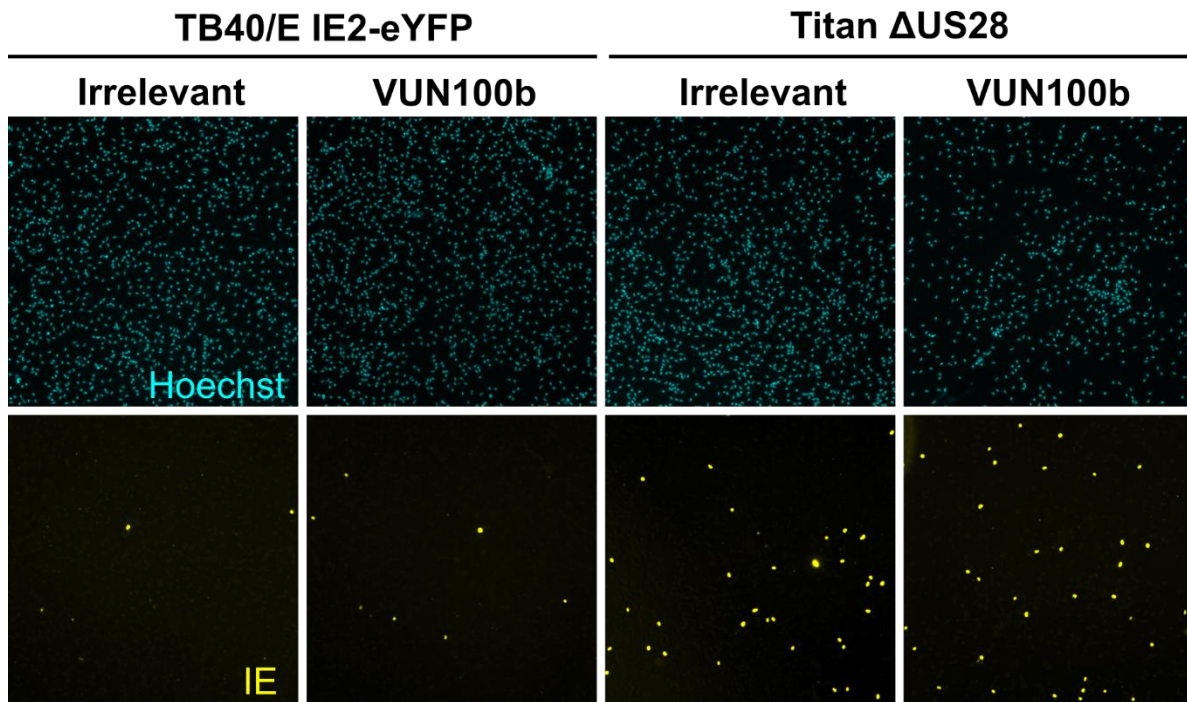


Figure 7-4 **VUN100b is only capable of activating IE gene expression in monocytes in the presence of US28.** Primary CD14⁺ monocytes (donor 3) were latently infected with TB40/E IE2-eYFP or Titan Δ US28 for 2 hours prior to incubation with the indicated nanobodies. Nanobodies were replenished every 2 or 3 days. At 6 d.p.i., infected monocytes were fixed and stained for total IE, and imaged using the ArrayScan XTI instrument.

7.2.3. VUN100b does not drive full virus reactivation

Published data have shown that treatment of latently infected monocytes with the US28 inhibitor VUF2274 leads to full viral reactivation [189]. In our previous shock and kill strategies, reactivation of expression of lytic HCMV antigens in latently infected monocytes led to T cell recognition and killing [145]. However, in any such strategy, full virus reactivation would be unfavourable because of the potential for an acute infection and the likelihood of expression of viral immune evasion genes known to be expressed at early and late times of lytic infection [20,386]. Therefore, I wished to ensure that VUN100 and VUN100b do not drive full virus reactivation. I analysed viral gene expression by RT-qPCR and production of infectious virus via coculture with indicator fibroblasts in the absence or presence of nanobodies. As shown in Figure 7-5 A, substantial production of infectious virus occurred when latently infected monocytes are differentiated with PMA to induce full virus reactivation. These levels were not produced when latently infected monocytes were treated with VUN100 or VUN100b, despite the similar levels of IE2 expressed in latently infected monocytes from that same donor treated with VUN100b or PMA (Figure 7-2 D). These results are supported by the analysis of expression of a panel of viral genes (Figure 7-5 B). While IE1/IE72 gene expression was increased by VUN100b, the expression of UL32, a

true-late gene encoding tegument protein pp150, was undetected in latently infected monocytes treated with nanobodies. In contrast, monocytes differentiated with PMA or infected with HCMV Δ US28, which causes lytic infection, do express UL32.

The expression of the early gene and viral DNA polymerase complex component UL44 was increased by VUN100b, but not to the same extent as PMA differentiation or Δ US28 infection. The same pattern was present with the immune evasion gene US11. US11 participates in virally-induced MHC Class I downregulation during lytic infection [386–390]. Since we were interested in US28-specific nanobodies as reagents for shock and kill interventions, we wished to avoid major induction of T-cell immune evasins like US11. Pleasingly, these results indicated that there was only a small upregulation of US11 after reactivation of viral gene expression in latently infected monocytes after nanobody treatment.

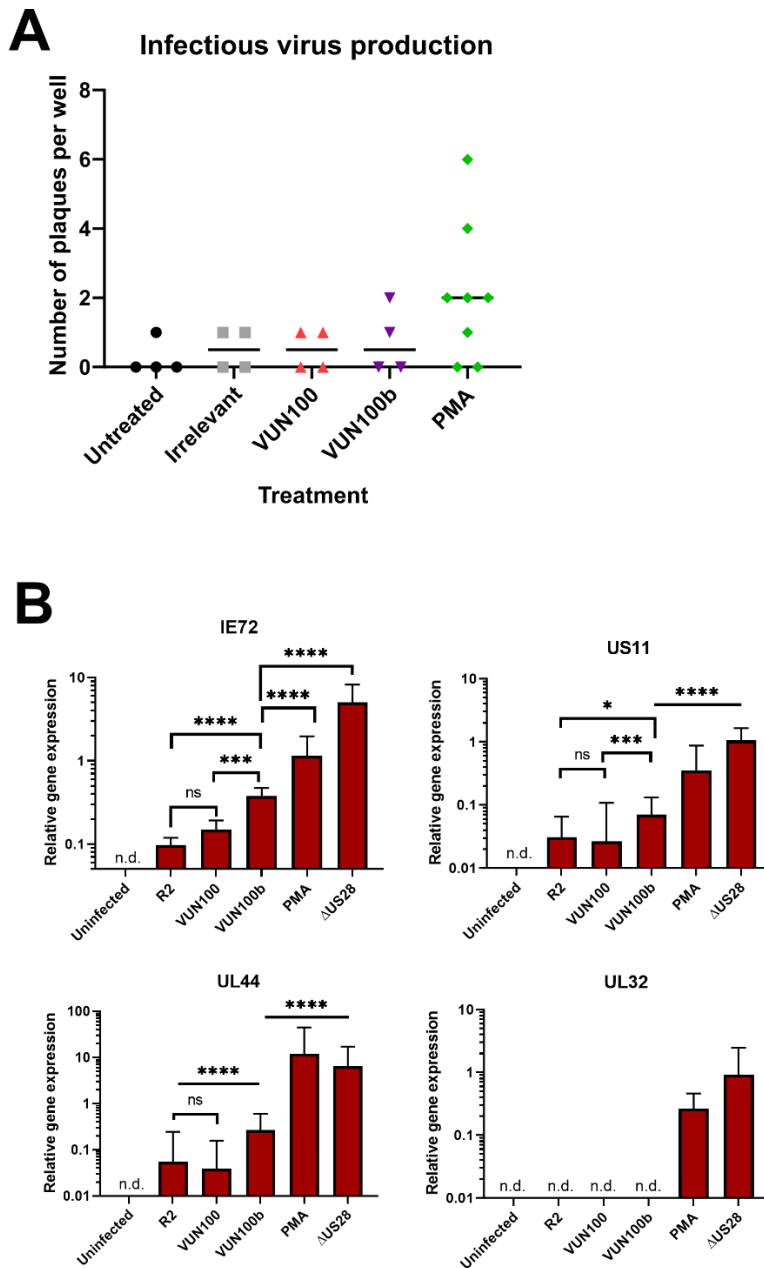


Figure 7-5 VUN100 and VUN100b treatment does not lead to full lytic replication in monocytes. Primary CD14⁺ monocytes were latently infected with TB40/E IE2-eYFP for 2 hours prior to incubation with the indicated nanobodies, or left untreated, or treated with PMA to induce differentiation and virus reactivation. Nanobodies were replenished every 2 or 3 days. Alternatively, primary CD14⁺ monocytes were infected with Titan ΔUS28. A) Monocytes from donor 4 were cocultured with indicator fibroblasts. After 7 days, IE2 positive plaques were counted. B) At 6 d.p.i., total RNA from monocytes from donor 3 were isolated and subjected to RT-qPCR for the indicated viral transcripts. Expression was normalised to GAPDH and is presented as 2^{ΔCt}. Where transcript was not detected, 'n.d.' replaces a bar. statistical analysis performed by one-way ANOVA followed by Tukey's multiple comparison test. *, P<0.05; **, P<0.01; ***, P<0.001; ****, P<0.0001; ns, P>0.05.

7.3. US28-specific nanobody treatment of latent monocytes directs their T cell killing

Following my promising results using nanobodies to activate IE gene expression in latently infected cells, I assessed whether this ability of nanobodies to activate IE expression in latently infected monocytes also allowed their T-cell recognition and killing and also whether this led to a reduction in differentiation-induced reactivation of HCMV from them. I isolated PBMC from a seropositive individual and separated the CD14⁺ monocytes from these PBMC. I then latently infected monocytes with the IE2-eYFP reporter virus and treated with either irrelevant nanobody or VUN100b. The IE2-eYFP reporter would allow tracking of IE2-positive monocytes during latency and reactivation in living cells. One major caveat to the use of this virus is that it is a BAC-derived strain of HCMV and is deleted in the US2-US6 region, which encode several proteins that downregulate MHC Class I and II molecules or otherwise interfere with antigen presentation [386,391]. However, as described above, this virus does encode US11, which is sufficient to downregulate some MHC Class I molecules [388–390].

After 6 days' treatment of latently infected monocytes with nanobodies, PBMC were separated into a CD4⁺/CD8⁺ population (T cells) and the remaining, CD4⁺/CD8⁺ depleted, PBMC (Figure 7-6, Figure 7-7). I included CD4⁺ T cells because there are HCMV-specific CD4⁺ CTLs in healthy donors [392,393]. IE positive cells were counted, and then the latently infected monocytes were cocultured with T cells or depleted PBMC at an effector:target ratio of 5:1 in the presence of nanobody (Figure 7-7 A). The count just prior to coculture indicated that VUN100b increase IE gene expression and this difference was consistent in the replicate wells (Figure 7-7 B, C).

IE positive cells were then counted at 18 and 40 hours after addition of PBMC/T cells. In all cases, there was a drop in the number of monocytes expressing IE protein which, formally, might have been due to increasing suppression of the MIEP as latency was being established. However, VUN100b/depleted PBMC treated wells continued to have higher numbers of IE positive cells than irrelevant nanobody treated controls, while VUN100b/T cell treated wells had low levels of IE positive cells, suggesting that IE positive cells were being killed in the presence of VUN100b and T cells (Figure 7-7 B, D).

At 48 hours post addition, the PBMC/T cells were also removed and the monocytes differentiated to immature DCs using GM-CSF/IL-4 in the absence of nanobodies. This differentiation to immature DCs is known not to reactivate IE gene expression [152] and, consistent with this, all four conditions (irrelevant antibody +/- T cells, VUN 100b +/- T cells) generated very low levels of IE positive cells. After 5 days'

incubation with GM-CSF/IL-4, differentiating cells were matured with LPS stimulation, which induces full virus reactivation [152]. Two days later, reactivating IE positive cells were counted (Figure 7-7 B, E). In the presence of depleted PBMC, both VUN100b and irrelevant nanobody-treated cells saw IE reactivation. Irrelevant nanobody-treated cells also saw IE reactivation if they had been cocultured with T cells, though admittedly at slightly lower levels than PBMC-depleted cells; this might be because the T cells in this condition kill any monocytes that spontaneously express IE. However, VUN100b/T cell treated cells showed almost no reactivation, demonstrating that VUN100b directs T cell killing of experimentally latent monocytes which is reflected in a lack of subsequent levels of reactivation.

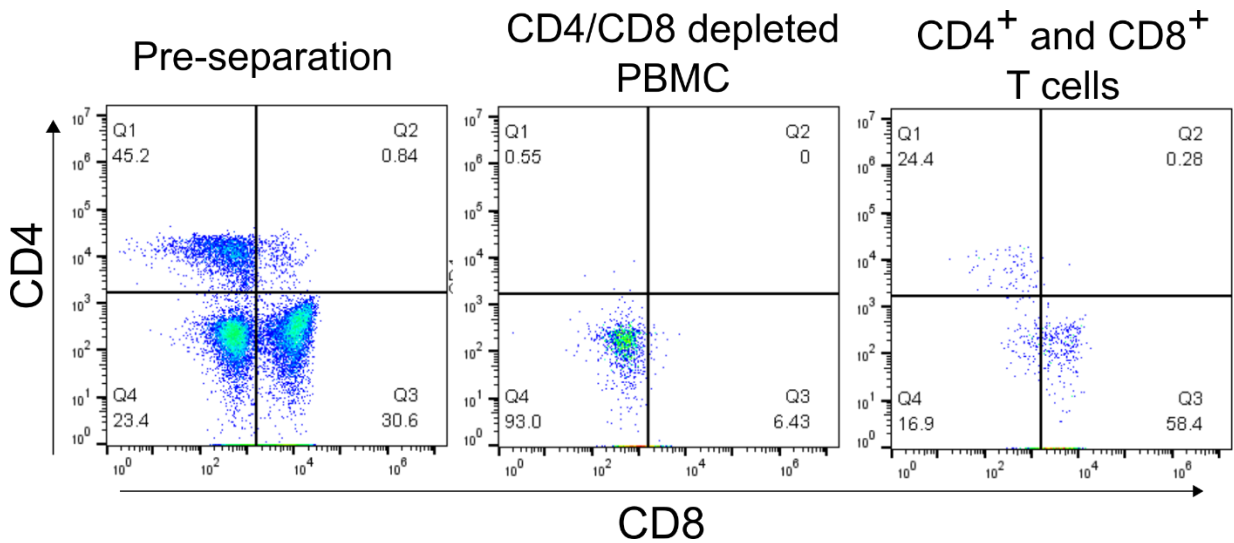


Figure 7-6 **T cell separations from PBMC.** CD4⁺ and CD8⁺ cells were separated from the previously monocyte-depleted PBMC (Pre-separation) by MACS. Purity of the CD4/CD8 depleted PBMC and CD4⁺ and CD8⁺ fractions was assessed by flow cytometry. These procedures were performed by Eleanor Lim.

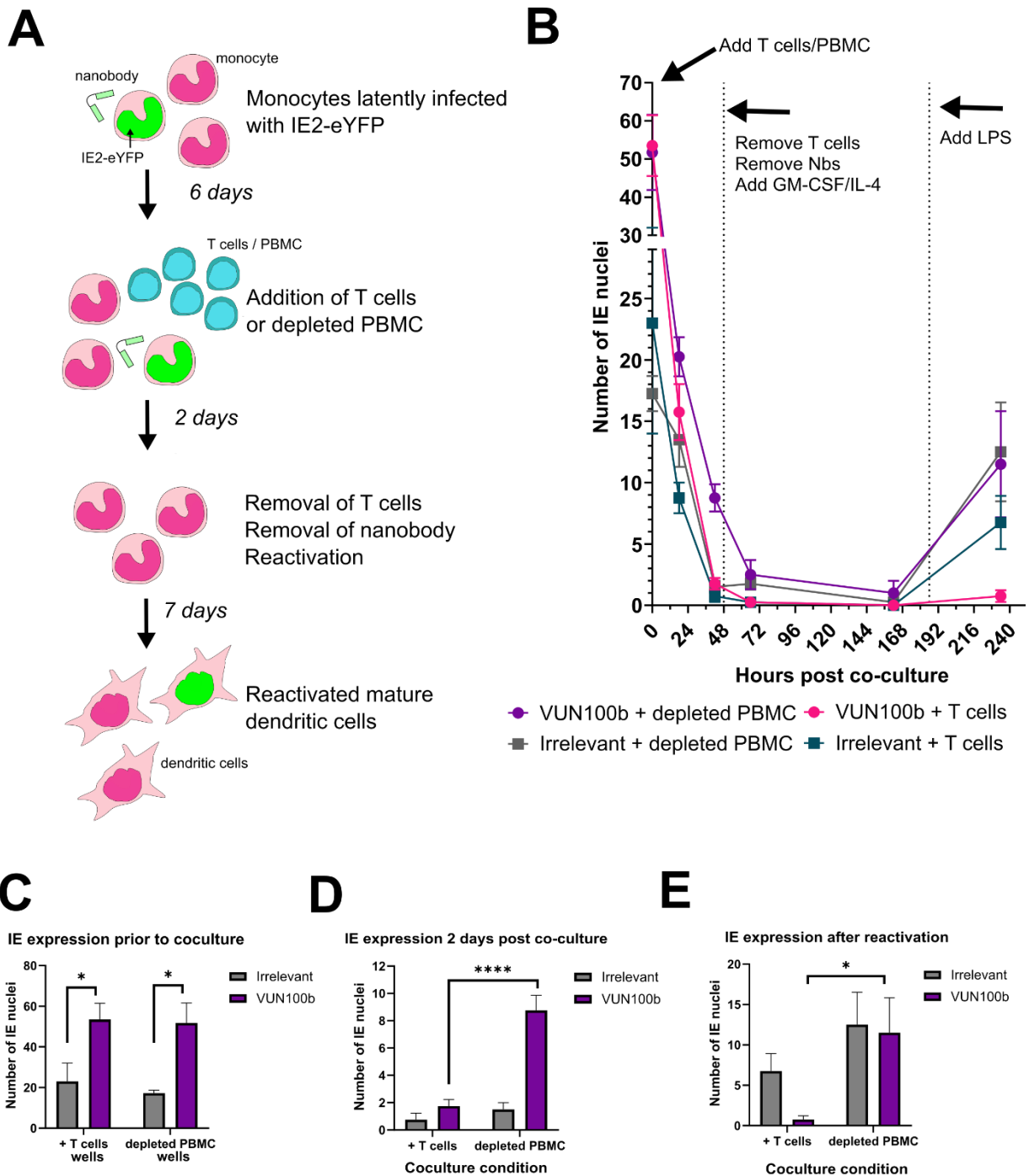


Figure 7-7 VUN100b directs T cell killing of latently infected monocytes. A) Schematic of the experimental design. I isolated monocytes, latently infected these cells, and treated with nanobody/cytokines, and performed all counting. Eleanor Lim isolated T cells, added these to monocytes, and washed the cells away at the appropriate time. B) Time course of IE positive cells following co-culture with autologous T cells or depleted PBMC in the presence of irrelevant or VUN100b nanobodies. C) IE2 positive cells in latently infected monocytes at 6 d.p.i. in the presence of indicated nanobodies. These data represent the wells that subsequently had either T cells or depleted PBMC added. D) IE2 positive cells 2 days post co-culture with the indicated nanobodies and cells. E) IE2 positive cells in reactivated, mature dendritic cells, after T-cell/PBMC and nanobody removal.

7.4. Discussion

The HCMV latent reservoir is a significant barrier to eradication of the virus from hosts [20,320]. Reactivation of latently infected cells can lead to disease or mortality in immunosuppressed transplant patients and immunocompromised individuals, but despite this, no current antiviral agents target this latent viral reservoir [14,28,394]. Our laboratory continues to examine the shock and kill strategy for targeting latent viral reservoirs using molecules that target epigenetic modifiers, like HDACi [145], to induce transient activation of IE gene expression, an antigen recognised by up to 5% of a seropositive individual's CD8⁺ T cells [395]. However, a virus-specific strategy may be preferable in terms of avoiding off-target effects within patients.

US28 is essential for HCMV latency in monocytes [189], and likely in CD34⁺ HPCs [159,173,193], at least in part because US28 suppresses the MIEP in undifferentiated myeloid cells. Therefore, targeting the function of US28 during latency disrupts latency establishment, as shown using the small molecule inhibitor VUF2272 [189]. However, this leads to full virus reactivation, which could harm patients, and will also lead to the expression of virally-encoded immune evasion genes. In this chapter, I collaborated with a group from Vrije Universiteit to examine the effects of a US28-targeting nanobody that partially inhibits US28 signalling.

The previously described US28-targeting nanobody VUN100 was used to develop a new bivalent format VUN100b [308]. The new nanobody had a higher affinity for US28 than VUN100 and was able to inhibit US28 signalling in myeloid cells, while both VUN100 and VUN100b specifically bound US28 expressed in isolation in THP-1 cells. How the bivalent nanobody has the additional signalling blockade function is unknown, but is consistent with other bivalent nanobodies that target cell surface GPCRs [317,318,396].

When used at saturating concentrations, both VUN100 and VUN100b could induce IE gene expression in latently infected monocytes. It would be interesting to analyse the dose dependency of this effect from a mechanistic perspective, as well as with a view to treatment. VUN100 blocks ligand binding, and the ligand binding activity of US28 has been shown to be required for the establishment in some, but not all, experimental latency systems [189,193,195]. Our results suggest that some mode of ligand binding by US28 is important for efficient latency establishment. However, the magnitude of the dependency appeared to show donor-to-donor variability, raising questions about the role of US28 ligand binding during HCMV latency *in vivo*.

VUN100b, a partial inverse agonist of US28, consistently upregulated IE gene expression without substantial induction of expression of viral immune evasins, nor full virus reactivation. This is a major advantage for a shock and kill strategy, which requires detection by T cells [320]. Furthermore, these findings suggest that there is a threshold of inhibition of US28 signalling to induce full virus reactivation. This potential 'sweet spot' of IE reactivation induced by VUN100b could then lead to recognition and killing by T cells from seropositive individuals and makes VUN100b a candidate for shock and kill therapy of living donors and transplant recipients prior to immunosuppression and transplant. However, additional experiments will need to be performed in *ex vivo* myeloid cells and PBMC to check the efficiency of this strategy. The T cell experiment presented in Figure 7-7 should be repeated with a different virus strain that has an intact US2-11 region and is therefore fully competent for viral interference for antigen presentation. The experiment can then be extended to analyse production of infectious virus after reactivation. The analysis then needs to be repeated on naturally latent myeloid cells from a seropositive donor, that is, not experimentally infected, to see that naturally latent virus may be partially reactivated and recognised following VUN100b treatment. These experiments are in progress.

Finally, I believe that the nanobody could also be coupled to toxins, effector molecules, and affinity tags to facilitate manipulation of latency infected cells in clinical and experimental settings. The potential of a US28-binding molecule coupled to a toxin is described in Chapter 8. The effector molecule could be something that enhances T cell recognition, such as the anti-CD3 single-chain variable fragment conjugated to an anti-EGFR nanobody for use in cancer immunotherapy [397]. The most exciting potential use for those studying HCMV latency is a nanobody-affinity tag conjugate that would allow the enrichment of experimentally and naturally latent cells from populations that contain low numbers of *bona fide* latently infected cells; typically, this is less than 10% in experimental latency and less than 0.01% of monocytes or HPCs from seropositive individuals [398]. We have now generated a VUN100-biotin conjugate that awaits testing for enrichment of latently infected cells.

8. Improved US28-specific immunotoxins kill latently infected monocytes

8.1. Introduction

The US28-specific immunotoxin F49A-FTP kills lytically and latently infected cells in culture following 48 or 72 hours of incubation [172,334]. In conjunction with Synklino ApS, I wanted to test newer candidate US28-specific immunotoxins for (i) antiviral activity at low concentrations and (ii) efficacy following shorter incubation times. These modifications to improve F49A-FTP would be beneficial to any strategy for killing latently infected cells in solid organs using *ex vivo* normothermic perfusion (EVNP). While the exact modifications/mutations in F49A-FTP made by Synklino ApS is proprietary information, modifications were generated in the N-terminal region, containing the modified CX3CL1, and in the linker region between CX3CL1 and the endotoxin domains. SYN001 is the 'original' F49A-FTP compound; SYN002 has a modified linker; SYN004 has a modified N-terminal region; SYN005 has both the modified linker and the modified N-terminal region.

Here, I show that SYN002 and SYN005 can kill US28-expressing THP-1 cells and latently infected monocytes with greater efficacy than SYN001 and are also efficacious after only a short incubation with cells.

8.2. US28-specific immunotoxins kill US28-expressing THP-1 cells

I began by comparing the ability of the original F49A-FTP and the three new immunotoxins to kill THP-1 cells that overexpress US28 or control THP-1 cells (described in Chapter 3). I chose to analyse killing using the MTS assay (see Materials and Methods). Strictly speaking, this colorimetric assay measures cell viability, as the tetrazolium compound in the assay reagent is converted to a formazan compound by metabolically active cells that are producing NADH or NADPH. The absorbance of the formazan product in the cell culture medium is directly proportional to the number of living cells. In the initial experiment, I treated cells with a range of concentrations of each immunotoxin, and assayed cell viability after 48 hours (Figure 8-1). This initial experiment indicated that, up to 10^{-8} M, none of the four immunotoxins killed THP-1 cells that do not express US28, but all four could kill US28-expressing THP-1 cells. Furthermore, SYN002 and SYN005 seemed to kill more US28-expressing THP-1 cells at lower concentrations.

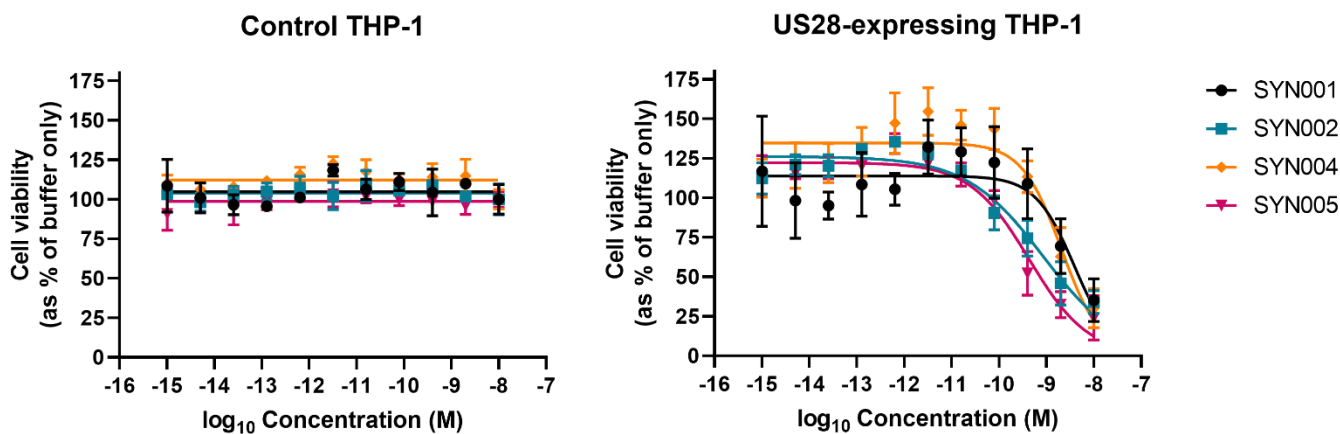


Figure 8-1 **US28-specific immunotoxins kill US28-expressing THP-1 cells but not control THP-1 cells.** Empty vector control or US28-expressing THP-1 cells (described in Chapter 3) were treated with the indicated immunotoxins for 48 hours before assaying for cell viability by MTS assay. Cell viability is presented as percentage of the assay value obtained for cells treated with the immunotoxin-solubilisation buffer only. Curve fitting was performed using GraphPad Prism 8, comparing the fits of a 'four-parameter log(concentration) vs response curve' with a 'horizontal line'; the curve which fitted better according to least squares regression analysis was then plotted.

I then repeated this analysis but, in addition to incubating US28-expressing THP-1 cells with immunotoxins for 48 hours, I also removed immunotoxin at 3, 6, and 24 hours post treatment. I then assayed cell viability at 48 hours post initial incubation with immunotoxin. I also chose to use a slightly different range of concentrations to give more data points on the killing curves for more accurate modelling, and determination of 50% cellular cytotoxicity values (CC_{50}). In this analysis, I found that short incubations of as little as 3 hours with the immunotoxins could still kill US28-expressing cells (Figure 8-2, Table 8-1). Increasing incubation times increases the efficacy of killing marginally (for example, CC_{50} for SYN005 was 0.115 nM at 3 hours, 0.063 nM at 6 hours, and 0.029 at 24 hours), but that 48 hours gave no additional benefit to 24 hours. This is consistent with the mechanism of action of this immunotoxin; once sufficient immunotoxin is internalised (perhaps only 1000 individual molecules), translation is arrested and apoptosis is irreversibly induced [337].

Furthermore, this analysis confirmed the individual immunotoxins did not perform equally well. Quite clearly, SYN002 and SYN005 can kill more US28-expressing THP-1 cells at lower concentrations than SYN001, the original immunotoxin; with a 24-hour incubation, the difference between CC_{50} values for SYN005 and SYN001 was approximately 10-fold. In contrast, SYN004 appears less potent than SYN001. SYN005 was also between 2- and 5-fold more potent than SYN002 at 3 of the 4 incubation times tested;

on this basis, I decided to take forward SYN002 and SYN005 for further testing in latently infected monocytes.

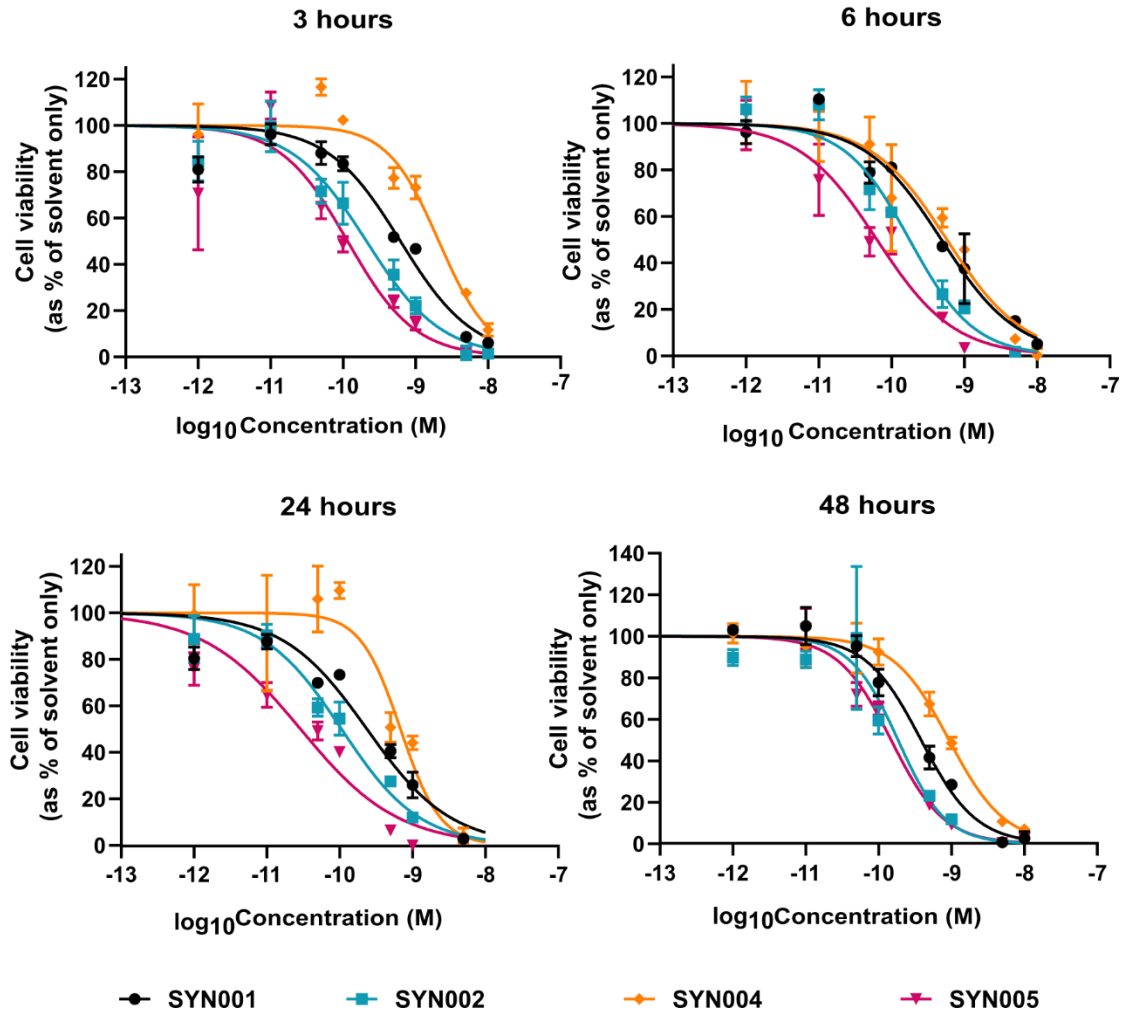


Figure 8-2 **US28-specific immunotoxins kill US28-expressing cells after short incubation times.** US28-expressing THP-1 cells were treated with the indicated immunotoxins for the indicated incubation times. 48 hours after initial incubation with immunotoxin, cell viability was assessed by MTS assay. Cell viability is presented as percentage of the assay value obtained for cells treated with the immunotoxin-solubilisation buffer only. Curve fitting was performed using GraphPad Prism 8, specifically the non-linear regression analysis using a 'four-parameter log(concentration) vs response' model.

Table 8-1 **CC₅₀ and respective 95% confidence intervals (CI) for immunotoxins at given incubations times**. All values in nM. Values were interpolated using GraphPad Prism 8, specifically the non-linear regression analysis using a' four-parameter log(concentration) vs response' model.

Incubation time	Parameter	SYN001	SYN002	SYN004	SYN005
3 hours	CC ₅₀	0.619	0.211	2.09	0.115
	95% CI	0.476, 0.802	0.158, 0.281	1.25, 3.54	0.073, 0.186
6 hours	CC ₅₀	0.485	0.177	0.577	0.063
	95% CI	0.371, 0.635	0.139, 0.225	0.383, 0.854	0.043, 0.090
24 hours	CC ₅₀	0.237	0.106	0.684	0.029
	95% CI	0.167, 0.330	0.081, 0.139	0.514, 0.924	0.017, 0.046
48 hours	CC ₅₀	0.384	0.185	0.928	0.149
	95% CI	0.322, 0.455	0.127, 0.271	0.780, 1.11	0.126, 0.175

8.3. US28-specific immunotoxins kill latently infected monocytes

Before assessing efficacy of SYN002 and SYN005 on latently infected primary CD14+ monocytes, I needed to formally confirm that neither immunotoxin was toxic to uninfected monocytes, as is predicted by Figure 8-1. Once again, I used the MTS assay to determine cell viability after both a 4 hour and a 48 hour incubation with SYN002 and SYN005, with blasticidin as a positive control for cell killing. Four hours was chosen as a realistic incubation time for any potential normothermic perfusion of kidneys with the immunotoxins. I found no evidence of cytotoxicity up to 10^{-7} M with either immunotoxin (Figure 8-3) and could, therefore, move on to testing specific killing of latently infected cells by SYN002 and SYN005.

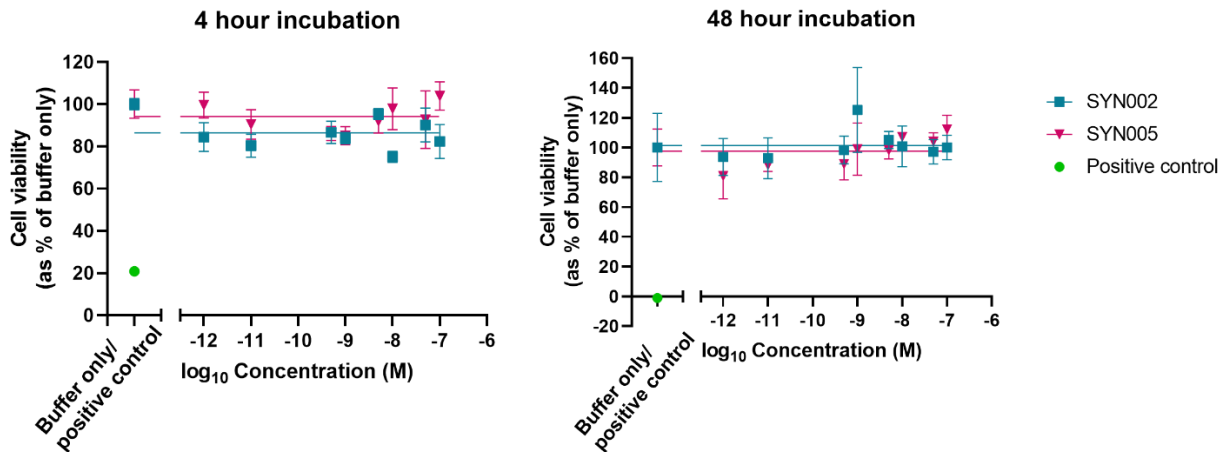


Figure 8-3 US28-specific immunotoxins do not kill uninfected primary monocytes at relevant concentrations

Primary CD14⁺ monocytes were incubated with the indicated immunotoxins for 4 or 48 hours, or blasticidin at 10 X lethal concentration as a positive control. 48 hours after initial incubation, cell viability was determined by MTS assay. Cell viability is presented as percentage of the assay value obtained for cells treated with the immunotoxin-solubilisation buffer only. Curve fitting was performed using GraphPad Prism 8, comparing the fits of a 'four-parameter log(concentration) vs response curve' with a 'horizontal line'; the curve which fitted better according to least squares regression analysis was then plotted.

I initially chose 1 nM as the concentration to test to kill latently infected cells as it represents a concentration able to kill 80-95% of US28-expressing THP-1 cells. I latently infected primary CD14⁺ monocytes with TB40/E *mCherry* US28-3XF, or ΔUS28 as a control for the specificity of immunotoxin for US28. At 5 days post infection, I treated infected cells with immunotoxins SYN002 and SYN005, as well as SYN001 at 1 nM and SYN001 at 10 nM for comparison. After 4 hours, I changed the media on half the wells. At the end of 48 hours, I counted all infected cells as marked by mCherry fluorescence. As shown in Figure 8-4, all four immunotoxin treatments killed a proportion (50-70%) of latently infected cells, but not those infected with ΔUS28-HCMV. This reconfirms the specificity of the immunotoxins for US28. The absolute differences between treatments were small, but there was a trend to suggest that SYN002 and SYN005, with a 4 hour incubation and at a concentration of 1 nM, were better able to kill latently infected monocytes compared with SYN001.

Immunotoxin-mediated loss of infected cells

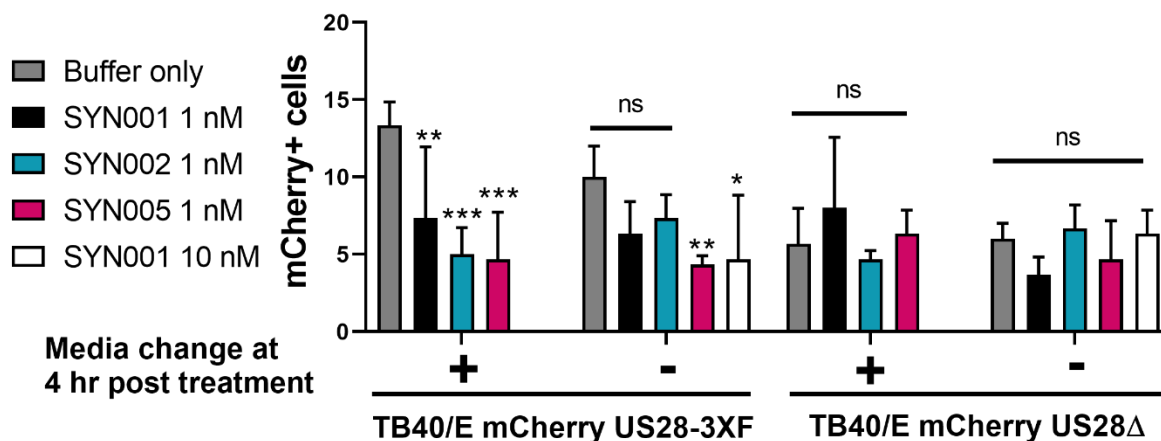


Figure 8-4 **SYN002 and SYN005 kill latently infected monocytes.** Primary CD14⁺ monocytes were latently infected with the indicated viruses. At 5 d.p.i., cells were treated with the indicated immunotoxins. Four hours later, the media was changed to immunotoxin-free media (+) or left unchanged (-). Then, 48 hours after initial immunotoxin incubation, mCherry positive cells were counted. Note that a media change experiment with SYN001 at 10 nM was not performed. Statistical analysis was performed using 2-way ANOVA followed by Dunnett's multiple comparison test between immunotoxin treatment and buffer only. *, P<0.05; **, P<0.01; ***, P<0.001; ns, not significant.

The analysis represented in Figure 8-4 did not allow me to categorically determine whether SYN002 or SYN005 was more potent. I therefore compared the antiviral performance of these two immunotoxins against latently infected monocytes and productively infected fibroblasts across a further range of concentrations. As shown in Figure 8-5, there was still little difference between the performances of SYN002 and SYN005 against latent cells (Figure 8-5 A) or lytically infected cells (Figure 8-5 B-D) regardless of MOI, or whether IE2 protein or the late protein pp28 was analysed. Furthermore, SYN005 was toxic to fibroblasts at high concentrations if it was not removed from culture medium. In these analyses, SYN002 and SYN005 had almost identical potencies; perhaps this is not surprising given that they both contain the same modifications in the linker region and only differ in the N-terminal region.

The final analysis I performed addressed whether the killing of latently infected cells with SYN002 and SYN005 resulted in subsequent loss of reactivation of the latently infected cells in the population following their differentiation. To do this, I latently infected monocytes with TB40/E GATA2mCherry, which maintains red fluorescence for longer than mCherry driven by the SV40 promoter [349]. I used a 4 or 48 hour treatment with immunotoxin, and counted remaining mCherry⁺ cells at 48 hours post treatment (Figure 8-6 A). I then differentiated the cells to immature dendritic cells using GM-CSF/IL-4 for 6 days. At the end of this time (8 days post treatment), I counted red cells again (Figure 8-6 B), before

maturing the dendritic cells with LPS, which induces full virus reactivation [152]. Four days post LPS treatment, I fixed cells and dual-stained for mCherry and IE, and then counted double-positive cells (Figure 8-6 D). I also transferred supernatants from these cells to fibroblasts, to assess release of infectious virions (Figure 8-6 E). These analyses confirmed results from the previous donors, and additionally showed that the immunotoxin treatments lead to a loss of reactivation that matched the levels of lost latently infected cells. The 8-day time point (after differentiation of latently infected monocytes to immature dendritic cells) additionally suggested that SYN005 is more potent with a 48 hour immunotoxin treatment, but not with a 4 hour treatment. A summary of the results from 3 donors is shown in Figure 8-6 C, demonstrating approximately 50% average loss of latently infected cells treated with immunotoxin for 4 hours.

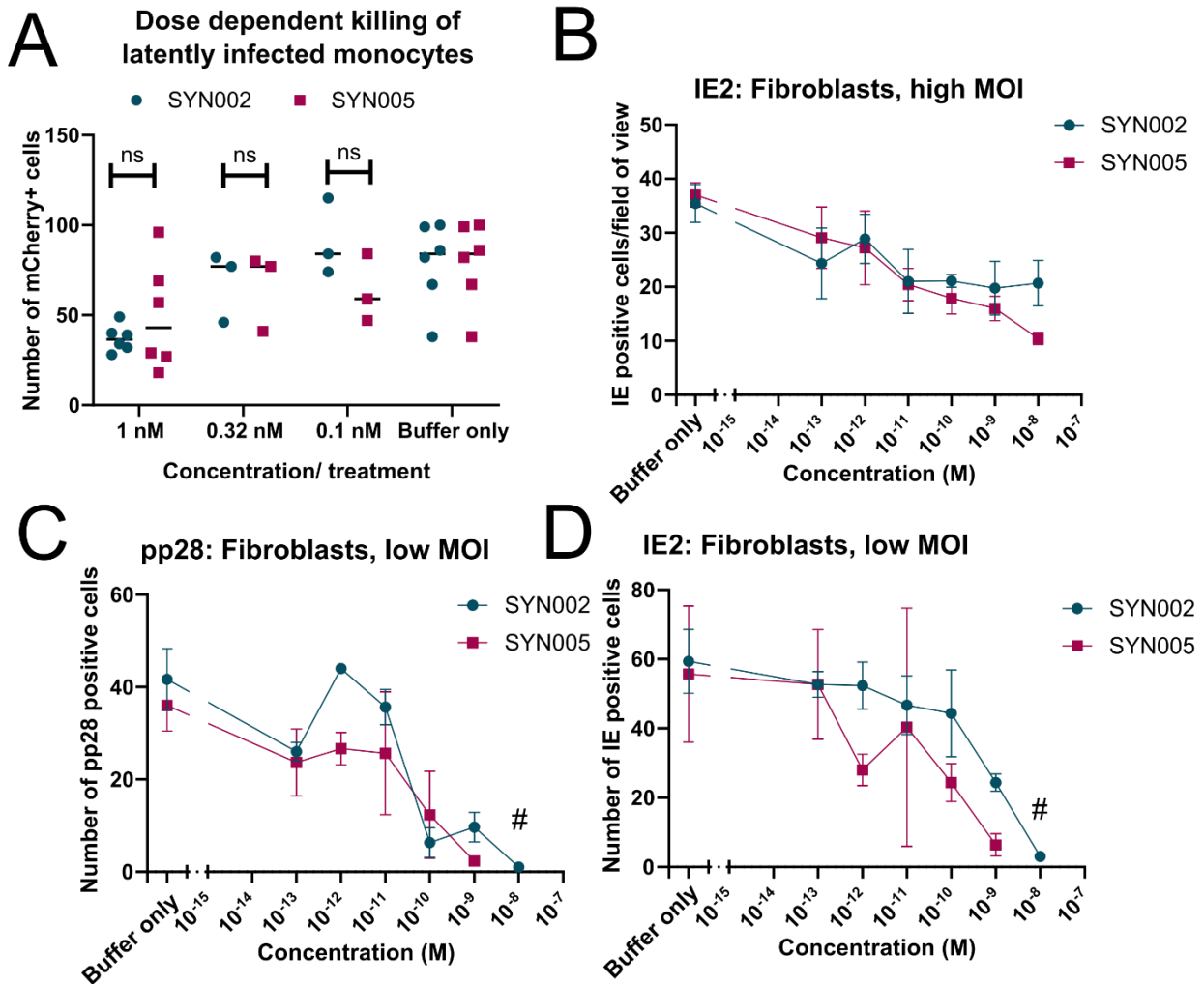


Figure 8-5 **SYN002 and SYN005 have similar antiviral activities against lytic and latent infections.** A) CD14⁺ monocytes were latently infected with TB40/*EmCherry* US28-3XFLAG. At 6 d.p.i., cells were treated with the indicated immunotoxins (n= 3 or n=6) for 4 hours before media removal. Then, 48 hours after treatment, mCherry⁺ cells were counted. Individual counts for each well are graphed. Buffer only controls are shared. Statistical analysis by 2-way ANOVA using Sidak's multiple comparison test; ns, not significant/P>0.05. B) Hff1 cells were infected with TB40/E IE2-eYFP at MOI of 1. At 24 h.p.i., cells were treated with the indicated immunotoxins in triplicate, and then 24 hours later the immunotoxin was removed. After a further 24 hours, IE2 positive cells in three fields of view were averaged for each well. Data points show mean of three wells \pm SD. C, D) Hff1 cells were infected with TB40/E IE2-eYFP at MOI of 0.01. At 24 h.p.i., cells were treated with the indicated immunotoxins in triplicate. Four days after this, cells were fixed and counterstained for pp28. The total number of pp28 (C) or IE2 (D) positive cells in each well was counted. # indicates that Hff1 cells (infected and uninfected) were killed by SYN005 at 10^{-8} M. Data points show mean \pm SD.

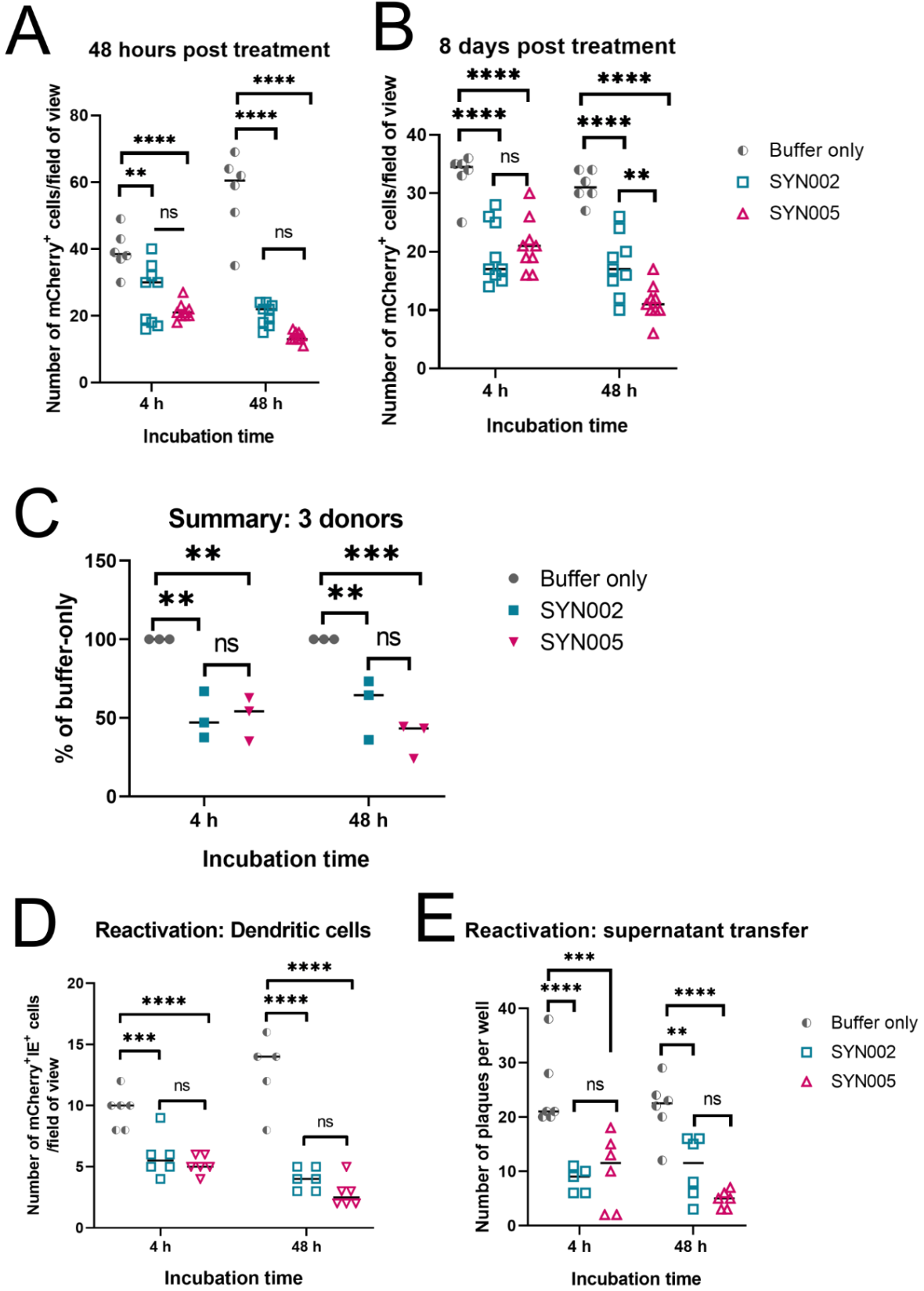


Figure 8-6 **SYN002 and SYN005 kill latently infected monocytes and reduce reactivation.** A, B) Primary CD14⁺ monocytes were latently infected with TB40/E GATA2mCherry. At 5 d.p.i., cells were treated with the indicated immunotoxins. At 4 or 48 hours post treatment, immunotoxin was removed. Then, 48 hours after initial immunotoxin incubation, mCherry⁺ cells were counted (A) before differentiating cells with GM-CSF/IL-4 for 6 days; at this point (8 days post treatment), mCherry⁺ cells were counted again (B). C) Summary of killing experiments from three donors, normalised to buffer only killing counts 48 hours after immunotoxin incubation. D, E) Differentiating cells from B were stimulated with LPS to induce maturation of dendritic cells and full virus reactivation. After 4 days of stimulation, supernatants were transferred to Hff1 cells and the mature DCs were fixed and stained for IE and mCherry; double positive cells were counted (D). Supernatants were incubated with Hff1 cells for 21 days and then mCherry⁺ plaques were counted. Statistical analysis was performed using 2-way ANOVA followed by Tukey's multiple comparison test. **, P<0.01; ***, P<0.001; ****, P<0.0001; ns, not significant.

8.4. Discussion

A proportion of pUS28 is expressed on the outer membrane of infected cells during both lytic replication and latency [172,174] (Chapter 3, §3.4.4). This makes US28 a druggable target, and exploiting the chemokine-binding properties of US28 is one approach to remove latent viral reservoirs and lytically infected cells from patients or grafts. A previous US28-targetting immunotoxin, F49A-FTP, could kill lytically infected cells *in vitro* and *in vivo*, and experimentally and naturally latent myeloid cells following 72 hour incubations [172,334].

Here, I tested the ability of three derivations of F49A-FTP to kill US28-expressing cells over a shorter time frame and at lower concentrations, with the aim of finding candidate immunotoxins suitable for treatment of solid organ grafts using EVNP. SYN004 did not show any improvement over the original immunotoxin, but SYN002 and SYN005 were more potent, and functioned after short (< 6 hour) incubations with US28-expressing THP-1 cells. These results were supported by the specific killing of latently infected monocytes at 1 nM, and concomitant loss in reactivation following their differentiation: I found an approximate 50% drop in survival of latently infected cells and reactivation.

However, in the published analysis of F49A-FTP-mediated killing of latently infected monocytes and CD34⁺ progenitor cells, a 72 hour incubation killed 50-70% of latent cells and reduced reactivation by 80-100% [172]. There are several differences between my experiments and the previous published analysis: the concentration of immunotoxin, the incubation length, and the virus strains used. Figure 8-4 suggests that SYN002 and SYN005 at 1 nM are equally effective as SYN001 at 10 nM in my experimental set up, so this concentration difference is unlikely to explain why I did not see an 80-100% drop in reactivation with SYN002 and SYN005. Figure 8-6 suggests that increasing the FTP incubation time (from 4 hours to 48 hours) did not increase killing substantially, making it less likely, but still possible, that a 72 hour

incubation has added benefit to latent cell killing. The previously published analysis also used both TB40/E SV40 GFP and Titan strains of HCMV; I have used TB40/E SV40 mCherry and TB40/E GATA2mCherry. I cannot rule out that there were differences in US28 expression or anti-apoptotic activity with the virus sets, which could explain the discrepancies between the datasets. It would be informative to immunostain for US28 expression in my analysis, to assess whether cells that are not killed by immunotoxin have typical levels of cell-surface US28, and to sequence viruses that replicate following reactivation to check for resistance mutations.

To understand the difference between my results and those previously published, I believe it would be informative to compare killing of latently infected monocytes by SYN001, SYN002, and SYN005 at 1 nM, 10 nM, and an intermediate concentration such as 5 nM using a short incubation time (4 hours) and the long incubation time (72 hours). It is also necessary to extend the experiments presented here and analyse killing naturally latent monocytes from seropositive individuals. This would hopefully also help to determine whether SYN002 or SYN005 is more potent, which I was unable to do in my experiments.

Overall, there is promise for an improved immunotoxin to be used for targeting of latent reservoirs in solid organ grafts prior to transplantation via EVNP. A schematic of the EVNP system for kidneys is shown in Figure 8-7. In a collaboration with the Department of Surgery, here at the University of Cambridge, we plan to access paired kidneys from seropositive cadavers. These will be perfused with heated buffer to improve renal function but, at the same time, an immunotoxin will be added to the perfusate and delivered to the kidney. As we are also able to collect leukocytes that are flushed from the kidney, we will then reactivate these leukocytes *ex vivo* to analyse whether immunotoxin can kill naturally infected cells within the kidney to reduce viral loads and prevent subsequent reactivation. This, we hope, could lead to a novel strategy to reduce the incidence of CMV reactivation and disease from seropositive grafts in transplant recipients.

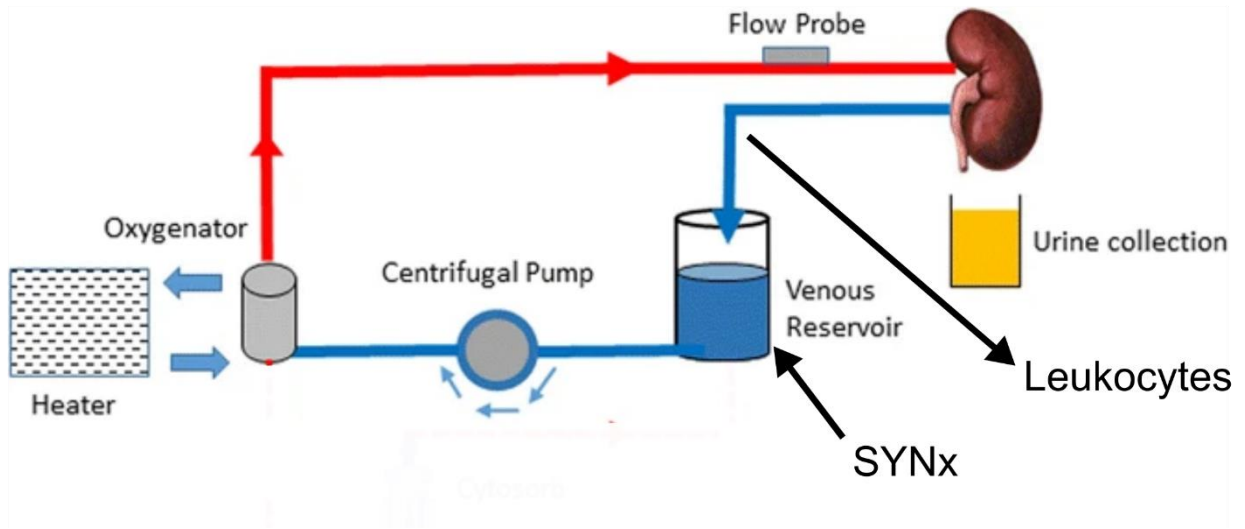


Figure 8-7 **Ex vivo normothermic perfusion configuration, adapted from [399].** The donor organ is cannulated at the renal artery and vein, and ureter (for urine collection). Prior to oxygenation and heating, a venous reservoir containing buffers to improve organ viability can be supplemented with the US28-targeting immunotoxin (SYNx). This enters the kidney through the renal artery and exits through the renal vein where a leukocyte filter can collect leukocytes flushed from the kidney for analysis.

9. General Discussion

I have presented results in this thesis that advance our understanding of the HCMV protein US28, and the potential for targeting US28 in a therapeutic intervention. I have also established roles for two host factors, namely IFI16 and MNDA, in HCMV latent infections.

I analysed the results of a proteomic screen which compared THP-1 cells that express US28-WT, US28-R129A, or empty vector control. This allowed both the analysis of signalling-dependent and signalling-independent changes to host factors induced by US28. Because G protein-mediated signalling is critical to HCMV latency [189,193], I focussed my attention on the signalling-dependent changes. A large number of ISGs were downregulated by US28-WT. I validated that three of these proteins, namely IFI16, MNDA, and HLA-DR, were indeed downregulated by US28-WT expressed in isolation, and also downregulated during HCMV latency in primary monocytes; IFI16 was also downregulated in CD34⁺ HPCs. I believe this is indicative of the quality of the proteomic screen in detecting US28-mediated changes during HCMV latency and the results of the screen will hopefully be useful to other HCMV investigators, as well as my own laboratory. I did not investigate other 'hits' in the proteomic screen except for caveolin-1, but I was unable to develop robust methods for detecting caveolin gene expression by RT-qPCR or protein analysis during the course of the project. Future investigations into the screen may provide additional insights into the biology of HCMV latency; for example, caveolin-1, which is downregulated by US28-WT, could affect cellular trafficking, a phenomenon shown by other to be extensively manipulated by HCMV latency [400,401]. Other potentially interesting 'hits' were discussed in Chapter 3.

I have considered, though not extensively investigated, the potential implications of a general downregulation of interferon-inducible genes during HCMV latency. Previous analysis in bulk populations of monocytes latently infected with HCMV has suggested that ISGs, are actually *induced* following latent infection [402]. I believe this can be linked back to the fact that in a population of infected monocytes, some are *bona fide* infected and carry viral genomes, and some are uninfected bystander monocytes, but all have still seen virus particles and any cytokines in the viral inoculum. The secretome of latently infected monocytes also has effects on bystander cells [127]. In my experimental system, bystander monocytes comprise the vast majority of monocytes in the population, and thus bulk analysis of latently infected monocyte populations is compromised by the presence of bystander cells. It was for this reason that I analysed latency-associated effects on specific genes by immunofluorescence or cell-sorting using fluorescence reporter viruses. I therefore propose that there is a downregulation in ISG expression in

bona fide latently infected monocytes, which could be important for the maintenance of the polarisation of the monocyte [371,372], since latently infected cells are proposed to have an immunosuppressive monocyte phenotype [173], or to avoid anti-viral activities of ISGs. Interestingly, a single-cell transcriptomic analysis of latently infected CD34⁺ HPCs also saw downregulation of ISGs including MND4 and IFI16 [108], and my own work also showed a decrease in IFI16 in latently infected CD34⁺ cells, suggesting that this phenomenon is conserved in different sites of HCMV latency.

The downregulation of ISGs and, in particular, IFI16, begs the question of whether the production of interferon itself is avoided. In Chapter 6, I presented some evidence that US28 may be attenuating the response to DNA stimuli, and that both IFI16 and MND4 overexpression enhance Type I interferon responses to transfected DNA. I also found some weak evidence that in bulk populations of latently infected monocytes, Type I interferon is produced. What I was unable to determine is whether *bona fide* latently infected cells produce interferon, whether this is modulated by US28, and, indeed, whether this has a positive or negative effect on HCMV latency. To investigate these questions, I would perform intracellular cytokine staining for IFN α /IFN β in cells latently infected with fluorescent reporter viruses, with or without US28. I would also treat latently infected monocytes with Type I interferon and measure the maintenance of viral genome, maintenance of latent phenotype by lack of IE expression and infectious virus production, and levels of reactivation following differentiation. It would also be informative to know whether any substrates for pathogen sensing are produced during latent infection. One way to perform this would be to follow procedures described by Alandijany et al. [262]. In their study of the early events of HSV-1 infection, they labelled viral genomes within viral inocula with 5-Ethynyl-2'-deoxyuridine (EdU). After infection, viral genome can be visualised using 'click chemistry', and any sensing machinery components associated with viral genomes can be identified by immunofluorescence staining. For IFI16 and MND4 in particular, an immunoprecipitation (IP) with viral genome would also be informative, however, I have doubts about the specificities of the antibodies available for these genes, and good antibody is crucial for such IP experiments. Epitope tagging IFI16 and MND4 may be appropriate, but it is difficult to genetically modify *ex vivo* hematopoietic lineage cells. Members of my laboratory have recently established an inducible pluripotent stem cell model for HCMV latency [121], which may make this sort of experiment feasible in the future.

My analysis of IFI16 overexpression in THP-1 cells confirmed that IFI16 is part of the DNA sensing machinery, as has been proposed by many other studies (see Introduction). However, it also revealed that a separate activity of IFI16 is at play during HCMV latency; the ability of IFI16 to modulate viral gene

expression. While the majority of viral genes (herpesvirus family, HBV, HIV-1) are transcriptionally repressed in some manner by IFI16 [257,264,268,271,274], the HCMV MIEP is activated by IFI16 in fibroblasts [79,264]. During this project, I confirmed that IFI16 could activate the MIEP in undifferentiated THP-1 cells, and that this occurred independently of other viral gene products. I also identified that the activation of the MIEP was mediated by NF- κ B binding at the MIEP, but not how IFI16 activates NF- κ B. I provided evidence that it was not via Sp1 sequestration from I κ B α promoters, a mechanism previously proposed to occur in endothelial cells [250]. It would be interesting to determine whether MIEP activation and DNA sensing by IFI16 are linked by NF- κ B activation, since a recent study found a mechanism by which IFI16, in concert with ATM, can activate STING and non-canonical NF- κ B signalling in response to nuclear DNA damage [224].

In response to transfected DNA, cells in which I had overexpressed MNDA had the same phenotype as cells overexpressing IFI16 with respect to increased interferon production, suggesting that MNDA is also a component of DNA sensing machinery. To date, no report has been published which demonstrates this function of MNDA, though one lab has reported similar results at a conference (A. Bowie, personal communication). This phenomenon deserves greater investigation; what is the mechanism of sensing? Does MNDA interact directly with DNA to enact this response? What kind of nucleic acid substrates can invoke an MNDA-mediated Type I interferon response? Knocking down or knocking out MNDA would also help to determine the role of MNDA, but I would need a robust system to test interferon induction, since I had great difficulty getting robust interferon responses in undifferentiated THP-1 cells (until, of course, I overexpressed MNDA or IFI16 within them). I also identified MNDA as a potential restriction factor for HCMV latency. I discussed the additional experiments required for characterisation of this function of MNDA in Chapter 5, but it is interesting that, whilst MNDA and IFI16 overexpression both lead to increased interferon responses, MNDA leads to a failure to express viral reporter cassettes. In contrast, IFI16 increases IE gene expression. Understanding the differences between MNDA and IFI16 function will be important in addressing the role of PYHIN proteins in HCMV latency, and during other viral infections.

For many of my observations, I could rely upon evidence from infection of primary cells, which is a highly relevant model for studying HCMV latency. For many other observations, I relied up protein overexpression in the model cell line THP-1. I discussed the limitations of THP-1 cells as a model for HCMV latency in the introduction (§1.3.2), but protein overexpression also has its limitations as a way in which to investigate protein function. For example, overexpression of the membrane protein US28 in

isolation in THP-1 cells could lead to abnormal processing and localisation of pUS28 which could lead to abnormal protein function, and not reflect what occurs when expressed during latency. Some mammalian expression systems give tuneable protein expression which could give more physiologically relevant results (e.g. [403]). However, I was able to validate several of the results seen with overexpression with US28 in the context of HCMV latent infection. For the analyses of MND4 and IFI16 function, it would be helpful to adopt a complementary approach, such as gene knock-out by CRISPR-Cas9 [404] or knock-down by shRNA [405], to validate the phenotypes seen with overexpression.

During the course of this project, I was also able to investigate two reagents that really illustrate that US28 is an 'Achilles Heel' for HCMV latency and persistence. A summary of the evidence (see Introduction) suggests that US28 is likely essential for HCMV persistence *in vivo* [159,173,189,193,195]. At least some proportion of US28 protein is expressed on the cell surface during latent and lytic infections [172,174] (Chapter 3), and can be targeted by nanobodies and immunotoxins to induce T cell-mediated killing, and direct cytotoxicity, respectively. In using the nanobodies, I was also able to confirm that US28-signalling is important for latency in monocytes, and provide evidence that ligand binding by US28 also has a role in the maintenance of HCMV latency in monocytes. These molecules, or derivatives thereof, could have therapeutic potential for reducing latent viral loads in transplant donors, grafts, or recipients, which, it is hoped, would reduce adverse CMV disease in transplant patients. Since US28 is essential for HCMV latency, important for cell-cell spread in endothelial cells [178], and likely immunomodulatory [175], resistance mutations to nanobodies and immunotoxins may decrease viral fitness. As US28 represents an entirely separate viral target to ganciclovir, I believe combination therapy involving GCV and a US28-targeting molecule is worth pursuing as a strategy for reducing the burden of HCMV disease.

10. References

- [1] Lefkowitz EJ, Dempsey DM, Hendrickson RC, Orton RJ, Siddell SG, Smith DB. Virus taxonomy: the database of the International Committee on Taxonomy of Viruses (ICTV). *Nucleic Acids Res* 2018;46:D708–17. doi:10.1093/nar/gkx932.
- [2] Chang Y, Cesarman E, Pessin M, Lee F, Culpepper J, Knowles D, et al. Identification of herpesvirus-like DNA sequences in AIDS-associated Kaposi's sarcoma. *Science* (80-) 1994;266:1865–9. doi:10.1126/science.7997879.
- [3] Ho M. The history of cytomegalovirus and its diseases. *Med Microbiol Immunol* 2008;197:65–73. doi:10.1007/s00430-007-0066-x.
- [4] Mocarski Jr. ES. Comparative analysis of herpesvirus-common proteins. *Hum. Herpesviruses Biol. Ther. Immunoprophyl.*, Cambridge University Press; 2007, p. 44–60.
- [5] Preston CM, Efstathiou S. HSV-1 and 2: Molecular basis of HSV latency and reactivation. *Hum. Herpesviruses Biol. Ther. Immunoprophyl.*, Cambridge University Press; 2007, p. 602–15. doi:10.1017/CBO9780511545313.034.
- [6] Cohen JI. VZV: Molecular basis of persistence (latency and reactivation). *Hum. Herpesviruses Biol. Ther. Immunoprophyl.*, Cambridge University Press; 2007, p. 689–99. doi:10.1017/CBO9780511545313.039.
- [7] Sinclair J. Human cytomegalovirus: Latency and reactivation in the myeloid lineage. *J Clin Virol* 2008;41:180–5. doi:10.1016/j.jcv.2007.11.014.
- [8] Kondo K, Yamanishi K. HHV-6A, 6B, and 7: molecular basis of latency and reactivation. *Hum. Herpesviruses Biol. Ther. Immunoprophyl.*, Cambridge University Press; 2007, p. 843–9.
- [9] Pantry SN, Medveczky PG. Latency, integration, and reactivation of human herpesvirus-6. *Viruses* 2017;9. doi:10.3390/v9070194.
- [10] Lieberman PM, Hu J, Renne R. Gammaherpesvirus maintenance and replication during latency. In: Arvin A, Campadelli-Fiume G, Mocarski E, Moore PS, Roizman B, Whitley R, et al., editors. *Hum. Herpesviruses Biol. Ther. Immunoprophyl.*, Cambridge: Cambridge University Press; 2007, p. 379–402.
- [11] Lukac DM, Yuan Y. Reactivation and lytic replication of KSHV. *Hum. Herpesviruses Biol. Ther.*

Immunoprophyl., Cambridge University Press; 2007, p. 434–60.

- [12] Cannon MJ, Schmid DS, Hyde TB. Review of cytomegalovirus seroprevalence and demographic characteristics associated with infection. *Rev Med Virol* 2010;20:202–13. doi:10.1002/rmv.655.
- [13] Zuhair M, Smit GSA, Wallis G, Jabbar F, Smith C, Devleeschauwer B, et al. Estimation of the worldwide seroprevalence of cytomegalovirus: A systematic review and meta-analysis. *Rev Med Virol* 2019;29. doi:10.1002/rmv.2034.
- [14] Griffiths P, Baraniak I, Reeves M. The pathogenesis of human cytomegalovirus. *J Pathol* 2015;235:288–97. doi:10.1002/path.4437.
- [15] Boppana SB, Fowler KB. HCMV: Persistence in the population: Epidemiology and transmission. *Hum. Herpesviruses Biol. Ther. Immunoprophyl.*, Cambridge University Press; 2007, p. 795–813. doi:10.1017/CBO9780511545313.045.
- [16] Forman MS, Vaidya D, Bolorunduro O, Diener-West M, Pass RF, Arav-Boger R. Cytomegalovirus Kinetics Following Primary Infection in Healthy Women. *J Infect Dis* 2017;215:1523–6. doi:10.1093/infdis/jix188.
- [17] Cannon MJ, Hyde TB, Schmid DS. Review of cytomegalovirus shedding in bodily fluids and relevance to congenital cytomegalovirus infection. *Rev Med Virol* 2011;21:240–55. doi:10.1002/rmv.695.
- [18] Jackson SE, Mason GM, Wills MR. Human cytomegalovirus immunity and immune evasion. *Virus Res* 2011;157:151–60. doi:10.1016/j.virusres.2010.10.031.
- [19] Méndez AC, Rodríguez-Rojas C, Del Val M. Vaccine vectors: the bright side of cytomegalovirus. *Med Microbiol Immunol* 2019;208:349–63. doi:10.1007/s00430-019-00597-7.
- [20] Wills MR, Poole E, Lau B, Krishna B, Sinclair JH. The immunology of human cytomegalovirus latency: Could latent infection be cleared by novel immunotherapeutic strategies? *Cell Mol Immunol* 2015;12:128–38. doi:10.1038/cmi.2014.75.
- [21] Poole E, Juss JK, Krishna B, Herre J, Chilvers ER, Sinclair J. Alveolar Macrophages Isolated Directly From Human Cytomegalovirus (HCMV)-Seropositive Individuals Are Sites of HCMV Reactivation In Vivo. *J Infect Dis* 2015;211:1936–42. doi:10.1093/infdis/jiu837.
- [22] Reeves MB, Sinclair JH. Circulating Dendritic Cells Isolated from Healthy Seropositive Donors Are

- Sites of Human Cytomegalovirus Reactivation In Vivo. *J Virol* 2013;87:10660–7.
doi:10.1128/JVI.01539-13.
- [23] Lim Y, Lyall H. Congenital cytomegalovirus – who, when, what-with and why to treat? *J Infect* 2017;74:S89–94. doi:10.1016/S0163-4453(17)30197-4.
- [24] Kagan KO, Hamprecht K. Cytomegalovirus infection in pregnancy. *Arch Gynecol Obstet* 2017;296:15–26. doi:10.1007/s00404-017-4380-2.
- [25] Hadar E, Dorfman E, Bardin R, Gabbay-Benziv R, Amir J, Pardo J. Symptomatic congenital cytomegalovirus disease following non-primary maternal infection: A retrospective cohort study. *BMC Infect Dis* 2017;17. doi:10.1186/s12879-016-2161-3.
- [26] Wang C, Zhang X, Bialek S, Cannon MJ. Attribution of Congenital Cytomegalovirus Infection to Primary Versus Non-Primary Maternal Infection. *Clin Infect Dis* 2011;52:e11–3.
doi:10.1093/cid/ciq085.
- [27] Reddehase MJ, Lemmermann NAW. Cellular reservoirs of latent cytomegaloviruses. *Med Microbiol Immunol* 2019;208:391–403. doi:10.1007/s00430-019-00592-y.
- [28] Ramanan P, Razonable RR. Cytomegalovirus infections in solid organ transplantation: a review. *Infect Chemother* 2013;45:260–71. doi:10.3947/ic.2013.45.3.260.
- [29] Stern L, Withers B, Avdic S, Gottlieb D, Abendroth A, Blyth E, et al. Human Cytomegalovirus Latency and Reactivation in Allogeneic Hematopoietic Stem Cell Transplant Recipients. *Front Microbiol* 2019;10:1186. doi:10.3389/fmicb.2019.01186.
- [30] Yong MK, Gottlieb D, Lindsay J, Kok J, Rawlinson W, Slavin M, et al. New Advances in the Management of Cytomegalovirus in Allogeneic Haemopoietic Stem Cell Transplantation. *Intern Med J* 2019. doi:10.1111/imj.14462.
- [31] Springer KL, Weinberg A. Cytomegalovirus infection in the era of HAART: fewer reactivations and more immunity. *J Antimicrob Chemother* 2004;54:582–6. doi:10.1093/jac/dkh396.
- [32] Marandu T, Dombek M, Cook CH. Impact of cytomegalovirus load on host response to sepsis. *Med Microbiol Immunol* 2019;208:295–303. doi:10.1007/s00430-019-00603-y.
- [33] Simanek AM, Dowd JB, Pawelec G, Melzer D, Dutta A, Aiello AE. Seropositivity to cytomegalovirus, inflammation, all-cause and cardiovascular disease-related mortality in the United States. *PLoS*

One 2011;6. doi:10.1371/journal.pone.0016103.

- [34] Savva GM, Pachnio A, Kaul B, Morgan K, Huppert FA, Brayne C, et al. Cytomegalovirus infection is associated with increased mortality in the older population. *Aging Cell* 2013;12:381–7. doi:10.1111/accel.12059.
- [35] Firth C, Harrison R, Ritchie S, Wardlaw J, Ferro CJ, Starr JM, et al. Cytomegalovirus infection is associated with an increase in systolic blood pressure in older individuals. *QJM* 2016;109:595–600. doi:10.1093/qjmed/hcw026.
- [36] Cobbs CS, Harkins L, Samanta M, Gillespie GY, Bharara S, King PH, et al. Human cytomegalovirus infection and expression in human malignant glioma. *Cancer Res* 2002;62:3347–50.
- [37] Soroceanu L, Matlaf L, Bezrookove V, Harkins L, Martinez R, Greene M, et al. Human cytomegalovirus US28 found in glioblastoma promotes an invasive and angiogenic phenotype. *Cancer Res* 2011;71:6643–53. doi:10.1158/0008-5472.CAN-11-0744.
- [38] Cobbs C. Cytomegalovirus is a tumor-associated virus: armed and dangerous. *Curr Opin Virol* 2019;39:49–59. doi:10.1016/j.coviro.2019.08.003.
- [39] Herbein G. The human cytomegalovirus, from oncomodulation to oncogenesis. *Viruses* 2018;10. doi:10.3390/v10080408.
- [40] Maussang D, Verzijl D, van Walsum M, Leurs R, Holl J, Pleskoff O, et al. Human cytomegalovirus-encoded chemokine receptor US28 promotes tumorigenesis. *Proc Natl Acad Sci* 2006;103:13068–73. doi:10.1073/pnas.0604433103.
- [41] Söderberg-Nauclér C, Rahbar A, Stragliotto G. Survival in Patients with Glioblastoma Receiving Valganciclovir. *N Engl J Med* 2013;369:985–6. doi:10.1056/NEJMc1302145.
- [42] Adler SP, Lewis N, Conlon A, Christiansen MP, Al-Ibrahim M, Rupp R, et al. Phase 1 Clinical Trial of a Conditionally Replication-Defective Human Cytomegalovirus (CMV) Vaccine in CMV-Seronegative Subjects. *J Infect Dis* 2019;220:411–9. doi:10.1093/infdis/jiz141.
- [43] Gomes AC, Griffiths PD, Reeves MB. The Humoral Immune Response Against the gB Vaccine: Lessons Learnt from Protection in Solid Organ Transplantation. *Vaccines* 2019;7:67. doi:10.3390/vaccines7030067.
- [44] Krishna BA, Wills MR, Sinclair JH. Advances in the treatment of cytomegalovirus. *Br Med Bull*

2019. doi:10.1093/bmb/ldz031.

- [45] Demmler-Harrison GJ. Congenital cytomegalovirus: Public health action towards awareness, prevention, and treatment. *J Clin Virol* 2009;46. doi:10.1016/j.jcv.2009.10.007.
- [46] Midgley G, Smithers-Sheedy H, McIntyre S, Badawi N, Keogh J, Jones CA. Congenital cytomegalovirus prevention, awareness and policy recommendations - a scoping study. *Infect Disord - Drug Targets* 2018;18. doi:10.2174/1871526518666181009093725.
- [47] Crumacker CS. Ganciclovir. *N Engl J Med* 1996;335:721–9. doi:10.1056/NEJM199609053351007.
- [48] Kaul DR, Stoelben S, Cober E, Ojo T, Sandusky E, Lischka P, et al. First report of successful treatment of multidrug-resistant cytomegalovirus disease with the novel anti-CMV compound AIC246. *Am J Transplant* 2011;11:1079–84. doi:10.1111/j.1600-6143.2011.03530.x.
- [49] Marty FM, Ljungman P, Chemaly RF, Maertens J, Dadwal SS, Duarte RF, et al. Letermovir Prophylaxis for Cytomegalovirus in Hematopoietic-Cell Transplantation. *N Engl J Med* 2017;377:2433–44. doi:10.1056/NEJMoa1706640.
- [50] Staczek J. Animal cytomegaloviruses. *Microbiol Rev* 1990;54:247–65.
- [51] McGeoch DJ, Cook S, Dolan A, Jamieson FE, Telford EAR. Molecular phylogeny and evolutionary timescale for the family of mammalian herpesviruses. *J Mol Biol* 1995;247:443–58. doi:10.1006/jmbi.1995.0152.
- [52] Powers C, Früh K. Rhesus CMV: An emerging animal model for human CMV. *Med Microbiol Immunol* 2008;197:109–15. doi:10.1007/s00430-007-0073-y.
- [53] Shellam GR, Redwood AJ, Smith LM, Gorman S. Murine Cytomegalovirus and Other Herpesviruses. *Mouse Biomed. Res.*, vol. 2, Elsevier Inc.; 2007, p. 1–48. doi:10.1016/B978-012369454-6/50029-7.
- [54] Schleiss MR. Nonprimate models of congenital cytomegalovirus (CMV) infection: Gaining insight into pathogenesis and prevention of disease in newborns. *ILAR J* 2006;47:65–72. doi:10.1093/ilar.47.1.65.
- [55] Geyer H, Ettinger J, Möller L, Schmolz E, Nitsche A, Brune W, et al. Rat cytomegalovirus (RCMV) English isolate and a newly identified Berlin isolate share similarities with but are separate as an anciently diverged clade from Mouse CMV and the Maastricht isolate of RCMV. *J Gen Virol*

2015;96:1873–82. doi:10.1099/vir.0.000109.

- [56] Bia FJ, Griffith BP, Fong CK, Hsiung GD. Cytomegaloviral infections in the guinea pig: experimental models for human disease. *Rev Infect Dis* 1983;5:177–95. doi:10.1093/clinids/5.2.177.
- [57] Voigt S, Ettinger J, Streblow DN. The Rat Model of Cytomegalovirus Infection and Vascular Disease. In: Reddehase M, Lemmermann N, editors. *Cytomegaloviruses From Mol. Pathog. to Interv.*, Caister Academic Press; 2013, p. 312–36.
- [58] Stinski MF, Meier JL. Immediate–early viral gene regulation and function. *Hum. Herpesviruses Biol. Ther. Immunoprophyl.*, Cambridge University Press; 2007, p. 241–63.
- [59] Liu X, Swaminathan S, Yan S, Engelmann F, Abbott DA, VanOsdol LA, et al. A novel murine model of differentiation-mediated cytomegalovirus reactivation from latently infected bone marrow haematopoietic cells. *J Gen Virol* 2019. doi:10.1099/jgv.0.001327.
- [60] Reddehase MJ, Lemmermann NAW. Cellular reservoirs of latent cytomegaloviruses. *Med Microbiol Immunol* 2019;208:391–403. doi:10.1007/s00430-019-00592-y.
- [61] Almanan M, Raynor J, Sholl A, Wang M, Chougnet C, Cardin RD, et al. Tissue-specific control of latent CMV reactivation by regulatory T cells. *PLoS Pathog* 2017;13. doi:10.1371/journal.ppat.1006507.
- [62] Dai X, Yu X, Gong H, Jiang X, Abenes G, Liu H, et al. The smallest capsid protein mediates binding of the essential tegument protein pp150 to stabilize DNA-containing capsids in human cytomegalovirus. *PLoS Pathog* 2013;9:e1003525. doi:10.1371/journal.ppat.1003525.
- [63] Davison AJ, Bhella D. Comparative betaherpes viral genome and virion structure. *Hum. Herpesviruses Biol. Ther. Immunoprophyl.*, vol. 2, Cambridge University Press; 2007, p. 177–203. doi:10.1017/CBO9780511545313.015.
- [64] McVoy MA, Adler SP. Human cytomegalovirus DNA replicates after early circularization by concatemer formation, and inversion occurs within the concatemer. *J Virol* 1994;68:1040–51.
- [65] Woodhall DL, Groves IJ, Reeves MB, Wilkinson G, Sinclair JH. Human Daxx-mediated repression of human cytomegalovirus gene expression correlates with a repressive chromatin structure around the major immediate early promoter. *J Biol Chem* 2006;281:37652–60. doi:10.1074/jbc.M604273200.

- [66] Stern-Ginossar N, Weisburd B, Michalski A, Le VTK, Hein MY, Huang SX, et al. Decoding human cytomegalovirus. *Science* (80-) 2012;338:1088–93. doi:10.1126/science.1227919.
- [67] Balázs Z, Tombácz D, Szűcs A, Csabai Z, Megyeri K, Petrov AN, et al. Long-Read Sequencing of Human Cytomegalovirus Transcriptome Reveals RNA Isoforms Carrying Distinct Coding Potentials. *Sci Rep* 2017;7:15989. doi:10.1038/s41598-017-16262-z.
- [68] Van Damme E, Van Loock M. Functional annotation of human cytomegalovirus gene products: An update. *Front Microbiol* 2014;5. doi:10.3389/fmicb.2014.00218.
- [69] Sinzger C, Digel M, Jahn G. Cytomegalovirus cell tropism. *Curr Top Microbiol Immunol* 2008;325:63–83. doi:10.1007/978-3-540-77349-8_4.
- [70] Compton T, Feire A. Early events in human cytomegalovirus infection. *Hum. Herpesviruses Biol. Ther. Immunoprophyl.*, Cambridge University Press; 2007, p. 231–40. doi:10.1017/CBO9780511545313.017.
- [71] Haspot F, Lavault A, Sinzger C, Sampaio KL, Stierhof YD, Pilet P, et al. Human cytomegalovirus entry into dendritic cells occurs via a macropinocytosis-like pathway in a pH-independent and cholesterol-dependent manner. *PLoS One* 2012;7. doi:10.1371/journal.pone.0034795.
- [72] Lee J-H, Kalejta RF. Human Cytomegalovirus Enters the Primary CD34+ Hematopoietic Progenitor Cells where it Establishes Latency by Macropinocytosis. *J Virol* 2019. doi:10.1128/JVI.00452-19.
- [73] Gerna G, Kabanova A, Lilleri D. Human Cytomegalovirus Cell Tropism and Host Cell Receptors. *Vaccines* 2019;7. doi:10.3390/vaccines7030070.
- [74] Li Q, Fischer E, Cohen JI. Cell Surface THY-1 Contributes to Human Cytomegalovirus Entry via a Macropinocytosis-Like Process. *J Virol* 2016;90:9766–81. doi:10.1128/jvi.01092-16.
- [75] Murphy E, Yu D, Grimwood J, Schmutz J, Dickson M, Jarvis MA, et al. Coding potential of laboratory and clinical strains of human cytomegalovirus. *Proc Natl Acad Sci U S A* 2003;100:14976–81. doi:10.1073/pnas.2136652100.
- [76] Cha TA, Tom E, Kemble GW, Duke GM, Mocarski ES, Spaete RR. Human cytomegalovirus clinical isolates carry at least 19 genes not found in laboratory strains. *J Virol* 1996;70:78–83.
- [77] Kalejta RF. Pre-Immediate Early Tegument Protein Functions. In: Reddehase MJ, Lemmermann NAW, editors. *Cytomegaloviruses, From Mol. Pathog. to Interv.*, Norfolk, UK: Caister Academic

Press; 2013, p. 141–51.

- [78] Fu YZ, Su S, Gao YQ, Wang PP, Huang ZF, Hu MM, et al. Human Cytomegalovirus Tegument Protein UL82 Inhibits STING-Mediated Signaling to Evade Antiviral Immunity. *Cell Host Microbe* 2017;21:231–43. doi:10.1016/j.chom.2017.01.001.
- [79] Cristea IM, Moorman NJ, Terhune SS, Cuevas CD, O’Keefe ES, Rout MP, et al. Human Cytomegalovirus pUL83 Stimulates Activity of the Viral Immediate-Early Promoter through Its Interaction with the Cellular IFI16 Protein. *J Virol* 2010;84:7803–14. doi:10.1128/JVI.00139-10.
- [80] Honess RW, Roizman B. Regulation of herpesvirus macromolecular synthesis. I. Cascade regulation of the synthesis of three groups of viral proteins. *J Virol* 1974;14:8–19.
- [81] Ghazal P. DNA microarrays of human cytomegalovirus genome: Profiling kinetic class with drug sensitivity of viral gene expression. *J Clin Virol* 1999;12:120. doi:10.1016/s1386-6532(99)90445-6.
- [82] Weekes MP, Tomasec P, Huttlin EL, Fielding CA, Nusinow D, Stanton RJ, et al. Quantitative temporal viromics: An approach to investigate host-pathogen interaction. *Cell* 2014;157:1460–72. doi:10.1016/j.cell.2014.04.028.
- [83] Meier JL, Stinski MF. Major Immediate-Early Enhancer and Its Gene Products. In: Reddehase M, Lemmermann N, editors. *Cytomegaloviruses From Mol. Pathog. to Interv.*, Caister Academic Press; 2013, p. 152–73.
- [84] Mocarski Jr. ES. *Betaherpes viral genes and their functions*. Hum. Herpesviruses Biol. Ther. Immunoprophyl., Cambridge University Press; 2007, p. 204–30.
- [85] Stinski MF, Isomura H. Role of the cytomegalovirus major immediate early enhancer in acute infection and reactivation from latency. *Med Microbiol Immunol* 2008;197:223–31. doi:10.1007/s00430-007-0069-7.
- [86] Sinclair J. Chromatin structure regulates human cytomegalovirus gene expression during latency, reactivation and lytic infection. *Biochim Biophys Acta - Gene Regul Mech* 2010;1799:286–95. doi:10.1016/J.BBAGRM.2009.08.001.
- [87] Arend KC, Ziehr B, Vincent HA, Moorman NJ. Multiple Transcripts Encode Full-Length Human Cytomegalovirus IE1 and IE2 Proteins during Lytic Infection. *J Virol* 2016;90:8855–65. doi:10.1128/JVI.00741-16.

- [88] Martínez FP, Cruz R, Lu F, Plasschaert R, Deng Z, Rivera-Molina YA, et al. CTCF binding to the first intron of the major immediate early (MIE) gene of human cytomegalovirus (HCMV) negatively regulates MIE gene expression and HCMV replication. *J Virol* 2014;88:7389–401. doi:10.1128/JVI.00845-14.
- [89] Collins-McMillen D, Rak M, Buehler JC, Igarashi-Hayes S, Kamil JP, Moorman NJ, et al. Alternative promoters drive human cytomegalovirus reactivation from latency. *Proc Natl Acad Sci* 2019;116:17492–7. doi:10.1073/pnas.1900783116.
- [90] Groves IJ, Reeves MB, Sinclair JH. Lytic infection of permissive cells with human cytomegalovirus is regulated by an intrinsic “pre-immediate-early” repression of viral gene expression mediated by histone post-translational modification. *J Gen Virol* 2009;90:2364–74. doi:10.1099/vir.0.012526-0.
- [91] Boshart M, Weber F, Jahn G, Dorsch-Häsler K, Fleckenstein B, Schaffner W. A very strong enhancer is located upstream of an immediate early gene of human cytomegalovirus. *Cell* 1985;41:521–30.
- [92] Nelson JA, Groudine M. Transcriptional regulation of the human cytomegalovirus major immediate-early gene is associated with induction of DNase I-hypersensitive sites. *Mol Cell Biol* 1986;6:452–61.
- [93] Patro ARK. Subversion of Immune Response by Human Cytomegalovirus. *Front Immunol* 2019;10:1155. doi:10.3389/fimmu.2019.01155.
- [94] Stempel M, Chan B, Brinkmann MM. Coevolution pays off: Herpesviruses have the license to escape the DNA sensing pathway. *Med Microbiol Immunol* 2019;208:495–512. doi:10.1007/s00430-019-00582-0.
- [95] Brune W, Andoniou CE. Die another day: Inhibition of cell death pathways by cytomegalovirus. *Viruses* 2017;9. doi:10.3390/v9090249.
- [96] Mocarski Jr. ES. Immunomodulation by cytomegaloviruses: manipulative strategies beyond evasion. *Trends Microbiol* 2002;10:332–9.
- [97] Biolatti M, Gugliesi F, Dell’Oste V, Landolfo S. Modulation of the innate immune response by human cytomegalovirus. *Infect Genet Evol* 2018;64:105–14. doi:10.1016/j.meegid.2018.06.025.
- [98] Sinclair J, Sissons P. Latency and reactivation of human cytomegalovirus. *J Gen Virol*

2006;87:1763–79. doi:10.1099/vir.0.81891-0.

- [99] Taylor-Wiedeman J, Sissons JGP, Borysiewicz LK, Sinclair JH. Monocytes are a major site of persistence of human cytomegalovirus in peripheral blood mononuclear cells. *J Gen Virol* 1991;72:2059–64. doi:10.1099/0022-1317-72-9-2059.
- [100] Mendelson M, Monard S, Sissons P, Sinclair J. Detection of endogenous human cytomegalovirus in CD34+ bone marrow progenitors. *J Gen Virol* 1996;77:3099–102. doi:10.1099/0022-1317-77-12-3099.
- [101] Kondo K, Xu J, Mocarski ES. Human cytomegalovirus latent gene expression in granulocyte-macrophage progenitors in culture and in seropositive individuals. *Proc Natl Acad Sci U S A* 1996;93:11137–42.
- [102] Hahn G, Jores R, Mocarski ES. Cytomegalovirus remains latent in a common precursor of dendritic and myeloid cells. *Proc Natl Acad Sci U S A* 1998;95:3937–42.
- [103] Reeves MB, MacAry PA, Lehner PJ, Sissons JGP, Sinclair JH. Latency, chromatin remodeling, and reactivation of human cytomegalovirus in the dendritic cells of healthy carriers. *Proc Natl Acad Sci* 2005;102:4140–5. doi:10.1073/pnas.0408994102.
- [104] Reeves MB, Lehner PJ, Sissons JGP, Sinclair JH. An in vitro model for the regulation of human cytomegalovirus latency and reactivation in dendritic cells by chromatin remodelling. *J Gen Virol* 2005;86:2949–54. doi:10.1099/vir.0.81161-0.
- [105] Forte E, Swaminathan S, Schroeder MW, Kim JY, Terhune SS, Hummel M. Tumor Necrosis Factor Alpha Induces Reactivation of Human Cytomegalovirus Independently of Myeloid Cell Differentiation following Posttranscriptional Establishment of Latency. *MBio* 2018;9. doi:10.1128/mBio.01560-18.
- [106] Jarvis MA, Nelson JA. Human cytomegalovirus persistence and latency in endothelial cells and macrophages. *Curr Opin Microbiol* 2002;5:403–7.
- [107] Sinclair J, Reeves M. The intimate relationship between human cytomegalovirus and the dendritic cell lineage. *Front Microbiol* 2014;5:389. doi:10.3389/fmicb.2014.00389.
- [108] Galinato M, Shimoda K, Aguiar A, Hennig F, Boffelli D, McVoy MA, et al. Single-Cell Transcriptome Analysis of CD34+ Stem Cell-Derived Myeloid Cells Infected With Human Cytomegalovirus. *Front*

Microbiol 2019;10:577. doi:10.3389/fmicb.2019.00577.

- [109] Poole EL, Kew VG, Lau JCH, Murray MJ, Stamminger T, Sinclair JH, et al. A Virally Encoded DeSUMOylase Activity Is Required for Cytomegalovirus Reactivation from Latency. *Cell Rep* 2018;24:594–606. doi:10.1016/j.celrep.2018.06.048.
- [110] Umashankar M, Goodrum F. Hematopoietic long-term culture (hLTC) for human cytomegalovirus latency and reactivation. *Methods Mol Biol* 2014;1119:99–112. doi:10.1007/978-1-62703-788-4_7.
- [111] Poole E, Reeves M, Sinclair JH. The Use of Primary Human Cells (Fibroblasts, Monocytes, and Others) to Assess Human Cytomegalovirus Function. *Methods Mol. Biol.*, vol. 1119, Humana Press, Totowa, NJ; 2014, p. 81–98. doi:10.1007/978-1-62703-788-4_6.
- [112] Collins-McMillen D, Kim JH, Nogalski MT, Stevenson E V., Chan GC, Caskey JR, et al. Human Cytomegalovirus Promotes Survival of Infected Monocytes via a Distinct Temporal Regulation of Cellular Bcl-2 Family Proteins. *J Virol* 2016;90:2356–71. doi:10.1128/JVI.01994-15.
- [113] Chan G, Nogalski MT, Yurochko AD. Human cytomegalovirus stimulates monocyte-to-macrophage differentiation via the temporal regulation of caspase 3. *J Virol* 2012;86:10714–23. doi:10.1128/JVI.07129-11.
- [114] Chan G, Nogalski MT, Bentz GL, Smith MS, Parmater A, Yurochko AD. PI3K-Dependent Upregulation of Mcl-1 by Human Cytomegalovirus Is Mediated by Epidermal Growth Factor Receptor and Inhibits Apoptosis in Short-Lived Monocytes. *J Immunol* 2010;184:3213–22. doi:10.4049/jimmunol.0903025.
- [115] Meier JL. Reactivation of the human cytomegalovirus major immediate-early regulatory region and viral replication in embryonal NTera2 cells: role of trichostatin A, retinoic acid, and deletion of the 21-base-pair repeats and modulator. *J Virol* 2001;75:1581–93. doi:10.1128/JVI.75.4.1581-1593.2001.
- [116] Liu R, Baillie J, Sissons JG, Sinclair JH. The transcription factor YY1 binds to negative regulatory elements in the human cytomegalovirus major immediate early enhancer/promoter and mediates repression in non-permissive cells. *Nucleic Acids Res* 1994;22:2453–9.
- [117] O'Connor CM, Murphy EA. A Myeloid Progenitor Cell Line Capable of Supporting Human

- Cytomegalovirus Latency and Reactivation, Resulting in Infectious Progeny. *J Virol* 2012;86:9854–65. doi:10.1128/JVI.01278-12.
- [118] Van Damme E, Sauviller S, Lau B, Kesteley B, Griffiths P, Burroughs A, et al. Glucocorticosteroids trigger reactivation of human cytomegalovirus from latently infected myeloid cells and increase the risk for HCMV infection in D+R+ liver transplant patients. *J Gen Virol* 2015;96:131–43. doi:10.1099/vir.0.069872-0.
- [119] Keyes LR, Bego MG, Soland M, St. Jeor S. Cyclophilin A is required for efficient human cytomegalovirus DNA replication and reactivation. *J Gen Virol* 2012;93:722–32. doi:10.1099/vir.0.037309-0.
- [120] Albright ER, Kalejta RF. Myeloblastic Cell Lines Mimic Some but Not All Aspects of Human Cytomegalovirus Experimental Latency Defined in Primary CD34+ Cell Populations. *J Virol* 2013;87:9802–12. doi:10.1128/jvi.01436-13.
- [121] Poole E, Huang C, Forbester J, Shnyder M, Nachshon A, Kweider B, et al. An iPSC derived myeloid lineage model of herpes virus latency and reactivation. *Front Microbiol* 2019;10:2233. doi:10.3389/FMICB.2019.02233.
- [122] Crawford LB, Streblow DN, Hakki M, Nelson JA, Caposio P. Humanized mouse models of human cytomegalovirus infection. *Curr Opin Virol* 2015;13:86–92. doi:10.1016/j.coviro.2015.06.006.
- [123] Poole E, Avdic S, Hodgkinson J, Jackson S, Wills M, Slobedman B, et al. Latency-Associated Viral Interleukin-10 (IL-10) Encoded by Human Cytomegalovirus Modulates Cellular IL-10 and CCL8 Secretion during Latent Infection through Changes in the Cellular MicroRNA hsa-miR-92a. *J Virol* 2014;88:13947–55. doi:10.1128/JVI.02424-14.
- [124] Jenkins C, Abendroth A, Slobedman B. A novel viral transcript with homology to human interleukin-10 is expressed during latent human cytomegalovirus infection. *J Virol* 2004;78:1440–7.
- [125] Slobedman B, Mocarski ES, Arvin AM, Mellins ED, Abendroth A. Latent cytomegalovirus down-regulates major histocompatibility complex class II expression on myeloid progenitors. vol. 100. 2002. doi:10.1182/blood.V100.8.2867.
- [126] Aslam Y, Williamson J, Romashova V, Elder E, Krishna B, Wills M, et al. Human Cytomegalovirus

Upregulates Expression of HCLS1 Resulting in Increased Cell Motility and Transendothelial Migration during Latency. *IScience* 2019;20:60–72. doi:10.1016/j.isci.2019.09.016.

- [127] Mason GM, Poole E, Sissons JGP, Wills MR, Sinclair JH. Human cytomegalovirus latency alters the cellular secretome, inducing cluster of differentiation (CD)4+ T-cell migration and suppression of effector function. *Proc Natl Acad Sci U S A* 2012;109:14538–43. doi:10.1073/pnas.1204836109.
- [128] Crawford LB, Kim JH, Collins-McMillen D, Lee B-J, Landais I, Held C, et al. Human Cytomegalovirus Encodes a Novel FLT3 Receptor Ligand Necessary for Hematopoietic Cell Differentiation and Viral Reactivation. *MBio* 2018;9. doi:10.1128/mBio.00682-18.
- [129] Poole E, Sinclair J. Sleepless latency of human cytomegalovirus. *Med Microbiol Immunol* 2015;204:421–9. doi:10.1007/s00430-015-0401-6.
- [130] Reeves M, Sinclair J. Regulation of human cytomegalovirus transcription in latency: Beyond the major immediate-early promoter. *Viruses* 2013;5:1395–413. doi:10.3390/v5061395.
- [131] Goodrum FD, Jordan CT, High K, Shenk T. Human cytomegalovirus gene expression during infection of primary hematopoietic progenitor cells: a model for latency. *Proc Natl Acad Sci U S A* 2002;99:16255–60. doi:10.1073/pnas.252630899.
- [132] Cheung AKL, Abendroth A, Cunningham AL, Slobedman B. Viral gene expression during the establishment of human cytomegalovirus latent infection in myeloid progenitor cells. *Blood* 2006;108. doi:10.1182/blood-2005-12-026682.
- [133] Goodrum F, Reeves M, Sinclair J, High K, Shenk T. Human cytomegalovirus sequences expressed in latently infected individuals promote a latent infection in vitro. *Blood* 2007;110:937–45. doi:10.1182/blood-2007-01-070078.
- [134] Shnayder M, Nachshon A, Krishna B, Poole E, Boshkov A, Binyamin A, et al. Defining the Transcriptional Landscape during Cytomegalovirus Latency with Single-Cell RNA Sequencing. *MBio* 2018;9. doi:10.1128/mBio.00013-18.
- [135] Cheng S, Caviness K, Buehler J, Smithey M, Nikolich-Žugich J, Goodrum F. Transcriptome-wide characterization of human cytomegalovirus in natural infection and experimental latency. *Proc Natl Acad Sci U S A* 2017;114:E10586–95. doi:10.1073/pnas.1710522114.
- [136] Rossetto CC, Tarrant-Elorza M, Pari GS. Cis and Trans Acting Factors Involved in Human

Cytomegalovirus Experimental and Natural Latent Infection of CD14 (+) Monocytes and CD34 (+) Cells. *PLoS Pathog* 2013;9:e1003366. doi:10.1371/journal.ppat.1003366.

- [137] Reeves MB, Sinclair JH. Analysis of latent viral gene expression in natural and experimental latency models of human cytomegalovirus and its correlation with histone modifications at a latent promoter. *J Gen Virol* 2010;91:599–604. doi:10.1099/vir.0.015602-0.
- [138] Söderberg-Nauclér C, Fish KN, Nelson JA. Reactivation of Latent Human Cytomegalovirus by Allogeneic Stimulation of Blood Cells from Healthy Donors. *Cell* 1997;91:119–26. doi:10.1016/S0092-8674(01)80014-3.
- [139] Cheung AKL, Gottlieb DJ, Plachter B, Pepperl-Klindworth S, Avdic S, Cunningham AL, et al. The role of the human cytomegalovirus UL111A gene in down-regulating CD4+ T-cell recognition of latently infected cells: implications for virus elimination during latency. *Blood* 2009;114:4128–37. doi:10.1182/blood-2008-12-197111.
- [140] Keyes LR, Hargett D, Soland M, Bego MG, Rossetto CC, Almeida-Porada G, et al. HCMV Protein LUNA Is Required for Viral Reactivation from Latently Infected Primary CD14+ Cells. *PLoS One* 2012;7:e52827. doi:10.1371/journal.pone.0052827.
- [141] Lau B, Poole E, Van Damme E, Bunkens L, Sowash M, King H, et al. Human cytomegalovirus miR-UL112-1 promotes the down-regulation of viral immediate early-gene expression during latency to prevent T-cell recognition of latently infected cells. *J Gen Virol* 2016;97:2387–98. doi:10.1099/jgv.0.000546.
- [142] Poole E, Walther A, Raven K, Benedict CA, Mason GM, Sinclair J. The myeloid transcription factor GATA-2 regulates the viral UL144 gene during human cytomegalovirus latency in an isolate-specific manner. *J Virol* 2013;87:4261–71. doi:10.1128/JVI.03497-12.
- [143] Murphy JC, Fischle W, Verdin E, Sinclair JH. Control of cytomegalovirus lytic gene expression by histone acetylation. *EMBO J* 2002;21:1112–20. doi:10.1093/emboj/21.5.1112.
- [144] Rauwel B, Jang SM, Cassano M, Kapopoulou A, Barde I, Trono D. Release of human cytomegalovirus from latency by a KAP1/TRIM28 phosphorylation switch. *Elife* 2015;4. doi:10.7554/eLife.06068.
- [145] Krishna BA, Lau B, Jackson SE, Wills MR, Sinclair JH, Poole E. Transient activation of human

cytomegalovirus lytic gene expression during latency allows cytotoxic T cell killing of latently infected cells. *Sci Rep* 2016;6:24674. doi:10.1038/srep24674.

- [146] Kew V, Yuan J, Meier J, Reeves M. Mitogen and Stress Activated Kinases Act Co-operatively with CREB during the Induction of Human Cytomegalovirus Immediate-Early Gene Expression from Latency. *PLoS Pathog* 2014;10:e1004195. doi:10.1371/journal.ppat.1004195.
- [147] Nelson JA, Reynolds-Kohler C, Smith BA. Negative and positive regulation by a short segment in the 5'-flanking region of the human cytomegalovirus major immediate-early gene. *Mol Cell Biol* 1987;7:4125–9.
- [148] Sinclair J, Sissons P. Latent and Persistent Infections of Monocytes and Macrophages. *Intervirology* 1996;39:293–301. doi:10.1159/000150501.
- [149] Sissons JGP, Bain M, Wills MR, Sinclair JH. Latency and Reactivation of Human Cytomegalovirus. *J Infect* 2002;44:73–7. doi:10.1053/jinf.2001.0948.
- [150] Wright E, Bain M, Teague L, Murphy J, Sinclair J. Ets-2 repressor factor recruits histone deacetylase to silence human cytomegalovirus immediate-early gene expression in non-permissive cells. *J Gen Virol* 2005;86:535–44. doi:10.1099/vir.0.80352-0.
- [151] Bain M, Mendelson M, Sinclair J. Ets-2 Repressor Factor (ERF) mediates repression of the human cytomegalovirus major immediate-early promoter in undifferentiated non-permissive cells. *J Gen Virol* 2003;84:41–9. doi:10.1099/vir.0.18633-0.
- [152] Reeves MB, Compton T. Inhibition of inflammatory interleukin-6 activity via extracellular signal-regulated kinase-mitogen-activated protein kinase signaling antagonizes human cytomegalovirus reactivation from dendritic cells. *J Virol* 2011;85:12750–8. doi:10.1128/JVI.05878-11.
- [153] Saffert RT, Penkert RR, Kalejta RF. Cellular and Viral Control over the Initial Events of Human Cytomegalovirus Experimental Latency in CD34+ Cells. *J Virol* 2010;84:5594–604. doi:10.1128/JVI.00348-10.
- [154] Groves IJ, Sinclair JH. Knockdown of hDaxx in normally non-permissive undifferentiated cells does not permit human cytomegalovirus immediate-early gene expression. *J Gen Virol* 2007;88:2935–40. doi:10.1099/vir.0.83019-0.
- [155] Wagenknecht N, Reuter N, Scherer M, Reichel A, Müller R, Stamminger T. Contribution of the

Major ND10 Proteins PML, hDaxx and Sp100 to the Regulation of Human Cytomegalovirus Latency and Lytic Replication in the Monocytic Cell Line THP-1. *Viruses* 2015;7:2884–907. doi:10.3390/v7062751.

- [156] Goodrum F. Human Cytomegalovirus Latency: Approaching the Gordian Knot. *Annu Rev Virol* 2016;3:333–57. doi:10.1146/annurev-virology-110615-042422.
- [157] Lee SH, Albright ER, Lee J-H, Jacobs D, Kalejta RF. Cellular defense against latent colonization foiled by human cytomegalovirus UL138 protein. *Sci Adv* 2015;1:e1501164. doi:10.1126/sciadv.1501164.
- [158] Kim JH, Collins-McMillen D, Buehler JC, Goodrum FD, Yurochko AD. Human Cytomegalovirus Requires Epidermal Growth Factor Receptor Signaling To Enter and Initiate the Early Steps in the Establishment of Latency in CD34⁺ Human Progenitor Cells. *J Virol* 2017;91. doi:10.1128/JVI.01206-16.
- [159] Humby MS, O'Connor CM. Human Cytomegalovirus US28 Is Important for Latent Infection of Hematopoietic Progenitor Cells. *J Virol* 2016;90:2959–70. doi:10.1128/JVI.02507-15.
- [160] Elder E, Sinclair J. HCMV latency: what regulates the regulators? *Med Microbiol Immunol* 2019. doi:10.1007/s00430-019-00581-1.
- [161] Chee MS, Bankier AT, Beck S, Bohni R, Brown CM, Cerny R, et al. Analysis of the protein-coding content of the sequence of human cytomegalovirus strain AD169. *Curr Top Microbiol Immunol* 1990;154:125–69.
- [162] Gompels UA, Nicholas J, Lawrence G, Jones M, Thomson BJ, Martin MED, et al. The DNA Sequence of Human Herpesvirus-6: Structure, Coding Content, and Genome Evolution. *Virology* 1995;209:29–51. doi:10.1006/viro.1995.1228.
- [163] Krishna BA, Miller WE, O'Connor CM. US28: HCMV's Swiss Army Knife. *Viruses* 2018;10. doi:10.3390/v10080445.
- [164] Casarosa P, Waldhoer M, LiWang PJ, Vischer HF, Kledal T, Timmerman H, et al. CC and CX3C chemokines differentially interact with the N terminus of the human cytomegalovirus-encoded US28 receptor. *J Biol Chem* 2005;280:3275–85. doi:10.1074/jbc.M407536200.
- [165] Miles TF, Spiess K, Jude KM, Tsutsumi N, Burg JS, Ingram JR, et al. Viral GPCR US28 can signal in

response to chemokine agonists of nearly unlimited structural degeneracy. *Elife* 2018;7.
doi:10.7554/eLife.35850.

- [166] Vomazke J, Nelson JA, Streblow DN. Human Cytomegalovirus US28: a functionally selective chemokine binding receptor. *Infect Disord Drug Targets* 2009;9:548–56.
doi:10.2174/187152609789105696.
- [167] Minisini R, Tulone C, Lüske A, Michel D, Mertens T, Gierschik P, et al. Constitutive inositol phosphate formation in cytomegalovirus-infected human fibroblasts is due to expression of the chemokine receptor homologue pUS28. *J Virol* 2003;77:4489–501. doi:10.1128/jvi.77.8.4489-4501.2003.
- [168] Casarosa P, Bakker RA, Verzijl D, Navis M, Timmerman H, Leurs R, et al. Constitutive signaling of the human cytomegalovirus-encoded chemokine receptor US28. *J Biol Chem* 2001;276:1133–7. doi:10.1074/jbc.M008965200.
- [169] Stropes MP, Schneider OD, Zagorski W a, Miller JLC, Miller WE. The carboxy-terminal tail of human cytomegalovirus (HCMV) US28 regulates both chemokine-independent and chemokine-dependent signaling in HCMV-infected cells. *J Virol* 2009;83:10016–27. doi:10.1128/JVI.00354-09.
- [170] Beisser PS, Laurent L, Virelizier J-LL, Michelson S. Human cytomegalovirus chemokine receptor gene US28 is transcribed in latently infected THP-1 monocytes. *J Virol* 2001;75:5949–57. doi:10.1128/JVI.75.13.5949-5957.2001.
- [171] Hargett D, Shenk TE. Experimental human cytomegalovirus latency in CD14+ monocytes. *Proc Natl Acad Sci U S A* 2010;107:20039–44. doi:10.1073/pnas.1014509107.
- [172] Krishna BA, Spiess K, Poole EL, Lau B, Voigt S, Kledal TN, et al. Targeting the latent cytomegalovirus reservoir with an antiviral fusion toxin protein. *Nat Commun* 2017;8:14321. doi:10.1038/ncomms14321.
- [173] Zhu D, Pan C, Sheng J, Liang H, Bian Z, Liu Y, et al. Human cytomegalovirus reprogrammes haematopoietic progenitor cells into immunosuppressive monocytes to achieve latency. *Nat Microbiol* 2018;3:503–13. doi:10.1038/s41564-018-0131-9.
- [174] Fraile-Ramos A, Kledal TN, Pelchen-Matthews A, Bowers K, Schwartz TW, Marsh M. The human cytomegalovirus US28 protein is located in endocytic vesicles and undergoes constitutive

endocytosis and recycling. *Mol Biol Cell* 2001;12:1737–49.

- [175] Randolph-Habecker J-R, Rahill B, Torok-Storb B, Vieira J, Kolattukudy PE, Rovin BH, et al. The expression of the cytomegalovirus chemokine receptor homolog US28 sequesters biologically active CC chemokines and alters IL-8 production. *Cytokine* 2002;19:37–46.
- [176] Boomker JM, The TH, de Leij LFMH, Harmsen MC. The human cytomegalovirus-encoded receptor US28 increases the activity of the major immediate-early promoter/enhancer. *Virus Res* 2006;118:196–200. doi:10.1016/j.virusres.2005.12.011.
- [177] Vieira J, Schall TJ, Corey L, Geballe AP. Functional analysis of the human cytomegalovirus US28 gene by insertion mutagenesis with the green fluorescent protein gene. *J Virol* 1998;72:8158–65.
- [178] Noriega VM, Gardner TJ, Redmann V, Bongers G, Lira SA, Tortorella D. Human cytomegalovirus US28 facilitates cell-to-cell viral dissemination. *Viruses* 2014;6:1202–18. doi:10.3390/v6031202.
- [179] Farrell HE, Bruce K, Ma J, Davis-Poynter N, Stevenson PG. Human cytomegalovirus US28 allows dendritic cell exit from lymph nodes. *J Gen Virol* 2018;99:1509–14. doi:10.1099/jgv.0.001154.
- [180] Soroceanu L, Matlaf L, Bezrookove V, Harkins L, Martinez R, Greene M, et al. Human Cytomegalovirus US28 Found in Glioblastoma Promotes an Invasive and Angiogenic Phenotype. *Cancer Res* 2011;71:6643–53. doi:10.1158/0008-5472.CAN-11-0744.
- [181] Maussang D, Langemeijer E, Fitzsimons CP, Stigter-van Walsum M, Dijkman R, Borg MK, et al. The human cytomegalovirus-encoded chemokine receptor US28 promotes angiogenesis and tumor formation via cyclooxygenase-2. *Cancer Res* 2009;69:2861–9. doi:10.1158/0008-5472.CAN-08-2487.
- [182] Heukers R, Fan TS, de Wit RH, van Senten JR, De Groof TWM, Bebelman MP, et al. The constitutive activity of the virally encoded chemokine receptor US28 accelerates glioblastoma growth. *Oncogene* 2018;37:4110–21. doi:10.1038/s41388-018-0255-7.
- [183] Omasits U, Ahrens CH, Müller S, Wollscheid B. Protter: interactive protein feature visualization and integration with experimental proteomic data. *Bioinformatics* 2014;30:884–6. doi:10.1093/bioinformatics/btt607.
- [184] Miller WE, Zagorski WA, Brenneman JD, Avery D, Miller JLCC, O’Connor CM. US28 Is a Potent Activator of Phospholipase C during HCMV Infection of Clinically Relevant Target Cells. *PLoS One*

2012;7:e50524. doi:10.1371/journal.pone.0050524.

- [185] Billstrom MA, Johnson GL, Avdi NJ, Worthen GS. Intracellular signaling by the chemokine receptor US28 during human cytomegalovirus infection. *J Virol* 1998;72:5535–44.
- [186] Wu S, Miller WE. The HCMV US28 vGPCR induces potent $G\alpha_q/PLC-\beta$ signaling in monocytes leading to increased adhesion to endothelial cells. *Virology* 2016;497:233–43. doi:10.1016/j.virol.2016.07.025.
- [187] Vomaske J, Melnychuk RM, Smith PP, Powell J, Hall L, DeFilippis V, et al. Differential ligand binding to a human cytomegalovirus chemokine receptor determines cell type-specific motility. *PLoS Pathog* 2009;5:e1000304. doi:10.1371/journal.ppat.1000304.
- [188] Melnychuk RM, Streblov DN, Smith PP, Hirsch AJ, Pancheva D, Nelson JA. Human cytomegalovirus-encoded G protein-coupled receptor US28 mediates smooth muscle cell migration through $G\alpha_{12}$. *J Virol* 2004;78:8382–91. doi:10.1128/JVI.78.15.8382-8391.2004.
- [189] Krishna BA, Poole EL, Jackson SE, Smit MJ, Wills MR, Sinclair JH. Latency-associated expression of human cytomegalovirus US28 attenuates cell signaling pathways to maintain latent infection. *MBio* 2017;8:e01754-17. doi:10.1128/mBio.01754-17.
- [190] Soroceanu L, Matlaf L, Bezrookove V, Harkins L, Martinez R, Greene M, et al. Human cytomegalovirus US28 found in glioblastoma promotes an invasive and angiogenic phenotype. *Cancer Res* 2011;71:6643–53. doi:10.1158/0008-5472.CAN-11-0744.
- [191] Slinger E, Maussang D, Schreiber A, Siderius M, Rahbar A, Fraile-Ramos A, et al. HCMV-Encoded Chemokine Receptor US28 Mediates Proliferative Signaling Through the IL-6-STAT3 Axis. *Sci Signal* 2010;3:ra58–ra58. doi:10.1126/scisignal.2001180.
- [192] de Wit RH, Mujic-Delic A, van Senten JR, Fraile-Ramos A, Siderius M, Smit MJ. Human cytomegalovirus encoded chemokine receptor US28 activates the HIF-1 α /PKM2 axis in glioblastoma cells. *Oncotarget* 2016;7:67966–85. doi:10.18632/ONCOTARGET.11817.
- [193] Krishna BA, Humby MS, Miller WE, O'Connor CM. Human cytomegalovirus G protein-coupled receptor US28 promotes latency by attenuating c-fos. *Proc Natl Acad Sci* 2019:201816933. doi:10.1073/pnas.1816933116.
- [194] Waldhoer M, Kledal TN, Farrell H, Schwartz TW. Murine cytomegalovirus (CMV) M33 and human

- CMV US28 receptors exhibit similar constitutive signaling activities. *J Virol* 2002;76:8161–8.
- [195] Crawford LB, Caposio P, Kreklywich C, Pham AH, Hancock MH, Jones TA, et al. Human Cytomegalovirus US28 Ligand Binding Activity Is Required for Latency in CD34 + Hematopoietic Progenitor Cells and Humanized NSG Mice . *MBio* 2019;10. doi:10.1128/mbio.01889-19.
- [196] Amsler L, Verweij MC, Defilippis VR. The tiers and dimensions of evasion of the type I interferon response by human cytomegalovirus. *J Mol Biol* 2013;425:4857–71. doi:10.1016/j.jmb.2013.08.023.
- [197] Paijo J, Döring M, Spanier J, Grabski E, Nooruzzaman M, Schmidt T, et al. cGAS Senses Human Cytomegalovirus and Induces Type I Interferon Responses in Human Monocyte-Derived Cells. *PLoS Pathog* 2016;12:e1005546. doi:10.1371/journal.ppat.1005546.
- [198] Murray MJ, Peters NE, Reeves MB. Navigating the host cell response during entry into sites of latent cytomegalovirus infection. *Pathogens* 2018;7. doi:10.3390/pathogens7010030.
- [199] Horan KA, Hansen K, Jakobsen MR, Holm CK, Sjøby S, Unterholzner L, et al. Proteasomal degradation of herpes simplex virus capsids in macrophages releases DNA to the cytosol for recognition by DNA sensors. *J Immunol* 2013;190:2311–9. doi:10.4049/jimmunol.1202749.
- [200] Sun C, Schattgen SA, Pisitkun P, Jorgensen JP, Hilterbrand AT, Wang LJ, et al. Evasion of Innate Cytosolic DNA Sensing by a Gammaherpesvirus Facilitates Establishment of Latent Infection. *J Immunol* 2015;194:1819–31. doi:10.4049/jimmunol.1402495.
- [201] Orzalli MH, Broekema NM, Diner BA, Hancks DC, Elde NC, Cristea IM, et al. cGAS-mediated stabilization of IFI16 promotes innate signaling during herpes simplex virus infection. *Proc Natl Acad Sci* 2015;112:E1773–81. doi:10.1073/pnas.1424637112.
- [202] Liu H, Zhang H, Wu X, Ma D, Wu J, Wang L, et al. Nuclear cGAS suppresses DNA repair and promotes tumorigenesis. *Nature* 2018;563:131–6. doi:10.1038/s41586-018-0629-6.
- [203] Biolatti M, Dell’Oste V, Pautasso S, Gugliesi F, von Einem J, Krapp C, et al. Human Cytomegalovirus Tegument Protein pp65 (pUL83) Dampens Type I Interferon Production by Inactivating the DNA Sensor cGAS without Affecting STING. *J Virol* 2017;92. doi:10.1128/jvi.01774-17.
- [204] Ansari MA, Dutta S, Veetil MV, Dutta D, Iqbal J, Kumar B, et al. Herpesvirus Genome Recognition Induced Acetylation of Nuclear IFI16 Is Essential for Its Cytoplasmic Translocation, Inflammasome

- and IFN- β Responses. *PLoS Pathog* 2015;11:e1005019. doi:10.1371/journal.ppat.1005019.
- [205] Volkman HE, Cambier S, Gray EE, Stetson DB. Tight nuclear tethering of cGAS is essential for preventing autoreactivity. *Elife* 2019;8. doi:10.7554/eLife.47491.
- [206] Jønsson KL, Laustsen A, Krapp C, Skipper KA, Thavachelvam K, Hotter D, et al. IFI16 is required for DNA sensing in human macrophages by promoting production and function of cGAMP. *Nat Commun* 2017;8:14391. doi:10.1038/ncomms14391.
- [207] Bianco C, Mohr I. Restriction of Human Cytomegalovirus Replication by ISG15, a Host Effector Regulated by cGAS-STING Double-Stranded-DNA Sensing. *J Virol* 2017;91:e02483-16. doi:10.1128/JVI.02483-16.
- [208] Biolatti M, Dell'Oste V, Pautasso S, von Einem J, Marschall M, Plachter B, et al. Regulatory Interaction between the Cellular Restriction Factor IFI16 and Viral pp65 (pUL83) Modulates Viral Gene Expression and IFI16 Protein Stability. *J Virol* 2016;90:8238–50. doi:10.1128/JVI.00923-16.
- [209] Almine JF, O'Hare CAJ, Dunphy G, Haga IR, Naik RJ, Atrih A, et al. IFI16 and cGAS cooperate in the activation of STING during DNA sensing in human keratinocytes. *Nat Commun* 2017;8:14392. doi:10.1038/ncomms14392.
- [210] Hancock MH, Hook LM, Mitchell J, Nelson JA. Human cytomegalovirus microRNAs miR-US5-1 and miR-UL112-3p block proinflammatory cytokine production in response to NF- κ B-activating factors through direct downregulation of IKK α and IKK β . *MBio* 2017;8. doi:10.1128/mBio.00109-17.
- [211] Huang ZF, Zou HM, Liao BW, Zhang HY, Yang Y, Fu YZ, et al. Human Cytomegalovirus Protein UL31 Inhibits DNA Sensing of cGAS to Mediate Immune Evasion. *Cell Host Microbe* 2018;24:69-80.e4. doi:10.1016/j.chom.2018.05.007.
- [212] Tavalai N, Stamminger T. Intrinsic cellular defense mechanisms targeting human cytomegalovirus. *Virus Res* 2011;157:128–33. doi:10.1016/j.virusres.2010.10.002.
- [213] Rai TS, Glass M, Cole JJ, Rather MI, Marsden M, Neilson M, et al. Histone chaperone HIRA deposits histone H3.3 onto foreign viral DNA and contributes to anti-viral intrinsic immunity. *Nucleic Acids Res* 2017;45:11673–83. doi:10.1093/nar/gkx771.
- [214] Scherer M, Schilling EM, Stamminger T. The human CMV IE1 protein: An offender of PML nuclear bodies. *Adv. Anat. Embryol. Cell Biol.*, vol. 223, Springer Verlag; 2017, p. 77–94. doi:10.1007/978-

3-319-53168-7_4.

- [215] Li T, Chen J, Cristea IM. Human cytomegalovirus tegument protein pUL83 inhibits IFI16-mediated DNA sensing for immune evasion. *Cell Host Microbe* 2013;14:591–9. doi:10.1016/j.chom.2013.10.007.
- [216] Scherer M, Stamminger T. Emerging Role of PML Nuclear Bodies in Innate Immune Signaling. *J Virol* 2016;90:5850–4. doi:10.1128/JVI.01979-15.
- [217] Rossini G, Cerboni C, Santoni A, Landini MP, Landolfo S, Gatti D, et al. Interplay between human cytomegalovirus and intrinsic/innate host responses: A complex bidirectional relationship. *Mediators Inflamm* 2012;2012. doi:10.1155/2012/607276.
- [218] Kapoor A, Forman M, Arav-Boger R. Activation of nucleotide oligomerization domain 2 (NOD2) by human cytomegalovirus initiates innate immune responses and restricts virus Replication. *PLoS One* 2014;9. doi:10.1371/journal.pone.0092704.
- [219] Scott I. Degradation of RIG-I following cytomegalovirus infection is independent of apoptosis. *Microbes Infect* 2009;11:973–9. doi:10.1016/j.micinf.2009.07.001.
- [220] Ziehr B, Vincent HA, Moorman NJ. Human Cytomegalovirus pTRS1 and pIRS1 Antagonize Protein Kinase R To Facilitate Virus Replication. *J Virol* 2016;90:3839–48. doi:10.1128/JVI.02714-15.
- [221] Vincent HA, Ziehr B, Moorman NJ. Mechanism of Protein Kinase R Inhibition by Human Cytomegalovirus pTRS1. *J Virol* 2017;91. doi:10.1128/JVI.01574-16.
- [222] Kimkong I, Avihingsanon Y, Hirankarn N. Expression profile of HIN200 in leukocytes and renal biopsy of SLE patients by real-time RT-PCR. *Lupus* 2009;18:1066–72. doi:10.1177/0961203309106699.
- [223] Lee J-H, Kalejta RF. Human Cytomegalovirus Enters the Primary CD34 + Hematopoietic Progenitor Cells Where It Establishes Latency by Macropinocytosis . *J Virol* 2019;93. doi:10.1128/jvi.00452-19.
- [224] Dunphy G, Flannery SM, Almine JF, Connolly DJ, Paulus C, Jønsson KL, et al. Non-canonical Activation of the DNA Sensing Adaptor STING by ATM and IFI16 Mediates NF-κB Signaling after Nuclear DNA Damage. *Mol Cell* 2018;71:745-760.e5. doi:10.1016/j.molcel.2018.07.034.
- [225] Cridland JA, Curley EZ, Wykes MN, Schroder K, Sweet MJ, Roberts TL, et al. The mammalian PYHIN

gene family: phylogeny, evolution and expression. *BMC Evol Biol* 2012;12:140. doi:10.1186/1471-2148-12-140.

- [226] Khare S, Ratsimandresy RA, de Almeida L, Cuda CM, Rellick SL, Misharin A V, et al. The PYRIN domain-only protein POP3 inhibits ALR inflammasomes and regulates responses to infection with DNA viruses. *Nat Immunol* 2014;15:343–53. doi:10.1038/ni.2829.
- [227] Connolly DJ, Bowie AG. The emerging role of human PYHIN proteins in innate immunity: Implications for health and disease. *Biochem Pharmacol* 2014;92:405–14. doi:10.1016/j.bcp.2014.08.031.
- [228] DeYoung KL, Ray ME, Su YA, Anzick SL, Johnstone RW, Trapani JA, et al. Cloning a novel member of the human interferon-inducible gene family associated with control of tumorigenicity in a model of human melanoma. *Oncogene* 1997;15:453–7. doi:10.1038/sj.onc.1201206.
- [229] Harada M, Li YF, El-Gamil M, Ohnmacht GA, Rosenberg SA, Robbins PF. Melanoma-reactive CD8+ T cells recognize a novel tumor antigen expressed in a wide variety of tumor types. *J Immunother* 2001;24:323–33. doi:10.1097/00002371-200107000-00008.
- [230] Roberts TL, Idris A, Dunn JA, Kelly GM, Burnton CM, Hodgson S, et al. HIN-200 Proteins Regulate Caspase Activation in Response to Foreign Cytoplasmic DNA. *Science (80-)* 2009;323:1057–60. doi:10.1126/science.1169841.
- [231] Fernandes-Alnemri T, Yu J-W, Datta P, Wu J, Alnemri ES. AIM2 activates the inflammasome and cell death in response to cytoplasmic DNA. *Nature* 2009;458. doi:10.1038/nature07710.
- [232] Bürckstümmer T, Baumann C, Blüml S, Dixit E, Dürnberger G, Jahn H, et al. An orthogonal proteomic-genomic screen identifies AIM2 as a cytoplasmic DNA sensor for the inflammasome. *Nat Immunol* 2009;10:266–72. doi:10.1038/ni.1702.
- [233] Hornung V, Ablasser A, Charrel-Dennis M, Bauernfeind F, Horvath G, Caffrey DR, et al. AIM2 recognizes cytosolic dsDNA and forms a caspase-1-activating inflammasome with ASC. *Nature* 2009;458:514–8. doi:10.1038/nature07725.
- [234] Man SM, Karki R, Kanneganti TD. AIM2 inflammasome in infection, cancer, and autoimmunity: Role in DNA sensing, inflammation, and innate immunity. *Eur J Immunol* 2016;46:269–80. doi:10.1002/eji.201545839.

- [235] Lugrin J, Martinon F. The AIM2 inflammasome: Sensor of pathogens and cellular perturbations. *Immunol Rev* 2018;281:99–114. doi:10.1111/imr.12618.
- [236] Rathinam VAK, Jiang Z, Waggoner SN, Sharma S, Cole LE, Waggoner L, et al. The AIM2 inflammasome is essential for host defense against cytosolic bacteria and DNA viruses. *Nat Immunol* 2010;11:395–402. doi:10.1038/ni.1864.
- [237] Huang Y, Ma D, Huang H, Lu Y, Liao Y, Liu L, et al. Interaction between HCMV pUL83 and human AIM2 disrupts the activation of the AIM2 inflammasome. *Virology* 2017;14. doi:10.1186/s12985-016-0673-5.
- [238] Huang Y, Liu L, Ma D, Liao Y, Lu Y, Huang H, et al. Human cytomegalovirus triggers the assembly of AIM2 inflammasome in THP-1-derived macrophages. *J Med Virol* 2017;89:2188–95. doi:10.1002/jmv.24846.
- [239] Botto S, Abraham J, Mizuno N, Pryke K, Gall B, Landais I, et al. Human cytomegalovirus immediate early 86-kDa protein blocks transcription and induces degradation of the immature interleukin-1 β protein during virion-mediated activation of the AIM2 inflammasome. *MBio* 2019;10. doi:10.1128/mBio.02510-18.
- [240] Reinholz M, Kawakami Y, Salzer S, Kreuter A, Dombrowski Y, Koglin S, et al. HPV16 activates the AIM2 inflammasome in keratinocytes. *Arch Dermatol Res* 2013;305:723–32. doi:10.1007/s00403-013-1375-0.
- [241] Zhen J, Zhang L, Pan J, Ma S, Yu X, Li X, et al. AIM2 mediates inflammation-associated renal damage in hepatitis B virus-associated glomerulonephritis by regulating caspase-1, IL-1 β , and IL-18. *Mediators Inflamm* 2014;2014:1–9. doi:10.1155/2014/190860.
- [242] Maruzuru Y, Ichinohe T, Sato R, Miyake K, Okano T, Suzuki T, et al. Herpes Simplex Virus 1 VP22 Inhibits AIM2-Dependent Inflammasome Activation to Enable Efficient Viral Replication. *Cell Host Microbe* 2018;23:254-265.e7. doi:10.1016/j.chom.2017.12.014.
- [243] Diner BA, Li T, Greco TM, Crow MS, Fuesler JA, Wang J, et al. The functional interactome of PYHIN immune regulators reveals IFIX is a sensor of viral DNA. *Mol Syst Biol* 2015;11:787.
- [244] Crow MS, Cristea IM. Human Antiviral Protein IFIX Suppresses Viral Gene Expression during Herpes Simplex Virus 1 (HSV-1) Infection and Is Counteracted by Virus-induced Proteasomal

- Degradation. *Mol Cell Proteomics* 2017;16:S200–14. doi:10.1074/mcp.M116.064741.
- [245] Trapani J, Browne K, Dawson M, Ramsay R, Eddy R, Shows T, et al. A novel gene constitutively expressed in human lymphoid cells is inducible with interferon-gamma in myeloid cells. *Immunogenetics* 1992;36:369–76. doi:10.1007/BF00218044.
- [246] Xin H, Curry J, Johnstone RW, Nickoloff BJ, Choubey D. Role of IFI 16, a member of the interferon-inducible p200-protein family, in prostate epithelial cellular senescence. *Oncogene* 2003;22:4831–40. doi:10.1038/sj.onc.1206754.
- [247] Xin H, Pereira-Smith OM, Choubey D. Role of IFI 16 in cellular senescence of human fibroblasts. *Oncogene* 2004;23:6209–17. doi:10.1038/sj.onc.1207836.
- [248] Aglipay JA, Lee SW, Okada S, Fujiuchi N, Ohtsuka T, Kwak JC, et al. A member of the Pyrin family, IFI16, is a novel BRCA1-associated protein involved in the p53-mediated apoptosis pathway. *Oncogene* 2003;22:8931–8. doi:10.1038/sj.onc.1207057.
- [249] Johnstone RW, Wei W, Greenway A, Trapani JA. Functional interaction between p53 and the interferon-inducible nucleoprotein IFI 16. *Oncogene* 2000;19:6033–42. doi:10.1038/sj.onc.1204005.
- [250] Caposio P, Gugliesi F, Zannetti C, Sponza S, Mondini M, Medico E, et al. A novel role of the interferon-inducible protein IFI16 as inducer of proinflammatory molecules in endothelial cells. *J Biol Chem* 2007;282:33515–29. doi:10.1074/jbc.M701846200.
- [251] Baggetta R, De Andrea M, Gariano GR, Mondini M, Rittà M, Caposio P, et al. The interferon-inducible gene IFI16 secretome of endothelial cells drives the early steps of the inflammatory response. *Eur J Immunol* 2010;40:2182–9. doi:10.1002/eji.200939995.
- [252] Piccaluga PP, Agostinelli C, Fuligni F, Righi S, Tripodo C, Re MC, et al. IFI16 Expression Is Related to Selected Transcription Factors during B-Cell Differentiation. *J Immunol Res* 2015;2015:747645. doi:10.1155/2015/747645.
- [253] Bawadekar M, De Andrea M, Lo Cigno I, Baldanzi G, Caneparo V, Graziani A, et al. The Extracellular IFI16 Protein Propagates Inflammation in Endothelial Cells Via p38 MAPK and NF-κB p65 Activation. *J Interf Cytokine Res* 2015;35:441–53. doi:10.1089/jir.2014.0168.
- [254] Jakobsen MR, Paludan SR. IFI16: At the interphase between innate DNA sensing and genome

- regulation. *Cytokine Growth Factor Rev* 2014;25:649–55. doi:10.1016/j.cytogfr.2014.06.004.
- [255] Dell’Oste V, Gatti D, Giorgio AG, Gariglio M, Landolfo S, De Andrea M. The interferon-inducible DNA-sensor protein IFI16: a key player in the antiviral response. *New Microbiol* 2015;38:5–20.
- [256] Unterholzner L, Keating SE, Baran M, Horan KA, Jensen SB, Sharma S, et al. IFI16 is an innate immune sensor for intracellular DNA. *Nat Immunol* 2010;11:997–1004. doi:10.1038/ni.1932.
- [257] Orzalli MH, Conwell SE, Berrios C, DeCaprio JA, Knipe DM. Nuclear interferon-inducible protein 16 promotes silencing of herpesviral and transfected DNA. *Proc Natl Acad Sci* 2013;110:E4492–501. doi:10.1073/pnas.1316194110.
- [258] Thompson MR, Sharma S, Atianand M, Jensen SB, Carpenter S, Knipe DM, et al. Interferon γ -inducible protein (IFI) 16 transcriptionally regulates type I interferons and other interferon-stimulated genes and controls the interferon response to both DNA and RNA viruses. *J Biol Chem* 2014;289:23568–81. doi:10.1074/jbc.M114.554147.
- [259] Diner BA, Lum KK, Toettcher JE, Cristea IM. Viral DNA sensors IFI16 and cyclic GMP-AMP synthase possess distinct functions in regulating viral gene expression, immune defenses, and apoptotic responses during herpesvirus infection. *MBio* 2016;7:e01553-16. doi:10.1128/mBio.01553-16.
- [260] Johnson KE, Bottero V, Flaherty S, Dutta S, Singh VV, Chandran B. IFI16 Restricts HSV-1 Replication by Accumulating on the HSV-1 Genome, Repressing HSV-1 Gene Expression, and Directly or Indirectly Modulating Histone Modifications. *PLoS Pathog* 2014;10:e1004503. doi:10.1371/journal.ppat.1004503.
- [261] Orzalli MH, DeLuca NA, Knipe DM. Nuclear IFI16 induction of IRF-3 signaling during herpesviral infection and degradation of IFI16 by the viral ICPO protein. *Proc Natl Acad Sci U S A* 2012;109:E3008-17. doi:10.1073/pnas.1211302109.
- [262] Alandijany T, Roberts APE, Conn KL, Loney C, McFarlane S, Orr A, et al. Distinct temporal roles for the promyelocytic leukaemia (PML) protein in the sequential regulation of intracellular host immunity to HSV-1 infection. *PLoS Pathog* 2018;14:e1006769. doi:10.1371/journal.ppat.1006769.
- [263] Eriksson K, Svensson A, Hait AS, Schlüter K, Tunbäck P, Nordström I, et al. Cutting Edge: Genetic Association between IFI16 Single Nucleotide Polymorphisms and Resistance to Genital Herpes Correlates with IFI16 Expression Levels and HSV-2-Induced IFN- β Expression. *J Immunol*

2017;199:2613–7. doi:10.4049/jimmunol.1700385.

- [264] Gariano GR, Dell'Oste V, Bronzini M, Gatti D, Luganini A, De Andrea M, et al. The Intracellular DNA Sensor IFI16 Gene Acts as Restriction Factor for Human Cytomegalovirus Replication. *PLoS Pathog* 2012;8:e1002498. doi:10.1371/journal.ppat.1002498.
- [265] Dutta D, Dutta S, Veettil MV, Roy A, Ansari MA, Iqbal J, et al. BRCA1 Regulates IFI16 Mediated Nuclear Innate Sensing of Herpes Viral DNA and Subsequent Induction of the Innate Inflammasome and Interferon- β Responses. *PLOS Pathog* 2015;11:e1005030. doi:10.1371/journal.ppat.1005030.
- [266] Singh V V., Kerur N, Bottero V, Dutta S, Chakraborty S, Ansari MA, et al. Kaposi's Sarcoma-Associated Herpesvirus Latency in Endothelial and B Cells Activates Gamma Interferon-Inducible Protein 16-Mediated Inflammasomes. *J Virol* 2013;87:4417–31. doi:10.1128/JVI.03282-12.
- [267] Roy A, Dutta D, Iqbal J, Pisano G, Gjyshi O, Ansari MA, et al. Nuclear Innate Immune DNA Sensor IFI16 Is Degraded during Lytic Reactivation of Kaposi's Sarcoma-Associated Herpesvirus (KSHV): Role of IFI16 in Maintenance of KSHV Latency. *J Virol* 2016;90:8822–41. doi:10.1128/jvi.01003-16.
- [268] Roy A, Ghosh A, Kumar B, Chandran B. IFI16, a nuclear innate immune DNA sensor, mediates epigenetic silencing of herpesvirus genomes by its association with H3K9 methyltransferases SUV39H1 and GLP. *Elife* 2019;8. doi:10.7554/eLife.49500.
- [269] Lo Cigno I, De Andrea M, Borgogna C, Albertini S, Landini MM, Peretti A, et al. The Nuclear DNA Sensor IFI16 Acts as a Restriction Factor for Human Papillomavirus Replication through Epigenetic Modifications of the Viral Promoters. *J Virol* 2015;89:7506–20. doi:10.1128/JVI.00013-15.
- [270] Jakobsen MR, Bak RO, Andersen A, Berg RK, Jensen SB, Tengchuan J, et al. IFI16 senses DNA forms of the lentiviral replication cycle and controls HIV-1 replication. *Proc Natl Acad Sci U S A* 2013;110:E4571-80. doi:10.1073/pnas.1311669110.
- [271] Hotter D, Bosso M, Jønsson KL, Krapp C, Stürzel CM, Das A, et al. IFI16 Targets the Transcription Factor Sp1 to Suppress HIV-1 Transcription and Latency Reactivation. *Cell Host Microbe* 2019;25:858-872.e13. doi:10.1016/J.CHOM.2019.05.002.
- [272] Monroe KM, Yang Z, Johnson JR, Geng X, Doitsh G, Krogan NJ, et al. IFI16 DNA sensor is required for death of lymphoid CD4 T cells abortively infected with HIV. *Science (80-)* 2014;343:428–32.

doi:10.1126/science.1243640.

- [273] Yang B, Song D, Liu Y, Cui Y, Lu G, Di W, et al. IFI16 regulates HTLV-1 replication through promoting HTLV-1 RTI-induced innate immune responses. *FEBS Lett* 2018;592:1693–704. doi:10.1002/1873-3468.13077.
- [274] Yang Y, Zhao X, Wang Z, Shu W, Li L, Li Y, et al. Nuclear Sensor IFI 16 Inhibits the Function of HBV ccc DNA by Integrating Innate Immune Activation and Epigenetic Suppression . *Hepatology* 2019. doi:10.1002/hep.30897.
- [275] Wichit S, Hamel R, Yainoy S, Gumpangseth N, Panich S, Phuadraksa T, et al. Interferon-inducible protein (IFI) 16 regulates chikungunya and zika virus infection in human skin fibroblasts. *EXCLI J* 2019;18:467–76. doi:10.17179/excli2019-1271.
- [276] Kerur N, Veettil MV, Sharma-Walia N, Bottero V, Sadagopan S, Otageri P, et al. IFI16 Acts as a Nuclear Pathogen Sensor to Induce the Inflammasome in Response to Kaposi Sarcoma-Associated Herpesvirus Infection. *Cell Host Microbe* 2011;9:363–75. doi:10.1016/j.chom.2011.04.008.
- [277] Morrone SR, Wang T, Constantoulakis LM, Hooy RM, Delannoy MJ, Sohn J. Cooperative assembly of IFI16 filaments on dsDNA provides insights into host defense strategy. *Proc Natl Acad Sci* 2014;111:E62–71. doi:10.1073/pnas.1313577111.
- [278] Jin T, Perry A, Jiang J, Smith P, Curry JA, Unterholzner L, et al. Structures of the HIN Domain: DNA Complexes Reveal Ligand Binding and Activation Mechanisms of the AIM2 Inflammasome and IFI16 Receptor. *Immunity* 2012;36:561–71. doi:10.1016/j.immuni.2012.02.014.
- [279] Stratmann SA, Morrone SR, van Oijen AM, Sohn J. The innate immune sensor IFI16 recognizes foreign DNA in the nucleus by scanning along the duplex. *Elife* 2015;4:e11721. doi:10.7554/eLife.11721.
- [280] Everett RD. The dynamic response of IFI16 and PML Nuclear Body components to HSV-1 infection. *J Virol* 2015;90:JVI.02249-15. doi:10.1128/JVI.02249-15.
- [281] Brázda V, Coufal J, Liao JCC, Arrowsmith CH. Preferential binding of IFI16 protein to cruciform structure and superhelical DNA. *Biochem Biophys Res Commun* 2012;422:716–20. doi:10.1016/j.bbrc.2012.05.065.
- [282] Hároníková L, Coufal J, Kejnovská I, Jagelská EB, Fojta M, Dvořáková P, et al. IFI16 Preferentially

- Binds to DNA with Quadruplex Structure and Enhances DNA Quadruplex Formation. *PLoS One* 2016;11:e0157156. doi:10.1371/journal.pone.0157156.
- [283] Merkl PE, Knipe DM. Role for a Filamentous Nuclear Assembly of IFI16, DNA, and Host Factors in Restriction of Herpesviral Infection. *MBio* 2019;10. doi:10.1128/mBio.02621-18.
- [284] Lum KK, Howard TR, Pan C, Cristea IM. Charge-Mediated Pyrin Oligomerization Nucleates Antiviral IFI16 Sensing of Herpesvirus DNA. *MBio* 2019;10. doi:10.1128/mbio.01428-19.
- [285] Pisano G, Roy A, Ahmed Ansari M, Kumar B, Chikoti L, Chandran B. Interferon- γ -inducible protein 16 (IFI16) is required for the maintenance of Epstein-Barr virus latency. *Virol J* 2017;14:221. doi:10.1186/s12985-017-0891-5.
- [286] Johnstone RW, Kerry JA, Trapani JA. The human interferon-inducible protein, IFI 16, is a repressor of transcription. *J Biol Chem* 1998;273:17172–7. doi:10.1074/jbc.273.27.17172.
- [287] Briggs JA, Burrus GR, Stickney BD, Briggs RC. Cloning and expression of the human myeloid cell nuclear differentiation antigen: Regulation by interferon α . *J Cell Biochem* 1992;49:82–92. doi:10.1002/jcb.240490114.
- [288] Briggs R, Briggs J, Ozer J, Sealy L, Dworkin L, Kingsmore S, et al. The human myeloid cell nuclear differentiation antigen gene is one of at least two related interferon-inducible genes located on chromosome 1q that are expressed specifically in hematopoietic cells. *Blood* 1994;83.
- [289] Briggs RC, Kao WY, Dworkin LL, Briggs JA, Dessypris EN, Clark J. Regulation and specificity of MND4 expression in monocytes, macrophages, and leukemia/B lymphoma cell lines. *J Cell Biochem* 1994;56:559–67. doi:10.1002/jcb.240560417.
- [290] Kao WY, Dworkin LL, Briggs JA, Briggs RC. Characterization of the human myeloid cell nuclear differentiation antigen gene promoter. *Biochim Biophys Acta* 1996;1308:201–4.
- [291] Fukushi M, Higuchi M, Oie M, Tetsuka T, Kasolo F, Ichiyama K, et al. Latency-associated nuclear antigen of Kaposi's sarcoma-associated herpesvirus interacts with human myeloid cell nuclear differentiation antigen induced by interferon alpha. *Virus Genes* 2003;27:237–47.
- [292] Li H, Wang ZX, Wu JW. Purification, characterization and docking studies of the HIN domain of human myeloid nuclear differentiation antigen (MND4). *Biotechnol Lett* 2014;36:899–905. doi:10.1007/s10529-013-1432-y.

- [293] Murao S, Epstein AL, Clevenger C V, Huberman E. Expression of maturation-specific nuclear antigens in differentiating human myeloid leukemia cells. *Cancer Res* 1985;45:791–5.
- [294] Suzuki T, Nakano-Ikegaya M, Yabukami-Okuda H, de Hoon M, Severin J, Saga-Hatano S, et al. Reconstruction of monocyte transcriptional regulatory network accompanies monocytic functions in human fibroblasts. *PLoS One* 2012;7:e33474. doi:10.1371/journal.pone.0033474.
- [295] Novershtern N, Subramanian A, Lawton LN, Mak RH, Haining WN, McConkey ME, et al. Densely interconnected transcriptional circuits control cell states in human hematopoiesis. *Cell* 2011;144:296–309. doi:10.1016/j.cell.2011.01.004.
- [296] Doggett KL, Briggs JA, Linton MF, Fazio S, Head DR, Xie J, et al. Retroviral mediated expression of the human myeloid nuclear antigen in a null cell line upregulates Dlk1 expression. *J Cell Biochem* 2002;86:56–66. doi:10.1002/jcb.10190.
- [297] Gaczynski M, Briggs JA, Wedrychowski A, Olinski R, Briggs RC, Uskokovic M, et al. cis-Diamminedichloroplatinum(II) Cross-Linking of the Human Myeloid Cell Nuclear Differentiation Antigen to DNA in HL-60 Cells following 1,25-Dihydroxy Vitamin D3-induced Monocyte Differentiation. *Cancer Res* 1990;50:1183–8.
- [298] Xie J, Briggs JA, Briggs RC. Human hematopoietic cell specific nuclear protein MNDA interacts with the multifunctional transcription factor YY1 and stimulates YY1 DNA binding. *J Cell Biochem* 1998;70:489–506.
- [299] Hofmann W-K, de Vos S, Komor M, Hoelzer D, Wachsmann W, Koeffler HP. Characterization of gene expression of CD34+ cells from normal and myelodysplastic bone marrow. *Blood* 2002;100.
- [300] Pradhan A, Mijovic A, Mills K, Cumber P, Westwood N, Mufti GJ, et al. Differentially expressed genes in adult familial myelodysplastic syndromes. *Leukemia* 2004;18:449–59. doi:10.1038/sj.leu.2403265.
- [301] Somasundaram V, Soni S, Chopra A, Rai S, Mahapatra M, Kumar R, et al. Value of Quantitative assessment of Myeloid Nuclear Differentiation Antigen expression and other flow cytometric parameters in the diagnosis of Myelodysplastic syndrome. *Int J Lab Hematol* 2016;38:141–50. doi:10.1111/ijlh.12458.
- [302] Parker JE, Mufti GJ. The Myelodysplastic Syndromes: A Matter of Life or Death. *Acta Haematol*

2003;111:78–99. doi:10.1159/000074488.

- [303] Briggs RC, Shults KE, Flye LA, McClintock-Treep SA, Jagasia MH, Goodman SA, et al. Dysregulated Human Myeloid Nuclear Differentiation Antigen Expression in Myelodysplastic Syndromes: Evidence for a Role in Apoptosis. *Cancer Res* 2006;66.
- [304] Fotouhi-Ardakani N, Kebir D El, Pierre-Charles N, Wang L, Ahern SP, Filep JG, et al. Role for Myeloid Nuclear Differentiation Antigen in the Regulation of Neutrophil Apoptosis during Sepsis. *Am J Respir Crit Care Med* 2010;182:341–50. doi:10.1164/rccm.201001-0075OC.
- [305] Reeves MB, Breidenstein A, Compton T. Human cytomegalovirus activation of ERK and myeloid cell leukemia-1 protein correlates with survival of latently infected cells. *Proc Natl Acad Sci U S A* 2012;109:588–93. doi:10.1073/pnas.1114966108.
- [306] Janeway CA, Travers P, Walport M, Al E. Principles of innate and adaptive immunity. *Immunobiol. Immune Syst. Heal. Dis.* 5th Ed., Garland Science; 2001, p. 1–9.
- [307] Könning D, Zielonka S, Grzeschik J, Empting M, Valldorf B, Krah S, et al. Camelid and shark single domain antibodies: structural features and therapeutic potential. *Curr Opin Struct Biol* 2017;45:10–6. doi:10.1016/J.SBI.2016.10.019.
- [308] De Groof TWM, Mashayekhi V, Fan TS, Bergkamp ND, Sastre Toraño J, van Senten JR, et al. Nanobody-Targeted Photodynamic Therapy Selectively Kills Viral GPCR-Expressing Glioblastoma Cells. *Mol Pharm* 2019;16:3145–56. doi:10.1021/acs.molpharmaceut.9b00360.
- [309] De Groof TWM, Bobkov V, Heukers R, Smit MJ. Nanobodies: New avenues for imaging, stabilizing and modulating GPCRs. vol. 484. 2019. doi:10.1016/j.mce.2019.01.021.
- [310] Bannas P, Hambach J, Koch-Nolte F. Nanobodies and Nanobody-Based Human Heavy Chain Antibodies As Antitumor Therapeutics. *Front Immunol* 2017;8:1603. doi:10.3389/fimmu.2017.01603.
- [311] Heukers R, De Groof TWM, Smit MJ. Nanobodies detecting and modulating GPCRs outside in and inside out. *Curr Opin Cell Biol* 2019;57:115–22. doi:10.1016/j.ceb.2019.01.003.
- [312] Estcourt LJ. Caplacizumab treatment for acquired thrombotic thrombocytopenic purpura (HERCULES trial). *Transfus Med* 2019;29:146–8. doi:10.1111/tme.12615.
- [313] le Besnerais M, Veyradier A, Benhamou Y, Coppo P. Caplacizumab: a change in the paradigm of

thrombotic thrombocytopenic purpura treatment. *Expert Opin Biol Ther* 2019;1–8.
doi:10.1080/14712598.2019.1650908.

- [314] Peyvandi F, Scully M, Kremer Hovinga JA, Cataland S, Knöbl P, Wu H, et al. Caplacizumab for Acquired Thrombotic Thrombocytopenic Purpura. *N Engl J Med* 2016;374:511–22.
doi:10.1056/NEJMoa1505533.
- [315] Detalle L, Stohr T, Palomo C, Piedra PA, Gilbert BE, Mas V, et al. Generation and Characterization of ALX-0171, a Potent Novel Therapeutic Nanobody for the Treatment of Respiratory Syncytial Virus Infection. *Antimicrob Agents Chemother* 2016;60:6–13. doi:10.1128/AAC.01802-15.
- [316] Van Hout A, Klarenbeek A, Bobkov V, Doijen J, Arimont M, Zhao C, et al. CXCR4-targeting nanobodies differentially inhibit CXCR4 function and HIV entry. *Biochem Pharmacol* 2018;158:402–12. doi:10.1016/j.bcp.2018.10.015.
- [317] Jähnichen S, Blanchetot C, Maussang D, Gonzalez-Pajuelo M, Chow KY, Bosch L, et al. CXCR4 nanobodies (VHH-based single variable domains) potently inhibit chemotaxis and HIV-1 replication and mobilize stem cells. *Proc Natl Acad Sci U S A* 2010;107:20565–70.
doi:10.1073/pnas.1012865107.
- [318] Maussang D, Mujčić-Delić A, Descamps FJ, Stortelers C, Vanlandschoot P, Stigter-van Walsum M, et al. Llama-derived single variable domains (nanobodies) directed against chemokine receptor CXCR7 reduce head and neck cancer cell growth in vivo. *J Biol Chem* 2013;288:29562–72.
doi:10.1074/jbc.M113.498436.
- [319] Sadowski I, Hashemi FB. Strategies to eradicate HIV from infected patients: elimination of latent provirus reservoirs. *Cell Mol Life Sci* 2019;1–18. doi:10.1007/s00018-019-03156-8.
- [320] Nehme Z, Pasquereau S, Herbein G. Control of viral infections by epigenetic-targeted therapy. *Clin Epigenetics* 2019;11:55. doi:10.1186/s13148-019-0654-9.
- [321] Knipe DM, Raja P, Lee J. Viral gene products actively promote latent infection by epigenetic silencing mechanisms. *Curr Opin Virol* 2017;23:68–74. doi:10.1016/j.coviro.2017.03.010.
- [322] Turner AMW, Margolis DM. Chromatin regulation and the histone code in HIV latency. *Yale J Biol Med* 2017;90:229–43.
- [323] Hammerschmidt W. The epigenetic life cycle of epstein–barr virus. *Curr. Top. Microbiol.*

- Immunol., vol. 390, Springer Verlag; 2015, p. 103–17. doi:10.1007/978-3-319-22822-8_6.
- [324] Ruiz A, Blanch-Lombarte O, Jimenez-Moyano E, Ouchi D, Mothe B, Peña R, et al. Antigen production after latency reversal and expression of inhibitory receptors in CD8+ T cells limit the killing of HIV-1 reactivated cells. *Front Immunol* 2019;10. doi:10.3389/fimmu.2018.03162.
- [325] Rose R, Nolan DJ, Maidji E, Stoddart CA, Singer EJ, Lamers SL, et al. Eradication of HIV from Tissue Reservoirs: Challenges for the Cure. *AIDS Res Hum Retroviruses* 2018;34:3–8. doi:10.1089/AID.2017.0072.
- [326] Hopcraft SE, Pattenden SG, James LI, Frye S, Dittmer DP, Damania B. Chromatin remodeling controls Kaposi's sarcoma-associated herpesvirus reactivation from latency. *PLoS Pathog* 2018;14. doi:10.1371/journal.ppat.1007267.
- [327] Hui KF, Yiu SPT, Tam KP, Chiang AKS. Viral-targeted strategies against EBV-associated lymphoproliferative diseases. *Front Oncol* 2019;9. doi:10.3389/fonc.2019.00081.
- [328] Choudhary S, Mathew M, Verma RS. Therapeutic potential of anticancer immunotoxins. *Drug Discov Today* 2011;16:495–503. doi:10.1016/j.drudis.2011.04.003.
- [329] Naran K, Nundalall T, Chetty S, Barth S. Principles of Immunotherapy: Implications for Treatment Strategies in Cancer and Infectious Diseases. *Front Microbiol* 2018;9. doi:10.3389/fmicb.2018.03158.
- [330] Xu Z, Guo D, Jiang Z, Tong R, Jiang P, Bai L, et al. Novel HER2-Targeting Antibody-Drug Conjugates of Trastuzumab Beyond T-DM1 in Breast Cancer: Trastuzumab Deruxtecan(DS-8201a) and (Vic-)Trastuzumab Duocarmazine (SYD985). *Eur J Med Chem* 2019;183:111682. doi:10.1016/j.ejmech.2019.111682.
- [331] Lewis Phillips GD, Li G, Dugger DL, Crocker LM, Parsons KL, Mai E, et al. Targeting HER2-positive breast cancer with trastuzumab-DM1, an antibody-cytotoxic drug conjugate. *Cancer Res* 2008;68:9280–90. doi:10.1158/0008-5472.CAN-08-1776.
- [332] Wayne AS, Fitzgerald DJ, Kreitman RJ, Pastan I. Immunotoxins for leukemia. *Blood* 2014;123:2470–7. doi:10.1182/blood-2014-01-492256.
- [333] Hogan LE, Vasquez J, Hobbs KS, Hanhauser E, Aguilar-Rodriguez B, Hussien R, et al. Increased HIV-1 transcriptional activity and infectious burden in peripheral blood and gut-associated CD4+ T

- cells expressing CD30. PLoS Pathog 2018;14:e1006856. doi:10.1371/journal.ppat.1006856.
- [334] Spiess K, Jeppesen MG, Malmgaard-Clausen M, Krzywkowski K, Dulal K, Cheng T, et al. Rationally designed chemokine-based toxin targeting the viral G protein-coupled receptor US28 potently inhibits cytomegalovirus infection in vivo. Proc Natl Acad Sci U S A 2015;112:8427–32. doi:10.1073/pnas.1509392112.
- [335] Kledal TN, Rosenkilde MM, Schwartz TW. Selective recognition of the membrane-bound CX3C chemokine, fractalkine, by the human cytomegalovirus-encoded broad-spectrum receptor US28. FEBS Lett 1998;441:209–14. doi:10.1016/S0014-5793(98)01551-8.
- [336] Krishna BA. Investigating and exploiting the latency-associated expression of the human cytomegalovirus gene US28 in early myeloid lineage cells. University of Cambridge, 2017.
- [337] Vallera DA, Kreitman RJ. Immunotoxins targeting B cell malignancy-progress and problems with immunogenicity. Biomedicines 2019;7. doi:10.3390/biomedicines7010001.
- [338] Hamar M, Selzner M. Ex-vivo machine perfusion for kidney preservation. Curr Opin Organ Transplant 2018;23:369–74. doi:10.1097/MOT.0000000000000524.
- [339] Nicholson ML, Hosgood SA. Renal Transplantation After *Ex Vivo* Normothermic Perfusion: The First Clinical Study. Am J Transplant 2013;13:1246–52. doi:10.1111/ajt.12179.
- [340] Spiess K, Jeppesen MG, Malmgaard-Clausen M, Krzywkowski K, Kledal TN, Rosenkilde MM. Novel Chemokine-Based Immunotoxins for Potent and Selective Targeting of Cytomegalovirus Infected Cells. J Immunol Res 2017;2017:1–12. doi:10.1155/2017/4069260.
- [341] Timms RT, Duncan LM, Tchasovnikarova IA, Antrobus R, Smith DL, Dougan G, et al. Haploid genetic screens identify an essential role for PLP2 in the downregulation of novel plasma membrane targets by viral E3 ubiquitin ligases. PLoS Pathog 2013;9:e1003772. doi:10.1371/journal.ppat.1003772.
- [342] van den Boomen DJH, Timms RT, Grice GL, Stagg HR, Skødt K, Dougan G, et al. TMEM129 is a Derlin-1 associated ERAD E3 ligase essential for virus-induced degradation of MHC-I. Proc Natl Acad Sci U S A 2014;111:11425–30. doi:10.1073/pnas.1409099111.
- [343] Groom HCT, Boucherit VC, Makinson K, Randal E, Baptista S, Hagan S, et al. Absence of xenotropic murine leukaemia virus-related virus in UK patients with chronic fatigue syndrome. Retrovirology

2010;7:10. doi:10.1186/1742-4690-7-10.

- [344] Norrander J, Kempe T, Messing J. Construction of improved M13 vectors using oligodeoxynucleotide-directed mutagenesis. *Gene* 1983;26:101–6. doi:10.1016/0378-1119(83)90040-9.
- [345] Sambrook J, Russell DW. Purification of Nucleic Acids by Extraction with Phenol:Chloroform. *Cold Spring Harb Protoc* 2006;2006:pdb.prot4455. doi:10.1101/pdb.prot4455.
- [346] Spector DJ, Yetming K. UL84-independent replication of human cytomegalovirus strain TB40/E. *Virology* 2010;407:171–7. doi:10.1016/J.VIROL.2010.08.029.
- [347] Weekes MP, Tan SYL, Poole E, Talbot S, Antrobus R, Smith DL, et al. Latency-associated degradation of the MRP1 drug transporter during latent human cytomegalovirus infection. *Science* 2013;340:199–202. doi:10.1126/science.1235047.
- [348] Straschewski S, Warmer M, Frascaroli G, Hohenberg H, Mertens T, Winkler M. Human cytomegaloviruses expressing yellow fluorescent fusion proteins--characterization and use in antiviral screening. *PLoS One* 2010;5:e9174. doi:10.1371/journal.pone.0009174.
- [349] Elder E, Krishna B, Williamson J, Aslam Y, Farahi N, Wood A, et al. Monocytes latently infected with human cytomegalovirus evade neutrophil killing. *IScience* 2019. doi:10.1016/J.ISCI.2019.01.007.
- [350] De Wit RH, Heukers R, Brink HJ, Arsova A, Maussang D, Cutolo P, et al. CXCR4-specific nanobodies as potential therapeutics for WHIM syndrome. *J Pharmacol Exp Ther* 2017;363:35–44. doi:10.1124/jpet.117.242735.
- [351] Mi H, Muruganujan A, Ebert D, Huang X, Thomas PD. PANTHER version 14: more genomes, a new PANTHER GO-slim and improvements in enrichment analysis tools. *Nucleic Acids Res* 2019;47:D419–26. doi:10.1093/nar/gky1038.
- [352] Ashburner M, Ball CA, Blake JA, Botstein D, Butler H, Cherry JM, et al. Gene ontology: tool for the unification of biology. The Gene Ontology Consortium. *Nat Genet* 2000;25:25–9. doi:10.1038/75556.
- [353] Carbon S, Douglass E, Dunn N, Good B, Harris NL, Lewis SE, et al. The Gene Ontology Resource: 20 years and still GOing strong. *Nucleic Acids Res* 2019;47:D330–8. doi:10.1093/nar/gky1055.

- [354] Boehm U, Klamp T, Groot M, Howard JC. CELLULAR RESPONSES TO INTERFERON- γ . *Annu Rev Immunol* 1997;15:749–95. doi:10.1146/annurev.immunol.15.1.749.
- [355] Rusinova I, Forster S, Yu S, Kannan A, Masse M, Cumming H, et al. Interferome v2.0: an updated database of annotated interferon-regulated genes. *Nucleic Acids Res* 2013;41:D1040-6. doi:10.1093/nar/gks1215.
- [356] Fisyunov AI. Molecular mechanisms of G protein-independent signaling mediated by 7-transmembrane receptors. *Neurophysiology* 2012;44:255–64. doi:10.1007/s11062-012-9295-8.
- [357] Tilley DG. G protein-dependent and G protein-independent signaling pathways and their impact on cardiac function. *Circ Res* 2011;109:217–30. doi:10.1161/CIRCRESAHA.110.231225.
- [358] Clarke CJP, Apostolidis V, Hii LLP, Gough DJ, Trapani JA, Johnstone RW. Critical role of the transcription factor AP-1 for the constitutive and interferon-induced expression of IFI 16. *J Cell Biochem* 2003;89:80–93. doi:10.1002/jcb.10475.
- [359] Ono SJ, Bazil V, Levi BZ, Ozato K, Strominger JL. Transcription of a subset of human class II major histocompatibility complex genes is regulated by a nucleoprotein complex that contains c-fos or an antigenically related protein. *Proc Natl Acad Sci* 1991;88:4304–8. doi:10.1073/pnas.88.10.4304.
- [360] Ono SJ, Liou HC, Davidon R, Strominger JL, Glimcher LH. Human X-box-binding protein 1 is required for the transcription of a subset of human class II major histocompatibility genes and forms a heterodimer with c-fos. *Proc Natl Acad Sci U S A* 1991;88:4309–12. doi:10.1073/pnas.88.10.4309.
- [361] Wang C, Krishnakumar S, Wilhelmy J, Babrzadeh F, Stepanyan L, Su LF, et al. High-throughput, high-fidelity HLA genotyping with deep sequencing. *Proc Natl Acad Sci U S A* 2012;109:8676–81. doi:10.1073/pnas.1206614109.
- [362] Francastel C, Mazouzi Z, Robert-Lézénès J. Co-induction of c-fos and junB during the latent period preceding commitment of Friend erythroleukemia cells to differentiation. *Leukemia* 1992;6:935–9.
- [363] Ding B, Liu C, Huang Y, Hickey RP, Yu J, Kong W, et al. p204 is required for the differentiation of P19 murine embryonal carcinoma cells to beating cardiac myocytes: its expression is activated by

the cardiac Gata4, Nkx2.5, and Tbx5 proteins. *J Biol Chem* 2006;281:14882–92.
doi:10.1074/jbc.M511747200.

- [364] Kristiansen M, Hughes R, Patel P, Jacques TS, Clark AR, Ham J. Mkp1 Is a c-Jun Target Gene That Antagonizes JNK-Dependent Apoptosis in Sympathetic Neurons. *J Neurosci* 2010;30:10820–32. doi:10.1523/JNEUROSCI.2824-10.2010.
- [365] Smith MS, Bentz GL, Alexander JS, Yurochko AD. Human Cytomegalovirus Induces Monocyte Differentiation and Migration as a Strategy for Dissemination and Persistence. *J Virol* 2004;78:4444–53. doi:10.1128/jvi.78.9.4444-4453.2004.
- [366] Fraile-Ramos A, Kledal TN, Pelchen-Matthews A, Bowers K, Schwartz TW, Marsh M. The human cytomegalovirus US28 protein is located in endocytic vesicles and undergoes constitutive endocytosis and recycling. *Mol Biol Cell* 2001;12:1737–49. doi:10.1091/mbc.12.6.1737.
- [367] Nightingale K, Lin K-M, Ravenhill BJ, Davies C, Nobre L, Fielding CA, et al. High-Definition Analysis of Host Protein Stability during Human Cytomegalovirus Infection Reveals Antiviral Factors and Viral Evasion Mechanisms. *Cell Host Microbe* 2018;24:447-460.e11. doi:10.1016/j.chom.2018.07.011.
- [368] Zhang G, Zhang H, Liu Y, He Y, Wang W, Du Y, et al. CD44 clustering is involved in monocyte differentiation. *Acta Biochim Biophys Sin (Shanghai)* 2014;46:540–7. doi:10.1093/abbs/gmu042.
- [369] Schmid MA, Kingston D, Boddupalli S, Manz MG. Instructive cytokine signals in dendritic cell lineage commitment. *Immunol Rev* 2010;234:32–44. doi:10.1111/j.0105-2896.2009.00877.x.
- [370] Watowich SS, Liu Y-J. Mechanisms regulating dendritic cell specification and development. *Immunol Rev* 2010;238:76–92. doi:10.1111/j.1600-065X.2010.00949.x.
- [371] Garrett S, Dietzmann-Maurer K, Song L, Sullivan KE. Polarization of primary human monocytes by IFN-gamma induces chromatin changes and recruits RNA Pol II to the TNF-alpha promoter. *J Immunol* 2008;180:5257–66.
- [372] Chistiakov DA, Myasoedova VA, Revin V V., Orekhov AN, Bobryshev Y V. The impact of interferon-regulatory factors to macrophage differentiation and polarization into M1 and M2. *Immunobiology* 2018;223:101–11. doi:10.1016/j.imbio.2017.10.005.
- [373] Jenkins C, Garcia W, Godwin MJ, Spencer J V., Stern JL, Abendroth A, et al. Immunomodulatory

- Properties of a Viral Homolog of Human Interleukin-10 Expressed by Human Cytomegalovirus during the Latent Phase of Infection. *J Virol* 2008;82:3736–50. doi:10.1128/JVI.02173-07.
- [374] Orzalli MH, Broekema NM, Knipe DM. Relative Contributions of Herpes Simplex Virus 1 ICP0 and vhs to Loss of Cellular IFI16 Vary in Different Human Cell Types. *J Virol* 2016;90:8351–9. doi:10.1128/JVI.00939-16.
- [375] Solt LA, May MJ. The I κ B kinase complex: master regulator of NF- κ B signaling. *Immunol Res* 2008;42:3–18. doi:10.1007/s12026-008-8025-1.
- [376] Paciolla M, Boni R, Fusco F, Pescatore A, Poeta L, Ursini M V., et al. Nuclear factor-kappa-B-inhibitor alpha (NFKBIA) is a developmental marker of NF- B/p65 activation during in vitro oocyte maturation and early embryogenesis. *Hum Reprod* 2011;26:1191–201. doi:10.1093/humrep/der040.
- [377] Paijo J, Döring M, Spanier J, Grabski E, Nooruzzaman M, Schmidt T, et al. cGAS Senses Human Cytomegalovirus and Induces Type I Interferon Responses in Human Monocyte-Derived Cells. *PLoS Pathog* 2016;12. doi:10.1371/journal.ppat.1005546.
- [378] Maréchal A, Zou L. DNA damage sensing by the ATM and ATR kinases. *Cold Spring Harb Perspect Biol* 2013;5. doi:10.1101/cshperspect.a012716.
- [379] Li X, Shu C, Yi G, Chaton CT, Shelton CL, Diao J, et al. Cyclic GMP-AMP Synthase Is Activated by Double-Stranded DNA-Induced Oligomerization. *Immunity* 2013;39:1019–31. doi:10.1016/j.immuni.2013.10.019.
- [380] Iqbal J, Ansari MA, Kumar B, Dutta D, Roy A, Chikoti L, et al. Histone H2B-IFI16 Recognition of Nuclear Herpesviral Genome Induces Cytoplasmic Interferon- β Responses. *PLoS Pathog* 2016;12:e1005967. doi:10.1371/journal.ppat.1005967.
- [381] Ansari MA, Singh VV, Dutta S, Veettil MV, Dutta D, Chikoti L, et al. Constitutive Interferon-Inducible Protein 16-Inflammasome Activation during Epstein-Barr Virus Latency I, II, and III in B and Epithelial Cells. *J Virol* 2013;87:8606–23. doi:10.1128/JVI.00805-13.
- [382] Yoo JW, Hong SW, Kim S, Lee D. Inflammatory cytokine induction by siRNAs is cell type- and transfection reagent-specific. *Biochem Biophys Res Commun* 2006;347:1053–8. doi:10.1016/j.bbrc.2006.07.001.

- [383] Brownell J, Bruckner J, Wagoner J, Thomas E, Loo Y-M, Gale M, et al. Direct, interferon-independent activation of the CXCL10 promoter by NF- κ B and interferon regulatory factor 3 during hepatitis C virus infection. *J Virol* 2014;88:1582–90. doi:10.1128/JVI.02007-13.
- [384] Chehimi J, Starr SE, Kawashima H, Miller DS, Trinchieri G, Perussia B, et al. Dendritic cells and IFN- α -producing cells are two functionally distinct non-B, non-monocytic HLA-DR⁺ cell subsets in human peripheral blood. *Immunology* 1989;68:486–90.
- [385] Hillyer P, Mane VP, Schramm LM, Puig M, Verthelyi D, Chen A, et al. Expression profiles of human interferon- α and interferon- λ subtypes are ligand- and cell-dependent. *Immunol Cell Biol* 2012;90:774–83. doi:10.1038/icb.2011.109.
- [386] Noriega V, Redmann V, Gardner T, Tortorella D. Diverse immune evasion strategies by human cytomegalovirus. *Immunol Res* 2012;54:140–51. doi:10.1007/s12026-012-8304-8.
- [387] Van der Wal FJ, Kikkert M, Wiertz E. The HCMV gene products US2 and US11 target MHC class I molecules for degradation in the cytosol. *Curr Top Microbiol Immunol* 2002;269:37–55. doi:10.1007/978-3-642-59421-2_3.
- [388] Wiertz EJHJ, Jones TR, Sun L, Bogyo M, Geuze HJ, Ploegh HL. The human cytomegalovirus US11 gene product dislocates MHC class I heavy chains from the endoplasmic reticulum to the cytosol. *Cell* 1996;84:769–79. doi:10.1016/S0092-8674(00)81054-5.
- [389] Ameres S, Besold K, Plachter B, Moosmann A. CD8 T Cell–Evasive Functions of Human Cytomegalovirus Display Pervasive MHC Allele Specificity, Complementarity, and Cooperativity. *J Immunol* 2014;192:5894–905. doi:10.4049/jimmunol.1302281.
- [390] Zimmermann C, Kowalewski D, Bauersfeld L, Hildenbrand A, Gerke C, Schwarzmüller M, et al. HLA-B locus products resist degradation by the human cytomegalovirus immunoevasin US11. *PLoS Pathog* 2019;15. doi:10.1371/journal.ppat.1008040.
- [391] Johnson DC, Hegde NR. Inhibition of the MHC class II antigen presentation pathway by human cytomegalovirus. *Curr Top Microbiol Immunol* 2002;269:101–15. doi:10.1007/978-3-642-59421-2_7.
- [392] Jackson SE, Sedikides GX, Mason GM, Okecha G, Wills MR. Human Cytomegalovirus (HCMV)-Specific CD4⁺ T Cells Are Polyfunctional and Can Respond to HCMV-Infected Dendritic Cells In

Vitro. *J Virol* 2017;91. doi:10.1128/JVI.02128-16.

- [393] Pachnio A, Ciaurriz M, Begum J, Lal N, Zuo J, Beggs A, et al. Cytomegalovirus Infection Leads to Development of High Frequencies of Cytotoxic Virus-Specific CD4⁺ T Cells Targeted to Vascular Endothelium. *PLoS Pathog* 2016;12. doi:10.1371/journal.ppat.1005832.
- [394] Chan ST, Logan AC. The clinical impact of cytomegalovirus infection following allogeneic hematopoietic cell transplantation: Why the quest for meaningful prophylaxis still matters. *Blood Rev* 2017;31:173–83. doi:10.1016/j.blre.2017.01.002.
- [395] Khan N, Cobbold M, Keenan R, Moss PAH. Comparative Analysis of CD8⁺ T Cell Responses against Human Cytomegalovirus Proteins pp65 and Immediate Early 1 Shows Similarities in Precursor Frequency, Oligoclonality, and Phenotype. *J Infect Dis* 2002;185:1025–34. doi:10.1086/339963.
- [396] Bradley ME, Dombrecht B, Manini J, Willis J, Vlerick D, De Taeye S, et al. Potent and efficacious inhibition of CXCR2 signaling by biparatopic nanobodies combining two distinct modes of action. *Mol Pharmacol* 2015;87:251–62. doi:10.1124/mol.114.094821.
- [397] Harwood SL, Alvarez-Cienfuegos A, Nuñez-Prado N, Compte M, Hernández-Pérez S, Merino N, et al. ATTACK, a novel bispecific T cell-recruiting antibody with trivalent EGFR binding and monovalent CD3 binding for cancer immunotherapy. *Oncoimmunology* 2017. doi:10.1080/2162402X.2017.1377874.
- [398] Slobedman B, Mocarski ES. Quantitative analysis of latent human cytomegalovirus. *J Virol* 1999;73:4806–12.
- [399] Hosgood SA, Moore T, Kleverlaan T, Adams T, Nicholson ML. Haemoadsorption reduces the inflammatory response and improves blood flow during ex vivo renal perfusion in an experimental model. *J Transl Med* 2017;15. doi:10.1186/s12967-017-1314-5.
- [400] Zeltzer S, Zeltzer CA, Igarashi S, Wilson J, Donaldson JG, Goodrum F. Virus control of trafficking from sorting endosomes. *MBio* 2018;9. doi:10.1128/mBio.00683-18.
- [401] Kim JH, Collins-McMillen D, Caposio P, Yurochko AD. Viral binding-induced signaling drives a unique and extended intracellular trafficking pattern during infection of primary monocytes. *Proc Natl Acad Sci U S A* 2016;113:8819–24. doi:10.1073/pnas.1604317113.
- [402] Noriega VM, Haye KK, Kraus TA, Kowalsky SR, Ge Y, Moran TM, et al. Human cytomegalovirus

modulates monocyte-mediated innate immune responses during short-term experimental latency in vitro. *J Virol* 2014;88:9391–405. doi:10.1128/JVI.00934-14.

[403] Pedone E, Postiglione L, Aulicino F, Rocca DL, Montes-Olivas S, Khazim M, et al. A tunable dual-input system for on-demand dynamic gene expression regulation. *Nat Commun* 2019;10. doi:10.1038/s41467-019-12329-9.

[404] Wang H, La Russa M, Qi LS. CRISPR/Cas9 in Genome Editing and Beyond. *Annu Rev Biochem* 2016;85:227–64. doi:10.1146/annurev-biochem-060815-014607.

[405] Bos T, De Bruyne E, Heirman C, Vanderkerken K. In Search of the Most Suitable Lentiviral shRNA System. *Curr Gene Ther* 2009;9:192–211. doi:10.2174/156652309788488578.

Appendix A: Publications authored during this project

1. Elder EG, Krishna BA, Williamson J, Lim EY, Poole E, Sedikides GX, et al. Interferon-Responsive Genes Are Targeted during the Establishment of Human Cytomegalovirus Latency. *MBio* 2019;10. <https://doi.org/10.1128/mBio.02574-19>.
2. Elder E, Sinclair J. HCMV latency: what regulates the regulators? *Med Microbiol Immunol* 2019. <https://doi.org/10.1007/s00430-019-00581-1>.
3. Elder E, Krishna B, Williamson J, Aslam Y, Farahi N, Wood A, et al. Monocytes latently infected with human cytomegalovirus evade neutrophil killing. *IScience* 2019. <https://doi.org/10.1016/J.ISCI.2019.01.007>.
4. Aslam Y, Williamson J, Romashova V, Elder E, Krishna B, Wills M, et al. Human Cytomegalovirus Upregulates Expression of HCLS1 Resulting in Increased Cell Motility and Transendothelial Migration during Latency. *IScience* 2019;20:60–72. <https://doi.org/10.1016/j.isci.2019.09.016>.